GENETIC AND GENE EXPRESSION ANALYSIS OF NASOPHARYNGEAL CARCINOMA (NPC)

By

Chunfang Hu

A thesis submitted to The University of Birmingham

for the degree of

DOCTOR OF PHILOSOPHY

School of Cancer Sciences

College of Medical and Dental Sciences

The University of Birmingham

November 2010

ABSTRACT

Nasopharyngeal carcinoma (NPC) is a highly malignant tumour arising from the epithelial lining of the nasopharynx and has geographical, genetic, environmental and viral cofactors. During the development and progression of NPC, a number of genetic abnormalities and expression changes in a wide variety of cellular genes are accumulated. Therefore, identification of these aberrations is critical for understanding the molecular basis of this disease. Here we examined both the chromosomal copy number changes and differential RNA expression profiles in NPC. Gene expression profiles identified a large number of differentially regulated genes involved in diverse functional processes (e.g. tumour promoting, tumour suppressing, apoptosis/anoikis- suppressing, and metastatic promotion), while genetic analysis detected extensive genomic abnormalities including large and small, discrete regions of copy number change and loci that exhibit uniparental disomy (UPD). The relationship between chromosomal copy number and level of gene expression were analysed in the list of tumour associated genes. This revealed that the direct copy number/expression link applies in about 60% of the instances of copy number loss/down-expression and less than 35% of instances of copy number gain/up-expression that were examined. When the gene expression data were analysed in the context of signalling pathways, it revealed that numerous components involved in the TGF-β, Wnt/β-catenin and Hedgehog pathways were universally upregulated in NPC tumours. The C666-1 cell line is the only line used in this study, and sample correlation and signalling pathway analysis demonstrated that the gene expression pattern of this line approximated to other NPC tumours, indicating that it could be a good tumour model for analysis of NPC. A preliminary *in vitro* investigation of signalling pathways revealed that the C666-1 cell line is intact in the activin and Hh signalling pathways but not in the TGF-β pathway. However, the C666-1 cells appear to resist activin-mediated cell growth inhibition.

ACKNOWLEDGEMENTS

I would like to take the opportunity to thank the Dorothy Hodgkin programme and Cancer Research UK for funding my research. I would also like to thank Professor Lawrence Young for giving me the opportunity to work within his group and for his intellectual support during the course of this project.

I owe my deepest gratitude to my supervisor Dr John Arrand for his immense help, support, guidance and patience from the initial to the final level of my PhD. Thanks for pushing me to write, reading every word of every draft, pointing out the mistakes and helping me to clarify my ideas. I could not have managed this without his invaluable support and advice. I would also like to thank supervisor Dr Chris Dawson for his massive guidance and assistance on the signalling pathways and cell biology work.

I would like to thank Professor Ciaran Woodman and Dr Wenbin Wei for their time and expertise in analysing microarray data, and thank Professor Paul Murray for instruction in cutting tissue sections and providing facilities and advice for IHC staining. A thank you also goes to the remaining NPC group members, past and present, for their support and kindness: especially to Jia, thanks so much for caring and looking after me throughout my PhD life in the UK; and to Sim, thanks for running microarray experiments and supporting me in the lab.

I offer my regards and blessings to all of those who supported me in any respect during the completion of this project.

Finally, I would like to thank my parents and my sisters for their support, encouragement and love throughout my life. The last, and the most important thank you I would like to give to my dear husband, Zuogui. Without his unconditional love and encouragement this thesis wouldn’t be possible. Thanks for always being there for me and here’s to many more great times together in the future.

CONTENTS

LIST OF FIGURES

Chapter 1 Introduction

Chapter 3 Expression changes in cellular tumour-associated genes

Chapter 4 Cellular genetic alterations of nasopharyngeal carcinoma

Chapter 5 Dysregulated signalling pathways

Chapter 6 *In vitro* investigation of signalling pathways in NPC cells

LIST OF TABLES

Chapter 2 Materials and Methods

Chapter 3 Expression changes in cellular tumour-associated genes

Chapter 4 Cellular genetic alterations of nasopharyngeal carcinoma

Chapter 5 Dysregulated signalling pathways

ABBREVIATIONS

aCGH	Array-based CGH
ALTER	Agitated low temperature epitope retrieval
APC	Adenomatous polyposis coli
BARTs	BamHI-A rightwards transcripts
BL	Burkitt's lymphoma
BMP	Bone morphogenic proteins
BPE	Bovine pituitary extract
BSA	Bovine serum albumin
CCND1	Cyclin D1
CDK	Cyclin-dependent kinase
CGH	Comparative genomic hybridisation
cIAP	Cellular inhibitor of apoptosis protein
CNAT	Copy number analysis tool
COX-2	Cyclooxygenase-2
CR2	Complement receptor type 2
CTNNB1	β-catenin
DAB	Diaminobenzidine
DEPC	Diethylpyrocarbonate
DKK	Dickkopf
DLEC1	Deleted in lung or esophageal cancer 1
DNA	Deoxyribonucleic acid
DVL	Dishevilled
EA	Early antigen
EBERs	Epstein-Barr virus encoded RNAs
EBNA	Epstein-Barr virus nuclear antigen
EBV	Epstein-Barr virus
ECL	Enhanced Chemiluminescence
ECM	Extracellular matrix
EDTA	Ethylenediaminetetra-acetic acid
EMT	Epithelial-mesenchymal transition
FBS	Foetal bovine serum
FCS	Foetal calf serum
FFPE	Formalin fixed paraffin embedded
FHIT	Fragile histidine triad
FISH	Fluorescence *in situ* hybridisation
FITC	Fluorescein isothiocyanate
GAPDH	Glyceraldehyde-3-phosphate dehydrogenase
GAS1	Growth arrest-specific 1
GCOS	GeneChip Operating Software
gp	Glycoprotein
H&E	Haematoxylin and eosin

HINGS	Heat inactivated normal goat serum
HIP	Hh-binding proteins
HL	Hodgkin's lymphomas
HLA	Human leukocyte antigen
hTERT	Human telomerase reverse transcriptase
ID1	Inhibitor of DNA binding 1
IF	Immunofluorescence
Ig	Immunoglobulin
IHC	Immunohistochemistry
IM	Infectious mononucleosis
ISH	*In situ* hydridisation
JNK	c-Jun N-terminal kinase
LCL	Lymphoblastoid cell lines
LMP	Latent membrane protein
LMPC	Laser microdissection and pressure catapulting
LOH	Loss of heterozygosity
LRP	Low-density-lipoprotein receptor-related protein
LTF	Lactotransferrin
LTβR	Lymphotoxin beta receptor
MAPK	Mitogen activated protein kinase
MHC	Major histocompatability complex
MLH1	MutL homologue 1
MMP	Matrix metalloproteinase
NF-κB	Nuclear factor-kappa B
NP	Nasopharyngeal epithelial
NPC	Nasopharyngeal carcinoma
OCT	Optimal cutting temperature
Ori-P	Plasmid origin of viral replication
PAGE	Polyacrylamide gel electrophoresis
PAI1	Plasminogen activator inhibitor-1
PBS	Phosphate buffered saline
PCR	Polymerase chain reaction
PFA	Paraformaldehyde
PI3K	Phosphatidylinositol 3-kinase
PTCH1	Patched 1
PTLD	Post-transplant lymphoproliferative disease
Q-PCR	Quantitative polymerase chain reaction
RASSF1	Ras Association Domain Family 1A
Rb	Retinoblastoma protein
RMA	Log scale robust multi-array analysis
RNA	Ribonucleic acid
RP	Rank products
RT	Reverse transcriptase
SCC	Squamous-cell carcinomas

SD	Standard deviation
SDS	Sodium dodecyl sulphate
SDW	Sterile distilled water
SHH	Sonic hedgehog
SMO	Smoothened
SNP	Single nucleotide polymorphism
TBS	Tris buffered saline
TGFβ1	Transforming growth factor Beta 1
TMA	Tissue microarray
TNF	Tumour necrosis factor
TRITC	Tetramethyl rhodamine iso-thiocyanate
TSG	Tumour suppressor gene
UPD	Uniparental disomy
VCA	Viral capsid antigen
VEGF	Vascular endothelial growth factor
WHO	World Health Organisation
WIF-1	Wnt inhibitory factor-1

CHAPTER 1

Introduction

1.1 Nasopharyngeal carcinoma (NPC)

Nasopharyngeal carcinoma is a highly malignant tumour arising from the epithelial lining of the nasopharynx and is distinguished from other cancers of the head and neck by its distinct histopathology, racial and geographical distribution, clinical characteristics and treatment.

1.1.1 Histopathology

NPC is a squamous cell carcinoma with a worldwide distribution. Therefore, it is important to have a universal histopathological classification for standardised and comparable diagnosis and therapy around the world. However, since the beginning of the 20th century, several classification schemes for NPC have been proposed and this has led to considerable confusion. In 1978 the first international classification was proposed by the World Health Organisation (WHO) which classified NPC into 3 subtypes based on the differentiation status of the tumour cells (Shanmugaratnam & Sobin, 1993). WHO type I is characterised by keratinising squamous-cell carcinomas (SCC). This type of NPC tumour presents as squamous differentiation with the presence of intracellular bridges and/or keratinisation, and the absence of cellular infiltrate. Type II is non-keratinising squamous carcinoma, which is neither anaplastic nor keratinising. It is a differentiated tumour with a stratified appearance and well-defined cell borders. Cytologically, the tumour cells are of moderate size, variable in cell morphology (polygonal and/or spindled) and differentiation. Type III represents undifferentiated carcinomas that have distinct cytological characteristics. Typically, the cells appear to have prominent nucleoli, indistinct cytoplasm and poorly

delineated cell boundaries. The tumour cell morphology of this type is highly variable as it can feature clear cells, spindle cells or anaplastic cells. In areas with low incidence of NPC such as North America, around 25% of NPC patients are WHO type I, 12% are type II, and 63% are type III whereas in endemic areas such as South China, the histological distribution is approximately 2%, 3% and 95%, respectively (Wei & Sham, 2005).

A modified WHO classification was proposed in 1991, which divided NPC tumours into two groups: keratinising squamous-cell carcinomas and non-keratinising carcinomas. The latter was then subdivided into differentiated and undifferentiated carcinomas. A criterion used in this classification is significantly correlated with EBV since non-keratinising carcinoma has a stronger association with EBV infection. In addition, in this classification therapeutic and prognostic significance has also been taken into account. It has been shown that non-keratinising carcinomas are more sensitive to radiotherapy and have better patient survival than keratinising squamous-cell carcinoma (Marks *et al.*, 1998).

There is an even newer, 2005, WHO classification for NPC, which maintains the separation between keratinising squamous-cell carcinomas and non-keratinising carcinomas but they are more flexible in their subclassification. The main consideration for this classification is for determining treatment options and prognosis regardless of EBV infection, differentiation status or other factors. The histopathological classification of NPC has been reviewed in detail (Nicholls & Niedobitek, 2008).

NPC is heterogeneous, often containing substantial numbers of tumour-infiltrating leucocytes, the majority of which are reactive T-lymphocytes (Nicholls *et al.*, 1997; Gourzones *et al.*, 2009). A large proportion of NPC cases show an extensive lymphocytic infiltrate. Although keratinising squamous cell carcinomas do not typically display lymphoid stroma, non-keratinising carcinomas have a predominant lymphoid infiltrate in up to 80% of this type of cases. Infiltrating leucocytes are often located around malignant tumour cell clusters but sometimes disseminated within epithelial cell nests. Depending on the pattern of tumour infiltrate, non-keratinising NPC can be further classified as either Regaud type if the tumour presents as a well-defined collection of epithelial cells surrounded by infiltrate (solid cell type) or Schmincke type if the tumour cells are scattered and intermingle with the infiltrating cells (isolated cell type). Increasing lines of evidence suggest that the presence of infiltrating leucocytes plays an essential role in NPC progression by communicating with tumour cells in the microenvironment of NPC and secreting various cytokines and exosomes that suppress the immune system and facilitate NPC tumour growth (Tang *et al.*, 1999; Gourzones *et al.*, 2009; Yip *et al.*, 2009). Nonetheless, on the other hand, it seems that it may also have adverse effects on tumour growth since earlier studies suggested that patients whose tumour cells are surrounded by an abundant leucocyte infiltrate have better prognosis (Zong *et al.*, 1993).

1.1.2 Epidemiology

1.1.2.1 Racial and geographical distribution

In most regions of the world, NPC is a rare malignancy with an incidence of less than 1 per 100,000 population per year. For example, in the United States, incidence rates in white males and females are only 0.5 and 0.2 per 100,000 person-years,

respectively. In its endemic areas including Southern China, NPC reaches a frequency of up to 20 – 30 per 100,000 per year. Highest rates are reported among Cantonese in Southern China who inhabit the central region of Guangdong province as well as Hong Kong. Other provinces in mainland China next to Guangdong (Hunan, Fujian, Guangxi and Hainan) also have a relatively high incidence of NPC, whereas the incidence in Northern China is significantly lower than that in the South. An intermediate incidence (approximately 8 per 100,000 per year) has been observed in other areas of Southeast Asia (e.g. Thailand, Philippines, Malaysia and Singapore), Greece, Turkey and the Maghreb region of North Africa (Yu & Yuan, 2002; Chang & Adami, 2006; Tao & Chan, 2007).

1.1.2.2 Aetiology of NPC

The observation that Chinese emigrants from endemic areas, irrespective of their country of immigration, continue to have a high incidence of NPC, whereas the rate of this disease among ethnic Chinese born in North America is considerably lower than those born in China (Buell, 1974) suggests that both environmental and inherited factors play crucial roles in the development of NPC.

1.1.2.2.1 Environmental factors

There are some common features across the populations demonstrating an elevated risk of NPC. One of the strongest cultural habits correlated with carcinogenesis is the digestion of Cantonese-style salted fish. A large case-control study suggests that consumption of Cantonese-style salted fish during all time periods, especially in childhood, has a strong correlation with NPC (Yu *et al*., 1986). Intake of other preserved food and usage of Chinese herbs have been frequently observed in high-risk

populations of NPC, suggesting a link with NPC pathogenesis (Gallicchio *et al.*, 2006). Actually, extracts from preserved food including salted fish demonstrate the presence of carcinogenic nitrosamines/precursors, and genotoxic and EBV-activating substances (Shao *et al.*, 1988; Poirier *et al.*, 1989). EBV has been closely associated with NPC and will be introduced in the following sections. In addition, insufficient intake of fresh fruit and vegetables has been suggested to be another risk factor for NPC in endemic areas. Epidemiological studies indicate that occupational exposure to toxic pollutants in the air, wood dust, and textiles is linked to increased incidence of NPC (Armstrong *et al.*, 2000; Li *et al.*, 2006b). Long-term cigarette smoking and/or alcohol consumption have also been considered to be important contributions to NPC (Nam *et al.*, 1992; Cheng *et al.*, 1999).

1.1.2.2.2 Genetic susceptibility

Several lines of evidence suggest that genetic predispositions contribute to the high prevalence of NPC in southern Chinese populations. An earlier linkage study on Chinese sib pairs with NPC identified an NPC susceptibility locus at the HLA (human leucocyte antigen) region (Lu *et al.*, 1990). Further studies in Taiwanese suggest that genes associated with susceptibility to NPC in the HLA region are within the HLA-A locus (Lu *et al.*, 2003a; Lu *et al.*, 2005). In recent years, family-based association studies identified several putative genetic susceptibility loci in NPC including chromosomes 3p21, 4 and 5p13 (Zeng *et al.*, 2006; Hu *et al.*, 2008a). However, since the chromosomal regions identified are quite large, the candidate NPC-related genes have not been determined. A number of case-control studies reveal that genetic polymorphisms for several genes including CYP2E1, GSTM1, XRCC1 and hOGG1 are associated with susceptibility of NPC. CYP2E1 is responsible for metabolic

activation of nitrosamines (an EBV activating agent) and other related carcinogens. Several variant forms of this gene are strongly associated with NPC development in Chinese populations (Hildesheim *et al.*, 1997; Jia *et al.*, 2009). GSTM1 is mainly involved in the detoxification of carcinogens and the absence of GSTM1 (GSTM1 null genotype) moderately increases risk of NPC (Nazar-Stewart *et al*., 1999). XRCC1 and hOGG1 are two enzymes that participate in the DNA repair system, genetic polymorphisms of which are correlated with an elevated risk of NPC (Cho *et al.*, 2003). The development and progression of NPC have also included a number of acquired genetic changes (e.g. gene amplification, deletion and mutation) and epigenetic changes (methylation) that contribute to carcinogenesis by altering the expression of genes essential for a wide range of functions, such as proliferation, apoptosis, differentiation, invasiveness and metastasis. This will be discussed in Section 1.4.

1.1.2.2.3 EBV infection

In addition to the environmental and genetic factors, NPC is consistently associated with EBV infection (Raab-Traub, 2002). This association was initially suggested on the basis of serological studies and has been subsequently supported by the detection of viral genomes and gene products in NPC tumour cells. At least 95% of NPC tumours are associated with EBV. The WHO type II and III NPCs are consistently associated with EBV regardless of geographical distribution and ethnic origin (Andersson-Anvret *et al*., 1979), whereas WHO type I is less frequently EBV-associated, especially for the cases in nonendemic areas. In NPC tumour cells EBV exists in a state of type II latency (see Section 1.2.5) (Brooks *et al.*, 1992; Busson *et al.*, 1992). Since there are variable morphological characteristics of NPC-affected

tissues, the pathological diagnosis of NPC is usually based on the location of the tumour in the nasopharynx and the presence of EBV in the tumour cells. The presence of clonal EBV genomes in the early preinvasive dysplastic lesion or carcinoma *in situ* of the nasopharynx contrasts with its absence either in normal nasopharynx or in low-grade dysplasia, suggesting that EBV infection is an early, possibly initiating event in the progression of NPC (Pathmanathan *et al.*, 1995). EBV infection and viral gene function in NPC development will be further discussed in Section 1.2.

1.1.3 Clinical presentation and treatment

In Southeast Asia NPC develops in all age groups of the population with a peak incidence in the range of 40-60 years, whereas in North Africa the distribution of NPC according to age is bi-modal, with the first peak between 10 and 20 years of age accounting for up to 20% of NPC patients and the second between 40 and 60 years of age accounting for nearly 60% of patients (Ellouz *et al.*, 1978; Daoud *et al.*, 2003). Anatomically, NPC usually arises in the ostium of the Eustachian tube in the lateral wall of the nasopharynx also called “pharyngeal recesses”. The nasopharynx has a rich vascular supply and lymphatic drainage system. These characteristics of anatomy define the symptomatology, the route of tumour spread and treatment of NPC. Headache, a nose bleed, a stuffed nose with bloody drainage, and serious otitis media are usually the earliest clinical symptoms of this disease. The clinical diagnosis of NPC mainly depends on clinical presentation, nasopharyngoscopy and biopsy. However, the majority of NPC is diagnosed at an advanced stage because initial symptoms of the disease may appear relatively innocuous. NPC can easily spread regionally resulting in early lymph-node involvement in the neck, which could actually be the first clinical presentation. NPC is also highly metastatic, with most

distant metastases appearing within 18 months of the first symptoms (Cvitkovic *et al.*, 1993; Tao *et al.*, 2008). Bone is the most frequent metastatic site, followed by lung and liver (Micheau *et al.*, 1987; Hui *et al.*, 2004). Juvenile forms of NPC have an even higher frequency of lymph node and distant metastases than those of adult forms (Daoud *et al.*, 2003).

Following the development of various detection systems that take advantage of the presence of EBV in NPC, increasing numbers of patients can be diagnosed at an early stage of the disease, which is of great help to the therapy and prognosis of patients. In endemic areas such as Southern China, EBV serology has been generally used for screening of NPC. EBV antibody titres (IgA) are usually elevated in sera of NPC patients compared to healthy controls, in addition, the levels increase from early stage (stages I or II) to advanced stage (stages III or IV) (Henle & Henle, 1976). Furthermore, quantitative detection of circulating EBV DNA has been demonstrated to be a powerful method for NPC patients in early diagnosis, and prediction of progression and prognosis (Lo *et al.*, 2000b; Stevens *et al.*, 2006).

In contrast to other types of head and neck cancers, NPC is sensitive to radiation. Thus, the standard treatment for NPC is radiotherapy, whereas local relapses and distant metastases still frequently occur after radiotherapy alone, especially for locoregionally advanced patients. Concurrent chemoradiotherapy with or without adjuvant chemotherapy significantly improves patient survival rates (Al-Sarraf *et al.*, 1998). Despite the improvement in treatment, distant metastasis remains a major cause for failure of treatment. The median survival rate after distant metastasis is only around 9-12 months (Ma & Chan, 2006). The prognosis of NPC patients mainly

depends on disease stage (tumour size, lymph node involvement and distant metastasis), although it is also influenced by patients' characteristics (gender and age), and treatment. Patients that are diagnosed at an early stage (stage I and II) have better prognosis, whereas those with lymph-node and distant metastasis have a much poorer prognosis. Women appear to have better survival than men (Sham & Choy, 1990). Taking advantage of the close association between EBV and NPC, some novel treatment approaches such as immunotherapy and gene therapy targeting EBV genes have been recently investigated (Busson *et al.*, 2004). These may provide new avenues for the treatment of NPC patients.

1.2 Epstein-Barr virus

1.2.1 The natural history of EBV

EBV (Epstein-Barr virus) is a ubiquitous human gammaherpesvirus that was recognised and designated in 1964 (Epstein *et al.*, 1964). EBV infects more than 90% of the adult population of the world. Following primary infection, the individual remains a lifelong carrier. In developing countries, EBV infection typically occurs during early childhood and is often asymptomatic, whereas in developed countries, infection often occurs during adolescence or adulthood and may cause symptomatic disease presenting as the characteristic clinical features of infectious mononucleosis (IM), including fever, sore throat, malaise and lymphoadenopathy (Slots *et al.*, 2006). Saliva is the main vehicle for EBV transmission from individual to individual, whereas organ and bone marrow transplantation is another risk for EBV infection.

1.2.2 EBV and human disease

EBV is associated with a number of human diseases. In early serological studies, high antibody titres to EBV were observed in patients with Burkitt's lymphoma (BL) (Henle & Henle, 1966), IM, and undifferentiated NPC (Henle *et al.*, 1968). EBV is also associated with Hodgkin's lymphoma (HL), T-cell lymphoma and gastric carcinoma (Baumforth *et al.*, 1999). In individuals with primary immunodeficiencies e.g. X-linked lymphoproliferative syndrome, EBV infection frequently leads to fatal IM and B-cell lymphomas (Tatsumi & Purtilo, 1986), whereas patients with acquired immunosuppression will have increased risk of developing lymphoproliferative disorders (e.g. post-transplant lymphoproliferative disease (PTLD)) (Cohen, 2003). Experimental evidence in support of EBV having oncogenic potential is derived from its ability to infect and transform normal human B-cells *in vitro* resulting in indefinitely proliferating lymphoblastoid cell lines (LCLs) (Henle *et al.*, 1967).

1.2.3 EBV *in vitro* and *in vivo* infection

EBV preferentially infects B lymphocytes, inducing growth transformation. EBV infection of B-cells *in vivo* has been well characterised. It uses the normal biology of B-cells to gain access to and persist within memory B-cells for the lifetime of the host (Thorley-Lawson, 2005). Complement receptor type 2 (CR2/CD21) is essential for the attachment of EBV to the surface of B-cells in an interaction mediated by the viral envelope glycoprotein gp350 (Nemerow *et al.*, 1987; Young *et al.*, 2007).

Although EBV infection of B-cells is well documented, infection of epithelial cells remains poorly understood *in vitro*. The epithelial cell environment appears to be unfavourable to the establishment of EBV stable infection. The resistance of epithelial cells to EBV infection *in vitro* has been associated with the absence of EBV receptors, CD21 (Shapiro & Volsky, 1983; Fingeroth *et al.*, 1999), since epithelial cells overexpressing introduced CD21 can be efficiently infected by EBV (Li *et al.*, 1992; Knox *et al.*, 1996). In addition, the observation that only epithelial cells impaired in their ability to differentiate appear to be capable of sustaining a stable EBV infection suggests that EBV infection is related to the differentiation status of the epithelial cells (Knox *et al.*, 1996), an association that has also been observed *in vivo* (Young *et al.*, 1991).

In spite of the inefficiency of EBV infection of epithelial cells *in vitro*, early studies have observed EBV replication in epithelial cells *in vivo*. However, later work with more sensitive EBV detection techniques frequently failed to detect EBV in a variety of normal epithelial tissues (Niedobitek *et al.*, 1989; Karajannis *et al.*, 1997; Niedobitek *et al.*, 2000), including nasopharyngeal epithelial cells (Sam *et al.*, 1993), suggesting that EBV infection of normal epithelial cells is not a common event.

Successful infection of human epithelial cells by EBV *in vitro* was achieved by cell-to-cell contact between epithelial cells and EBV-producing B-cells (e.g. from the BL cell line, Akata) without any additional manipulations such as introduction of the known EBV receptor (CD21) gene or addition of polymeric immunoglobulin A against viral gp350 in culture (Imai *et al.*, 1998; Shannon-Lowe *et al.*, 2006). This raises the possibility that EBV's ability to infect epithelial tissues such as

nasopharyngeal epithelium *in vivo* might be due to the close proximity of lytically infected B-cells that have the ability to produce virus and release it into saliva.

1.2.4 The structure and variation of the EBV genome

The EBV genome is composed of linear double stranded DNA, approximately 172 kilobase (kb) pairs in length with a coding potential for more than 85 genes. The genome contains a series of 500bp terminal direct repeats (TRs) and internal repeat sequences (IRs), which divide the EBV genome into short and long, largely unique sequence domains. The B95.8 strain of EBV was the first human herpesvirus to have its genome completely cloned and sequenced (Baer *et al.*, 1984). The structure of the EBV genome and its latent genes are represented in Figure 1.1.

EBV is divided into two subtypes, EBV type 1 (EBV1) and EBV type 2 (EBV2), based on sequence variation in a subset of the EBNA genes including EBNA2, EBNA3A, EBNA3B, and EBNA3C (Dambaugh *et al.*, 1984; Sample *et al.*, 1990). EBV1 and EBV2 are also dramatically different in their geographical distribution. Although both types are widespread in equatorial Africa and Papua New Guinea (Young *et al.*, 1987), EBV1 is the predominant subtype in Caucasian and Asian populations including those showing a high frequency of NPC (Chang *et al.*, 2009).

Increasing development in molecular technology allows the identification of EBV strain variation in a wider range of loci. In particular, polymorphisms within LMP1 have been investigated extensively and the variations have been described in numerous EBV-associated tumours. There are six major variants of LMP1: Alaska, China 1, China 2, China 3, North Carolina, and Mediterranean, classified according to

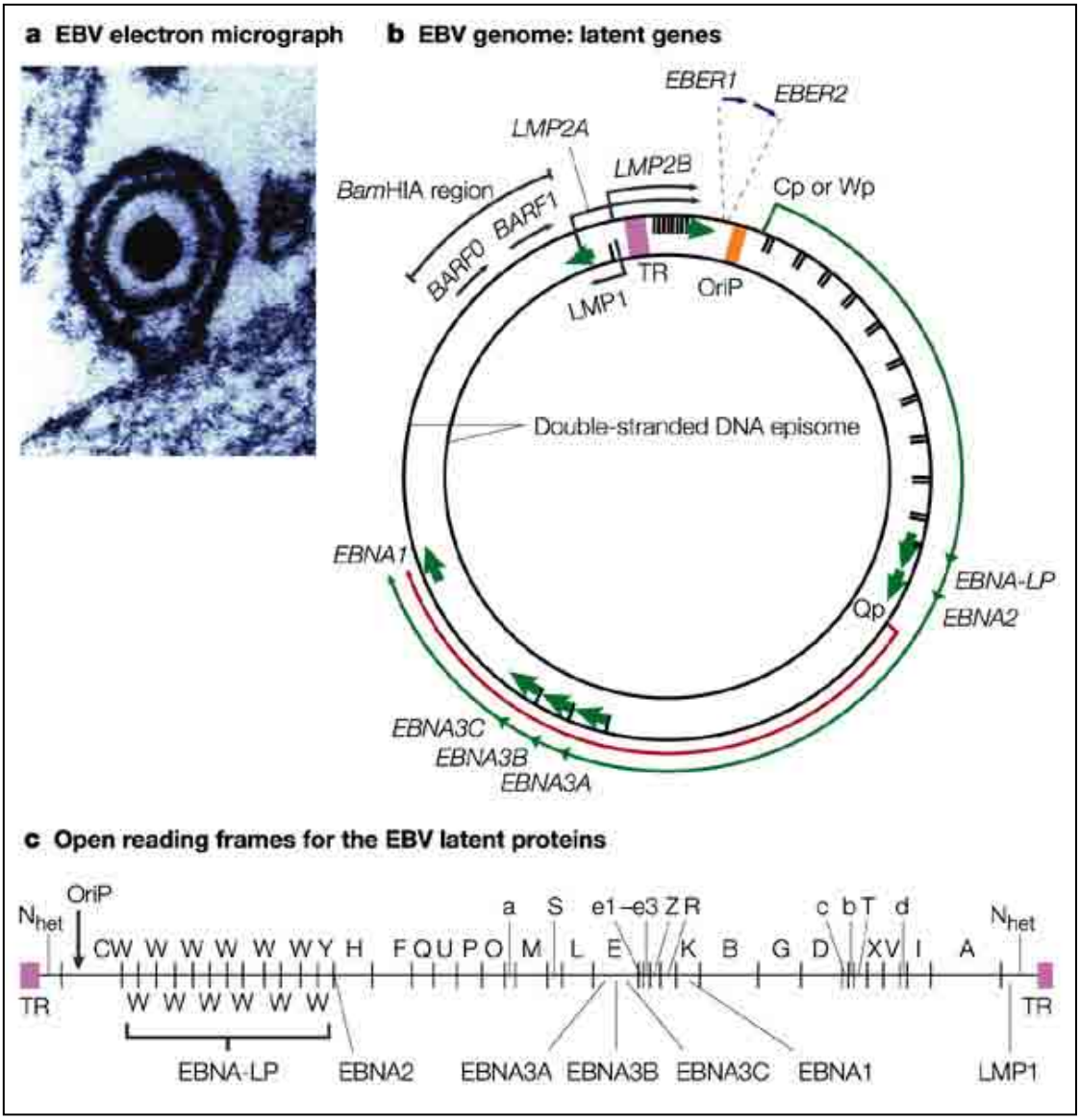

Figure 1.1: The Epstein–Barr virus genome.

(a) Electron micrograph of the EBV virion.
(b) Diagram showing the location and transcription of the EBV latent genes on the double-stranded viral DNA episome.
(c) Location of open reading frames for the EBV latent proteins on the BamHI restriction-endonuclease map of the prototype B95.8 genome.

Figure reproduced from: Lawrence S. Young & Alan B. Rickinson
Epstein–Barr virus: 40 years on
Nature Reviews Cancer 4: 757-768 (2004)

the geographical region from which the initial isolate was derived. A combined data analysis of 187 Asian LMP1 variants suggests that the China 1 LMP1 variant is the prevalent strain and is present in approximately 85% of the population in this area. In China 1 LMP1, two common polymorphisms have been reported containing a specific 30bp deletion in the C-terminus domain and loss of an XhoI restriction site in the N-terminus (Sung *et al.*, 1998; Saechan *et al.*, 2006; Nagamine *et al.*, 2007). The 30bp deletion of LMP1 was found in a higher frequency of Asian NPC patients compared to healthy controls (Miller *et al.*, 1994; Edwards *et al.*, 1999). In addition, this variation had a significantly higher frequency in advanced NPC patients (stage III and IV), suggesting a link with development and progression of this malignancy (Tiwawech *et al.*, 2008).

1.2.5 EBV lytic replication and latency states

Following EBV infection, cells display either a productive lytic infection or a latent infection. Lytic replication results in production of EBV virions by performing multiple rounds of replication. Whereas in latent infection, the virus does not replicate and produce virions but replicates along with the host DNA as an extrachromosomal episome. The host cells carrying the viral genome constitutively express a limited set of viral gene products called latent genes (see Figure 1.1). Three major patterns of EBV latent gene expression have been classified so far, and they are associated with particular human diseases (Young & Rickinson, 2004).

Latency III infection is found in LCLs and PTLD. All the viral latent genes are expressed in latency III: six nuclear antigens (EBNA1, EBNA2, EBNA3A, EBNA3B, EBNA3C and EBNA-LP), three latent membrane proteins (LMP1, LMP2A and

LMP2B), two non-polyadenylated RNAs (EBER1 and EBER2), the BamHI-A rightward transcripts (BARTs) and viral miRNAs (Young & Rickinson, 2004).

Latency II is found in NPC, Hodgkin's and T- and NK- lymphomas and is characterised by a more restricted pattern with the expression of only one of the nuclear antigens (EBNA1), all three latent membrane proteins, the EBERs and the BARTs (Brooks *et al*., 1992).

Type I latency is associated with BL and is characterised by the expression of only EBNA1, the EBERs and BARTs (Rowe *et al*., 1987). Some reports have documented expression of LMP1 and EBNA2 in a small proportion of cells in a few cases of endemic BL (Niedobitek *et al*., 1995).

1.2.6 The functions of EBV genes in NPC tumourigenesis

As mentioned in the previous section, EBV is consistently detected in NPC as a latency II infection. Functional studies have shown that viral latent genes have substantial functions in the regulation of cellular gene expression, alteration of cell phenotype, cell growth and differentiation, thereby leading to a highly invasive and malignant tumour. The potential contributions of the individual viral genes to the development of NPC are summarised in the following.

1.2.6.1 LMP1

LMP1 is the first EBV latent gene found to have oncogenic potential to transform established rodent cell lines and alter phenotypes of both lymphoid and epithelial cells (Wang *et al*., 1985; Martin *et al*., 1993). It is variably present in NPC and has also

been detected in preinvasive lesions of the nasopharynx (Pathmanathan *et al.*, 1995). Early studies in NPC biopsies using RT-PCR revealed that LMP1 transcripts are expressed in greater than 80% of NPC samples (Brooks *et al.*, 1992) whilst immunohistochemical staining data from different studies have shown LMP1 protein to be variably expressed in the range of 20% – 70% of NPC biopsies (Horikawa *et al.*, 2001; Sarac *et al.*, 2001; Shao *et al.*, 2004; Burgos, 2005; Li *et al.*, 2007; Chen *et al.*, 2010). However, when a more sensitive antibody was used, all NPC biopsies displayed positive LMP1 staining despite a variable proportion of positive tumour cells. In addition, a high frequency of LMP1 expression is closely associated with the juvenile form of NPC (Khabir *et al.*, 2005). Although the significance of heterogeneous expression of LMP1 protein in NPC has not been addressed, along with patient age it might be partly due to the sensitivity of the method used for detection.

LMP1 is involved in the regulation of several signalling pathways in NPC including the NF-κB, PI3K/Akt, MAPK, and JAK/STAT pathways (Tsao *et al.*, 2002; Zheng *et al.*, 2007), thereby modulating a number of target genes involved in a wide range of cellular functions including apoptosis, proliferation, differentiation, invasiveness and metastasis, all of which are important for the development and progression of NPC.

LMP1 may exert its function in apoptosis by upregulating anti-apoptotic genes e.g. Survivin, TNFAIP3 and BCL-2 (Laherty *et al.*, 1992; Deng *et al.*, 2003; Faqing *et al.*, 2005). However, a correlation between TNFAIP3, BCL-2 upregulation and LMP expression has not been demonstrated (Codd *et al.*, 1999; Murono *et al.*, 1999).

LMP1 regulates the cell cycle progression of NPC tumour cells either by increasing the kinase activity of the CDK4/Cyclin D1 complex or decreasing the activity of p16/p21 (Deng *et al.*, 2003; Ai *et al.*, 2005). LMP1 is also a key modulator in the differentiation process. Although the mechanisms by which LMP1 prevents epithelial cell terminal differentiation have not been fully addressed, it appears to be due, at least in part, to changes in the surface phenotype and differentiation responsiveness (Dawson *et al.*, 1990; Zheng *et al.*, 1994).

Transformation by LMP1 results in alterations in cell phenotypes. One of the alterations is reduction of cell-to-cell interactions, which facilitates invasiveness and metastasis of tumour cells. Loss of E-cadherin expression has been frequently observed in NPC and is closely associated with metastasis and poor prognosis (Zheng *et al.*, 1999). LMP1 is considered to be responsible for the reduction and switch of E-cadherin expression in NPC (Tsai *et al.*, 2002; Shair *et al.*, 2009). LMP1 upregulates the expression of the matrix metalloproteinases (MMPs) MMP1, MMP3 and MMP9 in NPC, and their upregulations are correlated with invasiveness and metastasis (Horikawa *et al.*, 2000; Lu *et al.*, 2003b; Lee *et al.*, 2007). Extensive growth of tumour cells also requires angiogenesis for nutrient supplement and metabolic waste trafficking. LMP1 induces expression of potent angiogenesis regulators, COX-2, VEGF, and receptor for advanced glycation end products (RAGE), contributing to tumour cell metastasis (Murono *et al.*, 2001; Fendri *et al.*, 2008; Tsuji *et al.*, 2008). However, in contrast with these observations, a study in North African NPCs shows that there is no relationship between LMP1 expression and metastatic behaviour (Khabir *et al.*, 2005), whilst in addition, an earlier study reported that LMP1-negative NPC tumours appear to have an increased tendency to recur and metastasise (Hu *et al.*,

1995). The molecular basis for these discrepancies is poorly understood and more studies are required to uncover the complexity of LMP1 functions in NPC.

1.2.6.2 LMP2A and LMP2B

Although the roles of LMP2A and LMP2B have been investigated mainly in B-cells (Longnecker, 2000), they have both been shown to alter epithelial cell behaviour such as adhesion and motility (Allen *et al.*, 2005). In agreement with this study, LMP2A-expressing epithelial cells have been observed to become more migratory and invasive (Pegtel *et al.*, 2005). LMP2A also has transforming properties in epithelial cells, and this is possibly mediated by activation of the PI3K/Akt pathway. LMP2A-expressing cells are more tumourigenic and the tumours show poorer differentiation and higher proliferation than LMP2A-negative controls (Scholle *et al.*, 2000).

In vivo studies indicate that LMP2A and LMP2B are consistently associated with NPC and might contribute to its pathogenesis. A serological study demonstrated that antibody responses to LMP2A and LMP2B were present in sera of more than 95% NPC patients (Lennette *et al.*, 1995). This finding supports earlier observations that LMP2A and -2B transcripts were consistently expressed in NPC (Brooks *et al.*, 1992; Busson *et al.*, 1992). More recent work reveals that LMP2A protein is expressed in approximately 50% of NPC tumours (Heussinger *et al.*, 2004) and that a high level of LMP2A expression correlates with poor prognosis (Pegtel *et al.*, 2005).

1.2.6.3 EBNA1 and EBERs

EBNA1 is consistently expressed in all EBV-associated malignancies including NPC. It has been suggested to have oncogenic potential in NPC in an early study (Brooks *et*

al., 1992). Further *in vitro* studies reveal that EBNA1-expressing NPC cells are able to form more metastatic, less differentiated tumours when inoculated into mice compared to their negative counterparts (Sheu *et al.*, 1996). Recent studies demonstrate that EBNA1 is a potent cellular transcriptional regulator in NPC cancer cells as it modulates TGF-β, NF-κB and AP-1 signalling pathways (Wood *et al.*, 2007; O'Neil *et al.*, 2008; Valentine *et al.*, 2010).

In addition to EBNA1, two small non-coding RNAs, EBERs 1 and 2 are ubiquitously expressed in all EBV-associated tumours including NPC. EBERs are the most abundant viral transcripts in NPC tumour cells, and a recent study reveals that the expression of EBERs can be regulated by EBNA1 (Owen *et al.*, 2010). The EBERs have been shown, by *in situ* hybridisation to be present in nearly all NPC tumour cells, but generally absent in the adjacent normal tissue or in only a few scattered lymphoid cells. Thus, they have been frequently used as target molecules for detection of EBV infection and for diagnosis of NPC (Wu *et al.*, 1991; Murono *et al.*, 1997). In addition, it has been shown that abundant expression of EBERs is essential to induce the initial transformation of epithelial cells. Thus they might make an important contribution to the oncogenesis of NPC (Yoshizaki *et al.*, 2007).

1.2.7 *In vitro* and *in vivo* model systems of NPC

To investigate NPC tumourigenesis and its metastatic potential, it is important to use EBV-positive NPC cell models since NPC is consistently associated with EBV infection. However, the establishment of NPC cell lines is difficult due to limited tissue quantity and contamination by other cell types. Moreover, as was mentioned in previous sections, EBV infection of epithelial cells is much less efficient than that of

B-cells because epithelial cells, including NPC cells, express no or only low levels of the CR2 receptor. Therefore, although there are several NPC cell lines that have been established, most of them either do not harbour EBV or have lost it during long-term culture (Gullo *et al.*, 2008). The single exception is the C666-1 cell line, which is a subclone of its parental cell line, C666, established from an NPC xenograft of a southern Chinese patient with undifferentiated NPC. This cell line consistently maintains EBV in long term culture. The expression pattern of EBV genes in C666-1 is latency type Π, as in authentic NPC tumours (Cheung *et al.*, 1999). In addition to the C666-1 cell line, the successful establishment and characterisation of EBV-positive NPC xenografts (e.g. C15, C17, xeno-666, xeno-2117 and xeno-1915) also provide good vehicles for investigation of NPC. They have been extensively used for identifying the genetic alterations and delineating aberrant signal transduction pathways in NPC (Busson *et al.*, 1988; Huang *et al.*, 1989; Wong *et al.*, 2003a; Friboulet *et al.*, 2008).

1.3 Cancer genetics

Cancer, which develops from single somatic cells and their progeny, is essentially a somatic genetic disease arising from the accumulation of a series of genetic changes at different chromosomal loci that lead to changes in gene activity, and so to altered cell phenotypes. Eventually, a cell population that evolves to be capable of escaping the normal controls in proliferation and territory can become a cancer (Ponder, 2001).

1.3.1 Somatic genetic changes in cancer

Genetic changes can be caused by genomic instability, which is a cardinal feature of almost all cancer cells and are usually a result of defects of the DNA repair system

that are either inherited from germinal cells and/or acquired in somatic cells during tumour development. The types of genetic aberrations in somatic cells underlying cancer include point mutations in coding or regulatory sequences, changes in whole chromosomes, high level chromosomal amplification, smaller regions of chromosomal loss/gain, loss of heterozygosity (LOH) and uniparental disomy (UPD) (Balmain *et al*., 2003).

Of these genetic alterations, LOH is defined as when both alleles of a chromosomal pair are heterozygous originally and they have become homozygous or hemizygous. This usually represents the loss of normal function of one allele of a gene by mutation in which the other allele was already inactivated (Presneau *et al.*, 2003). LOH represents a key step in the inactivation of multiple tumour suppressor genes. UPD arises when an individual inherits both copies of a chromosome pair from one parent (either maternal or paternal), whereas no copy of this chromosome comes from the other parent (Engel, 1980). Acquired UPD can be considered to be one form of LOH or called copy neutral LOH. A UPD region is typically larger than 2Mb and includes only copy-number-neutral changes. UPD, especially acquired whole chromosomal UPD, can occur in somatic cells and is usually associated with cancer (Tuna *et al.*, 2009).

1.3.2 Hallmarks of cancer

Genetic abnormalities will increase and involve more and more chromosomal regions following the progression of cancer and lead to further alterations in cell physiology. Six essential alterations to cell physiology that succeed genetic changes and collectively dictate malignant growth were summarised by Hanahan and Weinberg

and termed 'Hallmarks of Cancer' (Hanahan & Weinberg, 2000). They are self-sufficiency in growth signals, insensitivity to anti-growth signals, evasion of apoptosis, limitless replicative potential, sustained angiogenesis, and tissue invasion and metastasis. These altered cells are subjected to selection, and eventually only a cell population that manifests all the six characteristics can develop into cancer.

1.3.3 Tumour suppressor genes (TSGs) and oncogenes

To achieve and sustain these hallmarks, a number of genes that affect tumour cell behaviour are involved in this process. According to whether they activate or inhibit cellular proliferation, these cancer genes can be divided into two main groups, oncogenes or TSGs, respectively.

An oncogene is defined as a gene that contributes to the production of cancer by activating cellular proliferation, leading to unregulated cell growth and differentiation (Ponder, 2001). Oncogenes are generally mutated forms of proto-oncogenes that are functionally involved in the control of normal cellular growth and differentiation. Oncogenes are usually inappropriately activated by "gain-of-function mutations". The mechanism of oncogene activation has been associated with chromosomal amplification which could result in increased expression or activity of related genes (Mitelman *et al.*, 1997).

Tumour suppressor genes are also normal cellular genes with the function of inhibiting cellular proliferation, and they are usually inactivated by 'loss of function' mutations in cancer development (Weinberg, 1991). In 1971, Knudson proposed a "two hit" hypothesis of carcinogenesis based on an epidemiological investigation of

retinoblastoma (Knudson, 1971). The hypothesis suggests that cancer is caused by two mutational events. In the dominantly hereditary cancer, mutation in one of the two copies of a TSG is inherited from the germinal cells and mutation of the second copy of the gene occurs in somatic cells; whereas in the non-hereditary cases, both events occurring in a somatic cell are needed for it to develop into a tumour clone. This indicates that tumour-suppressor genes are inactivated either when a germline mutation occurs in one allele or somatic inactivation at a later stage occurs in the other allele or when sequential somatic inactivation of both alleles occurs. TSGs have been frequently detected at the DNA level in regions of chromosomal loss, especially regions with LOH (Solomon *et al.*, 1991).

1.3.4 Identifying chromosomal abnormalities and cancer-related genes in tumours

The ability to examine genetic aberrations that develop during the progression of cancer is increasing rapidly, owing to advanced molecular techniques, powerful analytical tools and the almost-complete genome sequence information. The regions of chromosomal loss, gain, and LOH give clues to the locations of abnormal genes involved in carcinogenesis.

In earlier genetic studies, karyotyping was used to calculate chromosome numbers, and to detect large chromosomal alterations such as rearrangements and deletions. In karyotyping chromosomes of cancer, tumour cells are grown in tissue culture, spread on glass slides and stained after cells have been arrested in metaphase by adding the drug colchicine. The chromosomes of these cells then can be photographed and analysed. To detect much smaller chromosomal abnormalities, other more sensitive

techniques have been used, such as fluorescence *in situ* hybridisation (FISH) and comparative genomic hybridisation (CGH). FISH uses a labelled specific segment of chromosome to hybridise with the chromosomal DNA of a tumour cell and is visualised under a fluorescence microscope. This technique allows a rapid detection of one gene or one specific region of chromosomal abnormality (deletion or gain) (Trask, 1991).

CGH is capable of detecting and mapping DNA copy-number variation across a whole genome. With CGH, tumour DNA and normal reference DNA are labelled with two different fluorescent markers and then hybridised simultaneously to normal chromosome spreads. Copy number changes in a tumour are determined by the comparison of the fluorescence ratios along the length of chromosomes. Multiple regions of chromosomal abnormalities can be detected by this technique (Kallioniemi *et al.*, 1992). More recently, the advanced CGH technique, array-based CGH (aCGH) that has high resolution and allows more accurate localisation of specific genetic alterations by hybridising with arrayed genomic DNA or cDNA clones on a genome-wide level, has been widely used to survey copy number aberrations in cancer (Kallioniemi, 2008).

Another method of screening for small areas of chromosomal imbalance is to use microsatellites (short tandem repeat sequences) as markers to do allelic imbalance analysis (Naidoo & Chetty, 1998). In this technique if one of the heterozygous markers (multiple repeats) becomes homozygous (a single repeat) in the tumour, this suggests that an allele has been lost, and this type of chromosomal abnormality is

determined as LOH. The alleles can also be gained in the case of chromosomal duplications.

1.3.5 Single nucleotide polymorphism microarrays (SNP arrays)

The techniques mentioned above have several limitations in detecting genetic abnormalities. Firstly, the resolution is limited. Although array-based CGH has highly increased resolution compared to the others, it is still limited by the number of clones that can be deposited on the arrays. Secondly, these techniques require large amounts of starting material. In addition, they cannot simultaneously detect copy number aberrations and LOH status. Recently developed SNP arrays provide a high-resolution platform for simultaneously detecting several types of genetic changes in cancer at the level of the individual allele, which allows more insight into the mechanism of tumourigenesis and is a more successful strategy for mapping TSGs and oncogenes (Dutt & Beroukhim, 2007; Kloth *et al.*, 2007; Lin *et al.*, 2008).

A SNP is defined as a single base polymorphism when the frequency of the minor allele exceeds 1% in at least one population; otherwise it is considered a variant or mutation (Botstein & Risch, 2003). The principle of detecting genetic changes by SNP array analysis is based on the correlation between alleles at nearby sites, predicting chromosome abnormalities on a genome-wide scale by using a smaller number of representative SNPs as markers (Gabriel *et al*., 2002).

The two major technologies of SNP arrays involve oligonucleotide probes either spotted on gene chips (Affymetrix) or adsorbed on beads (Illumina). Advances in Affymetrix SNP arrays in recent years have enabled rapid increases in the number of

SNPs (from 10K, 50K, 100K, 500K to commercially available 900K SNPs across the genome) that can be genotyped in parallel in a single experiment (Dutt & Beroukhim, 2007; McCarroll *et al.*, 2008). Taking advantage of the high resolution, SNP arrays have been widely used for combination analyses of genetic copy number changes and genetyping in a number of cancers and made great progress in exploring the mechanisms of cancer development and progression (Kloth *et al.*, 2007; Purdie *et al.*, 2007; Chen & Chen, 2008; Gardina *et al.*, 2008; Gunnarsson *et al.*, 2008).

1.4 NPC genetics

Like all other cancers, NPC is a genetic disease. During the development and progression of NPC, multiple acquired genetic aberrations (e.g. chromosomal loss, gain or LOH) are accumulated along with the effects of environmental factors, EBV infection as well as some inherited genetic susceptibilities, all acting together. These genetic abnormalities are often considered to be related to altered gene function, for example, activation of oncogenes is associated with amplification and inactivation of TSGs is correlated with homozygous deletion or LOH. The altered gene function is essential for NPC carcinogenesis by driving the progressive transformation of normal nasopharyngeal cells into highly malignant directions. Determining the genetic changes in NPC, therefore, can identify a number of TGSs and oncogenes that are involved in disruption of normal cellular mechanisms and multiple cellular signalling pathways. In addition, this could reveal the molecular basis of NPC pathogenesis and find biomarkers for early diagnosis and prediction of prognosis. Such findings could also provide insights for better planning of strategies of prevention and treatment for this disease.

1.4.1 Somatic genetic aberration in NPC

Since the late 1980s, cytogenetic studies such as karyotyping were firstly explored to detect genetic alterations in NPC. By karyotype analyses of EBV-positive NPC xenografts and cell lines, recurrent structural abnormalities on chromosomes 1, 3p, 11q, 12 and 17 were identified. Especially, deletions of 3p were consistently observed (Huang *et al.*, 1989; Bernheim *et al.*, 1993; Wong *et al.*, 2003a). However, the studies using karyotyping are limited due to the difficulty of culturing primary NPC tumour cells *in vitro*. Subsequently, CGH has been widely used for examination of chromosome losses or gains in a large number of primary NPC biopsies and has provided invaluable information. These studies have demonstrated a high incidence of multiple chromosome changes in NPC. Consistent findings include frequent deletions on chromosomes 1p, 3p, 9p, 9q, 11q, 13q, 14q and 16q and frequent gains on chromosomes 1q, 3q, 8q and 12. The most frequent chromosomal regions of loss or gain observed are 3p and 12 (Chen *et al.*, 1999; Hui *et al.*, 1999; Fang *et al.*, 2001). The delineation of the minimal overlapping regions of genetic changes provides important hints for the identification of potential oncogenes and/or TSGs in NPC. In recent years, the higher resolution of array-based CGH has been used to detect genetic abnormalities on a genome-wide level in NPC. In addition to previously characterised regions, several novel minimal regions of chromosomal gains (3q27.3-28, 8q21-24, 11q13.1-13.3, and 12q13) have been identified in 26 NPC biopsies with array-based CGH analysis, with oncogene cyclin D1 (CCND1) at 11q13.3 verified to be amplified and overexpressed in NPC (Hui *et al.*, 2005). Furthermore, several consistent small regions of amplification as well as novel potential oncogenes in NPC have been identified in other aCGH studies, for example, amplifications of MYCL1 in 1p34.3, TERC and PIK3CA at 3q26.3, and LTβR at 12p13.3 (Hui *et al.*, 2002b; Or *et al.*,

2010). In a comparison with findings from Asian NPC patients, one study using conventional CGH and aCGH demonstrates that Mediterranean NPCs have higher frequencies of gains at 1q and losses at 13q (Rodriguez *et al.*, 2005).

A meta analysis of a combination of 12 CGH studies in a total of 188 NPC cases from southern Asia also reveals hot spots for chromosomal gains in more than 20% of cases at 1q, 3q, 8q and 12, and chromosome losses on 3p, 11q, 14q and 16q (Li *et al.*, 2006c). A tree model analysis from 4 studies suggests that the loss of 3p and gain of 12q might be important early events (Shih-Hsin Wu, 2006). A recent study in Taiwanese NPC patients using aCGH demonstrates that amplification of GPR160 and SKIL at 3q26.2-q26.32, and deletion of TSGs ADAMTS9 and LRIG1 at 3p12.3-p14.2 have significance in predicting prognosis of NPC (Sheu *et al.*, 2009).

LOH, the somatic conversion of heterozygous germline alleles to homozygosity, is a critical event in the inactivation of multiple TSGs. Traditional study of LOH with highly informative polymorphic markers is the most common approach for the analysis of allelic imbalance in NPC. This technique can detect small regions of chromosomal changes that are usually overlooked by CGH analyses. Using microsatellite polymorphic markers, the most frequent allelic losses were found on chromosomes 3p, 9p, 11q and 14q (Huang *et al.*, 1991; Hu *et al.*, 1996; Hui *et al.*, 1996; Deng *et al.*, 1998; Mutirangura *et al.*, 1998; Shao *et al.*, 2001). Additional studies of normal nasopharyngeal epithelia, dysplastic lesions and NPC cases from a high-risk population (Southern Chinese) and a low-risk population (central/northern Chinese and/or Caucasians from Toronto) reveal precancerous lesions and NPC cases from both populations have a high incidence of LOH on chromosome 3p and 9p, whereas normal nasopharyngeal epithelia from the high-risk region show a

significantly higher incidence of 3p and 9p LOH than do those from the low-risk region (Chan *et al*., 2000; Chan *et al*., 2002). This indicates that LOH of 3p and 9p are early events in NPC development. In addition, the increased risk of NPC in Southern Chinese may be related to the high incidence of these early events occurring in the normal nasopharyngeal epithelium.

1.4.2 NPC-related genes

Recurrent chromosomal regions of loss or gain are generally considered to be associated with inactivation of TSGs or activation of oncogenes. To identify these NPC-related genes and elucidate the mechanisms of NPC tumourigenesis, particular interest has been put on the genes located within the critical and commonly involved regions of loss or gain.

1.4.2.1 Chromosome loss and TSGs

Chromosome 3p

Allelic loss of chromosome 3p is the most frequent genetic change in NPC, with an incidence of greater than 90% in all primary NPC patients from Southern China (Chan *et al.*, 2000; Lo *et al.*, 2000a). In particular, LOH studies have identified multiple tumour suppressor loci including 3p13-14.3, 3p21 and 3p21-25 (Huang *et al.*, 1991; Hu *et al.*, 1996; Deng *et al.*, 1998; Chan *et al.*, 2000).

3p21.3 is believed to be the region harbouring the most potential TSGs since a high incidence of deletion at 3p21.3 has been consistently observed (Huang *et al.*, 1991; Hu *et al.*, 1996; Cheng *et al.*, 1998; Chan *et al.*, 2000). Several well-established TSGs have been identified in this region, including RASSF1 and ZMYND10. RASSF1 has

been shown to function as an effector to mediate apoptosis and inhibit cell cycle progression (Vos *et al.*, 2000; Shivakumar *et al.*, 2002). Downregulation of RASSF1 has been associated with both the development and progression of NPC (Peng *et al.*, 2003). A more recent study reveals a possible role for EBV in this process, since LMP1 suppresses RASSF1 expression (Man *et al.*, 2007). Restoration of RASSF1 expression in a RASSF1 deficient NPC cell line, C666-1, inhibited cell growth *in vitro* and reduced tumourigenesis *in vivo*. This provides functional evidence for RASSF1 as a target tumour suppressor gene (Chow *et al.*, 2004). ZMYND10, also known as BLU, is a candidate 3p21.3 TSG located upstream of RASSF1. It is an E2F-regulated, stress-responsive gene whose transcripts are ubiquitously expressed in normal nasopharyngeal epithelia but frequently absent or reduced in NPC cell lines and biopsies (Liu *et al.*, 2003; Qiu *et al.*, 2004; Ayadi *et al.*, 2008). Functional studies demonstrate that stable expression of ZMYND10 suppresses tumour formation *in vivo* (Yau *et al.*, 2006).

There are several other potential TSGs identified at 3p21.3 such as LTF (lactotransferrin) and LFLARS2 (leucyl-tRNA synthetase 2, mitochondrial) or close to 3p21.3 such as DLEC1 (deleted in lung or esophageal cancer 1) and MLH1 (MutL homologue 1, colon cancer, nonpolyposis type 2) at 3p22.3, RARB (Retinoic acid receptor, beta) at 3p24, which have been shown to be inactivated in NPC and might contribute to carcinogenesis (Wong *et al.*, 2003b; Yi *et al.*, 2006; Kwong *et al.*, 2007; Zhou *et al.*, 2009). In addition to the above loci, 3p14.2 is another potential TSG locus on 3p with candidate TSG FHIT (fragile histidine triad protein) involvement (Sung *et al.*, 2000). Mutation, LOH and abnormal expression of FHIT have been observed in NPC tumours (Deng *et al.*, 2001; Ko *et al.*, 2002). A recent publication reveals that

LOH and abnormal expression of FHIT in NPC are correlated with advanced clinical stage and higher titres of EBV capsid antigen (EBVCA-IgA) (Deng *et al.*, 2010). Although these observations suggest that FHIT might play an important role in NPC tumourigenesis, functional evidence for its tumour suppressor effect is still lacking.

Chromosome 9p

In addition to 3p, 9p is another region showing high frequency of loss in NPC (Huang *et al.*, 1994; Mutirangura *et al.*, 1998; Lo *et al.*, 2000a). LOH analyses have delineated an overlapping tumour suppressor locus at 9p21-22 in which two CDK inhibitors, p16 (CDKN2A) and p15 (CDKN2B) are involved and considered to be candidate TSGs in NPC (Huang *et al.*, 1994; Lo *et al.*, 1995). P16 and p15 inhibit cell cycle progression from G1 to S phase, and inactivation of these two genes will result in uncontrolled cell proliferation. Loss of expression of p16 protein has been frequently detected in NPC tumours and is associated with NPC development, local recurrence and prognosis (Baba *et al.*, 2001; Hwang *et al.*, 2002; Makitie *et al.*, 2003; Lin *et al.*, 2006a). The observation that deletion of p16 during the establishment of immortalisation of nasopharyngeal epithelial cells suggests that it might have a critical function in the malignant transformation of nasopharyngeal epithelial cells (Li *et al.*, 2006a). Restoration of p16 expression in NPC cells significantly inhibited cell growth and tumourigenicity (Wang *et al.*, 1999).

Chromosome 11q

Loss of 11q is also a frequent event in NPC, and LOH studies delineated two distinct regions of deletion, 11q13.3-22 and 11q22-24 (Hui *et al.*, 1996; Lo *et al.*, 2000a; Fang *et al.*, 2001). Several potential TSGs have been identified in these two regions

including GSTP1 (11q13), TSLC1 (11q23.2), THY1 (11q23.3) and ATM (11q22-23) (Cheng *et al.*, 2002; Hui *et al.*, 2002a; Lo & Huang, 2002; Tao & Chan, 2007). TSLC1 (also called CADM1) that was firstly reported to be a TSG in human non-small cell lung cancer plays a role as a cell adhesion molecule and exerts its TSG function by altering cell-cell interactions and controlling growth. Loss of TSLC1 expression has been observed in NPC and this is associated with lymph node metastasis (Hui *et al*., 2003; Lung *et al*., 2004). Restoration of TSLC1 expression inhibits cell growth and suppresses tumour formation in NPC cell lines by arresting cells in G1 phase (Lung *et al*., 2006). A more recently identified TSG, THY1, has been found to have a very similar tumour suppressor function to TSLC1 in NPC tumour cells (Lung *et al.*, 2005; Lung *et al.*, 2008; Lung *et al.*, 2009).

Although ATM has long been postulated to be a TSG in NPC, a recent investigation provides new evidence supporting its tumour suppressor function. In this study, downregulation of ATM expression has been observed at the both mRNA and protein levels in NPC tumour biopsies. In addition, in NPC cell lines, ATM expression was reduced only in the EBV-positive NPC cell line, C666-1, but not in five EBV-negative cell lines, indicating its association with EBV-infection (Bose *et al*., 2009).

Chromosomes 13q, 14q and 16q

Two distinct, smaller regions of deletion at 13q14.3-22 and 13q31-34 were delineated by LOH studies. Mapping of the critical regions of these loci suggests that some candidate TSGs might be involved (Tsang *et al.*, 1999; Lo *et al.*, 2000a; Shao *et al.*, 2002). Of the genes encoded in these regions, EDNRB located at 13q22 has been shown to be downregulated in NPC tumour cells, an effect that has been speculated to

be associated with the high frequency of promoter hypermethylation in NPC (Lo *et al.*, 2002; Zhou *et al.*, 2007).

Allelic loss at 14q is a very common event in NPC, and it has been observed in more than 80% of NPC tumours (Mutirangura *et al.*, 1998; Shao *et al.*, 2002). Although the monochromosome transfer technique supports the growth suppressive activity of 14q, especially two critical regions, 14q11.2-13.1 and 14q32.1, the TSGs involved in this region have been poorly understood so far (Cheng *et al*., 2003).

LOH of 16q has been detected in greater than half of NPC cases, and high resolution allelotyping of microdissected primary NPC samples has mapped the deletion to a minimal region of 16q22-23 (Lo *et al.*, 2000a; Fang *et al.*, 2001). CDH1 (also called E-cadherin) is the only known candidate TSG involved in this minimal region. This gene encodes a cell adhesion molecule whose loss of function is thought to contribute to cancer progression by increasing proliferation, invasion, and/or metastasis. Downregulation of CDH1 expression has been consistently observed in NPC tumours and that is associated with NPC progression and prognosis (Zheng *et al.*, 1999; Huang *et al.*, 2001; Li *et al.*, 2004; Xie *et al.*, 2010). Potential TSGs involved in other regions of 16q have also been identified including BRD7 (16q12) and RBL2 (16q12.2). The observation that BRD7 expression was reduced in NPC biopsies and cell lines suggests its tumour suppressor potential, while the finding that BRD7 can inhibit NPC cell growth through negatively regulating β-catenin and ERK1/2 pathways provides further functional evidence (Peng *et al.*, 2007).

1.4.2.2 Chromosomal gain and oncogenes

In previous CGH studies, recurrent gains in NPC tumours have been frequently detected on chromosomes 1q, 3q, 8q 12p and 12q (Hui *et al.*, 1999), whereas the putative oncogenes involved are still poorly understood. Later high-resolution array-based CGH studies and FISH analysis delineated the minimal regions of gain (e.g. 3q27.3-28, 8q21-24, 11q13.1-13.3, and 12q13) and recognised several NPC-related oncogenes (e.g. CCND1, PIK3CA and LTβR) (Hui *et al.*, 2002b; Hui *et al.*, 2005; Or *et al.*, 2005; Or *et al*., 2010).

Chromosome 3q

Gain of 3q is one of the most frequent genetic events occurring in NPC. The candidate oncogenes identified so far are found at 3q26-28, including PIK3CA (3q26.3), TERC (3q26), EVI1 (3q26.2) and TP73L (3q28) (Hui *et al*., 2002b; Or *et al*., 2005; Tao & Chan, 2007). PIK3CA encodes the catalytic subunit of PI3Ks that regulate signalling pathways involved in cell proliferation, motility, and adhesion. A high frequency of amplification and overexpression of PIK3CA in NPC tumours has been observed. PIK3CA amplification has been associated with aggressive progression and poor prognosis of Tunisian NPC patients (Fendri *et al*., 2009). TP73L (also called p63) includes wild-type p63 and mutated p63 (DeltaN-p63), and the latter is the oncogenic form. DeltaN-p63 is invariably expressed in NPC tumours, and its expression is associated with the differentiation status of NPC (Guo *et al.*, 2006). The oncogenic function of DeltaN-p63 in NPC can be accomplished by blocking p53-mediated transactivation and apoptosis (Crook *et al.*, 2000).

Chromosomes 8q and 11q13

Frequent gains have also been found at 8q. However, the potential oncogenes involved in this region are not fully understood. Only the well-known oncogene, c-myc (8q24.2), was found to have high copy number gains and be overexpressed in NPC (Fan *et al.*, 2000). Although chromosome 11q is frequently deleted in NPC, gain of a small portion of 11q (11q13.1-13.3) was observed in more than 60% of NPC tumours (Hui *et al.*, 2005). Of the genes encoded in this region, CCND1 and FGF3 are considered to be candidate oncogenes (Fan *et al*., 2000; Hui *et al*., 2005). CCND1 (cyclin D1) interacts with cyclin dependent kinases CDK4 and CDK6 whose activity is required for cell cycle G1/S transition resulting in DNA synthesis. Amplification and overexpression of this gene have been frequently observed in NPC tumours. Silencing of CCND1 expression in NPC cell lines by using interfering RNA significantly decreased cell proliferation, suggesting an oncogenic function of this gene in NPC cells (Hui *et al.*, 2005).

Chromosome 12q13

12q has been considered to be another most frequent chromosomal gain in NPC. (Or *et al.*, 2005; Or *et al.*, 2010). FISH mapping delineated the amplicon to a 1.24 Mb region at 12q13.3 in which 13 genes were involved. Among these genes, LTβR (lymphotoxin beta receptor) is the only one consistently overexpressed in both NPC xenografts and primary tumours (Or *et al*., 2010). This gene is a member of the tumour necrosis factor (TNF) family of receptors, modulating activation of the NF-κB signalling pathway. Overexpression of LTβR results in increased NF-κB activity and cell proliferation in nasopharyngeal epithelial cells, whereas knockdown of LTβR

inhibits tumour growth. This suggests LTβR might be a potential oncogene facilitating NPC tumour growth (Or *et al*., 2010).

In addition to the potential oncogenes introduced above, several other genes such as BCL2 at 18q21.3 (Chen *et al.*, 2008; Fendri *et al.*, 2010), EGFR at 7p12.1 (Hui *et al.*, 2002b), TNFAIP3 (A20) at 6q23 (Codd *et al.*, 1999), BIRC3 at 11q22 (Friboulet *et al.*, 2008), MET at 7q31 (Horikawa *et al.*, 2001; Qian *et al.*, 2002), BMI1 at 10p11(Song *et al.*, 2006; Qin *et al.*, 2008), that are either involved in other regions of gain or have been shown to have oncogenic potential in carcinogenesis, have also been considered to be candidate NPC-associated oncogenes.

Genetic changes and TSGs/oncogenes in NPC have been reviewed (Lo & Huang, 2002; Tao & Chan, 2007; Lo, 2008).

1.4.3 Abnormal cellular signals in proliferation and apoptosis

Genetic analyses in NPC have identified a number of chromosomal abnormalities as well as TSGs/oncogenes that contribute to carcinogenesis. It is inevitable that for the NPC-associated genes already mapped, the emphasis will shift from genetics to functional analysis. In common with other cancers, the development of NPC can be considered as a disruption in normal cellular proliferation and apoptosis. The critical signals resulting in uncontrolled proliferation or abnormal apoptosis contribute to NPC tumourigenesis.

A number of cellular signals can affect cell proliferation including those genes involved in cell cycle progression such as CDKN2A (p16) and cyclin D1. The cell cycle progression is regulated by cyclin-CDK complexes, and their activity is

regulated by binding with CDK inhibitors. Cyclin D1 is one of the most important cyclins and is required for cell cycle progression from G1 to S phase. Normal cyclin D1 activity can be regulated by p16 (CDK4 inhibitor). Therefore, a balance between p16 and cyclin D1 expression is important for maintaining a normal cell cycle progression. However, frequent loss of p16 expression and overexpression of cyclin D1 in NPC tumours disrupt the balance of p16/cyclin D1 and lead to uncontrolled DNA synthesis (Zhang *et al.*, 2009). C-myc is another cell cycle-related gene that interferes with regulators of G1/S transition (de Nigris *et al.*, 2003). Downregulation of c-myc expression can cause a significant arrest of NPC cells in S phase and disturb cell proliferation (Liu *et al.*, 2009). In addition, a recent publication suggests that DeltaNp63 is also involved in the regulation of cell cycle progression in NPC. Silencing DeltaNp63 expression results in cell cycle arrest in G1 phase, which is probably achieved by upregulation of p27 and p57 (Chiang *et al.*, 2009). Loss of function of TSLC1 and THY1 in NPC are critical proliferative signals since overexpression of these two genes in NPC cell lines can result in G1 arrest and inhibit proliferation (Lung *et al.*, 2006; Lung *et al.*, 2009).

Critical signals for inhibition of apoptosis are also involved in NPC development. BCL-2 is believed to play an essential role in regulation of apoptosis. Overexpression of BCL-2 has been consistently detected in NPC tumours (Sheu *et al.*, 1997) and is associated with poor prognosis of patients (Chen *et al.*, 2009). An induction of cell apoptosis or a regression of tumour growth can be achieved in NPC tumours by blocking the antiapoptotic function of BCL-2 by a BCL-2 family inhibitor or antisense oligonucleotides. Especially, a significant effect has been observed in those NPC cells with high expression of BCL-2 (Yip *et al.*, 2005; Hu *et al.*, 2008b).

TNFAIP3 is also a protein that protects cancer cells from apoptosis. TNFAIP3 expression can be induced by LMP1, and stable expression of TNFAIP3 in epithelial cells blocks p53-mediated apoptosis (Fries *et al.*, 1996). TNFAIP3 expression has been shown to be upregulated in NPC. Another antiapoptotic protein, BIRC3, that has been shown to be amplified and overexpressed in several cancers, was recently found also to be overexpressed in NPC biopsies and xenografts. In addition, using an inhibitor of BIRC3 results in degradation of this gene product, induces apoptosis and blocks clonal cell growth in NPC cells (Lu *et al.*, 1993; Codd *et al.*, 1999; Friboulet *et al.*, 2008).

1.4.4 Dysregulation of signalling pathways

In addition to the dysfunction of TSGs and oncogenes, multiple, aberrant signalling pathways can also play essential roles in carcinogenesis. These include the NF-κB, Wnt/β-catenin, and TGF-β signalling pathways.

1.4.4.1 The NF-κB signalling pathway

Dysregulation of NF-κB signalling is one of the most important components for NPC tumourigenesis as almost all NPC tumours show overexpression of NF-κB signalling cascades (Lo *et al.*, 2006). The NF-κB signalling is activated by LMP1, and then results in activation of a number of antiapoptotic and proliferative signals, including BCL-2, COX-2, and VEGF (Murono *et al.*, 2001). It also induces the accumulation of p53 protein and upregulates its transactivity, disturbing cell cycle progression (Deng *et al.*, 2003). Furthermore, NF-κB modulates the activity of telomerase and results in cell immortalisation by binding with human telomerase reverse transcriptase (hTERT) (Ding *et al.*, 2005).

1.4.4.2 The TGF-β signalling pathway

The TGF-β superfamily constitutes a large number of growth and differentiation factors which include TGF-β, activin/inhibins, nodal and bone morphogenic proteins (BMPs). These proteins mobilise complex signalling networks to regulate cellular differentiation, proliferation, motility, adhesion and apoptosis. The deregulation of various components of this pathway plays a critical role in the progression of several types of cancer (Moses & Serra, 1996; Massague, 1998).

The process of intracellular signal transduction from membrane-bound receptors into the nucleus is straightforward and quite similar between TGF-β superfamily members. The TGF-β ligands bind to transmembrane kinase type II receptor and phosphorylate type I receptors. The activated type I receptors then phosphorylate and activate specific intracellular mediators, SMAD proteins, which are direct substrates with the demonstrated ability to mediate gene responses to TGF-β signalling. The activated SMAD signalling results in nuclear translocation and activation of substrate genes (Massague & Chen, 2000) (Figure 1.2). In vertebrates, the SMAD proteins are classified into three functional groups: 1) receptor activated SMADs, which include SMAD1, 2, 3, 5 and 8; 2) the co-mediator SMAD, SMAD4; and 3) inhibitory SMADs, SMAD6 and 7 (Heldin *et al.*, 1997). The type I receptors for TGF-β, activin and Nodal, utilise receptor SMADs 2 and 3, whereas BMP receptors utilise SMAD1, 5 and 8. Once phosphorylated, receptor SMADs associate with the co-activator SMAD4 to form active SMAD complexes, which in turn translocate into the nucleus and activate transcriptional responses (Abdollah *et al.*, 1997; Heldin *et al.*, 1997). TGF-β, activins and BMPs can induce the expression of inhibitors SMAD6 and SMAD7 which act as a negative-feedback loop to dampen TGFβ-mediated SMAD

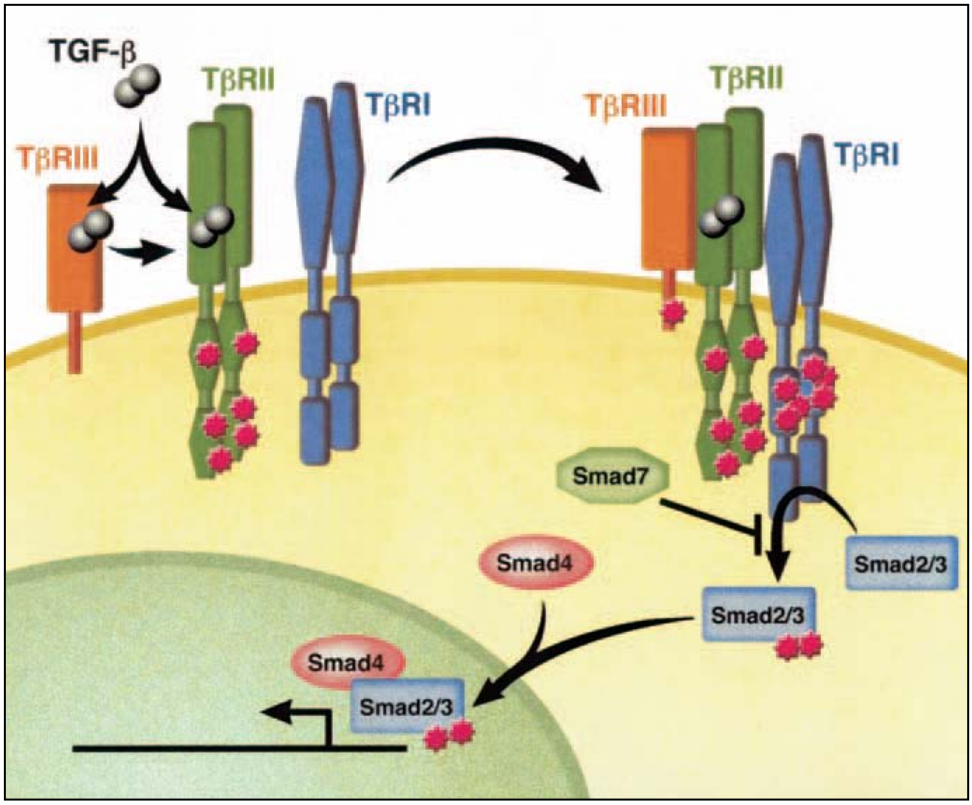

Figure 1.2: The transforming growth factor beta (TGF-β) signalling pathway.

TGF-β binds to the type II receptor (TGFBR2) and phosphorylates the type I receptor (TGFBR1), which then phosphorylates SMAD2 or SMAD3. Activated SMAD2 or SMAD3 associates with SMAD4 and they translocate into the nucleus where they modulate transcription of a number of target genes. SMAD7 inhibits TGF-β signalling by preventing the activation of SMAD2 or SMAD3 by TGFBR1.

Figure reproduced from: Rebecca L. Elliott and Gerard C. Blobe
Role of Transforming Growth Factor Beta in Human Cancer.
J Cli Oncol 23: 2078-2093 (2005)
.

transcription. The inhibitor SMADs bind to TGF-β family member receptors and inhibit the activation of receptor SMADs by these receptors (Nakao *et al.*, 1997). Normally, SMAD6 selectively inhibits BMP signalling, whereas SMAD7 mainly suppresses TGF-β and activin signalling (Nakao *et al.*, 1997; Hata *et al.*, 1998). Besides SMAD-mediated transcription, TGF-β also activates SMAD-independent signalling cascades, including MAPK, Rho-like GTPases, PI3K and PP2A signalling pathways, and induces various cellular functions (Derynck *et al.*, 2001).

TGF-β can function as a tumour suppressor during the early stages of cancer and a tumour promoter during the more advanced stages of tumour progression. Thus, TGF-β can either stimulate or inhibit cell proliferation depending on the cell type or the underlying genetic or epigenetic changes present within the cell (Hartsough & Mulder, 1997). TGF-β acts as a potent growth inhibitor for many tumour types of epithelial origin, a property that underscores its tumour suppressor function (Yue & Mulder, 2001; Marinari *et al.*, 2008). Although the precise mechanism for this growth inhibitory effect remains elusive, the ability of TGF-β to inhibit growth through cell cycle G1/S arrest by inducing the expression of cyclin kinase inhibitors p15(Ink4b), p21(Cip1) and p27(Kip1) has been well-established (Hannon & Beach, 1994; Zhang *et al.*, 2002; Nakamura *et al.*, 2009). The increased expression of cyclin kinase inhibitors block phosphorylation of the retinoblastoma protein by cyclin and cyclin-dependent kinases, allowing hypophosphorylated Rb protein binding to transcription factor E2F or directly suppressing c-myc (Laiho *et al.*, 1990; Li *et al.*, 1997). The growth inhibitory effects of TGF-β are mediated primarily through TGF-β -mediated SMADs activation. Mutations in either TGF-β receptors or downstream components such as SMADs can result in loss of responsiveness to TGF-β signalling, thereby

blocking the growth inhibitory effect of TGF-β on cancer cell growth (Markowitz & Roberts, 1996; Forrester *et al.*, 2005; Biswas *et al.*, 2008). For example, in one study, restoration of TGFBR2 expression in an RII-deficient cancer cell line reduced its tumourigenic potential (Wang *et al.*, 1995). Another convincing line of evidence supporting the tumour suppressor function of TGF-β signalling is that overexpression of TGF-β1 can suppress mammary tumour formation (Pierce *et al.*, 1995).

The loss of TGF-β receptor or SMAD function accounts for only a relatively small proportion of cases in which tumour cells become resistant to TGF-β mediated growth inhibition. More often, loss of TGF-β growth-inhibitory responsiveness in cancer cells occurs following changes in cellular phenotype and the surrounding microenvironment. At some point during the development and progression of malignancies, TGF-β switches to stimulate the proliferation of a number of epithelial-derived cancer cells acting as a tumour promoting factor by building a positive environment for tumour cell growth and survival. For example, TGF-β can enhance tumourigenesis by stimulating the proliferation of mesenchymal cells, increasing ECM (extracellular matrix) production and accelerating migration (Ellenrieder *et al.*, 2001; Zavadil & Bottinger, 2005). Advanced human tumours often become resistant to TGF-β induced growth inhibition and even secrete elevated levels of TGF-β (Derynck *et al.*, 2001). A study in a model of breast cancer cell lines further demonstrated that TGF-β switched from tumour suppressor in the early stage to a tumour promoter in the late stage of cancer (Tang *et al.*, 2003).

Aberrant expression of TGF-β signalling has been observed by microarray analysis of NPC (Sriuranpong *et al.*, 2004; Zeng *et al.*, 2007). Earlier studies revealed that NPC

patients had significantly higher TGF-β1 levels in serum than did controls. Moreover, the elevated TGF-β1 was closely associated with advanced stage, recurrence and survival of NPC patients (Xu *et al.*, 1999). Although the function of TGF-β signalling in NPC carcinogenesis still remains to be elucidated, this finding suggests it might act as a tumour promoter contributing to development and progression of NPC. Further studies are required to understand better its role in NPC.

1.4.4.3 The Wnt signalling pathway

The Wnt signalling pathway has a central role in embryogenesis and in adult tissue homeostasis (Logan & Nusse, 2004; Clevers, 2006). Wnt signalling can be subdivided into the canonical Wnt/β-catenin and the non-canonical Wnt signalling pathway. Non-canonical Wnt pathways transduce Wnt signalling either to the RhoA and JNK pathway or to the Ca^{2+}-releasing pathway involving diverse functions such as cochlear hair cell morphology, heart induction, tissue separation, as well as independent roles in both development and tumourigenesis in vertebrates by binding to Frizzled (FZD) receptors (Veeman *et al.*, 2003). The canonical Wnt pathway is the best understood Wnt pathway, given its frequent deregulation in epithelial cancers. The canonical Wnt ligands, such as WNT3A, regulate the stability of the transcription cofactor β-catenin which co-operates with Tcf/Lef transcription factors to regulate expression of a wide range of target genes such as CCND2 and MYC. Abnormal activation of the Wnt/β-catenin signalling pathway is associated with a number of human diseases including various types of human cancer (Giles *et al.*, 2003). As the general outline of the Wnt/β-catenin signalling pathway has been established, we will focus on this pathway in the following.

Wnt signalling is initiated by binding with two distinct cell surface receptors and inducing a ligand-receptor complex formation. The first receptor is a member of the FZD group of proteins, which are seven-span transmembrane receptors, and the second is the low-density-lipoprotein receptor-related proteins (LRP)-5 and -6. The interaction of WNTs with FZD receptors can be modulated by a number of secreted factors, which act as antagonists by binding either to Wnts or LRP receptors. Dickkopf (DKK) is one of the secreted proteins structurally distinct from WNTs, which can block Wnt signalling by binding with LRP6 receptor (Mao *et al.*, 2001). In the absence of antagonists, WNT ligand binding to receptors results in hyperphosphorylation of Dishevilled (DVL), which inhibits the activity of GSK3β and recruits AXIN to the plasma membrane. GSK3β substrates are generally functionally inhibited by the activation of GSK3β, as is the case for one of its substrates, β-catenin (CTNNB1). β-catenin undergoes ubiquitination and degradation after phosphorylation by GSK3β (Clevers, 2006). The β-catenin degradation complex consists of GSK3β, AXIN and Adenomatous polyposis coli (APC). AXIN and APC form a structural scaffold that allows GSK3β to phosphorylate β-catenin in the absence of Wnt signalling. When Wnt signalling is present, GSK3β is phosphorylated, inhibiting β-catenin phosphorylation and its subsequent degradation. Thus, the stabilised β-catenin accumulates in the nucleus and complexes with the DNA binding transcription factors (TCF/LEF) to enhance the expression of a specific subset of genes in determining cell fate and proliferation (Giles *et al.*, 2003; Huang & He, 2008).

More recent gene expression profiling demonstrates that expression of several central components engaged in the Wnt pathway are abnormally regulated, such as

upregulation of WNT5A, FZD7 and downregulation of AXIN2, indicating that dysregulation of the Wnt signalling pathway might be a key event in NPC tumourigenesis (Sriuranpong *et al.*, 2004; Zeng *et al.*, 2007). This has also been supported by the observation of constitutive activation of Wnt signalling and silencing of WIF-1 (Wnt inhibitory factor-1) in NPC cell lines (Lin *et al.*, 2006b). Although the Wnt pathway is involved in a wide range of biological functions including directing cell proliferation, the function of its constitutive activation in NPC tumourigenesis is still poorly understood. Therefore, a greater understanding of this pathway in NPC is likely to contribute to NPC diagnosis, treatment and prognosis.

1.5 A possible model for NPC pathogenesis

The development and progression of NPC is a multi-step process and may take a long time. Although the molecular basis is still unclear, environmental factors (e.g. intake of preserved food, exposure to various carcinogens), EBV infection and genetic susceptibility are believed to be three major contributors. To understand the process of NPC tumourigenesis, particular focus has been put on early lesions of the nasopharynx. As inflammation and infection are very common in the upper respiratory tract, mild dysplasia can usually be detected in normal nasopharyngeal tissue. This is a reversible lesion whereas precancerous lesions such as severe dysplasia and carcinoma *in situ* are irreversible changes. The precancerous lesions are rarely detected in routine examination of nasopharyngeal biopsies. This may be due to the fact that the process of transition from precancerous lesions to an NPC appears to be quick, probably as a result of the contributions of various tumour-promoting factors (e.g. some genetic changes, EBV infection as well as continuous environmental carcinogens).

Despite limited investigations from early events of NPC, genetic changes and EBV infection in precancerous lesions have been documented in several studies (e.g. deletions of 3p and 9p, overexpression of BCL-2, and activation of telomerase). LOH analyses in normal nasopharyngeal epithelia, dysplastic lesions and NPC cases from endemic and non-endemic areas reveal that a high frequency of LOH of 3p and 9p occurs not only in precancerous lesions and NPC cases but also in normal nasopharyngeal epithelia, suggesting that LOH of 3p and 9p are early events in NPC development. The observation that normal epithelial cells from high-risk regions show significantly higher incidence of 3p and 9p LOH than those from low-risk regions indicates that exposure to specific environmental factors in endemic areas may contribute to these genetic changes (Chan *et al.*, 2000; Chan *et al.*, 2002). The loss of 3p and 9p is closely associated with loss of function of RASSF1 and CDKN2A which will disturb cell cycle progression and result in unlimited cell proliferation. The findings that EBV infection is present in early high-grade dysplastic lesions or carcinoma *in situ* of the nasopharynx but absent either in normal nasopharynx or in low-grade dysplasia, suggest that EBV infection may be important for driving the malignant transformation of nasopharyngeal epithelial cells (Pathmanathan *et al.*, 1995). Expression of latent EBV genes such as LMP1, LMP2A and EBNA1 will lead to abnormal regulation of a number of signalling pathways, for example, the NFκB, and the TGFβ pathways that are involved in regulation of cell apoptosis and proliferation. Oncogene activation including BCL-2 overexpression and telomerase activation has also been observed in a high proportion of dysplastic lesions, suggesting that their functions in antiapoptosis and cell immortalisation occur from the early stages and contribute to NPC development (Sheu *et al.*, 1997).

Following these genetic alterations and EBV infection in precancerous lesions of the nasopharynx, multiple genetic changes are accumulated in the later stage of NPC development, such as deletions of 11q, 13q, 14q and 16q, and gains of 3q, 8q and 12q. These genetic aberrations are correlated with more TSG inactivation and oncogene activation (e.g. inactivation of THY1, ATM, TSLC1 and E-cadherin, and activation of Cyclin D1, PIK3CA and LTβR) that will either speed up NPC development or contribute to NPC invasiveness and metastasis. A possible model for NPC pathogenesis has been proposed and is represented in Figure 1.3.

1.6 Aims and objectives

NPC tumour cells carry a number of genetic abnormalities and exhibit expression changes in a wide variety of cellular genes as well as components of signalling pathways. Therefore, identification of these aberrations is critical for understanding the molecular basis of this disease. The aim of this study was to examine chromosomal aberrations using SNP array analysis, and to characterise cellular gene expression patterns using expression microarray analysis in NPC tumours. For doing this, frozen samples from 21 NPC biopsies and 4 normal epithelia, alongside the NPC cell line C666-1 were used. The DNA copy number and expression analyses were carried out in the same 13 NPC samples, thus, it is possible to assess the relationship between gene expression level and DNA copy number in the same sample set. The validation of array data was undertaken by using standard techniques such as q-PCR, RT-PCR and immunohistochemistry staining analysis.

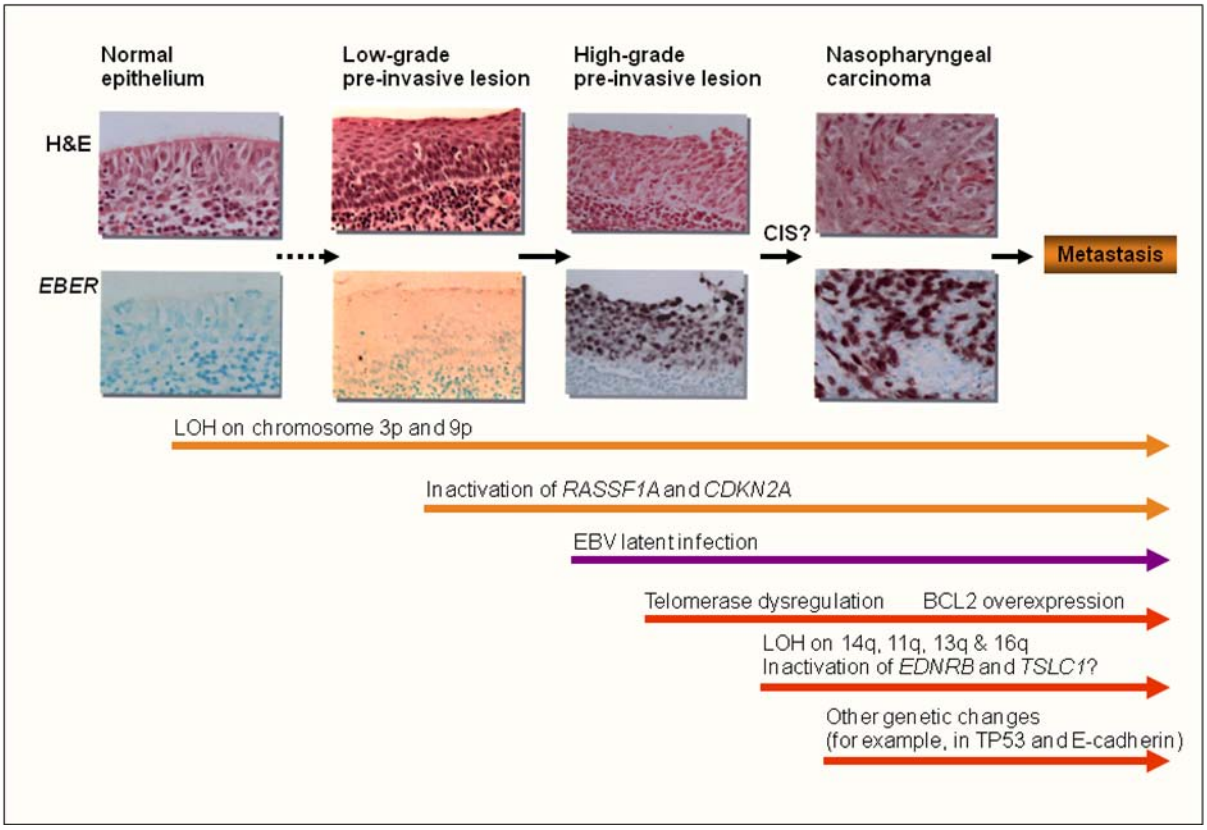

Figure 1.3: A possible model for NPC pathogenesis.

A possible model of NPC pathogenesis is proposed in the above scheme. Loss of heterozygosity (LOH) of 3p and 9p occurs early in the pathogenesis of NPC, possibly as a result of exposure to environmental cofactors. This leads to low-grade preinvasive lesions that, after additional genetic and epigenetic events become susceptible to EBV infection. Many more genetic changes are then accumulated, which act together with environmental and EBV cofactors, resulting in development and progression of NPC.

Figure reproduced from: Lawrence S. Young & Alan B. Rickinson
Epstein–Barr virus: 40 years on
Nature Reviews Cancer 4: 757-768 (2004)

The C666-1 cell line is the only line used in the array analysis. The gene expression pattern in C666-1 cells and in authentic NPC tumour samples can be analysed and compared. This would allow us to assess whether the C666-1 cell line is a good model to represent authentic NPC. It was hoped that the information obtained from array analysis would allow us to develop *in vitro* model systems for more detailed functional investigations of NPC pathogenesis.

CHAPTER 2

Materials and Methods

2.1 Microarray analysis

2.1.1 Sample preparation

2.1.1.1 Frozen tissue collection and selection

In all instances, local ethical rules applicable at the site and date of collection were followed. The work was approved by South Birmingham Research Ethics Committee, reference numbers H1207/95 and 06/Q2702/50.

The snap frozen biopsies diagnosed as NPC (undifferentiated, non-keratinising carcinoma) were obtained from the Associated Hospitals of Guangdong Medical College, Zhanjiang, China; Queen Mary Hospital, Hong Kong; Institut Gustave Roussy, Villejuif, France and Oran Hospital, Algeria. The biopsies were frozen immediately in liquid nitrogen with or without optimal cutting temperature compound (OCT) after isolation from patients. All the samples had concurrent formalin fixed material which was used and retained by local pathologists for diagnosis. Samples were transported on dry ice and stored in liquid nitrogen until used. A total of 21 frozen samples were used for array analysis. 17 samples that showed good quality of morphology and well-defined islands of tumour cells with minimal numbers of infiltrating lymphocytes were selected as tumour samples for array analysis. 4 biopsies were used as normal controls for expression array analysis, among them, 3 were chosen from the transported frozen samples that had sufficient areas of normal epithelium but without showing any tumour tissues. Another normal control was derived from tonsil tissue that contained an extensive region of stratified squamous epithelium. Except for gender and ethnic origin, no further patient or case information was available. One NPC cell line, C666-1, and 12 tumour biopsies were used for both

SNP array and expression array analysis, 2 tumour samples were used only for SNP array analysis, and 7 biopsies (3 tumours and 4 normals) were used only for expression array analysis. The EBV status of tumour biopsies was determined by PCR using BamHI-specific primers (Section 2.2.4). The biopsies and their information are listed in Table 2.1.

Table 2.1: Frozen biopsies used for array analysis

Designation	Definition	Origin	Patient Ethnicity	Gender	EBV Status
XY5	T	Guangdong	Cantonese	M	+
XY6	T	Guangdong	Cantonese	F	+
XY8	T	Guangdong	Cantonese	M	+
XY23	T	Guangdong	Cantonese	M	+
125855	T	Hong Kong	Cantonese	F	+
173570	T	Hong Kong	Cantonese	M	+
68(8)	T	Hong Kong	Cantonese	M	+
MDIG	T	France	Italian	M	+
MKAV	T	France	Italian	M	+
MKEC	T	France	Maghreb	M	+
MMAH	T	France	Maghreb	F	-
MOUZ	T	Algeria	Algerian	F	+
DNA only					
XY16	T	Guangdong	Cantonese	M	+
235326	T	Hong Kong	Cantonese	F	+
RNA only					
400(3)	T	Hong Kong	Cantonese	M	ND
YH7	T	Guangdong	Cantonese	F	ND
YH8	T	Guangdong	Cantonese	M	ND
MSTA	N	Algeria	Algerian	U	ND
MBEZ	N	Algeria	Algerian	U	ND
MHAU	N	France	Italian	M	ND
T3	N	UK	UK	U	ND

“DNA only” indicates that only SNP array data were obtained from these biopsies whilst “RNA only” signifies that only expression array data were obtained. T = tumour; N = normal; U = unknown; ND = not determined.

2.1.1.2 Cutting and staining for cryosections

Before being cut, the frozen biopsies transported from liquid nitrogen were kept within the cryotome at -20ºC for approximately 5 minutes, and then fixed in OCT (Tissue-Tek). 8 micron cryosections were cut using a cryotome (CM1900, Leica) and placed onto PALM membrane slides (P.A.L.M. Microlaser Technologies). The sections were then air dried on ice for about 1 minute followed by H&E (haematoxylin and eosin) staining. Briefly, the slides were immersed in ice-cold 75% ethanol for 2 minutes, tapped dry and stained with ice-cold haematoxylin and eosin (9:1) containing 1% NucleoGuard (AmpTec, Hamburg) for 30 seconds. Excess stain was tapped off and the slides were washed in ice-cold nuclease-free water for about 30 seconds, 75% ice-cold ethanol for 1 minute and then 100% ice-cold ethanol for 1 minute. The slides were air dried and kept on ice for microdissection immediately.

2.1.1.3 Laser microdissection and pressure catapulting (LMPC)

LMPC was performed using a PALM Microlaser system (PALM, Microlaser Technology, Bernried, Germany) containing a PALM MicroBeam instrument. Different areas of cells of interest were selected and caught on PALM Adhesive Caps. A minimum of 200,000 μm^2 (mostly between 300,000 to 500,000 μm^2) of cells was obtained for each RNA and DNA extraction, and the purity of target tumour or normal cells collected by PALM was more than 90% in all cases. Immediately, after LMPC, the collected cells in the PALM tubes were processed for RNA extraction and the cells for DNA extraction were kept at -20 ºC until required.

2.1.1.4 Total RNA preparation for expression array

RNA extraction and purification

The RNA from LMPC samples was extracted by using the RNeasy Mini kit (Qiagen) supplemented with N-carrier and NucleoGuard (AmpTec). 100µl of RLT buffer (Qiagen) supplemented with 1µl of N-carrier and 1 µl of NucleoGuard (AmpTec) were placed into each LMPC tube. The tubes were closed with adhesive caps containing LMPC samples, then inverted and incubated at room temperature for 15 minutes. Subsequently, the extracted RNA was cleaned up using a Qiagen RNeasy mini kit with on-column DNase treatment according to the manufacturer's instructions. 100 µl of column-eluted RNA were then collected by ethanol precipitation. 2 µl P-carrier (AmpTec), 10 µl of 3M sodium acetate and 220 µl of ethanol were added and mixed well. The RNA suspension was stored at - 20ºC until used. When required for the next experiment, the RNA suspension was spun in a microcentrifuge for 15 minutes at 13,000 rpm, and the pellet was washed twice with 80% ethanol, then air dried and dissolved in 12 µl of RNase-free water. The purified RNA was used immediately in the next process.

Total RNA extraction from C666-1 cells was as described in Section 2.2.1 and cleaned up as above.

RNA amplification and labelling

The purified RNA was then subjected to three rounds of mRNA amplification, followed by biotin labelling using an ExpressArt TR mRNA amplification Nano kit (AmpTec) and an Affymetrix IVT labelling kit. This experiment was performed by Dr. John Arrand and the detailed process was as described in the manufacturer's manuals.

2.1.1.5 Genomic DNA preparation for SNP array

DNA extraction from LMPC samples

The LMPC cells on PALM adhesive caps were suspended in 100 µl of lysis buffer (10 µl proteinase K (>600 mAU/ml), 50 µl 10% Tween 20, 440 µl TE buffer (10 mM Tris-HCl, 1 mM EDTA, pH 8). The tubes were inverted, sealed with Parafilm and incubated at 55 ºC for 3 hours, followed by shaking vigorously to resuspend any material still sticking to the caps. The samples were briefly spun and incubated at 95ºC for 5 minutes. After adding 4 µl of glycogen (20mg/ml) and 10 µl 3M sodium acetate (pH 5.5), the solution was transferred into a new 1.5 ml eppendorf tube, and then 250 µl of ethanol were added to precipitate the DNA. Subsequently, the samples were mixed well and incubated at room temperature for 2 minutes then centrifuged at room temperature for 15 minutes at 13,000rpm. The sample was washed with 200 µl of 70% ethanol and spun at 13,000rpm for 5 minutes at room temperature, then air dried.

DNA extraction from C666-1 cells was performed by Dr. John Arrand as described previously (Arrand *et al.*, 1983).

DNA amplification

The air dried DNA was subjected to DNA amplification using a Genomiphi V2 DNA amplification kit (GE Healthcare). Following the manufacturer's protocol, for multiple samples a master mix for each of the following steps was prepared. For each reaction, the air dried DNA was resuspended in the mixture of 1 µl of DEPC water and 9 µl sample buffer and incubated at 95 ºC for 3 minutes then cooled down to 4 ºC quickly. In the meantime, a 10 µl amplification reaction was prepared on ice with 9 µl of reaction buffer and 1 µl of enzyme mix. The cooled sample was added to 10 µl of the above reaction mix and incubated at 30ºC for 1.5 hours for amplification. This

was followed by enzyme inactivation by heating to 65 ºC for 10 minutes then cooling to 4ºC. The amplified DNA was precipitated by adding 20 µl water, 4 µl of a solution containing 1.5 M sodium acetate and 250mM EDTA, and 100 µl ethanol. DNA was recovered by centrifugation for 15 minutes at full speed using a microcentrifuge. The pellet was washed with 500 µl ethanol, centrifuged for 5 minutes at full speed, air dried and dissolved in 20 µl reduced TE buffer (10mM Tris, 0.1mM EDTA, pH 8.0). The final solution was stored at 4 ºC until used.

DNA quantity and quality control

The quantity of amplified DNA was measured using a Nanodrop 1000 spectrophotometer (Thermo Scientific). A minimum of 3 µg of DNA was obtained after amplification. Ratios (OD_{260}/OD_{280}) for all the amplified samples were between 1.8 – 1.9. The size of amplified DNA was checked by electrophoresis on a 0.8 % agarose gel. All cases showed a large proportion of DNA larger than the resolving capability of the gel, indicating that this material was greater than 2 kb in length.

2.1.2 500K SNP array protocol

2 x 250 ng of amplified DNA was used for the Mapping 500K SNP array experiment. The mapping 500K system consists of two 250K arrays (Nsp and Sty) that was provided by Affymetrix. All the reagents and protocols used in the 500K SNP array experiment were recommended by the manufacturer. A brief description is given in the following.

For each reaction, 5 µl of diluted DNA (50ng/µl) was added into a master mix containing either NspI or StyI enzyme and incubated at 37ºC for 2 hours then 65 ºC

for 20 minutes. The adaptor-primer NspI / StyI was then ligated to the digested DNA samples at 16 ºC for 3 hours, 70 ºC for 20 minutes. The ligated DNA was diluted and subjected to PCR amplification. The PCR conditions were optimised preferentially to amplify fragments in the range of 200 bp to 1,100 bp. For quality control, the PCR products were run on a 2% agarose gel. The product was purified and concentrated using a vacuum cleanup plate then quantified on a Nanodrop spectrophotometer. 90µg of each product was then fragmented by adding fragmentation reagent, incubated at 37 ºC for 35 minutes and 95 ºC for 15 minutes. The fragmented products were checked on a 4 % agarose gel to ensure that the size was less than 200 base pairs. The fragmented samples were then labelled using DNA labelling reagent. The labelled samples were stored at – 20 ºC until used.

2.1.3 Hybridisation to Affymetrix Arrays

The biotinylated RNA was fragmented and hybridised to Affymetrix Human Genome U133Plus2 Arrays containing nearly 33,000 substantiated human genes according to the Affymetrix protocol (Affymetrix, 2004, GeneChip Expression Analysis Technical Manual). The labelled DNA from C666-1 and LMPC samples was hybridised onto the Mapping 500K Arrays according to the Affymetrix protocol (Affymetrix, 2006, GeneChip Mapping 500K Assay Manual).

All arrays were washed and stained on an Affymetrix FS450 fluidics station then scanned using an Affymetrix GeneChip 3000 7G scanner as described in Affymetrix procedures. GCOS software (Affymetrix) was used for instrument control and data acquisition. All the steps described above can be found on the Affymetrix web

site http://www.affymetrix.com. The procedure of hybridisation to Affymetrix Arrays was performed by Ms Sim Sihota.

2.1.4 Microarray data analysis

SNP array data were processed by using GTYPE 4.1 (Affymetrix), analysed by both copy number analysis tool v4 (CNAT v4) and genotyping console v2.1 with default settings. An unpaired analysis was used for calculation of copy number. The reference samples used in the analysis were data from 40 healthy female controls with mixed origins (23 Chinese, 10 Japanese and 7 Utah residents of Central European descent) that were downloaded from the HapMap project (http:// www.hapmap.org/downloads/index.html.en). The physical position of all SNPs on the arrays was mapped according to the Human Genome (Build 35, hg17).

Expression array data were normalised and processed to give expression values using the "log scale robust multi-array analysis" (RMA) protocol (Irizarry *et al.*, 2003) within the "Affy" package of Bioconductor (http://www.bioconductor.org). Statistical analysis for significance and fold-change was performed using Rank Products (RP) analyses with percentage of false positives set to less than 10% (Breitling *et al.*, 2004). Data were also analysed using GCOS (Affymetrix) at the default settings except that the target signal was set to 100. Gene expression heatmaps were generated from the data obtained from the RP analysis using dChip software (Li & Wong, 2001). A sample correlation heatmap was generated with the "heatmap" function of R (http://www.r-project.org) using complete linkage clustering and 1-r (Pearson correlation) as the measure of dissimilarities. The expression array analyses were performed by Dr. Wenbin Wei.

2.2 Molecular biology techniques

2.2.1 RNA extraction

Cells were grown in 75cm^2 tissue culture flasks to approximately 80-90% confluence. Total RNA was extracted using Trizol Reagent (Invitrogen, UK), and the manufacturer's instructions were slightly modified. Briefly, monolayers of cells were lysed by the addition of 7.5ml Trizol reagent and the lysates were scraped and transferred to a 15ml polypropylene screw cap tube (Sarstedt, Germany). Samples were fully homogenised by shaking vigorously for 2 minutes. 1.5ml of chloroform were added, shaken for 2 minutes, and then centrifuged for 30 minutes, 4 ^{o}C at 3,000 rpm. The aqueous phase was transferred to a fresh 15ml polypropylene screw cap tube, and an equal volume of isopropanol was subsequently added, mixed by inversion and incubated at room temperature for 10 minutes to precipitate RNA. The pellet was obtained by centrifugation for 30 minutes, 4^{o}C at 3,000 rpm. The supernatant was carefully removed and the pellet was washed in 75% ethanol overnight at -20^{o}C. The following day, the sample was centrifuged for 10 minutes, 4^{o}C at 3,000 rpm, the ethanol was removed and the pellet was air dried for 5-10 minutes then resuspended in 200µl DEPC treated water.

RNA concentration was determined using a NanoDrop 1000 spectrophotometer (Thermo Scientific) and samples diluted to 1µg/µl using DEPC treated water. RNA was stored at -80°C ready for use.

2.2.2 cDNA synthesis

cDNA was synthesised using Superscript II reverse transcriptase (Invitrogen, UK). For each reverse transcription reaction, 1µg of RNA, 0.5µl of 3µg/µl random primers and DEPC treated water to a final volume of 11µl were added to a PCR tube and incubated at 70°C for 5 minutes to denature any dsRNA, and then cooled to 25°C. Meanwhile, master mixes were prepared by adding (per reaction) 4µl of 5x first strand buffer, 2 µl of 0.1M DTT, 1µl of RNase inhibitor, 1µl of dNTP mix and 1 µl of Superscript II. 9 µl of the above mix were added to each preheated tube and mixed well. The cDNA synthesis was then carried out in a thermal cycler using the programme: 25°C for 10 minutes, 42°C for 1 hour, 90°C for 5 minutes and then hold at 4°C.

2.2.3 Reverse Transcriptase-polymerase chain reaction (RT-PCR)

RT-PCR was performed in a 50 µl reaction mix consisting of 1µl cDNA, 1µl 100pM forward primer, 1µl 100pM reverse primer, 25µl 2x GoTaq Green Master Mix (Promega) and 22µl DEPC treated water. The GoTaq master mix contains Taq polymerase, PCR buffer, 400µM dNTP mix, 3mM $MgCl_2$ and DNA loading dye. PCR conditions were: an initial denaturation at 94 °C for 5 minutes, 35 cycles of amplification at 94 °C for 1 minute, annealing for 40 seconds (variable temperature for different primer sets) and 72 °C for 1 minute, a final extension at 72°C for 10 minutes. The products of RT-PCR were then kept at 4 °C prior to agarose gel electrophoresis.

2.2.4 Polymerase chain reaction (PCR)

PCR reactions and conditions were as described above except for using 200ng of genomic DNA as template rather then cDNA.

The primers used for RT-PCR and PCR were obtained from Alta Bioscience or Sigma-Aldrich. The sequences of primers and their annealing temperatures are presented in Table 2.2.

Table 2.2: Primer list for PCR

Primer Name	Primer Sequence 5'-3'	Annealing Temperature °c	Product Size (bp)
GAPDH Fwd	GCCTCCTGCACCACCAACTG	60	300
GAPDH Rev	GGACGCCTGCTTCACCACCTTCT		
TGFβ1 Fwd	GTTGAGCCGTGGAGGGGAAA	58	386
TGFβ1 Rev	CTGCGTGTCCAGGCTCCAAAT		
TGFβ2 Fwd	AAATGGATACACGAACCCAA	55	250
TGFβ2 Rev	GCTGCATTTGCAAGACTTTAC		
TGFβ3 Fwd	AAGTGGGTCCATGAACCTAA	55	250
TGFβ3 Rev	GCTACATTTACAAGACTTCAC		
TGFβRII Fwd	GCAGTGGGAGAAGTAAAAGAT	56	301
TGFβRII Rev	GGGAGCCGTCTTCAGGAAT		
SMAD2 Fwd	CGAAATGCCACGGTAGAAAT	57	259
SMAD2 Rev	CGGCTTCAAAACCCTGATTA		
SMAD3 Fwd	CCAGCCATGTCGTCCATCC	57	388
SMAD3 Rev	TTTTCCCCAAGCCTGCCCTC		
SERPINE1Fwd	GTGGTCTGTGTCACCGTATC	55	440
SERPINE1Rev	GTAGTTGAATCCGAGCTGCC		
TGFBI Fwd	GGAAGGAGTCTACACAGTCTTT	51	399
TGFBI Rev	CCTCTGGGAAGCCCTGGAAAA		
INHBB Fwd	GCCAGGAGCGCGCGTTTCCGAAATC	55	280
INHBB Rev	CCGCTCGCCCCGCTCAAACAAG		

ACVR2B Fwd ACVR2B Rev	TCCCTCACGGATTACCTCA CCTCCTCAAAAGGCAGCA	56	440
BAM HI-W Fwd BAM HI-W Rev	ACGTAAGCCAGACAGCAGCC TTTGTGTGGACTCCTGGCG	56	114

2.2.5 Agarose gel electrophoresis

PCR products were fractionated and analysed by electrophoresis on 0.8 – 2% w/v agarose gels depending on the size of PCR products. Agarose powder was dissolved in a suitable volume of 1x TBE buffer (Tris-borate-EDTA, 10.8g Tris, 4.5g Boric acid and 0.74g EDTA make up to 1 litre with SDW, pH 8.0) by boiling in a glass conical flask. The boiled solution was cooled by rinsing in tap water. Ethidium bromide was added into the cooled solution to a final concentration of 0.5µg/ µl and mixed gently. The solution was then poured into a sealed casting tray inserted with a gel comb. The gel was left to set for about 1 hour and the tray was placed into a horizontal electrophoresis tank filled with sufficient 1x TBE buffer. After removing the gel comb, a DNA ladder (100bp or 1kb plus, Invitrogen) and the PCR products were loaded into the wells. The samples were allowed to run for about 1 hour at a suitable voltage prior to visualisation of ethidium bromide stained bands using a UV transilluminator.

2.2.6 Quantitative PCR (q-PCR) for determination of gene copy number

DNA copy number predicted by SNP array analysis was verified by q-PCR using an ABI 7500 sequence Detection System (Applied Biosystems, ABI). All the probes and primers were designed by using Primer Express 3.0 software (ABI). The sequences are listed in Table 2.3. Taqman probes were synthesised containing a 5' FAM reporter dye and 3' TAMRA quencher (Eurogentec). 25µl PCR reactions were prepared by

the addition of 12.5 µl of 2 x Taqman Universal PCR Mastermix (Applied Biosystems), 5 µl of a combination of forward and reverse primers, 1 µl of probe (a final concentration of 300nM primers and 200 nM probe in each reaction), 1.5 µl DEPC treated water and 5 µl of genomic DNA containing either 1.32ng or 13.2ng input DNA. A calibrator DNA derived from the X50-7 cell line was serially diluted into 100,000, 20,000, 5,000, 1,000, 200, 50, and 10 copies on the basis of 3.3pg per haploid genome. Each sample was assayed at 2 concentrations in duplicate and calibration was also prepared at the same time in each assay. The PCR conditions consisted of an initial incubation (2 min, 50°C), an activation step (10 min, 95°C) and 40 rounds of amplification (denaturation for 15 s at 95°C, annealing and extension for 1 min at 60°C).

The data were analysed by using 7500 fast system SDS software v1.3.1 (ABI). The Ct value was determined according to the real time changes in fluorescence and a standard curve was then generated from the Ct value of the calibrator DNA. For each target gene, the copy number of the unknown DNA sample was quantified by comparing with the reference gene CYP7A1 for which a DNA copy number of 2 was confirmed by SNP array prediction and previous q-PCR analysis.

Table 2.3: Primer and probe list for q-PCR

Gene	Primer and Probe Sequences 5'-3'
FHIT	Primer Forward: TGGGAGGGAGATGGATTCTTTA Reverse: CTTCTGAGCCTAACCAGCCAAA Probe: TGGACAGACTGGAGGCCAATCTTGTATTTATATTC
IL20RA	Primer Forward: AAGTGTTGGCATCAGTTTTCCA Reverse: GAGAAAATGAAACCTATCTCATGCAA Probe: CTGCACATATAACCCCCATTCCTCCATG
MAP3K5	Primer Forward: GTCAATGATAGCCTTCCACAGTGT Reverse: GAAATGTTCGTTTCACCATGTTCT Probe: CACAGCATCCCTCCCCTGTTTAAAGACA

CDKN2A	Primer Forward: GCGTGAGCTGAGGCAAGAC Reverse: TCCAAAGCTCAGAGCATTCATTT Probe: CTGGTCTCCCGGGCTGAACTTTCTG
FGF20	Primer Forward: CCACTGGTCTAGGTAAGAAATGTGTAAA Reverse: CAAAGACGGAACTCCAAGAGATG Probe: TCTGATGCCTCTTGGACCTGGCG
KIAA1967	Primer Forward: GGGCGGTTCCTGGAGATT Reverse: GAGGAGGGCCCAGAAGAGAT Probe: TTCTCTTTCCCCATAGGCACAGCTTCAA
CLU	Primer Forward: TGGGAGGCGCCGTATTTATA Reverse: TTGGGCGTGAGTCATGCA Probe: CTCGCGCACACACCCCCTTTG
NRG1	Primer Forward: TCTACATCCACCACTGGGACAA Reverse: CCCCTCCATTCACACAGAAAG Probe: TTCTCCTTCTCCGCACATTTTACAAGATGG
IKBKB	Primer Forward: TTGCTTATAGAGTTAGCACGACATCA Reverse: TCCCAGGCCCCACATG Probe: ATGAGCTGGTCACCTTCCCTGACAACG
CYP7A1	Primer Forward: TGATATGTTGGTGGAAAGGATTACTAA Reverse: TAGACGGGTGCTTGTTGAATGT Probe: TCCATCCATTCATGCATCCGTCCATA

2.2.7 q-PCR for determination of gene expression changes

Cellular gene expression changes in C666-1 cells relative to controls cells were determined by q-PCR analysis using commercial Taqman Gene Expression Assay primer and probe mixes purchased from ABI (See Table 2.4). Each 25µl q-PCR reaction was prepared by adding 1µl (50ng) of cDNA, 1.25µl of primers and probe mix for both the target gene and the reference gene (GAPDH), 12.5µl of 2x Taqman Universal PCR Mastermix and 9µl of PCR H_2O. Each reaction was assayed in triplicate and analysed using 7500 fast system SDS software v1.3.1. The Ct value was generated according to the real time changes in fluorescence. The average Ct was calculated for both target and reference gene and the dCt ($Ct_{target} - Ct_{GAPDH}$) was

obtained. The ddCt ($dCt_{C666-1} - dCt_{control}$) was then determined and fold change of gene expression in C666-1 cells was calculated by using the formula 2^-ddCt.

Table 2.4: Taqman primer and probe mixes

Gene	ABI QPCR Primer/Probe Reference Number
GAPDH	4310884E
E2F5	Hs00231092_ml
BMP2	Hs00154192_ml
MAPK1	Hs01046830_ml
NEDD9	Hs00610590_ml
HES1	Hs00172878_ml
ID1	Hs00357821_ml
CLDN1	Hs01076359_ml

2.3 Immunohistochemistry staining (IHC)

2.3.1 Tissue array construction

The formalin-fixed, paraffin-embedded blocks were obtained from the archives of the Pathology Department, Cancer Center, Sun Yat-Sen University (Guangzhou, Guangdong, China) during 2007. The matching H&E-stained slides were reviewed and screened, and samples containing both NPC tumour and adjacent nasopharyngeal mucosae were chosen for tissue microarray construction. Each patient case was represented by a mean of 4 cores with 2 tumours and 2 normal nasopharyngeal mucosae taken using a 0.6-mm punch. In total, 40 cases were used to construct two TMAs with 176 cores. The final numbers assessed were slightly variable for different markers due to failure of taking target tissues and additional losses during block trimming and staining procedures.

2.3.2 IHC staining in formalin fixed paraffin embedded (FFPE) sections

FFPE sections were deparaffinised in xylene and rehydrated through ethanol to distilled water, then incubated with 3% hydrogen peroxide for 15 minutes to quench endogenous peroxidase. Antigen retrieval was performed using the agitated low temperature epitope retrieval (ALTER) method (Reynolds *et al.*, 2002)**,** or by heating in low pH retrieval buffer (Vector Laboratories) for 20 minutes at 880W in a microwave oven. Sections were then rinsed with PBS (see Section 2.5.2), primary antibody was added and incubated for 60 minutes at room temperature. After three brief washes with PBS containing 0.05% Tween 20 a peroxidase-based secondary antibody (Dako EnVision™ Detection System, Denmark; or Anti-goat Ig, Immpress) was added and incubated for 30 minutes at room temperature. The final peroxidase-labelled complex was visualised using diaminobenzidine (DAB). The tissue sections were counterstained with hematoxylin, dehydrated, and mounted with coverslips. When staining for individual genes, negative control included omission of primary antibody whilst positive controls included tissues of previously documented positive immunoreactivity.

The antibodies used in IHC are listed in Table 2.5.

Table 2.5: Primary antibody list for IHC staining

Primary antibody	Species	Dilution	Supplier
MSH3(S-16)	Goat	1:50	Santa Cruz
TGFBI(HPA008612)	Rabbit	1:150	Sigma
ITGA2(CD49b,611016))	Mouse	1:100	Becton Dickinson
CLU	Mouse	1:6000	Santa Cruz
EZH2	Mouse	1:200	Cell Signalling
JAK1(sc-1677)	Mouse	1:100	Santa Cruz

SKIL(HPA013920)	Rabbit	1:800	Sigma
WNT5A	Rabbit	1:50	Santa Cruz
KLF4(AF3640)	Goat	1:100	R&D
LCN2(HPA002695)	Rabbit	1:100	Sigma
ANXA1(HPA011271)	Rabbit	1:800	Sigma
TNFAIP3(HPA002116)	Rabbit	1:20	Sigma
CD44 (v6)	Mouse	1:200	R&D Systems
CTNNB1(610153)	Rabbit	1:400	Becton Dickinson
TGFBR1 (sc-398)	Rabbit	1:200	Santa Cruz
TGFBR2 (sc-220)	Rabbit	1:150	Santa Cruz
SMAD2(51-1300)	Rabbit	1:300	Zymed
SMAD4 (OP111)	Mouse	1:50	Cell Signalling
SP1 (sc-59)	Rabbit	1:400	Santa Cruz
SERPINE1 (sc-8979)	Rabbit	1:300	Santa Cruz
ID1 (sc-448)	Rabbit	1:300	Santa Cruz
BTG1(HPA005972)	Rabbit	1:50	Sigma
APC(SC-895)	Rabbit	1:25	Santa Cruz
PTCH1 (ab53715)	Rabbit	1:200	Abcam
SHH (ab73958)	Rabbit	1:20	Abcam

2.3.3 IHC staining for frozen sections

8 micron cryosections were cut, air dried and fixed in 10% formalin for about 20 minutes. The sections were then incubated in 3% hydrogen peroxide for 15 minutes, followed by antigen retrieval in low pH buffer for 20 minutes (High power, microwave). The remaining procedures were the same as for FFPE samples.

2.3.4 IHC scoring

For each tissue core on the tissue array, a semiquantitative scoring system was used for evaluation of IHC staining, in which both intensity of staining and percentage of positive cells of interest were represented. A staining index (values 0-9) was obtained by multiplying the intensity of staining (negative = 0, weak = 1, moderate =2, or strong = 3) by the proportion of positive cells of interest (≤30% = 1, 30% -70% = 2, >70% = 3). The expression values for tumour and normal controls of each individual case were obtained from the mean values of two representative cores.

2.4 *In situ* hydridisation (ISH)

EBERs staining was performed in the tissue arrays using digoxigenin-labelled probes. All the solutions and containers used in the experiment were sterile. Briefly, the sections were deparaffinised in xylene and dehydrated in absolute ethanol twice for 5 minutes then washed in PBS buffer for 5 minutes. The slides were then treated with 100 µl of pronase E (10mg/ml stock pronase E diluted at 1:160 in DEPC water) per slide for exactly 5 minutes at room temperature. After washing with PBS and dehydration in ethanol, a gene frame (AB gene house) was placed around the tissue section. Meanwhile, the digoxigenin-labelled sense and antisense probes to EBERs (Barletta *et al.*, 1993) were heated at 80ºC for 30 seconds and diluted with hybridisation solution at 1:100. A suitable amount of the above probe was applied to the slides (sense probe to EBERs used as a negative control), sealed with a siliconised cover slip and incubated at 50º C overnight. The following day, the cover slips and gene frames were removed and the sections were washed once with 2 x SSC for 5 min,

twice with 0.1 x SSC for 5 min and once with PBS. This was followed by incubation in diluted blocking serum according to the manufacturer's protocol (Vectastain universal quick kit) for 10 minutes and mouse anti-digoxigenin antibody (diluted at 1:1000 with PBS) for 1 hour. After washing with PBS, the diluted secondary antibody (Vectastain universal quick kit) was added to the slides and incubated for 10 minutes, washing with PBS again. The diluted tertiary complex was then added, incubated for 5 minutes then washed with PBS. Finally, the slides were visualised using diaminobenzidine (DAB), counterstained with hematoxylin, immersed in ethanol, and mounted with coverslips.

2.5 Tissue culture

2.5.1 Basic media

RPMI 1640 (1X) liquid supplemented with L-glutamine (2mM) and adjusted to pH 7.0, was purchased from GIBCO Ltd and supplied in 500ml sterile bottles. Medium was stored at 4^{o}C.

Keratinocyte serum-free (1X) liquid supplemented with 25mg of Bovine pituitary extract (BPE) and adjusted to pH 7.0, was purchased from GIBCO Ltd and supplied in 500ml sterile bottles. Medium was stored at 4^{o}C.

2.5.2 Other sterile solutions and supplements

Foetal bovine serum (FBS) pre-screened for virus/mycoplasma contamination was purchased in sterile 500ml bottles from GIBCO Ltd. FBS was aliquoted into 50ml sterile bottles and stored at -20^{o}C.

Penicillin/streptomycin antibiotic solution (5,000 units/ml penicillin-G and 5mg/ml streptomycin) was purchased from Gibco Ltd, filter sterilised and used at 5ml/500ml medium.

Trypsin (1x) supplied in 100ml sterile bottles containing 2.5g/L trypsin (0.25%) and 0.38g/L EDTA was purchased from GIBCO Ltd. Trypsin was aliquoted and stored at -20ºC.

Phosphate buffered saline (PBS) (8g/L NaCl, 0.2g/L KCl, 1.15g/L Na_2HPO_4, 0.2g/L KH_2PO_4) was purchased in tablet form Oxoid Ltd. 10 tablets were dissolved in 1L of distilled water, and 500ml aliquots were sterilised by autoclaving at 115ºC for 10min.

Fibronectin derived from human plasma was purchased at a concentration of 1mg/ml from Sigma-Aldrich and stored at 4^{o}C. To coat tissue culture vessels, the stock solutions were diluted into 10ng/ml in sterile PBS.

Opti-MEM reduced-serum medium (1X) liquid was purchased from Invitrogen and supplied in 500ml sterile bottles. Medium was stored at 4^{o}C.

2.5.3 Cell lines and their media

C666-1 is an EBV-positive NPC cell line (Cheung *et al.*, 1999).

Medium: 10% FBS, 2mM glutamine and antibiotics in RPMI 1640. Cells should be plated into vessels previously coated with 10ng/ml fibronectin by incubating at 37^{o}C for at least 1 hour or 4^{o}C overnight.

OKF6 tert-1 is a human immortalised normal oral epithelial line (Peng *et al.*, 2006).

Medium: 2mM glutamine and antibiotics in Keratinocyte serum-free medium.

2.5.4 Maintenance of cell lines

The cell lines were maintained in incubators at 37^{o}C supplied with 5% $CO_{2.}$

Adhesive cells grown in 75 cm^2 flasks were fed twice a week and split when they reached 90-95% confluence. The cells were washed in PBS and trypsinised with 5ml of 1x trypsin. The cells were returned to the incubator until they dislodged from vessels, usually spending 5-10 minutes depending on cell types. Cells were recovered in 10ml of complete growth medium containing serum to inactivate the trypsin and pelleted by centrifuge at 1500rpm for 5 minutes. The supernatants were removed. Cells were resuspended in fresh medium, counted using a haemocytometer, and plated out at a density required by the experimental design.

2.5.5 Cryopreservation of cell lines

Adhesive cells were trypsinised and pelleted as described as above. Pellets were resuspended in freezing medium containing 50% complete medium, 40% FCS and 10% DMSO (Dimethyl sulphoxide, Fisher Scientific) pre-chilled at -20^{o}C for 10 minutes. Typically, 1x10^{6} cells were resuspended in 1ml freezing medium and transferred to cryotubes (Nunc). The cryotubes were placed into a Mr Frosty (Nalgene) and stored at -80^{o}C overnight allowing cells to freeze gradually. The following day, the cryotubes were transferred to a liquid nitrogen freezer (-140^{o}C) for long-term storage.

Cells from frozen ampoules were recovered by thawing rapidly in a 37ºC water bath. Cell suspensions were gently transferred into a sterile universal tube (Sterlin) containing warm normal growth medium. The suspensions were spun at 1500rpm for 5 minutes. The cell pellets were resuspended in normal growth medium and seeded into a tissue culture flask.

2.6 Immunoblotting

2.6.1 Solutions

Resolving Gel Buffer

500ml solution of 1.5M Tris requires 90.86g Tris dissolved in SDW, pH 8.8 with concentrated HCl.

Stacking Gel Buffer

500ml solution of 0.25M Tris requires 15.14g Tris dissolved in SDW, pH 6.8 with concentrated HCl.

1x Running Buffer

A 10 x solution requires 30g Tris, 144g glycine, and 10g SDS. Make up to 1 litre with SDW, pH 8.3-8.8. Dilute 1/10 with SDW prior to use.

1x Transfer Buffer

10 litres requires 30g Tris and 144g glycine dissolved in 8 litres of SDW and 2 litres of methanol.

10x Tris Buffered Saline-Tween (TBS-T)

10 litres requires 60.5g Tris, 200g NaCl, 25ml Tween-20, pH 7.6 with concentrated HCl and made up to 2.5 litres with SDW.

*5% Milk blocking buffe*r

5% (w/v) powdered non-fat milk dissolved in TBS-T.

*5% bovine serum albumim (BSA) blocking buffe*r

5% (w/v) powdered BSA dissolved in TBS-T and filtered.

Stripping Buffer

100 mM Tris-HCl pH 6.8, 2% (w/v) SDS, 50mM 2-mercaptoethanol

2.6.2 Preparation of protein extracts and determination of protein concentration

Cells were washed once in PBS and lysed in 100µl protein lysis buffer containing protease inhibitors (Novagen). The cell lysates were collected using a cell scraper (Sarstedt, Germany) and transferred into pre-chilled eppendorf tubes. The samples were mixed well and kept on ice for a minimum of 30 minutes. Following sonication for 15 seconds, the samples were centrifuged at 13,000rpm for 5 minutes at 4ºC to pellet cell debris. The supernatants were transferred to new eppendorf tubes and protein concentrations were determined using a Bradford Protein Assay kit. Briefly, 10µl BSA standards were prepared in distilled water at concentrations of 100, 200, 300, 400 and 500µg/ml, and 10µl of protein samples at a dilution of 1:10 in distilled water were added into a 96-well plate in duplicate. 200µl of Bradford reagent at a dilution of 1:5 in distilled water were then added to each well and incubated at room temperature for 5 minutes. The absorbance at 595nm of the samples was read on a BioTek automated microtitre plate reader. A standard curve was generated and the sample protein concentrations were determined. A minimum of 30µg protein samples used for immunoblotting were diluted at 1:2 in Laemmli sample buffer (Bio-Rad) containing 10% β-mercaptoethanol, boiled at 95ºC for 5 minutes and stored at -20ºC until required.

2.6.3 SDS-polyacrylamide gel electrophoresis (SDS-PAGE)

BioRad apparatus (165-3322) was used for SDS-PAGE. An appropriate percentage resolving gel (5-15%) depending on the size of protein of interest was prepared and poured into the gel cassettes. Once the resolving gel had set, a 4% stacking gel was prepared and gel combs were inserted. Gel combs were removed after the gel had set and the gels were placed into an electrophoresis tank and submerged in running buffer. Equal amounts of protein samples were loaded onto the gel alongside a rainbow protein ladder (Fermentas). Electrophoresis was then carried out at 135V for about 90 minutes.

2.6.4 Western blotting

Following electrophoresis the resolved proteins were transferred to a nitrocellulose membrane (Pall-Life Sciences, 66-485). The gel and membrane were tightly sandwiched between two layers of 3MM filter paper (Whatman, UK) pre-soaked in transfer buffer. The sandwich was placed into a transfer tank filled with transfer buffer and run at 90v for 90 minutes on ice. The membrane was blocked in 5% milk at room temperature for one hour and then incubated at 4ºC overnight in primary antibodies at appropriate dilutions (Table 2.6). The following day, after 3 x 5 minute washes in 1x TBS-T buffer, the membrane was incubated in corresponding HRP-conjugated secondary antibody at room temperature for one hour (Table 2.7). Following a further 3 x 5 minute washes in 1x TBS-T buffer, the antigen-antibody complexes were detected by Enhanced Chemiluminescence **(**ECL, GE healthcare) according to the manufacturer's instructions, wrapped in Saran Wrap and exposed to Hyperfilm (GE healthcare) for an appropriate period of time. The film was developed on a Kodak X-OMAT-1000 Processor.

Table 2.6: Primary antibody list for immunoblotting

Antibody	Species	Dilution	Product Size (kDa)	Supplier
β-actin	Mouse monoclonal	1:5000	42	Sigma
SERPINE1-1	Mouse monoclonal	1:500	47	BD Biosciences (612024)
p21(c-19)	Rabbit polyclonal	1:500	21	Santa Cruz (sc-397)
pSMAD2 (Ser465/467)	Rabbit polyclonal	1:1000	58	Cell Signalling Technology (3101)

Table 2.7 Secondary antibody list for immunoblotting

Antibody	Dilution	Supplier
Anti-Mouse peroxidase	1: 1000	DAKO
Anti-Rabbit peroxidase	1: 1000	DAKO

2.7 Immunofluorescence (IF) staining

Cells were tryspinised and resuspended in normal growth medium at a concentration of 6 x 10^5/ml. 1.5 - 3 x 10^4 cells were seeded onto each dot of sterile teflon coated slides (Henley) in a sterile petri dish with 1ml of PBS, and then left to adhere for 24 hours at 37^{o}C. Cells were then washed in PBS and fixed in 4% PFA pH 7.4 (20g PFA in 500ml PBS) for 10min. Subsequently, the fixed cells were permeabilised in 0.5% Triton X-100 (in PBS) for 5min and blocked in 50µl of 20% HINGS (heat inactivated normal goat serum diluted in PBS) for at least 1hr. 25µl Primary antibody (diluted at the appropriate concentration in 20% HINGS) was added to each microdot and incubated at 37^{o}C for 1hr or at 4^{o}C overnight (Table 2.8). Following 3x 5min washes in PBS, the cells were incubated in 25 µl AlexaFluor488 or AlexaFluor594-conjugated goat anti-rabbit immunoglobulin (Molecular Probes, diluted in 20%

HINGS at 1:1000) for 1hr at room temperature in the dark. After 3x 5min washes in PBS, the slides were then mounted with DABCO (1,4-diazabicyclo[2.2.2]octane) anti-fading agent for visualisation by fluorescence microscopy.

Table 2.8: Primary antibody list for IF staining

Primary antibody	Species	Dilution	Supplier
PTCH1 (ab53715)	Rabbit	1:50	Abcam
SMO (ab38686)	Rabbit	1:100	Abcam
GLI1 (ab92611)	Rabbit	1:50	Abcam

2.8 Transfection of plasmid DNA into Mammalian cells

Liposome transfection of cultured eukaryotic cells was carried out using lipofectamine LTX and plus reagent (Invitrogen, UK). Briefly, 24-well plates were seeded at a density of 0.5-2x10^5cells/well and allowed to adhere overnight. The following day, the cells that reached 50-80% confluence were washed once with Opti-MEM and replaced with 500µl of fresh growth medium. For each transfection, a suitable amout of plasmid DNA was diluted in 100µl Opti-MEM. 1µl of plus reagent was then added and DNA complex was formed by incubating at room temperature for 5 minutes. 2 µl of lipofectamine LTX were added directly to the diluted DNA complex and incubated at room temperature for 30 minutes. The lipid–DNA transfection mix was added into each well and mixed by gentle swirling of each plate before being returned to the incubator. After 4-6 hours, the transfection mix was removed and replaced with normal growth medium. The cells were incubated at 37ºC with 5% CO_2 for 24 hours or 48 hours until further treatment.

2.9 Stimulation of cells with human recombinant cytokines

Cells were seeded at a suitable density in appropriate vessels depending on the nature of the experiments. 16 hours (for western blotting) or 5 hours (for luciferase reporter assays) prior to stimulation, the medium was replaced with serum free medium to reduce the background level of cytokines that are naturally present in serum. The cells were then stimulated in the serum free medium with the appropriate concentration of recombinant cytokine for varying lengths of time depending on the individual experiment, or left unstimulated as a control.

Table 2.9: Human recombinant cytokines

Cytokine	Supplier
Recombinant Human Transforming Growth Factor Beta 1 (TGFβ1)	Peprotech (100-21)
Recombinant Human activin A	Peprotech (120-14)
Recombinant Human Sonic Hedgehog (SHH)	Peprotech (100-45)

2.10 Luciferase reporter assays

Reporter assays were carried out using the Dual-Luciferase Reporter Assay System (Promega, UK) whereby the activities of both firefly (*Photinus pyralis*) and Renilla (*Renilla reniformis*) luciferase can be measured from the same sample sequentially. Firefly luciferase was used to measure the activity of the reporter of interest, whilst Renilla activity provided an internal control for transfection efficiency and cell viability. In triplicate, cells were plated in 24-well plates and grown in normal growth medium until 70% confluence was achieved. Cells were co-transfected with 50ng of a luciferase reporter construct and a plasmid expressing Renilla luciferase (See Table 2.10) for 24 hours using lipofectamine LTX and plus reagent as described in section 2.8. All wells were then serum starved for 5 hours, and incubated in the presence or absence of a serial dilution of either TGF-β1 or activin A cytokine, or SHH (2µg/ml)

for 16 hours. Cells were washed with PBS and wells drained completely prior to the addition of 120µl of 1x passive lysis buffer (PLB; Promega, UK). Complete lysis and homogenisation of samples was achieved by using a cell scraper. 20µl of sample from each well were added into a 96 well plate. Using the luminescence setting on a Victor plate reader firefly activity was determined immediately after the addition of 25µl of LARII. 25µl of Stop & Glo was then added to each well to quench the firefly luciferase activity and initiate measurement of the Renilla luciferase. Relative luciferase activity was determined by normalising the firefly luciferase value to that of the Renilla.

Table 2.10: Luciferase reporter constructs used in transfection of Mammalian cells.

Plasmid vector	**Abbreviation**
PAI-1 reporter	p3TP-lux
Smad3 reporter	(CAGA)12
GLI1 reporter	p8xGLI1
Renilla luciferase	p-RL-TK

2.11 Flow cytometry analysis (FACS analysis)

Cells were seeded at a density of 1-4x10^5 into 6cm dishes and grown in normal growth medium for 1 day before treatment. The following day, the cells were washed gently with PBS then serum free medium with or without TGF-β1 (10ng/ml) or activin A (100ng/ml) cytokines was added and the cells were incubated for 5 days. Following treatment, the cells were trypsinised, washed, and resuspended in 500µl PBS. These cells were fixed by adding 500µl of 70% ethanol and stored at -20 ^oC

overnight. The fixed cells were washed, resuspened in 500µl PBS containing 10µg PI (propidium iodide) and 5mg RNase A, and then incubated at 37 ^{o}C for 30 minutes. The cell cycle program was run on a FACS machine (XL-MCL, Beckman Coulter) for at least 20,000 individual events per reaction. Data were extracted and cell cycle analysis was done using Multicycle AV software (Phoenix).

CHAPTER 3

Expression changes in cellular tumour-associated genes

3.1 Introduction

NPC exhibits expression changes in a number of cellular genes. The expression microarray technique allows simultaneous monitoring of the expression of thousands of genes (Russo *et al*., 2003). Thus, identification of differences in the gene expression profile between NPC tumour and normal nasopharyngeal epithelial cells could reveal a variety of functional groups of genes and signalling pathways whose dysregulation may play critical roles in NPC development and progression.

Cellular gene expression profiles in NPC have been investigated in a number of previous studies. Earlier studies used low-density cDNA arrays on NPC biopsies or NPC-derived cells (Fung *et al*., 2000; Xie *et al*., 2000). More recently, advanced technologies such as the development of microdissection and increasingly higher-density microarrays have been widely used in expression profiling of NPC , which revealed aberrant expression of a number of genes involved in a variety of functions such as control of cell growth, survival, and invasion, and signalling pathways including Wnt/β-catenin, TGFβ, and MAPK pathways (Sriuranpong *et al*., 2004; Lee *et al*., 2007; Zeng *et al*., 2007; Liu *et al*., 2009; Zhang *et al*., 2009). PTPRG was identified as a candidate NPC TSG by comparing gene expression in tumourigenic and nontumorigenic NPC chromosome 3 microcell hybrids (Cheung *et al*., 2008). The potential TSG ATM was found to be associated only with EBV-positive cell lines (Bose *et al*., 2009), and downregulation of MHC class I antigen presentation genes is highly correlated with increased EBNA1 expression (Sengupta *et al*., 2006). A

comparison of gene expression profiles in NPC cell lines with or without metastasis revealed that the expression of several transcription factors was associated with NPC progression (Su *et al*., 2010)

In the present study, we compared global gene expression in microdissected cells from 4 normal epithelial samples, and 15 NPC tumour samples that were obtained from high- and intermediate- incidence areas, as well as C666-1 cells. The expression array data identified a large number of differentially-expressed oncogenes, tumour suppressor genes and genes involved in various functional processes and signalling pathways. The differential expression of several genes identified by expression array was verified at the protein level by IHC staining in NPC tumour and normal nasopharyngeal epithelial (NP) cells.

3.2 Sample correlation analysis

16 NPC samples (15 NPC biopsies and 1 NPC cell line, C666-1) together with 4 reference samples from normal epithelial cells were used for global gene expression profiling. The sample information is listed in Table 2.1. The quality of the data from expression arrays is highly dependent on RNA quality and tumour purity. A mixture of stromal cells, extensive lymphoid infiltrate and other non-neoplastic cells within the NPC tumour makes it difficult to obtain pure tumour cells. To overcome the noise of the admixed non-neoplastic cells, LMPC was carried out to collect purified populations of tumour or normal epithelial cells from frozen biopsies. Representative images of LMPC performed in NPC tumour and normal epithelia are shown in Figure 3.1. RNA was extracted from microdissected cells, amplified, labelled and hybridised to Affymetrix Human Genome U133Plus 2.0 microarrays.

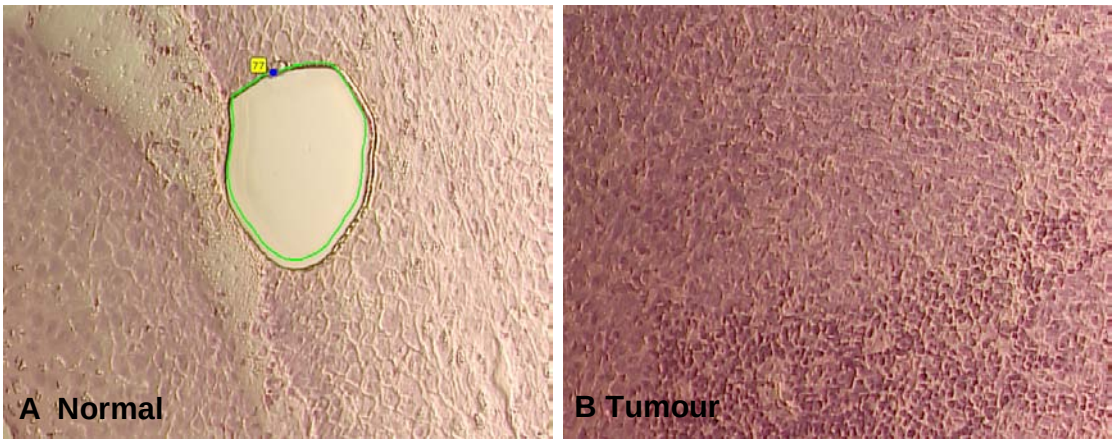

Figure 3.1: Microdissection of NPC tumour and normal epithelial cells. The selected frozen biopsies of NPC tumour and normal epithelia were cut into 8µm sections, stained with H&E then subjected to microdissection. Panel A displays normal epithelium and the cells within the circled area were microdissected. Panel B shows a well-defined island of NPC tumour cells.

As described in Table 2.1, the tumour and normal samples used for expression array analyses are from different geographical origins and contain both genders. To estimate the degree of relatedness between the samples a correlation heatmap was generated by analysing the normalised expression array intensity values of global gene probesets in individual samples (Figure 3.2). The figure indicates that 4 normal samples (MSTA, MBEZ, MHAU and T3) are closely correlated with each other, 13 tumours (12 biopsies and the C666-1 cell line) are tightly clustered with each other but not correlated with the normal controls. 3 tumour biopsies (YH8, 68(8) and XY8) do not correlate with the other 13 tumour samples, with the 4 normal controls or with each other. Taking the above results together: (i) no substantial geographical or gender differences are found between tumour samples; (ii) the C666-1 cell line appears to be a good tumour model to mimic real NPC tumours since it is closely correlated with the other 12 NPC biopsies; (iii) tonsillar epithelium appears to mimic nasopharyngeal epithelium. However, it is unclear why 3 of the NPC tumours do not cluster with the other 13.

3.3 Global gene expression array data analysis

Initially the gene expression array data generated from the 16 NPC samples and 4 normal samples were normalised and processed using RMA and RP to identify differentially expressed genes. The data were then subjected to further hierarchical clustering analysis using dChip software. The heatmap generated from dChip showed a distinct clustering of expression between tumour and normal. The results displayed that a large number of genes were differentially regulated, of which the majority were upregulated (Figure 3.3).

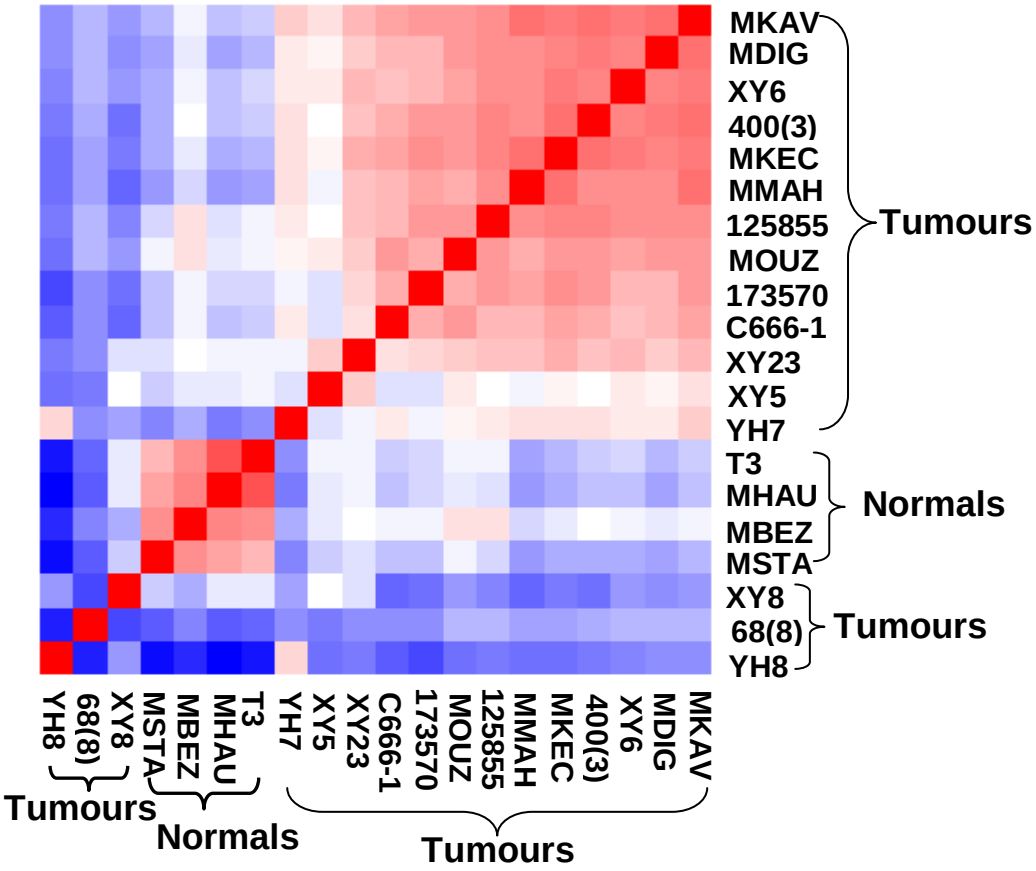

Figure 3.2: Sample correlation analysis. RNA from 15 NPC biopsies, 1 NPC cell line C666-1, and 4 reference samples from normal epithelial cells were used for gene expression profiling. A correlation heatmap was generated from the normalised expression array intensity values of global gene probesets in individual samples. 4 normal samples (MSTA, MBEZ, MHAU and T3) are closely correlated with each other. 13 tumours including 12 biopsies and the C666-1 cell line are tightly clustered with each other but not correlated with the normal controls. 3 tumour biopsies (YH8, 68(8) and XY8) do not correlate with the other 13 tumour samples, the 4 normal controls or each other.

Figure 3.3: Global gene expression profiling.

The expression array data generated from16 tumours and 4 normal controls were normalised and processed using RMA and RP. This identified a number of significantly differentially regulated genes, which were visualised using dChip software for hierarchical clustering analysis. The heatmap shows a distinct clustering of expression patterns between tumours and normal samples. The expression level of each gene in individual sample is colour coded: blue for down-regulation, red for up-regulation, and white for unchanged.

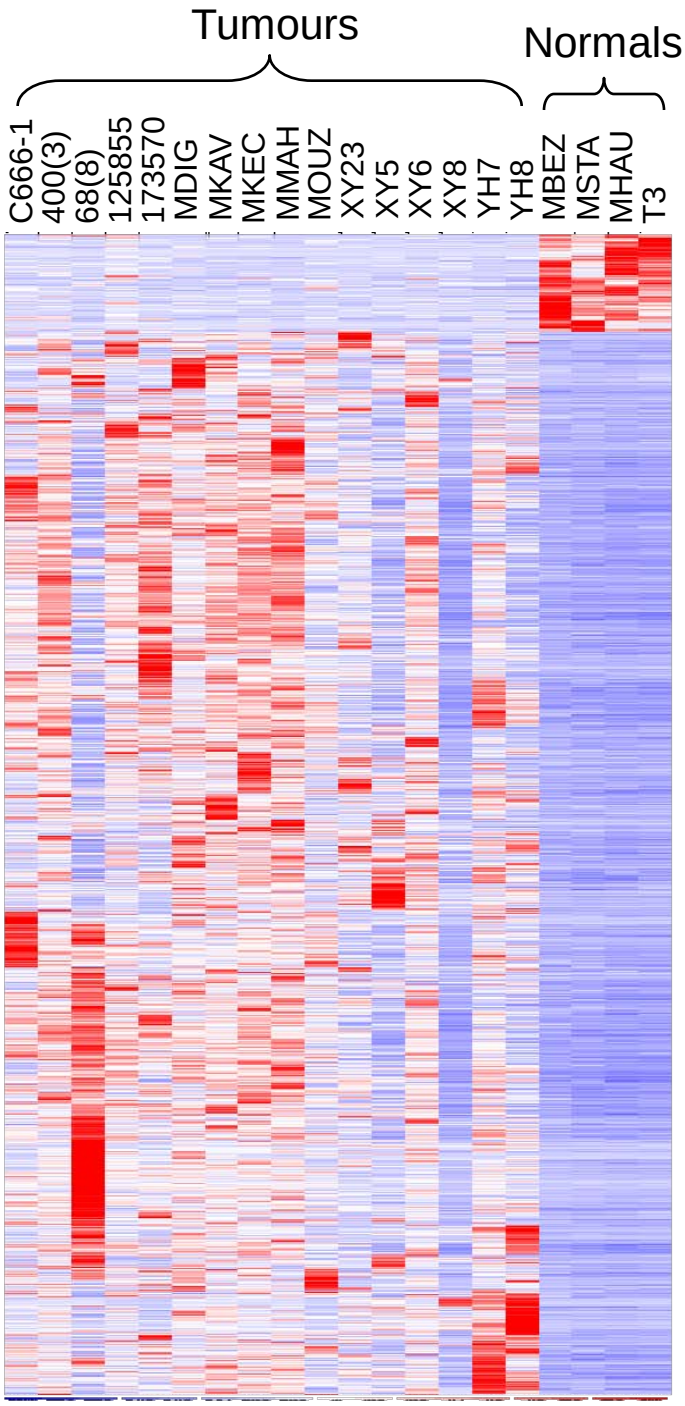
Tumours
Normals
C666-1
400(3)
68(8)
125855
173570
MDIG
MKAV
MKEC
MMAH
MOUZ
XY23
XY5
XY6
XY8
YH7
YH8
MBEZ
MSTA
MHAU
T3

When the data were processed using RP analysis, the differentially regulated genes and the overall fold change in the expression between tumours and normals were determined. However, because this method compares mean expression values it could miss some potential tumour-related genes whose expression changes occurred in only a minority of cases. Thus, the data were also analysed with GCOS taking advantage of the "present/absent" calls that this method provides. If a gene is called as "present" by GCOS, it indicates that the level of gene expression is clearly detected by the expression array, whereas if it is called as "absent", it indicates that the signal of gene expression is too low to be reliable. To define the up- and down- regulated genes the following criteria were used: within individual tumours, a gene was called upregulated if (1) it was called "present" in the sample of interest and (2) its GCOS normalised expression level was ≥1.5 times more than the mean of the normal samples. A downregulated gene was defined as one in which (1) the gene was called by GCOS as "present" in all of the 4 normal samples and (2) the gene expression level in the tumour sample was ≥1.5 times less than the mean of the normals.

3.4 Validation of expression array data

To validate the reliability of expression array data we constructed two tissue arrays containing NPC tumour and patient-matched normal epithelial cells. Figure 3.4 shows the two tissuearray blocks, corresponding slides with H&E staining, and representative images of NPC tumour tissue and its matched normal nasopharynx. There are 22 matched cases in each tissuearray block, and each case is represented by 4 cores containing 2 cores of tumour and 2 of normal. To confirm the EBV status in the samples, *in situ* hybridisation for the EBERs was performed (Figure 3.5). The

Figure 3.4: NPC tumour and matched normal tissuearrays.

To validate the expression array data, two tissuearrays containing NPC tumour and matched normal epithelial cells were constructed. There are 22 matched cases in each tissuearray, and each case is represented by 4 cores containing 2 cores of tumour and 2 of normal. The figure shows two tissuearray blocks (A), corresponding slides with H&E staining (B) and representative images of NPC tumour tissue and its matched normal nasopharynx (C). T = tumour, N = normal.

A

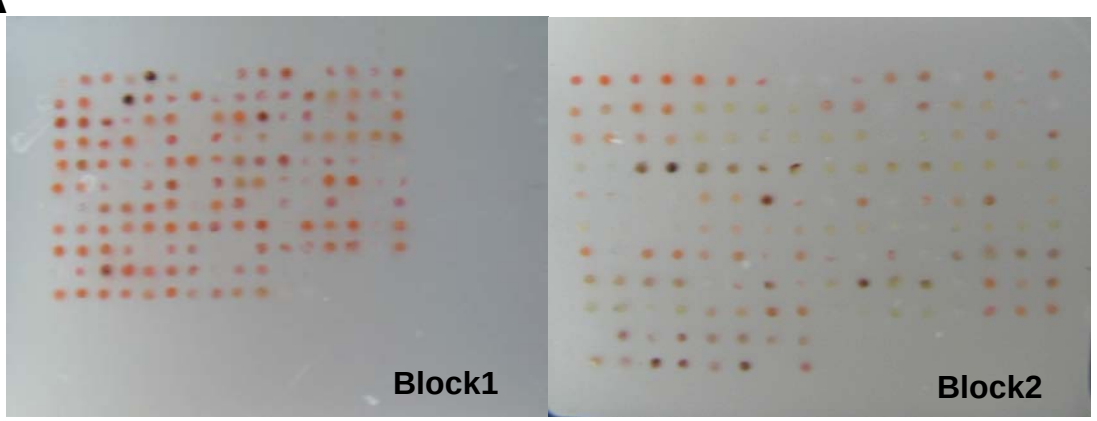

B

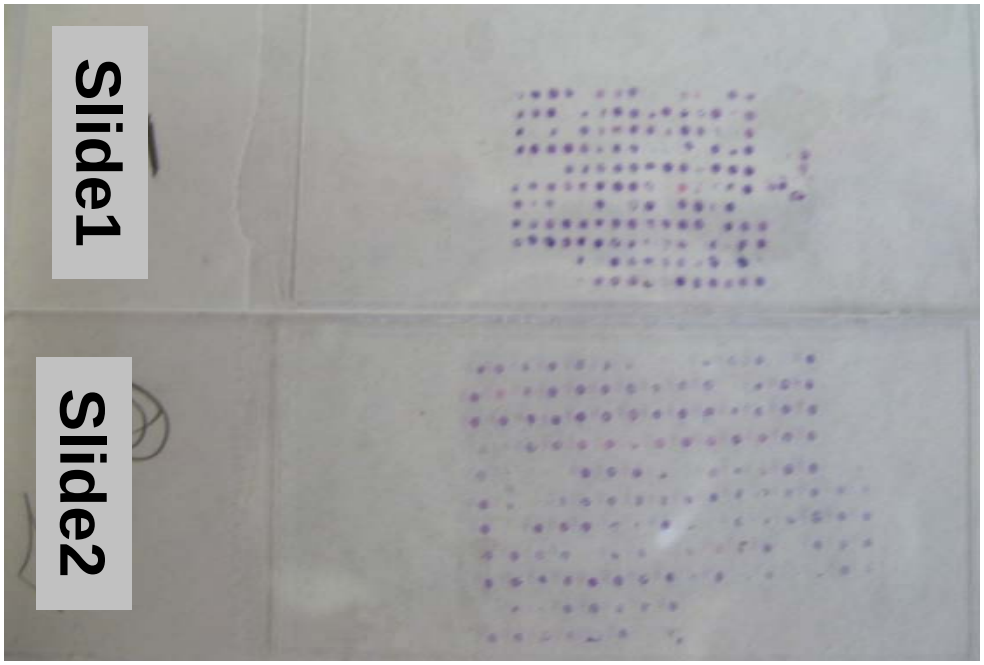

C

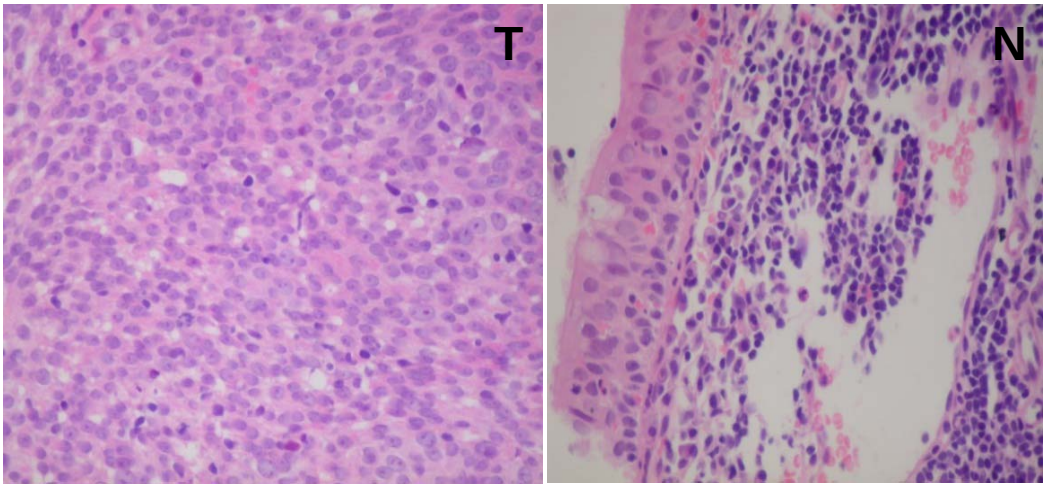

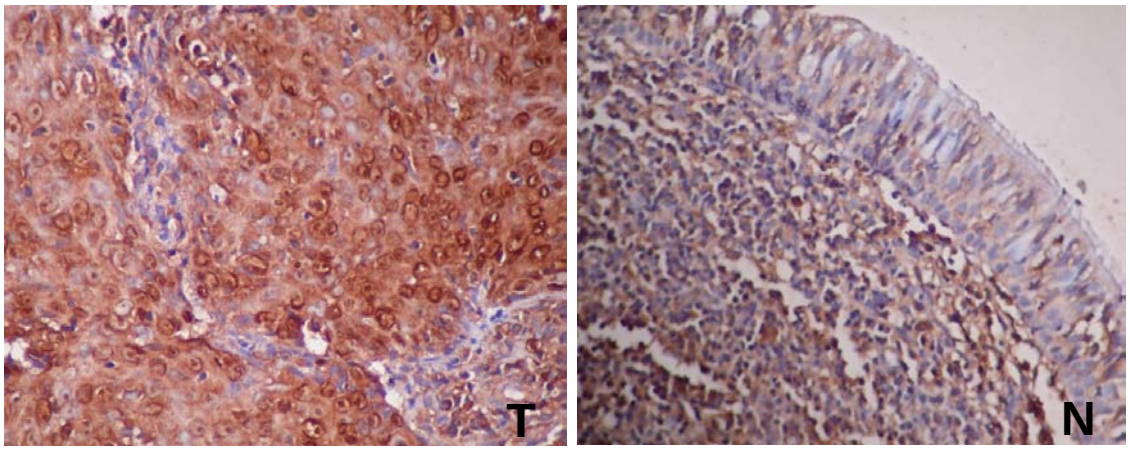

Figure 3.5: EBERs staining in NPC tumour and normal epithelial cells. EBERs staining was performed in tissuearrays. The examples of EBERs staining in NPC tumour (T) and normal epithelial cells (N) are presented. NPC tumour cells show positive nuclear localisation, whereas no or rare nuclear accumulation of EBERs is observed in normal epithelial cells and lymphocytes.

positive nuclear localisation of EBERs in the NPC tumours but absence in the normal epithelial cells confirmed the presence of EBV in NPC tumours and absence in the normal controls.

The differential expression of genes of interest identified by expression array analysis was validated at the protein level by IHC staining in tissuearrays. Because of the limited material in the tissuearrays, staining for most of the genes was performed in only one tissuearray. When evaluating the staining the following are excluded: (1) overlapped cores, (2) edge of the cores which can be overstained, (3) damaged cores (4) cores without target tissue. Additionally, due to losses in block trimming and staining procedures, the number of cases evaluated for individual genes was variable. The criteria used for scoring IHC staining are described in Section 2.3.4. In addition, IHC staining for some genes was also performed in frozen sections which were cut from the same biopsies used for array analysis.

3.5 Tumour-related genes

A large number of differentially expressed genes were identified, and we focused our attention on those genes with known function whose up- or down-regulation in NPC tumours may play critical roles in determining the malignant phenotypes of NPC. According to previous studies and the findings from our data, the differentially expressed genes were involved in diverse functions of biological processes including tumour promoting, tumour suppression, apoptosis/anoikis- suppressing or metastasis. For some of the genes of interest IHC staining data for validation of their array-predicted expression are presented. Since a large number of differentially expressed genes were identified, IHC staining could include only a small proportion of them.

Therefore, some of them were compared with previous published studies of IHC staining. The agreement of the current and previous data further verified the reliability of our array data and supports the idea that these genes are important for NPC tumourigenesis.

To find further information relating to the molecular basis of the pathogenesis of NPC, the expression array data of the individual tumour-related genes were also analysed in the context of their copy number changes determined by SNP array analysis. This is described in detail in Chapter 4. In some cases, the up-regulated genes were found to be amplified in several samples and down-regulated genes were frequently deleted, whereas for some of the genes of interest, the expression level did not correlate with DNA copy number.

3.5.1 Oncogenes

Activation of oncogenes and inactivation of tumour suppressor genes is a critical step in NPC tumourigenesis. In spite of the increased understanding of genetic changes and gene expression patterns in NPC in recent years, information of oncogene activation is still limited in this type of cancer. To identify putative oncogenes that may be important in NPC our expression array data were first analysed for differentially expressed genes that were up-regulated in 4 or more tumours. This gene list was then compared with a list of putative oncogenes derived from the literature. The common genes included in these two gene lists were defined as putative NPC oncogenes (Table 3.1). 159 putative oncogenes that showed upregulation in 4 or more NPC tumours are defined in this list. Examination of these oncogenes in individual tumours revealed that the mean number of oncogenes upregulated in each tumour was

Table 3.1: 159 Putative oncogenes upregulated in at least 25% of samples.

Gene Symbol	Gene Title	location	Number (%) with copy gain	Number (%) up regulated	Validated up regulated
ETS1	v-ets erythroblastosis virus E26 oncogene homolog 1 (avian)	11q24.3	1*(7)	16 (100)	
TFRC	transferrin receptor (p90, CD71)	3q29	0 (0)	16 (100)	
EIF4A2	eukaryotic translation initiation factor 4A, isoform 2	3q27.3	0 (0)	15 (94)	
TPR	translocated promoter region (to activated MET oncogene)	1q31.1	4*(27)	15 (94)	
NCOA3	nuclear receptor coactivator 3	20q13.12	1 (7)	15 (94)	NPC OG
RPL22	ribosomal protein L22	1p36.31	0*(0)	15 (94)	
RBM15	RNA binding motif protein 15	1p13.3	1*(7)	15 (94)	
RHEB	Ras homolog enriched in brain	7q36.1	2 (13)	15 (94)	
EZH2	enhancer of zeste homolog 2 (Drosophila)	7q36.1	2 (13)	15 (94)	10/14 (71%)
PSIP1	PC4 and SFRS1 interacting protein 1	9p22.3	0*(0)	14 (88)	
WHSC1	Wolf-Hirschhorn syndrome candidate 1	4p16.3	0*(0)	14 (88)	11/18 (61%)
LIFR	leukemia inhibitory factor receptor alpha	5p13.1	6 (40)	14 (88)	
AKT3	v-akt murine thymoma viral oncogene homolog 3 (protein kinase B, gamma)	1q44	3*(20)	14 (88)	
TOP1	topoisomerase (DNA) I	20q12	1 (7)	14 (88)	
ECT2	epithelial cell transforming sequence 2 oncogene	3q26.31	2 (13)	14 (88)	
FUS	fusion (involved in t(12;16) in malignant liposarcoma)	16p11.2	1*(7)	14 (88)	
RAB12	RAB12, member RAS oncogene family	18p11.22	2 (13)	14 (88)	
RAB18	RAB18, member RAS oncogene family	10p12.1	0*(0)	14 (88)	
RAB28	RAB28, member RAS oncogene family	4p15.33	6 (40)	14 (88)	
RAN	RAN, member RAS oncogene family	12q24.33	2 (13)	14 (88)	
RAP1A	RAP1A, member of RAS oncogene family	1p13.2	1*(7)	14 (88)	
DEK	DEK oncogene (DNA binding)	6p22.3	1*(7)	14 (88)	
JAK2	Janus kinase 2 (a protein tyrosine kinase)	9p24.1	0*(0)	14 (88)	
JUN	jun oncogene	1p32.1	3 (20)	14 (88)	
RAP2B	RAP2B, member of RAS oncogene family	3q25.2	0(0)	14 (88)	
RAP1B	RAP1B, member of RAS oncogene family	12q15	4 (27)	13 (81)	
SKIL	SKI-like oncogene	3q26.2	3 (20)	13 (81)	25/34 (73.5%)
TRIM33	tripartite motif-containing 33	1p13.2	1*(7)	13 (81)	
LCP1	lymphocyte cytosolic protein 1	13q14.12	0*(0)	13 (81)	

PICALM	phosphatidylinositol binding clathrin assembly protein	11q14.2	1*(7)	13 (81)	
TPM3	tropomyosin 3	1q21.3	4 (27)	13 (81)	
CIITA	class II, major histocompatibility complex, transactivator	16p13.13	1*(7)	13 (81)	
RAP2C	RAP2C, member of RAS oncogene family	Xq25	n/a	13 (81)	
CLTC	clathrin, heavy chain (Hc)	17q23.1	1 (70)	13 (81)	
TCF3	transcription factor 3 (E2A immunoglobulin enhancer binding factors E12/E47)	19p13.3	0*(0)	12 (75)	
CRKL	v-crk sarcoma virus CT10 oncogene homolog (avian)-like	22q11.21	0 (0)	12 (75)	
FGFR1OP2	FGFR1 oncogene partner 2	12p11.23	7 (47)	12 (75)	
FYN	FYN oncogene related to SRC, FGR, YES	6q21	3*(20)	12 (75)	
KRAS	v-Ki-ras2 Kirsten rat sarcoma viral oncogene homolog	12p12.1	7 (47)	12 (75)	
MLLT6	myeloid/lymphoid or mixed-lineage leukemia (trithorax homolog, Drosophila); translocated to, 6	17q12	0*(0)	12 (75)	
NOLC1	nucleolar and coiled-body phosphoprotein 1	10q24.32	0*(0)	12 (75)	NPC OG
PAFAH1B2	platelet-activating factor acetylhydrolase, isoform Ib, beta subunit 30kDa	11q23.3	0*(0)	12 (75)	
TRIM24	tripartite motif-containing 24	7q34	3 (20)	12 (75)	
ZNF384	zinc finger protein 384	12p13.31	6 (40)	12 (75)	
SET	SET translocation (myeloid leukemia-associated)	9q34.11	0*(0)	11 (69	
TPD52	tumor protein D52	8q21.13	5*(33)	11 (69	
WHSC1L1	Wolf-Hirschhorn syndrome candidate 1-like 1	8p12	7 (47)	11 (69)	
JAK1	Janus kinase 1 (a protein tyrosine kinase)	1p31.3	3 (20)	11 (69)	5/11 (45%)
BCL6	B-cell CLL/lymphoma 6 (zinc finger protein 51)	3q27.3	0 (0)	11 (69)	
SFRS3	splicing factor, arginine/serine-rich 3	6p21.31	0*(0)	11 (69)	
CCND2	cyclin D2	12p13.32	7 (47)	11 (69)	
LASP1	LIM and SH3 protein 1	17q12	0*(0)	11 (69)	
PATZ1	POZ (BTB) and AT hook containing zinc finger 1	22q12.2	1*(7)	11 (69)	
PML	promyelocytic leukemia	15q24.1	0*(0)	11 (69)	
GNA12	guanine nucleotide binding protein (G protein) alpha 12	7p22.2	1 (7)	11 (69)	
COX6C	cytochrome c oxidase subunit VIc	8q22.2	5*(33)	11 (69)	
DDX10	DEAD (Asp-Glu-Ala-Asp) box polypeptide 10	11q22.3	0*(0)	11 (69)	
GOLPH3	golgi phosphoprotein 3	5p13.3	6 (40)	11 (69)	
MAF	v-maf musculoaponeurotic fibrosarcoma oncogene homolog (avian)	16q23.1	2*(13)	11 (69)	
NRAS	neuroblastoma RAS viral (v-ras)	1p13.2	1*(7)	11 (69)	NPC OG
YES1	v-yes-1 Yamaguchi sarcoma viral	18p11.32	2 (13)	11 (69)	

	oncogene homolog 1				
MERTK	c-mer proto-oncogene tyrosine kinase	2q13	1 (7)	11 (69)	
RAB23	RAB23, member RAS oncogene family	6p12.1	4*(27)	11 (69)	
RAB27A	RAB27A, member RAS oncogene family	15q21.3	1*(7)	10 (63)	
RAB2A	RAB2A, member RAS oncogene family	8q12.1	5*(33)	10 (63)	
SOX2	SRY (sex determining region Y)-box 2	3q26.33	5 (33)	10 (63)	
HOXA9	homeobox A9	7p15.2	3 (20)	10 (63)	
RAB14	RAB14, member RAS oncogene family	9q33.2	0*(0)	10 (63)	
RAB21	RAB21, member RAS oncogene family	12q21.1	5 (33)	10 (63)	
RAB24	RAB24, member RAS oncogene family	5q35.3	0*(0)	10 (63)	
MYST3	MYST histone acetyltransferase (monocytic leukemia) 3	8p11.21	7 (47)	10 (63)	
GNA13	guanine nucleotide binding protein (G protein), alpha 13	17q24.1	2 (13)	10 (63)	
CRK	v-crk sarcoma virus CT10 oncogene homolog (avian)	17p13.3	0*(0)	10 (63)	
ETV7	ets variant gene 7 (TEL2 oncogene)	6p21.31	1*(7)	10 (63)	
AKT2	v-akt murine thymoma viral oncogene homolog 2	19q13.2	0 (0)	10 (63)	
CDK4	cyclin-dependent kinase 4	12q14.1	4 (27)	10 (63)	
COL1A1	collagen, type I, alpha 1	17q21.33	1 (7)	10 (63)	
BMI1	BMI1 polycomb ring finger oncogene	10p12.31	0*(0)	10 (63)	NPC OG
RAB1A	RAB1A, member RAS oncogene family	2p14	1 (7)	10 (63)	
GNAS	GNAS complex locus	20q13.32	1 (7)	10 (63)	
CCNB1IP1	cyclin B1 interacting protein 1	14q11.2	2*(13)	9 (56)	
RAB22A	RAB22A, member RAS oncogene family	20q13.32	1 (7)	9 (56)	
RAB7L1	RAB7, member RAS oncogene family-like 1	1q32.1	5 (33)	9 (56)	
CEBPA	CCAAT/enhancer binding protein (C/EBP), alpha	19q13.11	0*(0)	9 (56)	
HSP90AB1	heat shock protein 90kDa alpha (cytosolic), class B member 1	6p21.1	1*(7)	9 (56)	
LPP	LIM domain containing preferred translocation partner in lipoma	3q28	0 (0)	9 (56)	
RAB5A	RAB5A, member RAS oncogene family	3p24.3	0*(0)	9 (56)	
RABL5	RAB, member RAS oncogene family-like 5	7q22.1	2*(13)	9 (56)	
RRAS	related RAS viral (r-ras) oncogene homolog	19q13.33	0*(0)	9 (56)	
MYB	v-myb myeloblastosis viral oncogene homolog (avian)	6q23.3	3*(20)	9 (56)	
RAB40B	RAB40B, member RAS oncogene family	17q25.3	0 (0)	9 (56)	
IKZF1	IKAROS family zinc finger 1	7p12.2	2 (13)	8 (50)	

	(Ikaros)				
FLI1	Friend leukemia virus integration 1	11q24.3	1*(7)	8 (50)	
CBL	Cas-Br-M (murine) ecotropic retroviral transforming sequence	11q23.3	0*(0)	8 (50)	
TP63	tumor protein p63	3q28	0 (0)	8 (50)	NPC OG
MYBL1	v-myb myeloblastosis viral oncogene homolog (avian)-like 1	8q13.1	5 (33)	8 (50)	
MYCN	v-myc myelocytomatosis viral related oncogene, neuroblastoma derived (avian)	2p24.3	2 (13)	8 (50)	
RAB9A	RAB9A, member RAS oncogene family	Xp22.2	n/a	8 (50)	
RRAS2	related RAS viral (r-ras) oncogene homolog 2	11p15.2	2*(13)	8 (50)	
WNT5A	wingless-type MMTV integration site family, member 5A	3p14.3	0*(0)	8 (50)	10/23 (43.5%)
RAB43	RAB43, member RAS oncogene family	3q21.3	0 (0)	7 (44)	
RAF1	V-raf-1 murine leukemia viral oncogene homolog 1	3p25.1	0*(0)	7 (44)	
REL	v-rel reticuloendotheliosis viral oncogene homolog (avian)	2p16.1	1 (7)	7 (44)	
PIK3CA	Phosphoinositide-3-kinase, catalytic, alpha polypeptide	3q26.32	4 (27)	7 (44)	NPC OG
RAP2A	RAP2A, member of RAS oncogene family	13q32.1	0*(0)	7 (44)	
RAB27B	RAB27B, member RAS oncogene family	18q21.2	2*(13)	7 (44)	
RAB34	RAB34, member RAS oncogene family	17q11.2	2*(13)	7 (44)	
MSI2	musashi homolog 2 (Drosophila)	17q22	2 (13)	7 (44)	
RAB11A	RAB11A, member RAS oncogene family	15q22.31	0*(0)	7 (44)	
MALT1	mucosa associated lymphoid tissue lymphoma translocation gene 1	18q21.32	2*(13)	7 (44)	
PTTG1	pituitary tumor-transforming 1	5q33.3	0*(0)	7 (44)	
ELL	elongation factor RNA polymerase II	18p13.11	0*(0)	7 (44)	
KTN1	kinectin 1 (kinesin receptor)	14q22.3	1*(7)	7 (44)	
GMPS	guanine monphosphate synthetase	3q25.31	0 (0)	7 (44)	
ETV6	ets variant gene 6 (TEL oncogene)	12p13.2	7 (47)	7 (44)	
PDGFRA	platelet-derived growth factor receptor, alpha polypeptide	4q12	1*(7)	7 (44)	
DDIT3	DNA-damage-inducible transcript 3	12q13.3	5 (33)	7 (44)	
RALA	v-ral simian leukemia viral oncogene homolog A (ras related)	7p14.1	2 (13)	7 (44)	
RET	ret proto-oncogene	10q11.21	0*(0)	7 (44)	
AKT1	v-akt murine thymoma viral oncogene homolog 1	14q32.33	0 (0)	7 (44)	
IL21R	interleukin 21 receptor	16p12.1	1*(7)	6 (38)	
RELB	v-rel reticuloendotheliosis viral oncogene homolog B, nuclear factor of kappa light polypeptide gene enhancer in B-cells 3 (avian)	19q13.32	0 (0)	6 (38)	
SS18L1	synovial sarcoma translocation gene on chromosome 18-like 1	20q13.3	0*(0)	6 (38)	

THRB	thyroid hormone receptor, beta (erythroblastic leukemia viral (v-erb-a) oncogene homolog 2, avian)	3p24.2	0*(0)	6 (38)	
RAB6A	RAB6A, member RAS oncogene family	11q13.4	1*(7)	6 (38)	
HRAS	v-Ha-ras Harvey rat sarcoma viral oncogene homolog	11p15.5	0 (0)	6 (38)	NPC OG
MAFB	v-maf musculoaponeurotic fibrosarcoma oncogene homolog B (avian)	20q12	1 (7)	6 (38)	
MET	met proto-oncogene (hepatocyte growth factor receptor)	7q31.2	2 (13)	6 (38)	NPC OG
BRAF	v-raf murine sarcoma viral oncogene homolog B1	7q34	3 (20)	6 (38)	
MLLT3	myeloid/lymphoid or mixed-lineage leukemia (trithorax homolog, Drosophila); translocated to, 3	9p21.3	0*(0)	6 (38)	
HMGA2	high mobility group AT-hook 2	12q14.3	5 (33)	6 (38)	
MLL	myeloid/lymphoid or mixed-lineage leukemia (trithorax homolog, Drosophila)	11q23.3	0*(0)	6 (38)	
VAV1	vav 1 oncogene	19p13.3	0*(0)	5 (31)	
VAV2	vav 2 oncogene	9q34.2	0*(0)	5 (31)	
PBX1	Pre-B-cell leukemia homeobox 1	1q23.3	4 (27)	5 (31)	
SKI	v-ski sarcoma viral oncogene homolog (avian)	1p36.33	0*(0)	5 (31)	
USP6	ubiquitin specific peptidase 6 (Tre-2 oncogene)	17p13.2	0*(0)	5 (31)	
MYCL1	v-myc myelocytomatosis viral oncogene homolog 1, lung carcinoma derived (avian)	1p34.2	2 (13)	5 (31)	
ERBB4	v-erb-a erythroblastic leukemia viral oncogene homolog 4 (avian)	2q34	1 (7)	5 (31)	
FCRL4	Fc receptor-like 4	1q23.1	4 (27)	5 (31)	
HOXA13	homeobox A13	7p15.2	3 (20)	5 (31)	
MNX1	homeobox HB9	7q36.3	1 (7)	5 (31)	
NIN	ninein (GSK3B interacting protein)	14q22.1	1*(7)	5 (31)	
EGFR	epidermal growth factor receptor (erythroblastic leukemia viral (v-erb-b) oncogene homolog, avian)	7p11.2	3 (20)	5 (31)	NPC OG
FGFR1	fibroblast growth factor receptor 1 (fms-related tyrosine kinase 2, Pfeiffer syndrome)	8p12	6 (40)	5 (31)	
CHIC2	cysteine-rich hydrophobic domain 2	4q12	1*(7)	5 (31)	
ETV1	ets variant gene 1	7p21.2	2 (13)	4 (25)	
NUMA1	nuclear mitotic apparatus protein 1	11q13.4	1*(7)	4 (25)	
PDE4DIP	phosphodiesterase 4D interacting protein (myomegalin)	1q21.1	0 (0)	4 (25)	
PVT1	Pvt1 oncogene homolog, MYC activator (mouse)	8q24.21	5 (33)	4 (25)	
ABL1	v-abl Abelson murine leukemia viral oncogene homolog 1	9q34.12	0 (0)	4 (25)	
ERG	v-ets erythroblastosis virus E26 oncogene homolog (avian)	21q22.2	0 (0)	4 (25)	
FCGR2B	Fc fragment of IgG, low affinity IIb,	1q23.3	4 (27)	4 (25)	

	receptor (CD32)				
KDSR	3-ketodihydrosphingosine reductase	18q21.33	2*(13)	4 (25)	
ITK	IL2-inducible T-cell kinase	5q33.3	0*(0)	4 (25)	
KIT	v-kit Hardy-Zuckerman 4 feline sarcoma viral oncogene homolog	4q12	1*(7)	4 (25)	
RAB31	RAB31, member RAS oncogene family	18p11.22	2*(13)	4 (25)	
RAB33B	RAB33B, member RAS oncogene family	4q31.1	0*(0)	4 (25)	
RAB39B	RAB39B, member RAS oncogene family	Xq28	n/a	4 (25)	

* = locus that showed copy number loss in a number of samples.

n/a = copy number data not applicable on the X chromosome.

NPC OG = gene previously implicated as an oncogene in NPC.

93 (range 40 – 120). To determine whether the overexpression of the potential NPC oncogenes could be caused by their copy number status, the copy number data for these genes are also displayed.

Several oncogenes in our list (labelled "NPC OG" in the table) have previously been determined to be associated with NPC. Among these NCOA3 has been reported to be overexpressed in 51% and gained in 7% of NPC tumours (Liu *et al*., 2008), and our data show it to be upregulated in 94% and gained in 7% of NPC. A recent publication suggested that NOLC1 had a higher expression level in most NPC cell lines and biopsies compared with normal cells, and the activation of this gene is necessary for p53-mediated MDM2 expression and is associated with cell proliferation in NPC cells (Hwang *et al*., 2009). This gene showed 75% upregulation in our expression data. TP63 is a suppressor of wide type p53 and its expression was found to be elevated in primary NPC and immortalised nasopharyngeal epithelial cells at their proliferation stages (Crook *et al*., 2000; Yip & Tsao, 2008). TP63 was observed to be upregulated in 50% of our NPC tumours. Other genes including NRAS, PIK3CA and EGFR were identified by a genome-wide study of NPC (Hui *et al*., 2002; Or *et al*., 2005). They are also found to have a copy number gain in several samples and upregulated in most of NPC. Recent evidence suggested that polycomb group genes can act as oncogenes. BMI1 is one of the polycomb group proteins and has been shown to be overexpressed in 38.7% of primary NPC tumours. Furthermore, the oncogenic potential of this gene was revealed by its ability to immortalise normal nasopharyngeal epithelial cells, induce epithelial-mesenchymal transition (EMT) and enhance the motility and invasiveness of human nasopharyngeal epithelial cells (Song *et al.*, 2006; Song *et al.*, 2009). BMI1 was upregulated in 63% of NPC tumours in our data.

In addition to the candidate oncogenes revealed previously, the majority of genes in the oncogene list are novel potential NPC oncogenes although their upregulation has been reported to be associated with other types of cancer. The IHC staining for several genes of interest was performed in the tissuearrays and frozen sections from biopsies that have been used for array analysis.

EZH2 along with BMI1 which was introduced above is another member of the Polycomb group of genes. Elevated expression of this gene has been reported in several cancers including prostate cancer (Varambally *et al.*, 2002; van Leenders *et al.*, 2007), breast cancer (Kleer *et al*., 2003) and glioblastoma multiforme (Suva *et al*., 2009) based on its ability to modulate transcription of key genes implicated in cell cycle control, DNA repair, and cell differentiation and invasiveness (Shi *et al.*, 2007a; Cao *et al*., 2008; Friedman *et al.*, 2009). Our data demonstrated that EZH2 was also elevated in NPC tumours. In the expression data, EZH2 transcripts were upregulated in 94% (15/16) of NPC tumours. IHC staining of EZH2 in frozen sections from the biopsies used for array analysis confirmed increased expression in tumours at the protein level. In addition, tissuearray data revealed that EZH2 was overexpressed in 71% (10/14) of NPC tumours (Figure 3.6 A).

WHSC1 is expressed ubiquitously in early development and consistently appears in glioblastoma multiforme tissue but not in normal brain. Its expression increased tumour proliferation activity (Li *et al*., 2008). This indicates that WHSC1 might be a putative oncogene as emphasised by recent data showing overexpression in 15 types of cancer compared to their normal counterparts (Kassambara *et al*., 2009). In our

Figure 3.6: Expression array intensities and immunohistochemical staining for oncogenes.

The left panels show normalised expression array intensities for the 4 normal samples (grey) and 15 NPCs plus C666-1 (red). The centre panels show examples of immunohistochemical staining of NPC tissue samples. Normal epithelial cells (Normal) show weak expression, whilst tumour cells (Tumour) show strong expression. The right panels show the immunohistochemical scoring results from the tissue arrays (normal, grey: tumour, red). At the RNA and protein levels respectively, (A) EZH2 is upregulated in 15/16 (94%) and 10/14 (71%) samples, and positive EZH2 staining is predominantly observed in the nucleus; (B) SKIL is upregulated in 13/16 (81%) and 25/34 (74%) samples, and positive SKIL staining is predominantly observed in the cytoplasm and membrane; (C) JAK1 is upregulated in 11/16 (69%) and 5/11 (45%) samples, and positive JAK1 staining is predominantly observed in the nucleus; (D) WNT5A is upregulated in 8/16 (50%) and 10/23 (43%) samples, and positive WNT5A staining is predominantly observed in the cytoplasm. Note that in (A) the illustrated immunohistochemical staining was performed on frozen sections of samples that were used for array analysis (MHAU, XY23) whilst the IHC scoring data were obtained from tissue arrays.

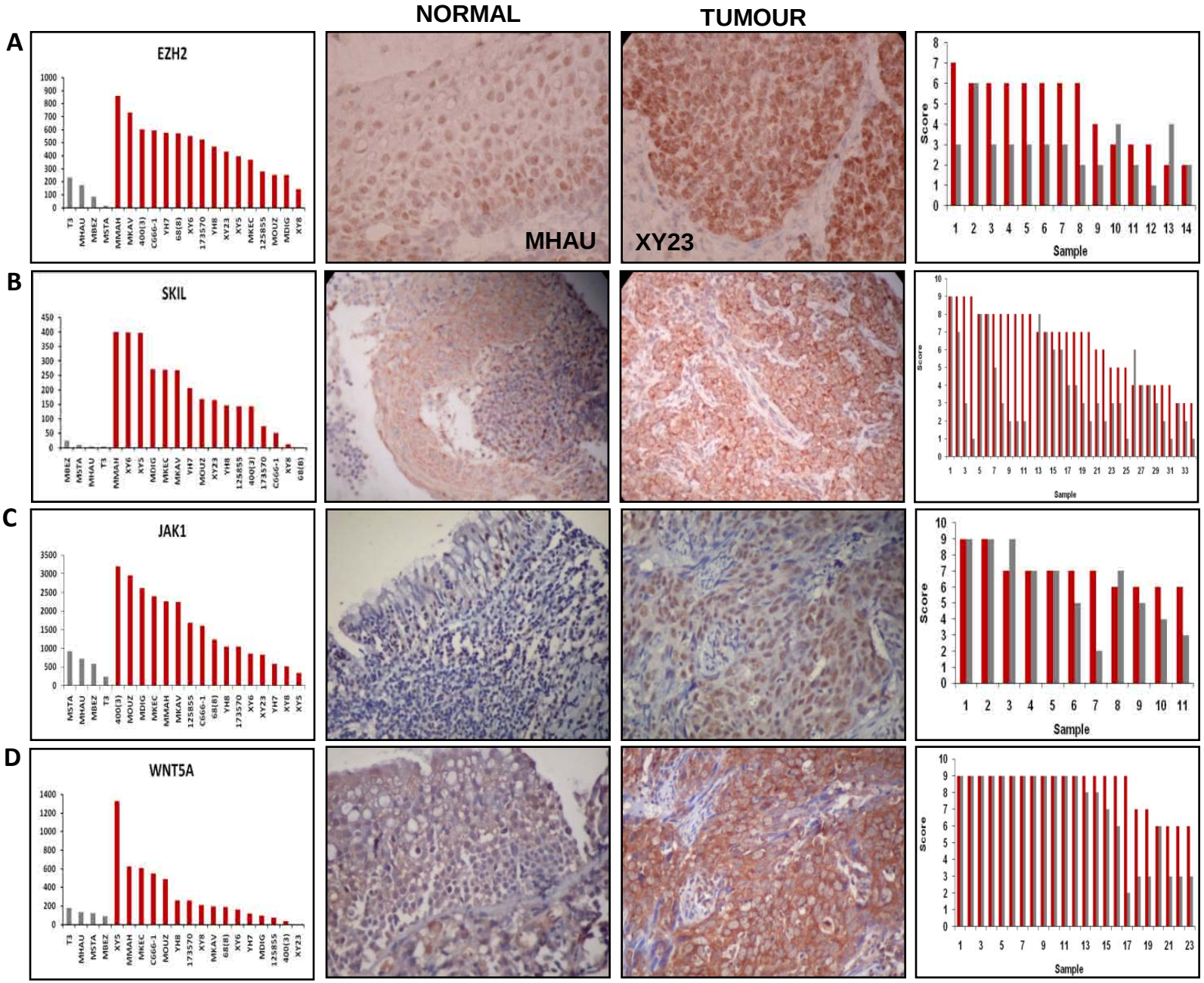
NORMAL
TUMOUR
A
EZH2
MHAU
XY23
Score
Sample
B
SKIL
Score
Sample
C
JAK1
Score
Sample
D
WNT5A
Score
Sample

expression data the WHSC1 transcript was upregulated in 88% (14/16) of tumours. IHC data revealed protein overexpression in 61% (11/18) of NPC tumours. Taken together, WHSC1 might be an NPC-related oncogene although confirmation and understanding of the tumour promoting function of this gene in NPC requires further study.

SKIL (SKI-like oncogene) is a member of the SKI family of proto-oncogenes. Human SKIL is considered to be expressed at a very low level in normal human tissues, whereas elevation of its expression is believed to occur in both development and tumourigenesis. In oesophageal carcinoma, SKIL is needed for smad3-protein complexes involved in TGF-β signalling, and increased expression of SKIL can block TGFβ-induced growth arrest (Edmiston *et al.*, 2005; Pot & Bonni, 2008). Genome-wide studies in NPC revealed that the gene locus of SKIL was amplified in 33% of advanced NPC tumours (Sheu *et al*., 2009). In addition, increased expression level of SKIL has been associated with EBV reactivation in NPC cells (Lee *et al*., 2008). In our SNP array data, 20% of NPC tumours showed copy number gain at the SKIL gene locus. Expression data revealed that 81% (13/16) of NPC tumours were upregulated at the transcript level. This was confirmed at the protein level by IHC staining where 73.5% (25/34) of tumours showed overexpression compared with normal controls (Figure 3.6 B).

JAK is a small family consisting of at least four different tyrosine kinases (JAK1, JAK2, JAK3 and Tyk2) that share significant structural homology with each other. They play an essential role in mediating biological responses including control of cell differentiation and proliferation by modulating several signalling pathways especially

the JAK-STAT pathway. The activity of JAK is generally required for STAT activation which has been implicated in the pathogenesis of a number of malignancies (Verma *et al*., 2003; Xiong *et al*., 2008). This indicates that JAK has potential oncogenic functions. Our expression data also support this thesis in NPC as both JAK1 and JAK2 are upregulated. JAK2 transcripts were upregulated in 88% (14/16) of tumours whereas JAK1 transcription was upregulated in 69% (11/16) of NPCs and IHC data revealed that its protein was overexpressed in 45% (5/11) of tumour samples (Figure 3.6 C).

WNT5A is a representative ligand of the Wnt gene family whose function is essential for activation of the Wnt/β-catenin signalling pathway. Wnt signalling will be considered in Chapter 5. Abnormal expression and tumour promotion activity of WNT5A has been observed in several tumours including gastric cancer (Saitoh *et al*., 2002), breast cancer (Leris *et al*., 2005) and prostate cancer (Yamamoto *et al*.). The expression data displayed upregulation of WNT5A transcripts in 50% (8/16) of NPC tumours and tissue array data revealed its protein was overexpressed in 43.5% (10/23) of NPCs (Figure 3.6 D).

3.5.2 Tumour suppressor genes

Aside from activation of tumour promoting genes, the loss of tumour suppressors is another important factor contributing to the development of NPC. To identify putative tumour suppressor genes, the list of downregulated genes identified by expression array analysis was compared with a list of previously identified putative tumour suppressor genes compiled by an extensive literature search. This revealed 165 putative tumour suppressor genes (Table 3.2). Examination of these TSGs in

Table 3.2: 165 Putative tumour suppressor genes downregulated in at least 25% of samples.

Gene Symbol	Gene Title	Location	Number (%) with Copy Loss	Number (%) Down regulated	Validated Down regulated
ANXA1	annexin A1	9q21.13	5 (33)	16 (100)	11/14 (79%)
BRD7	bromodomain containing 7	16q12.1	9 (60)	16 (100)	NPC tsg
CEACAM1	carcinoembryonic antigen-related cell adhesion molecule 1 (biliary glycoprotein)	19q13.2	0 (0)	16 (100)	
CLCA2	chloride channel, calcium activated, family member 2	1p22.3	3* (20)	16 (100)	
CLU	clusterin	8p21.1	3*(20)	16 (100)	13/13 (100%)
CSK	c-src tyrosine kinase	15q24.1	2 (13)	16 (100)	
DLG1	discs, large homolog 1 (Drosophila)	3q29	0 (0)	16 (100)	
DUOX2	dual oxidase 2	15q21.1	5* (33)	16 (100)	
EHF	ets homologous factor	11p13	1* (7)	16 (100)	
EPAS1	endothelial PAS domain protein 1	2p21	0* (0)	16 (100)	
FOXC1	forkhead box C1	6p25.3	3 (20)	16 (100)	
GLTSCR2	glioma tumor suppressor candidate region gene 2	19q13.32	1 (7)	16 (100)	
GPX3	glutathione peroxidase 3 (plasma)	5q33.1	5 (33)	16 (100)	
H19	H19, imprinted maternally expressed untranslated mRNA	11p15.5	†	16 (100)	NPC tsg
JUP	junction plakoglobin	17q21.2	1* (7)	16 (100)	
KLF5	Kruppel-like factor 5 (intestinal)	13q22.1	5* (33)	16 (100)	
KLK11	kallikrein-related peptidase 11	19q13.33	0 (0)	16 (100)	
LCN2	lipocalin 2 (oncogene 24p3)	9q34.11	6 (40)	16 (100)	18/19 (95%)
MSMB	microseminoprotein, beta	10q11.23	3 (20)	16 (100)	
MSRA	methionine sulfoxide reductase A	8p23.1	1*(7)	16 (100)	
PER2	period homolog 2 (Drosophila)	2q37.3	†	16 (100)	
S100A2	S100 calcium binding protein A2	1q21.3	0*(0)	16 (100)	
SERPINB13	serpin peptidase inhibitor, clade B (ovalbumin), member 13	18q21.33	2*(13)	16 (100)	
SFN	stratifin	1p36.11	8 (53)	16 (100)	NPC tsg
SOX7	SRY (sex determining region Y)-box 7	8p23.1	1*(7)	16 (100)	
YAP1	Yes-associated protein 1, 65kDa	11q22.1-q22.2	6 (40)	16 (100)	
ZNF185	zinc finger protein 185 (LIM domain)	Xq28	n/a	16 (100)	
CDHR2	cadherin-related family member 2	5q35.2	6 (40)	16 (100)	
CEBPD	CCAAT/enhancer binding protein (C/EBP), delta	8q11.21	2*(13)	15 (94)	

GJB2	gap junction protein, beta 2, 26kDa	13q12.11	7 (47)	15 (94)	
GRLF1	glucocorticoid receptor DNA binding factor 1	19q13.32	1 (7)	15 (94)	
IGFBP5	insulin-like growth factor binding protein 5	2q35	0*(0)	15 (94)	
ING2	inhibitor of growth family, member 2	4q35.1	5 (33)	15 (94)	
MCC	mutated in colorectal cancers	5q22.2	4 (27)	15 (94)	
NDUFA13	NADH dehydrogenase (ubiquinone) 1 alpha subcomplex, 13	19p13.11	4 (27)	15 (94)	
PDLIM4	PDZ and LIM domain 4	5q31.1	7 (47)	15 (94)	
PPP1R13B	protein phosphatase 1, regulatory (inhibitor) subunit 13B	14q32.33	10 (67)	15 (94)	
PRDX2	peroxiredoxin 2	19p13.13	0 (0)	15 (94)	
PYCARD	PYD and CARD domain containing	16p11.2	3*(20)	15 (94)	
SEMA3F	sema domain, immunoglobulin domain (Ig), short basic domain, secreted, (semaphorin) 3F	3p21.31	12 (80)	15 (94)	
TACC2	transforming, acidic coiled-coil containing protein 2	10q26.13	3 (20)	15 (94)	
GSTP1	glutathione S-transferase pi	11q13.2	1 (7)	15 (94)	NPC tsg
DUOX1	dual oxidase 1	15q21.1	5*(33)	15 (94)	
CBFA2T3	core-binding factor, runt domain, alpha subunit 2; translocated to, 3	16q24.3	14 (93)	14 (88)	
HINT1	histidine triad nucleotide binding protein 1	5q31.1	5 (33)	14 (88)	
LIMD1	LIM domains containing 1	3p21.31	12 (80)	14 (88)	
LLGL2	lethal giant larvae homolog 2 (Drosophila)	17q25.1	3 (20)	14 (88)	
PDCD4	programmed cell death 4 (neoplastic transformation inhibitor)	10q24	3 (20)	14 (88)	
PTPN6	protein tyrosine phosphatase, non-receptor type 6	12p13.31	0*(0)	14 (88)	
RARB	retinoic acid receptor, beta	3p24.2	8 (53)	14 (88)	NPCtsg
RPS6KA2	ribosomal protein S6 kinase, 90kDa, polypeptide 2	6q27	4 (27)	14 (88)	
SERPINB2	serpin peptidase inhibitor, clade B (ovalbumin), member 2	18q21.33	1*(7)	14 (88)	
SLC9A3R1	solute carrier family 9 (sodium/hydrogen exchanger), member 3 regulator 1	17q25.1	1*(7)	14 (88)	
SMAD3	SMAD family member 3	15q22.33	4 (27)	14 (88)	
SOD2	superoxide dismutase 2, mitochondrial	6q25.3	4*(27)	14 (88)	
CSNK1A1	casein kinase 1, alpha 1	5q33.1	6 (40)	13 (81)	
DUSP6	dual specificity phosphatase 6	12q21.33	0*(0)	13 (81)	
HRASLS	HRAS-like suppressor	3q29	0 (0)	13 (81)	
IFI16	interferon, gamma-inducible protein 16	1q23.1	0*(0)	13 (81)	
KLF6	Kruppel-like factor 6	10p15.1	2 (13)	13 (81)	
RASSF6	Ras association (RalGDS/AF-6) domain family 6	4q13.3	1*(7)	13 (81)	
SPTBN1	spectrin, beta, non-erythrocytic 1	2p16.2	0*(0)	13 (81)	
TMPRSS6	transmembrane protease, serine 6	22q12.3	0 (0)	13 (81)	

VTA1	Vps20-associated 1 homolog (S. cerevisiae)	6q24.1	1*(7)	13 (81)	
WASL	Wiskott-Aldrich syndrome-like	7q31.32	0*(0)	13 (81)	
ZC3H10	zinc finger CCCH-type containing 10	12q13.2	0*(0)	13 (81)	
ADAMTS9	ADAM metallopeptidase with thrombospondin type 1 motif, 9	3p14.1	11 (73)	12 (75)	NPC tsg
CXCL14	chemokine (C-X-C motif) ligand 14	5q31.1	8 (53)	12 (75)	
EXT2	exostoses (multiple) 2	11p11.2	1*(7)	12 (75)	
MFN2	mitofusin 2	1p36.22	7 (47)	12 (75)	
MZF1	myeloid zinc finger 1	19q13.43	†	12 (75)	
NPAS2	neuronal PAS domain protein 2	2q11.2	0*(0)	12 (75)	
MIIP	invasion inhibitory protein 45	1p36.22	7 (47)	12 (75)	
SERPINB5	serpin peptidase inhibitor, clade B (ovalbumin), member 5	18q21.33	2*(13)	12 (75)	
TIMP3	TIMP metallopeptidase inhibitor 3 (Sorsby fundus dystrophy, pseudoinflammatory)	22q12.3	0*(0)	12 (75)	
TMSB10	thymosin, beta 10	2p11.2	0*(0)	12 (75)	
TNFSF10	Tumor necrosis factor (ligand) superfamily, member 10	3q26.31	0*(0)	12 (75)	
CHFR	checkpoint with forkhead and ring finger domains	12q24.33	†	11 (69)	NPC tsg
DDB2	damage-specific DNA binding protein 2, 48kDa	11p11.2	1*(7)	11 (69)	
ETS2	v-ets erythroblastosis virus E26 oncogene homolog 2 (avian)	21q22.2	0 (0)	11 (69)	
FBXO31	F-box protein 31	16q24.2	11 (73)	11 (69)	
HPGD	hydroxyprostaglandin dehydrogenase 15-(NAD)	4q34.1	3 (20)	11 (69)	
KLF4	Kruppel-like factor 4 (gut)	9q31.2	4*(27)	11 (69)	31/37 (84%)
LATS1	LATS, large tumor suppressor, homolog 1 (Drosophila)	6q25.1	2*(13)	11 (69)	
PRDX1	peroxiredoxin 1	1p34.1	1*(7)	11 (69)	
VSNL1	visinin-like 1	2p24.2	0*(0)	11 (69)	
FH	fumarate hydratase	1q43	1*(7)	10 (63)	
GAK	cyclin G associated kinase	4p16.3	†	10 (63)	
GDI2	GDP dissociation inhibitor 2	10p15.1	2 (13)	10 (63)	
IER3	immediate early response 3	6p21.33	4*(27)	10 (63)	
IGFBP3	insulin-like growth factor binding protein 3	7p13	0*(0)	10 (63)	
SMARCA4	SWI/SNF related, matrix associated, actin dependent regulator of chromatin, subfamily a, member 4	19p13.2	0 (0)	10 (63)	
THRA	thyroid hormone receptor, alpha (erythroblastic leukemia viral (v-erb-a) oncogene homolog, avian)	17q21.1	1*(7)	10 (63)	NPC tsg
TLE4	transducin-like enhancer of split 4 (E(sp1) homolog, Drosophila)	9q21.31	4 (27)	10 (63)	
TP73	tumor protein p73	1p36.32	11 (73)	10 (63)	NPC tsg
TRIM35	tripartite motif-containing 35	8p21.2	3*(20)	10 (63)	

TRIM8	tripartite motif-containing 8	10q24.32	3 (20)	10 (63)	
WWOX	WW domain containing oxidoreductase	16q23.1	7 (47)	10 (63)	
BNIP3L	BCL2/adenovirus E1B 19kDa interacting protein 3-like	8p21.2	3*(20)	9 (56)	
CDKN2C	cyclin-dependent kinase inhibitor 2C (p18, inhibits CDK4)	1p33	0*(0)	9 (56)	
CTDSPL	CTD (carboxy-terminal domain, RNA polymerase II, polypeptide A) small phosphatase-like	3p22.2	11 (73)	9 (56)	
EGR1	early growth response 1	5q31.2	7 (47)	9 (56)	
HIPK2	homeodomain interacting protein kinase 2	7q34	0*(0)	9 (56)	
NDRG1	N-myc downstream regulated gene 1	8q24.22	0*(0)	9 (56)	
PFDN5	prefoldin subunit 5	12q13.13	0*(0)	9 (56)	
PRR5	proline rich 5 (renal)	22q13.31	8 (53)	9 (56)	
PSEN1	presenilin 1 (Alzheimer disease 3)	14q24.2	9 (60)	9 (56)	
RASEF	RAS and EF-hand domain containing	9q21.32	4 (27)	9 (56)	
REEP5	receptor accessory protein 5	5q22.2	4 (27)	9 (56)	
SAR1A	SAR1 gene homolog A (S. cerevisiae)	10q22.1	3 (20)	9 (56)	
TSC1	tuberous sclerosis 1	9q34.13	6 (40)	9 (56)	
SMARCA2	SWI/SNF related, matrix associated, actin dependent regulator of chromatin, subfamily a, member 2	9p24.3	6*(40)	9 (56)	
EPB41	erythrocyte membrane protein band 4.1 (elliptocytosis 1, RH-linked)	1p35.3	6 (40)	8 (50)	
GPNMB	glycoprotein (transmembrane) nmb	7p15.3	0*(0)	8 (50)	
MIA3	melanoma inhibitory activity family, member 3	1q41	0*(0)	8 (50)	
PERP	PERP, TP53 apoptosis effector	6q23.3	2*(13)	8 (50)	
RND3	Rho family GTPase 3	2q23.3	0*(0)	8 (50)	
RPS14	ribosomal protein S14	5q33.1	5 (33)	8 (50)	
YWHAE	tyrosine 3-monooxygenase/tryptophan 5-monooxygenase activation protein, epsilon polypeptide	17p13.3	5 (33)	8 (50)	
BLCAP	bladder cancer associated protein	20q11.23	0*(0)	7 (44)	
DNAJA3	DnaJ (Hsp40) homolog, subfamily A, member 3	16p13.3	4*(27)	7 (44)	
EEF1A1	eukaryotic translation elongation factor 1 alpha 1	6q13	2*(13)	7 (44)	
FOXO1	forkhead box O1	13q14.11	8 (53)	7 (44)	
GABARAP	GABA(A) receptor-associated protein	17p13.1	5 (33)	7 (44)	
IGFBP7	insulin-like growth factor binding protein 7	4q12	1*(7)	7 (44)	
PA2G4	proliferation-associated 2G4, 38kDa	12q13.2	0*(0)	7 (44)	
PHLDA1	pleckstrin homology-like domain, family A, member 1	12q21.2	0*(0)	7 (44)	

SDHB	succinate dehydrogenase complex, subunit B, iron sulfur (Ip)	1p36.13	7(47)	7 (44)	
SH3GLB1	SH3-domain GRB2-like endophilin B1	1p22.3	3*(20)	7 (44)	
TJP2	tight junction protein 2 (zona occludens 2)	9q21.11	4 (27)	7 (44)	
UTRN	utrophin	6q24.2	1*(7)	7 (44)	
BCLAF1	BCL2-associated transcription factor 1	6q23.3	1*(7)	6 (38)	
CD9	CD9 molecule	12p13.31	0*(0)	6 (38)	
DDX3X	DEAD (Asp-Glu-Ala-Asp) box polypeptide 3, X-linked	Xp11.4	n/a	6 (38)	
FOXO3	forkhead box O3	6q21	1*(7)	6 (38)	
MSH3	mutS homolog 3 (E. coli)	5q14.1	8 (53)	6 (38)	15/18 (83%)
PEBP1	phosphatidylethanolamine binding protein 1	12q24.23	0*(0)	6 (38)	
CD99	CD99 molecule	Xp22.33	n/a	5 (31)	
CREG1	cellular repressor of E1A-stimulated genes 1	1q24.2	1*(7)	5 (31)	
DDIT4	DNA-damage-inducible transcript 4	10q22.1	3 (20)	5 (31)	
HMGB1	high-mobility group box 1	13q12.3	7*(47)	5 (31)	
PHB	prohibitin	17q21.33	0*(0)	5 (31)	
TES	testis derived transcript (3 LIM domains)	7q31.2	0*(0)	5 (31)	
TFAP2A	transcription factor AP-2 alpha (activating enhancer binding protein 2 alpha)	6p24.3	2*(13)	5 (31)	
TLE1	transducin-like enhancer of split 1 (E(sp1) homolog, Drosophila)	9q21.31 - q21.32	4 (27)	5 (31)	
CCAR1	cell division cycle and apoptosis regulator 1	10q21.3	3 (20)	5 (31)	
PTEN	phosphatase and tensin homolog (mutated in multiple advanced cancers 1)	10q23.31	3 (20)	5 (31)	NPCtsg
TSC22D1	TSC22 domain family, member 1	13q14.11	8 (53)	5 (31)	
BECN1	beclin 1 (coiled-coil, myosin-like BCL2 interacting protein)	17q21.31	1 (7)	5 (31)	
RTN4	reticulon 4	2p16.1	0*(0)	5 (31)	
RASSF5	Ras association (RalGDS/AF-6) domain family 5	1q32.1	0*(0)	5 (31)	
CDH1	cadherin 1, type 1, E-cadherin (epithelial)	16q22.1	9 (60)	4 (25)	NPC tsg
RANBP2	RAN binding protein 2	2q13	0*(0)	4 (25)	
RBMX	RNA binding motif protein, X-linked	Xq26.3	n/a	4 (25)	
ZFHX3	AT-binding transcription factor 1	16q22.3	9 (60)	4 (25)	
BTG3	BTG family, member 3	21q21.1	0*(0)	4 (25)	
ENO1	enolase 1, (alpha)	1p36.23	12 (80)	4 (25)	
HTATIP2	HIV-1 Tat interactive protein 2, 30kDa	11p15.1	1*(7)	4 (25)	

STAT1	signal transducer and activator of transcription 1, 91kDa	2q32.2	0*(0)	4 (25)	
IRF3	interferon regulatory factor 3	19q13.33	6 (40)	4 (25)	
LITAF	lipopolysaccharide-induced TNF factor	16p13.13	4* (27)	4 (25)	
TOB1	transducer of ERBB2, 1	17q21.33	0*(0)	4 (25)	
TSG101	tumor susceptibility gene 101	11p15.1	1*(7)	4 (25)	

* = locus that showed copy number gain in a number of samples.

† = copy number data unreliable due to proximity to chromosomal end.

n/a = copy number data not applicable on the X chromosome.

NPCtsg = gene previously implicated as acting as a tsg in NPC.

individual tumours revealed that the mean number of TSGs downregulated in each tumour was 109 (range 90 – 135).

Several previously identified, candidate NPC-related TSGs are found in our list including BRD7, H19, SFN, GSTP1, RARB, ADAMTS9, CHFR, THRA, TP73, PTEN and CDH1. BRD7 transcripts were downregulated in 100% (16/16) of NPC tumours in our expression array. This gene has been reported to be downregulated in NPC biopsies and cell lines and its expression could inhibit cell cycle progression and induce apoptosis (Zhou *et al*., 2004; Zhou *et al*., 2006a; Zhou *et al*., 2006b). The transcripts of both H19 and SFN were also downregulated in 100% (16/16) of NPC tumours. SFN is a target of p53 and overexpression of SFN could inhibit cell growth and block DNA synthesis (Yang *et al*., 2006). GSTP1, RARB ADAMTS9, CHFR, TP73 and CDH1 have been identified as tumour suppressor genes in NPC by methylation analysis (Kwong *et al.*, 2002; Wong *et al.*, 2003; Lung *et al.*, 2008), and the expression data revealed that their transcripts were downregulated in 94% (15/16), 88% (14/16), 75% (12/16), 69% (11/16), 63% (10/16) and 25% (4/16) of NPC tumours compared with normal control cells, respectively.

Most of the candidate genes in our tumour suppressor gene list are relatively new in the context of NPC although their tumour suppressor behaviour has been observed in other types of cancer. IHC staining confirmed downregulation of the TSGs ANXA1, LCN2, KLF4, MSH3 and CLU at the protein level (Figures 3.7, 4.8 and 4.11).

ANXA1, at the top of our TSG list, was downregulated in 100% (16/16) of NPC tumours. IHC staining revealed the expression of its protein was reduced in 79%

Figure 3.7: Expression array intensities and immunohistochemical staining for tumour suppressor genes.

The left panels show normalised expression array intensities for the 4 normal samples (grey) and 15 NPCs plus C666-1 (red). The centre panels show examples of immunohistochemical staining of NPC tissue samples. Normal epithelial cells (Normal) show strong expression, whilst tumour cells (Tumour) show weak expression. The right panels show the immunohistochemical scoring results from the tissue arrays (normal, grey: tumour, red). At the RNA and protein levels respectively, (A) ANXA1 is downregulated in 16/16 (100%) and 11/14 (79%) samples, and positive ANXA1 staining is predominantly observed in the membrane; (B) LCN2 is downregulated in 16/16 (100%) and 18/19 (95%) samples, and positive LCN2 staining is predominantly observed in the cytoplasm and membrane; (C) KLF4 is downregulated in 11/16 (69%) and 31/37 (84%) samples, and positive KLF4 staining is predominantly observed in the nucleus.

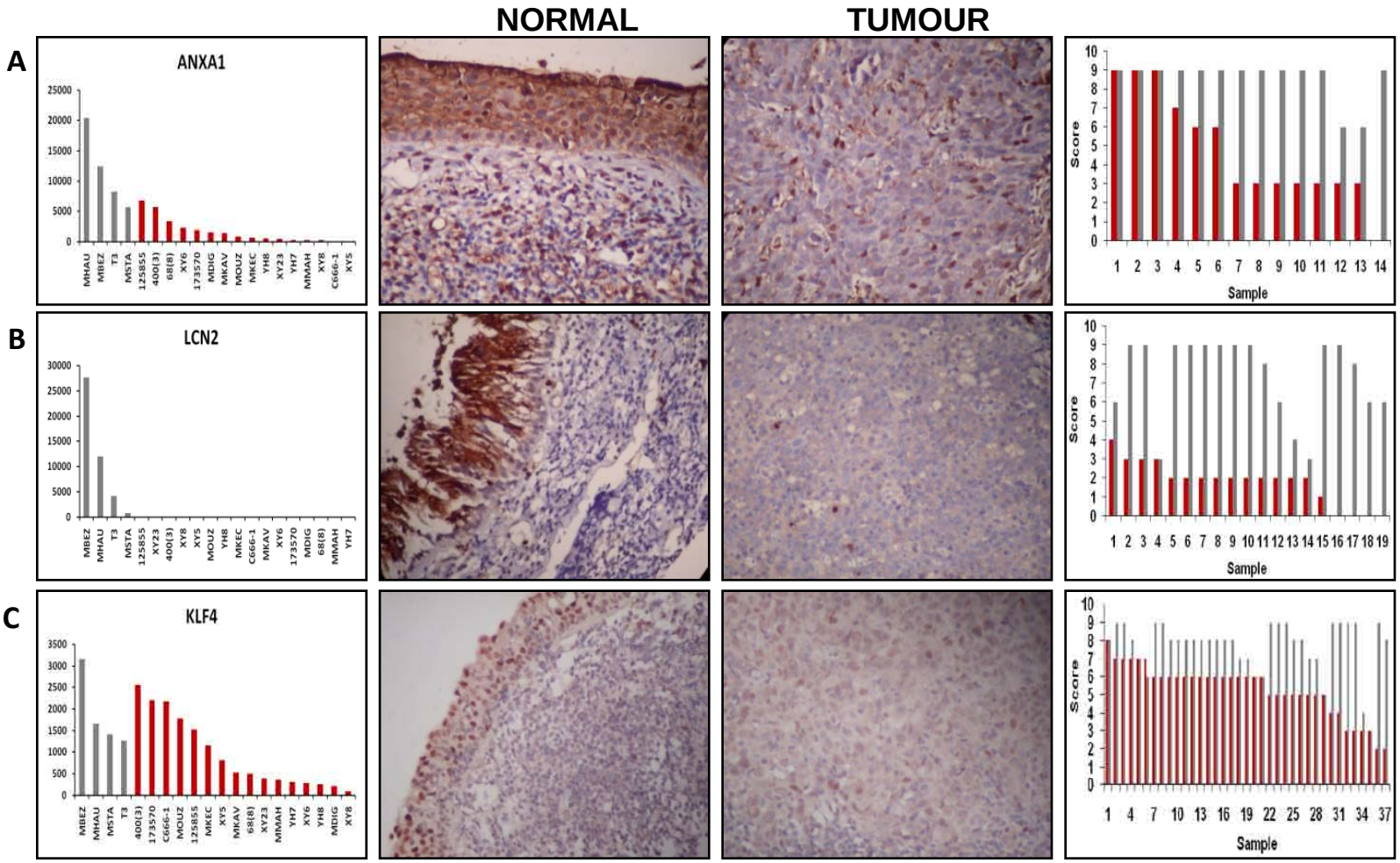
NORMAL
TUMOUR
A
ANXA1
MHAU
MBEZ
T3
MSTA
125855
400(3)
68(8)
XY6
173570
MDIG
MKAV
MOUZ
MKEC
YH8
XY23
YH7
MMAH
XY8
C666-1
XY5
Score
Sample
B
LCN2
MBEZ
MHAU
T3
MSTA
125855
XY23
400(3)
XY8
XY5
MOUZ
YH8
MKEC
C666-1
MKAV
XY6
173570
MDIG
68(8)
MMAH
YH7
Score
Sample
C
KLF4
MBEZ
MHAU
MSTA
T3
400(3)
173570
C666-1
MOUZ
125855
MKEC
XY5
MKAV
68(8)
XY23
MMAH
YH7
XY6
YH8
MDIG
XY8
Score
Sample

(11/14) of tumours compared with the normal counterparts (Figure 3.7A). Although the exact function of ANXA1 remains unknown, it has been suggested to play an important role in the regulation of tumour growth, invasiveness and metastasis (Ang *et al.*, 2009; Inokuchi *et al.*, 2009; Yi & Schnitzer, 2009). Downregulation of ANXA1 has been found in a number of cancers and the expression of this gene is associated with epithelial differentiation status (Garcia Pedrero *et al.*, 2004; Rodrigo *et al.*, 2005; Hummerich *et al.*, 2006; Petrella *et al.*, 2006; Shen *et al.*, 2006; Bose *et al.*, 2009).

In the expression array, LCN2 transcripts also showed 100% (16/16) downregulation in NPC tumours, and confirmation by IHC staining which revealed that the expression of LCN2 protein was decreased in 95% (18/19) of tumours (Figure 3.7 B). LCN2 is a 25kDa glycoprotein that was initially purified from neutrophil granules. A variety of functions of LCN2 have been reported including in cell proliferation. Two studies demonstrated that LCN2 might exert tumour suppressor functions as it suppresses tumour invasion and metastasis and induces apoptosis (Tong *et al.*, 2005; Lee *et al.*, 2006).

KLF4 (formerly GKLF) is a zinc-finger transcription factor expressed in the epithelia of the skin, lung, gastrointestinal tract and several other organs (Garrett-Sinha et al., 1996; Shields et al., 1996). *In vitro* and *in vivo* studies suggested that KLF4 plays important roles in cell proliferation and/or differentiation (Segre *et al.*, 1999; Katz *et al.*, 2002; Chen *et al.*, 2003). Loss of expression of KLF4 has been observed in several human tumours, especially in those of the gastrointestinal tract. In addition, the tumours with loss of KLF4 expression are associated with a more aggressive phenotype (Wong *et al.*, 2005). In our expression data, KLF4 transcripts were

downregulated in 69% (11/16) of NPC tumours and protein expression was decreased in 84% (31/37) of tumours (Figure 3.7C). This suggests that KLF4 might have tumour suppressor functions in NPC. However, functional studies are needed to confirm this thesis.

3.5.3 Metastasis promotion genes

Distant metastasis at a very early stage is one of the distinct features of NPC. The transition from *in situ* tumour growth to metastatic disease depends on the ability of tumours at the primary site to invade local tissues and to cross tissue barriers. This process requires the activation of a number of metastasis promoting genes to exert their various functions in cell adhesion, proliferation, migration and so on.

Expression array analysis revealed several differentially regulated genes whose upregulation might promote the progression of metastasis (Table 3.3). ASAP1 was upregulated in 94% of NPC tumours in the expression array data. Overexpression of ASAP1 has also been reported to be associated with invasiveness and metastasis of prostate cancer (Lin *et al*., 2008) and breast cancer (Sabe *et al*., 2009). TNFRSF11A, upregulated in 56% of NPC tumours in our data, has been found to be related to lymph node (Heymann *et al*., 2008) and bone metastasis (Armstrong *et al*., 2008). NUDCD1 and SPP1 were upregulated in 75% and 69% of NPC tumours, respectively, and have been observed to be involved in cervical cancer metastatic progression (Wang *et al*., 2008) and advanced NPC tumours (Wong *et al*., 2005). Downregulation of another metastasis-associated molecule, CD44, has been shown to inhibit the metastatic potential of an NPC cell line, whereas induction of its expression by LMP1 was associated with lymphoma dissemination (Shi *et al*., 2007). In the expression

Table 3.3: Upregulated genes involved in promotion of metastasis and resistance to anoikis or apoptosis.

Gene Symbol	Gene Title	Location	Number (%) with copy gain	Number (%) upregulated	Validation
Metastasis Promotion					
MALAT1	metastasis associated lung adenocarcinoma transcript 1 (non-protein coding)		0*(0)	16 (100)	
ASAP1	ArfGAP with SH3 domain, ankyrin repeat and PH domain 1	8q24.21	8 (53)	15 (94)	
NUDCD1	NudC domain containing 1	8q23.1	8 (53)	12 (75)	
TNFRSF10B	tumor necrosis factor receptor superfamily, member 10b	8p21.3	5*(33)	11 (69)	
TGFBI	transforming growth factor, beta-induced, 68kDa	5q31.1 - 31.2	0*(0)	11 (69)	
SPP1	secreted phosphoprotein 1 (osteopontin)	4q22.1	1*(7)	11 (69)	
TNFRSF11A	tumor necrosis factor receptor superfamily, member 11a, NFKB activator	18q21.33	2*(13)	9 (56)	
TNFRSF11B	tumor necrosis factor receptor superfamily, member 11b (osteoprotegerin)	8q24.12	8 (53)	6 (38)	
CD44	CD44 molecule (Indian blood group)	11p13	2*(13)	6 (38)	NPC-A 6/12 (50%)
Anoikis Resistance					
ITGAV	integrin, alpha V	2q32.1	1 (7)	16 (100)	
NTRK2	neurotrophic tyrosine kinase, receptor, type 2	9q21.33	0*(0)	15 (94)	
CFLAR	CASP8 and FADD-like apoptosis regulator	2q33.1	1 (7)	14 (88)	
XIAP	X-linked inhibitor of apoptosis	Xq25	n/a	14 (88)	
CTNNB1	catenin (cadherin-associated protein), beta 1, 88kDa	3p22.1	0*(0)	13 (81)	6/18 (33%)
PLAU	plasminogen activator, urokinase	10q22.2	0*(0)	10 (63)	
ITGB6	integrin, beta 6	2q24.2	1 (7)	10 (63)	
Apoptosis Resistance					
BCL2	B-cell CLL/lymphoma 2	18q21.33	2*(13)	16 (100)	NPC-A
TNFAIP3	tumor necrosis factor, alpha-induced protein 3	6q23.3	2*(13)	15 (94)	9/18 (50%)
BIRC3	baculoviral IAP repeat-containing 3	11q22.2	0*(0)	14 (88)	NPC-A
TNFAIP8	tumor necrosis factor, alpha-induced protein 8	5q23.1	0*(0)	13 (81)	
BCL2A1	BCL2-related protein A1	15q25.1	0*(0)	9 (56)	
CLDN1	Claudin 1	3q28	0 (0)	8 (50)	NPC-A

* = locus that showed copy number loss in a number of samples.

n/a = copy number data not applicable on the X chromosome.

NPC-A = NPC-associated.

array data, the transcript level of this gene was upregulated in 38% (6/16) of NPC and IHC staining in the NPC tissue array showed it to be upregulated at the protein level in 50% (6/12) of tumours (Figure 3.8A).

3.5.4 Apoptosis associated genes

Aberrant apoptosis, as in all malignancies, is also essential for NPC development. The inhibition of apoptosis is critical for the progression of malignant cell proliferation and NPC tumour formation. A number of antiapoptotic factors have been identified and are listed in Table 3.3. BCL-2, upregulated in 100% of NPC tumours, is an oncoprotein whose overexpression interferes with apoptosis (Hockenbery *et al.*, 1990), and it has also long been recognised as an oncogene in NPC (Lu *et al.*, 1993). TNFAIP3 (A20) was upregulated at the RNA level in 94% (15/16) of samples and IHC staining on tissue arrays showed upregulation at the protein level in 50% (9/18) of tumours (Figure 3.8 B). It has been suggested that stable expression of TNFAIP3 could inhibit p53-mediated apoptosis (Fries *et al.*, 1996) and upregulation of TNFAIP3 was associated with undifferentiated NPC tumours (Codd *et al.*, 1999). Another antiapoptotic gene BIRC3 (also called c-IAP2) which is upregulated in 88% of NPC tumours in our array data, has been recently found to be overexpressed in EBV-associated NPC and play critical roles in the resistance to Toll-like receptor 3-mediated apoptosis (Friboulet *et al.*, 2008). These apoptosis associated genes were also introduced in Section 1.4.3.

3.5.5 Anoikis Resistance genes

Anoikis, a form of apoptosis induced by loss of cell-matrix interactions, has been suggested to act as a physiological barrier to metastasis. Resistance to anoikis may

Figure 3.8: Expression array intensities and immunohistochemical staining for other tumour-associated genes.

The left panels show normalised expression array intensities for the 4 normal samples (grey) and 15 NPCs plus C666-1 (red). The centre panels show examples of immunohistochemical staining of NPC tissue samples. Normal epithelial cells (Normal) show weak expression, whilst tumour cells (Tumour) show strong expression. The right panels show the immunohistochemical scoring results from the tissue arrays (normal, grey: tumour, red). At the RNA and protein levels respectively, (A) the metastasis-related gene CD44 is upregulated in 6/16 (38%) and 6/12 (50%) samples; and positive CD44 staining is predominantly observed in the membrane; (B) the antiapoptotic gene TNFAIP3 is upregulated in 15/16 (94%) and 9/18 (50%) samples; and positive TNFAIP3 staining is predominantly observed in the cytoplasm; (C) the anoikis resistance gene CTNNB1 is upregulated in 13/16 (81%) and 6/18 (33%) samples, and positive CTNNB1 staining is predominantly observed in the cytoplasm and membrane.

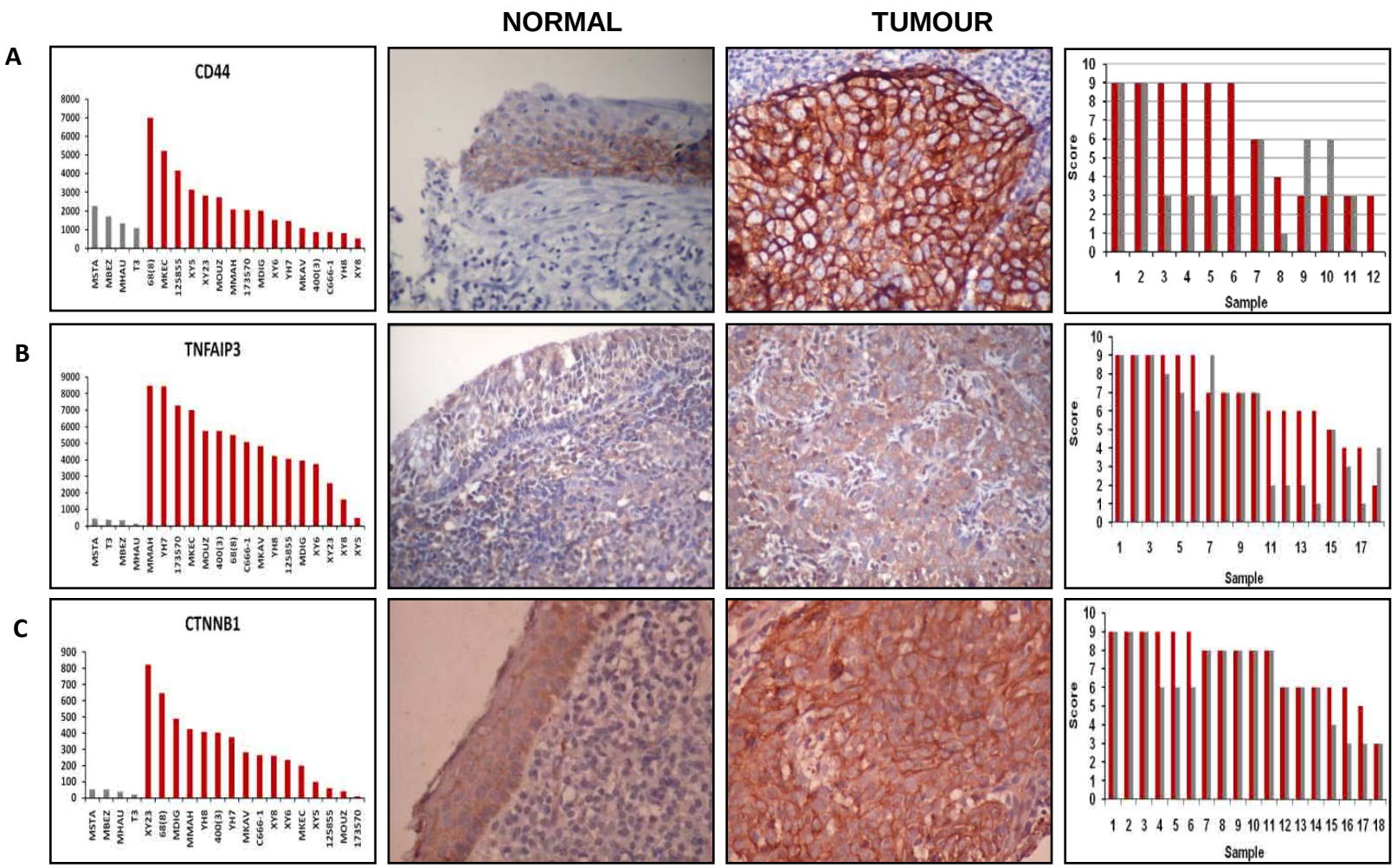
NORMAL
TUMOUR
A
CD44
MSTA MBEZ MHAU T3 68(8) MKEC 125855 XY5 XY23 MOUZ MMAH 173570 MDIG XY6 YH7 MKAV 400(3) C666-1 YH8 XY8
Score
Sample
B
TNFAIP3
MSTA T3 MBEZ MHAU MMAH YH7 173570 MKEC MOUZ 400(3) 68(8) C666-1 MKAV YH8 125855 MDIG XY6 XY23 XY8 XY5
Score
Sample
C
CTNNB1
MSTA MBEZ MHAU T3 XY23 68(8) MDIG MMAH YH8 400(3) YH7 MKAV C666-1 XY8 XY6 MKEC XY5 125855 MOUZ 173570
Score
Sample

allow survival of cancer cells during systemic circulation, thereby facilitating distant metastasis. In the expression array data, several genes involved in anoikis resistance were upreguated in many NPC tumours (Table 3.3). These include NTRK2, which showed suppression of anoikis and induction of metastasis in human cancers (Douma et al., 2004); PLAU, whose upregulation induces the resistance to anoikis in prostate cancer cells (Hasanuzzaman *et al*., 2007); and CTNNB1 that is also a key member of the Wnt signalling pathway (Chapter 5), which was found to be up regulated in 81% (13/16) of tumours at the RNA level and 6/18 (33%) samples at the protein level (Figure 3.8 C).

The metastasis-related, anti-apoptotic and anoikis-resistance genes are presented in Table 3.3, in which genes that have previously been reported as having an NPC association are labelled “NPC-A”.

3.6 Discussion

In this study, we performed expression array analysis in 16 NPC tumours and 4 normal epithelial samples. The RNA samples used in this work were extracted from microdissected NPC tumour and normal epithelial cells. This made it possible to compare the cellular gene expression level in pure populations of tumour and normal cells.

The samples consisted of 4 normal epithelial samples, one cell line C666-1, and 15 NPC biopsies from high- and intermediate- incidence areas. At a global gene expression level a sample correlation analysis was carried out. This clustering analysis revealed that there is no geographical difference of gene expression in the samples.

Tumour cells and normal controls have their distinct expression features, and more importantly, C666-1 was clustered with other tumours and thus appears to be a good tumour model for NPC.

To identify differentially regulated genes in NPC tumours, the expression data were normalised with RMA and analysed with RP and also analysed using GCOS. The RP analysis revealed a large number of differentially expressed genes but had a tendency to miss some important genes whose up- or down-regulation occurred in only a small proportion of NPC tumours. Regarding the behaviour of specific single genes in individual tumours, these genes are probably important in a small fraction of tumours. Thus, an analysis which concerned the gene expression levels in individual samples was used to determine up- or down-regulated genes. This revealed a number of genes that are involved in diverse functions of biological processes including oncogenes, tumour suppressor genes, apoptosis/anoikis- suppressing or metastasis-associated genes.

Our findings confirmed and also extended previous observations. Some genes displayed in the tables have been reported previously, but most of the genes identified have not been related to NPC. Although over 160 previously characterised TSGs were found to be downregulated in the current sample set, even this number is an underestimate. Several well-known candidate NPC TSGs were not defined in our list. For instance, TSGs W1F1 (Chan *et al*., 2007), RASSF1 (Chow *et al*., 2004), FHIT (Ko *et al*., 2002) and DLC1 (Peng *et al*., 2006) were expressed at low levels in both tumour and normal and called “absent” by the GCOS software. The relative expression level can not be compared, thus, these genes were excluded in our TSGs

list. Similarly, other NPC-associated TSGs CDKN2A (Baba *et al*., 2001), ZMYND10 (Agathanggelou *et al*., 2003; Liu *et al*., 2003) and ATM (Bose *et al*., 2009) were called "present" in only 3 of the 4 normal samples, so they also were not included in our list. On ther other hand, although some genes were found to be downregulated in a large propotion of NPC samples and defined as tumour suppressor genes, they appear to have both tumour suppressive and tumour promoting activities. For example, LCN2 was downregulated in 100% NPC tumours at the RNA level and 95% tumours at the protein level in our data. Nonetheless, it has been suggested to be a tumour promoting factor in several cancers *(*Cui *et al., 2008;* Moniaux *et al., 2008;* Yang *et al*., 2009). Our data revealed that KLF4 expression was significantly reduced in NPC tumours. However, it also seems to function as a dominant oncogene since it has been shown to be overexpressed in human breast tumours and squamous cell carcinomas and contributes to oncogenic transformation of cultured cells (Foster *et al*., 1999; Foster *et al*., 2000; Chen *et al*., 2008).

It is generally accepted that for the majority of genes, changes at the mRNA level will usually result in similar alterations at the protein level. On this basis, we used IHC staining to verify the reliability of the array data. The results revealed that the up- or down-regulation of the genes of interest in expression array data showed increased or reduced protein expression following IHC staining, but the proportion of samples are somewhat different (see Table 3.1-3.3). For example, in the expression array data, MSH3 was down-regulated in 38% NPC tumours, whilst the IHC data showed it to be down-expressed in 83% tumours. This observation that genes were differentially regulated in a different proportion of samples at the RNA and protein level could be

due to gene post-transcriptional regulation, but most likely, it was caused by the different sample sets that were used for expression array and IHC data analysis.

In conclusion, the expression array analyses revealed a large number of putative NPC-related genes that might play important roles in NPC development and progression. IHC staining confirmed the expression array data. To further explore the pathogenesis of NPC, functional analyses are needed to understand better the roles of these potential tumour-related genes.

CHAPTER 4

Cellular genetic alterations of nasopharyngeal carcinoma

4.1 Introduction

NPC is a genetic disease exhibiting a series of abnormalities such as chromosomal loss, gain or mutation during the process of carcinogenesis. Such abnormalities have been found by a number of previous studies that used karyotyping, FISH, CGH or microsatellite analyses. Most notably, consistent genetic changes in NPC include frequent deletions on chromosomes 1p, 3p, 9p, 9q, 11q, 13q, 14q and 16q and frequent gains on chromosomes 1q, 3q, 8q and 12 (see Section 1.4.1). However, the genetic analyses mentioned above have limited resolution and are inadequate in defining the fine boundaries of genetic changes and pinpointing tumour-associated genes. Some potential tumour-related genes within small regions of genetic aberrations might have been overlooked. Therefore, in this study, we took advantage of the high-resolution of Affymetrix 500K SNP arrays to profile the genetic changes in NPC biopsies and the NPC cell line C666-1. A number of genetic changes in NPC tumours were detected by the SNP array analyses. The extensive regions of loss or gain that are frequently detected in NPC tumours by SNP array are consistent with previous observations. Furthermore, the delineation of small genetic aberrations by this high-resolution array allows us to identify some potential tumour-related genes involved in the critical regions. Q-PCR analyses were used to validate SNP array-predicted copy number changes of the genes of interest.

13 NPC tumour samples used for SNP array analysis have also been used for expression array analysis (see Table 2.1), which makes it possible to compare gene

expression changes with chromosomal abnormalities in the same sample. It has been considered that gene copy number loss is often accompanied by downregulation of their expression, whereas gene copy number gain is associated with upregulation of expression. However, when analysing the relationship between copy number changes and gene expression levels, we found that in some instances this might be the case, whilst in others, copy number changes do not correlate directly with differential expression. None of the previous work performed the gene expression analysis and chromosomal genetic studies in the same NPC tumour, thus, our work will provide a valuable framework for the discovery of novel NPC-related genes as well as further exploration of the mechanism of NPC tumourigenesis.

As was mentioned in Section 1.3.5, SNP arrays can analyse DNA copy number and LOH in parallel in the same patient across the whole genome. By combining LOH with copy number data, this new technique is also capable of identifying UPD regions that are likely to harbour genes important for the carcinogenic process.

Usually, the size of NPC biopsies is quite small and the DNA extracted from microdissected tumour cells is insufficient for direct SNP array analysis as well as subsequent verification of SNP array data. In order to obtain enough material, a DNA amplification step is necessary. The bacteriophage φ29 polymerase-based Genomiphi kit has been successfully used for the amplification of small amounts of genomic DNA prior to SNP array analysis (Paez *et al.*, 2004; Wong *et al.*, 2004). Typically, the yield of amplified DNA is about 3-5 μg from 10 ng of genomic DNA as starting material. To study the fidelity of amplified DNA, a preliminary experiment was performed by Dr. John Arrand using the C666-1 cell line as a vehicle. 10ng and 1ng

of C666-1 DNA were amplified and analysed on 10K SNP arrays and compared with unamplified C666-1 DNA. The data revealed that concordance of SNP calls between unamplified DNA and DNA amplified from 10ng was 99.90%, whereas between unamplified DNA and DNA amplified from 1ng it was 99.89%. As a further confirmation, the LMP1 DNA was isolated by PCR from the 1ng-amplified DNA and sequenced by Ms Sim Sihota. The sequence was identical to that obtained from non-amplified C666-1 DNA. These preliminary data indicate that amplification of genomic DNA using the Genomiphi kit can produce a high fidelity, near-complete genome representation suitable for high resolution genetic analysis.

4.2 Comparison of unamplified and amplified C666-1 DNA on 500K arrays

Although genome representation of the amplified DNA on the 10K array is quite comprehensive and estimated to be 99.90%, when unamplified and DNA amplified were compared on 500K arrays it was found that the copy number profiles of the amplified samples were somewhat noisier than those obtained from intact DNA. In particular, comparing the copy number data generated from amplified and unamplified C666-1 DNA, we found that isolated, small (-200kb) apparent amplifications or deletions appeared in amplified DNA that were not present in the intact sample (Figure 4.1). For this reason, in all subsequent experiments, isolated, apparent copy number changes of 300kb or less were filtered out. In addition, losses close to chromosomal termini were often observed. This phenomenon has also been noted by others (Pan *et al.*, 2008) to be artefactual and such apparent losses were ignored.

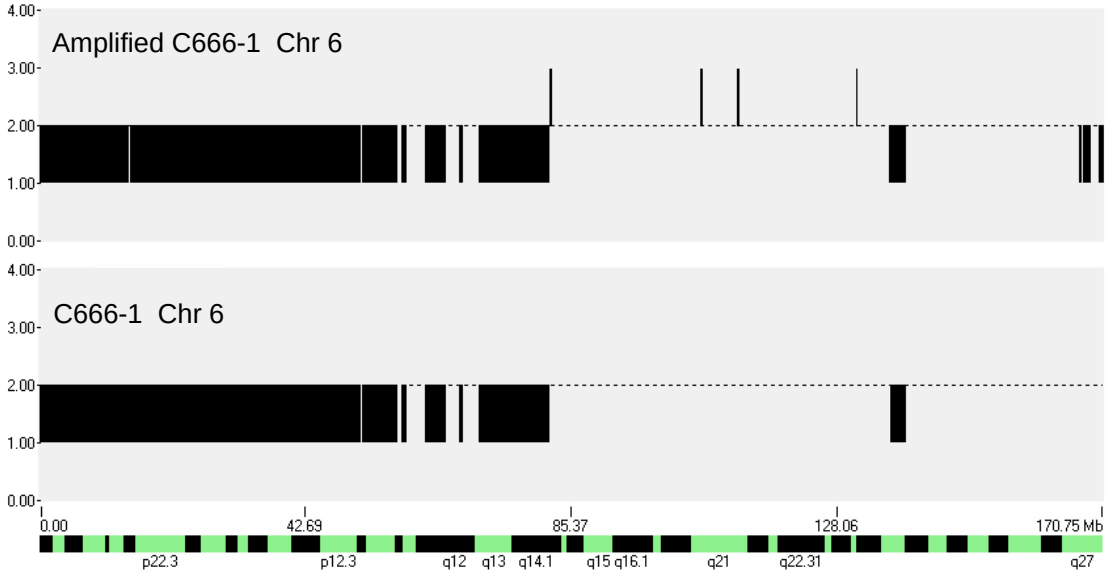

Figure 4.1: Comparison of unamplified and amplified C666-1 DNA on 500K SNP arrays. Unamplified and amplified C666-1 DNA were analysed on 500K SNP arrays. The traces show an example of copy number states of unamplified and amplified C666-1 on chromosome 6. The "2" dashed line is used as a baseline to depict DNA copy number 2, and the solid vertical line represents the value of smoothed DNA copy number. It is defined as copy number loss if the value of the solid vertical line is below the "2", and gain if above the "2" line. Compared to unamplified C666-1 DNA, the amplified DNA shows several additional isolated, small (-200kb) apparent gains or deletions, as well as losses close to chromosomal termini.

4.3 Characterisation of NPC biopsies and NPC cell line C666-1

14 NPC biopsies (Table 2.1) diagnosed as undifferentiated NPC and one NPC cell line, C666-1, were used for SNP array analysis. 9 biopsies were from Cantonese patients, 3 were from Maghreb patients, and 2 were Italian. Within the EBV genome, the BamHI-W region is a repetitive, highly conserved region. The EBV status in the NPC biopsies and the C666-1 cell line was determined by PCR using BamHI-W-specific primers (Hill *et al.*, 2006). As shown in Figure 4.2, all samples except one showed the expected amplified fragment. Considering the near 100% of EBV positivity in undifferentiated NPC tumours that was reported previously (Dickens *et al.*, 1992; Gulley *et al.*, 1995), sample MMAH was reviewed again by an experienced NPC pathologist who confirmed the diagnosis of undifferentiated NPC.

The detection of copy number changes in tumour DNA could be confounded by the presence of DNA from surrounding non-neoplastic tissue. Tumour-normal mixing experiments to assess the effects of contaminating non-neoplastic cells on genetic changes using SNP arrays found the best performance for LOH was achieved with 90% tumour purity and above, and DNA copy number gains can be detected in mixtures containing 60% tumour DNA, whereas copy number losses can be detected at more than 90% tumour purity (Lindblad-Toh *et al.*, 2000; Zhao *et al.*, 2004). Although the NPC biopsies selected for array analysis showed well-defined islands of tumour cells, they still had infiltrating lymphocytes. Therefore, for reliable and best results of genetic analysis, laser microdissection and pressure catapulting (LMPC) was carried out on NPC biopsies to obtain a pure and homogeneous population of tumour cells.

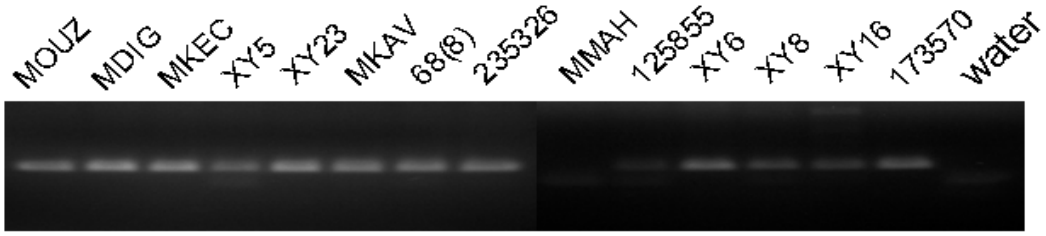

Figure 4.2: Determination of the EBV status of NPC samples used for SNP array analysis. Genomic DNA was extracted from microdissected NPC tumour cells and amplified using a Genomiphi kit. 200 ng of DNA from each sample were used for analysis of EBV status by amplifying the BamHI-W-specific region using PCR. Products were viewed by agrose gel electrophoresis. All samples except MMAH showed the expected 114-base-pair amplified product.

4.4 SNP array analysis

Since matched normal DNA is not always available as a reference, the recent release of the initial phase of a haplotype map of the human genome provides an opportunity for un-paired analysis of SNP array data, which has been successfully used to detect genetic alterations. In our SNP array analysis, the copy number data were obtained by unpaired analysis using array data derived from 40 normal individuals (23 Chinese, 10 Japanese and 7 Utah residents of Central European descent), which were downloaded from the HapMap project **(http://www.hapmap.org/downloads/index.html.en).** The Affymetrix GeneChip Chromosome Copy Number Tool v4 using the default settings and Genotyping Console v2.1 (Affymetrix) with genomic smoothing set to 1Mb estimate the copy number of individual SNPs by comparing the signal intensity of each SNP from the tumour sample with the mean of the corresponding SNP in the reference set. The SNP call rates generated from the analysis reached above 90% in all the samples. To locate the genes implicated in the regions of chromosomal aberrations, the physical position of corresponding SNPs on the arrays was mapped according to the Human Genome (Build 35, hg17).

4.5 Genetic aberrations in NPC tumour cells

4.5.1 Overall genetic changes of NPC biopsies

Amplified DNA from 14 NPC biopsies and DNA from the C666-1 cell line were analysed on 500K SNP arrays. Extensive regions of chromosomal copy number changes and UPD were observed. The overall genetic aberrations are shown in Figure

4.3, which displays the frequency and patterns of the genetic aberrations across the whole genome in all the samples. The most frequent deletions are observed in chromosomes 3p, 5q, 9, 13q, 14q and 16, and frequent gains are observed in chromosomes 1q, 3q, 8 and 12. Chromosome 6 exhibits most frequent UPD. The minimal overlapping regions of copy number loss or gain in all the 14 biopsies were also determined and are summarised in Table 4.1. These results are in broad agreement with the data obtained from conventional and array-based CGH analyses in a number of previous studies. These have been reviewed and summarised by meta analysis (Li *et al.*, 2006) as well as a tree model analysis (Shih-Hsin Wu, 2006).

4.5.2 Genetic changes of the C666-1 cell line

500K SNP array analysis identified several extensive regions of genetic changes in the C666-1 cell line including chromosome losses on 6pter-q14, 11q14-qter and 18q21-qter, and chromosome gains on 7q, 8pter-p22, 8p12-q12, 14q21-23, and 16pter-q12. It also additionally identified several smaller regions of copy number changes such as small deletions on chromosome 3p, 5q, 6q, 8q, 12p and gains on chromosome 14q. The genetic changes in the C666-1 line are shown in Figure 4.4.

In the SNP array analysis, the C666-1 cell line has been used as a vehicle for validation of copy number predicted by SNP array data. Regions of chromosome 8 that showed gain, loss or no change in C666-1 DNA were examined by q-PCR using the genes FGF20, NRG1, KIAA1967, CLU and CYP7A1 as markers and confirmed the copy number changes predicted by SNP array analysis (Figure 4.5). As CYP7A1 showed two copies in C666-1 and also in most of the NPC biopsies examined by SNP

Figure 4.3: Summary of Gains, Losses and uni-parental disomy (UPD).

An overview of genetic changes of 22 chromosomes in a total of 14 microdissected NPC biopsies and cell line C666-1 is presented. “Genetic gains” are shown as blue arrows, “losses” as red arrows and “UPD regions” as green bars aligned along each chromosome in each sample.

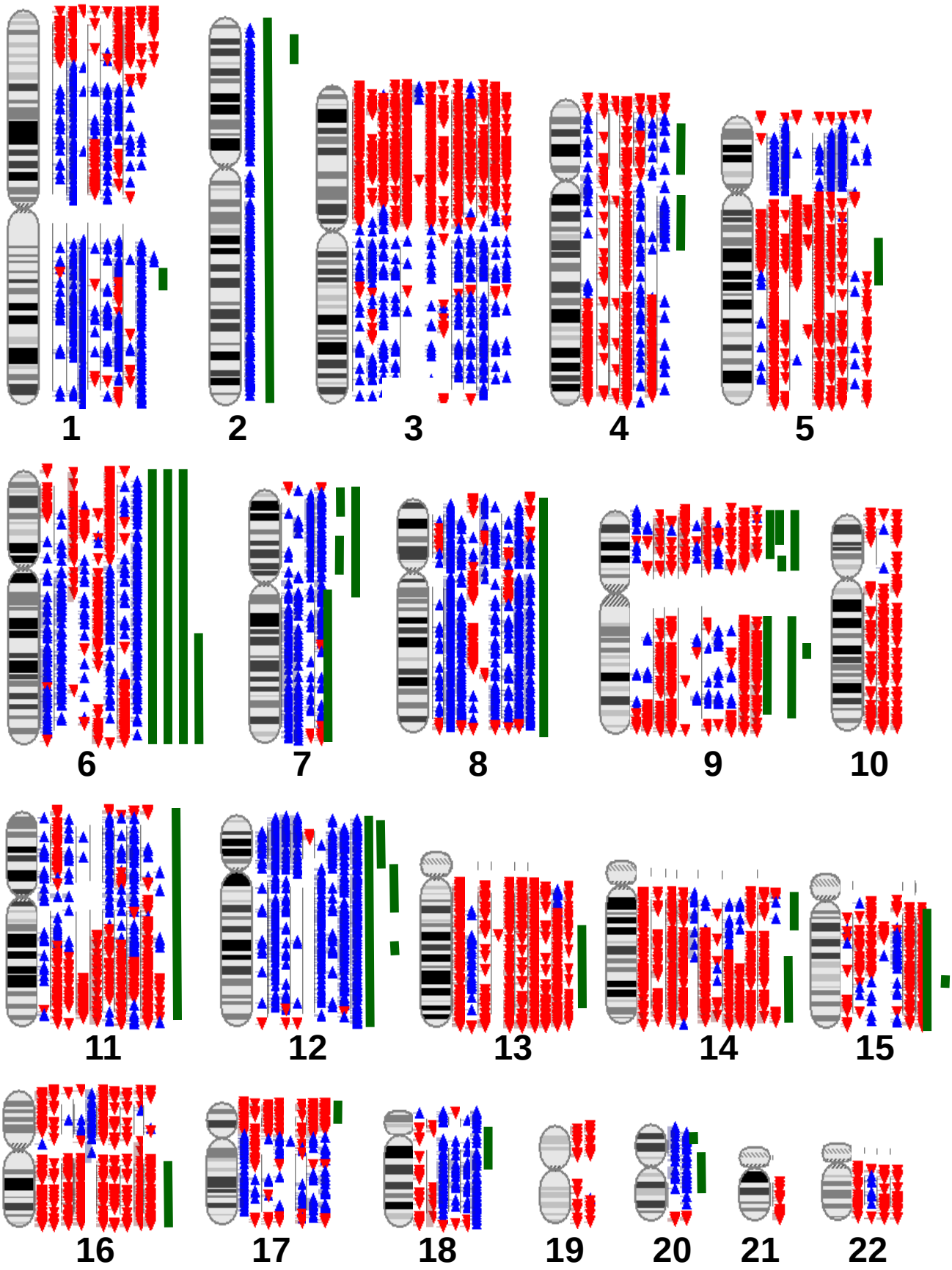
1
2
3
4
5
6
7
8
9
10
11
12
13
14
15
16
17
18
19
20
21
22

Table 4.1:

A. Minimal Regions of "Extensive" Loss in 14 Primary Tumours.

REGION	NUMBER	%
1pter - p35.1	6	43
1p22.1 - p13.3	3	21
3pter - p12.3	12	86
4p15.1 - p12	4	29
4q28.2 - qter	5	36
5q12.3 - q15	7	50
6p22.1 - p21.3	3	21
9pter - p21.2	7	50
9q12 - q32	4	29
9q34.11 - qter	8	57
10q21.1 - qter	3	21
11q22.3 - q23.3	9	64
13q	7	50
13q14.11 - 11qter	1	7 (57)
14q	6	43
14q24.2 - qter	2	14 (57)
15q14 - q21.1	5	36
16	5	36
16q	3	21 (57)
17p11.2 - pter	7	50

B. Minimal Regions of "Extensive" Gain in 14 Primary Tumours.

REGION	NUMBER	%
1p33 - p22.3	7	50
1q32.1 - q41	6	43
3q11.2 - q13.32	8	57
5p15.1 - p12	5	36
6q14.1 - 24.3	4	29
8p12 - q24.3	4	29
8q23.1 - q24.3	4	29 (58)
12p13.2 - p11.1	7	50
12q12 - q24.3	4	29

The numbers in parentheses indicate the frequency of chromosomal abnormality (including not only the smaller regions but also a larger region containing this smaller region).

Figure 4.4: Chromosomal copy number analysis of cell line C666-1.

C666-1 cell DNA was extracted and analysed on 500K SNP arrays. The traces show the log2 ratio of the copy number of C666-1 on several chromosomes compared to the reference. The "0" dashed line is used as a baseline to depict DNA copy number 2, and the solid black line represents the value of smoothed DNA copy number. It is defined as copy number loss if the value of the solid black line is below the "0", and defined as gain if above the "0" line. The sizes of the "small" deletions discussed in the text are indicated.

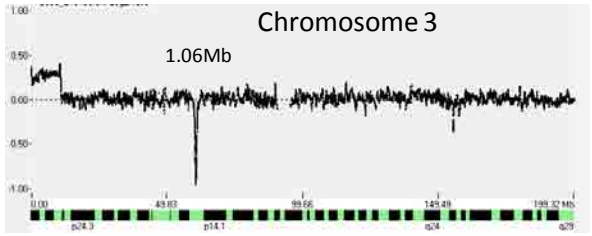
Chromosome 3
1.06Mb

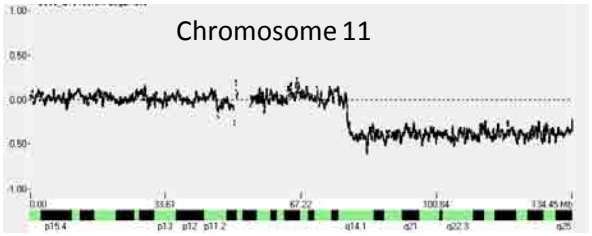
Chromosome 11

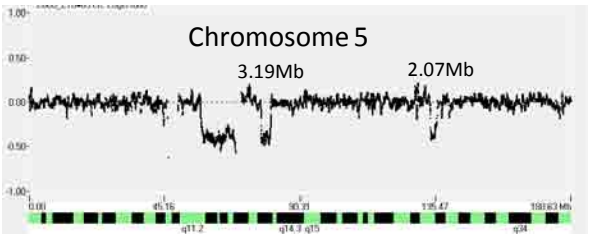
Chromosome 5
3.19Mb
2.07Mb

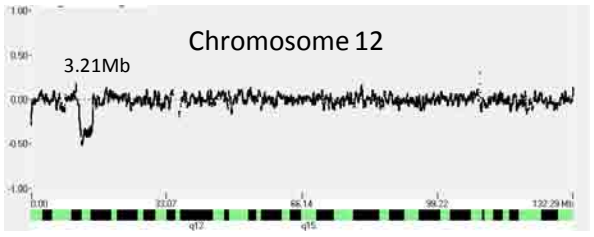
Chromosome 12
3.21Mb

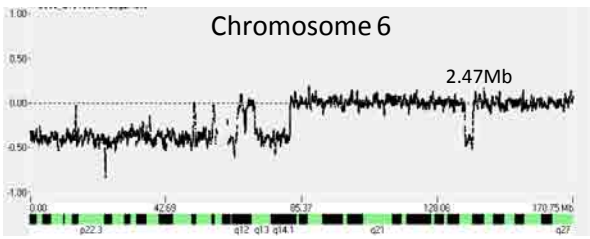
Chromosome 6
2.47Mb

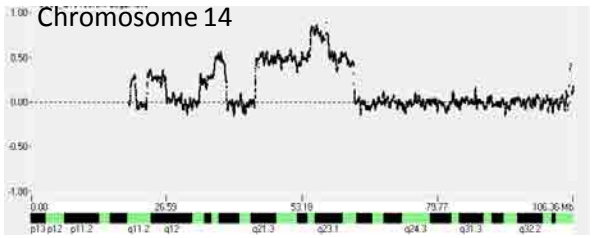
Chromosome 14

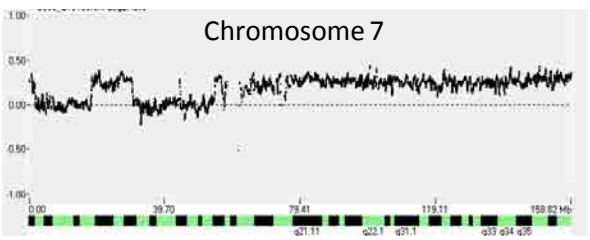
Chromosome 7

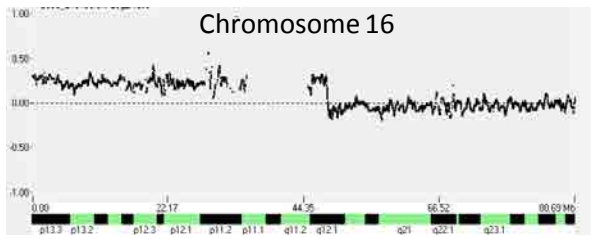
Chromosome 16

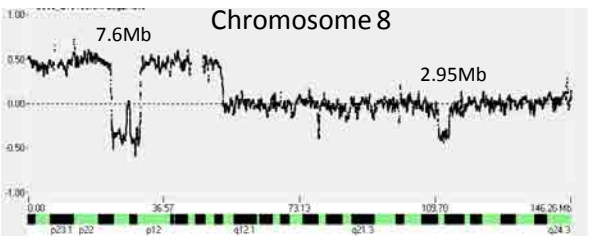
Chromosome 8
7.6Mb
2.95Mb

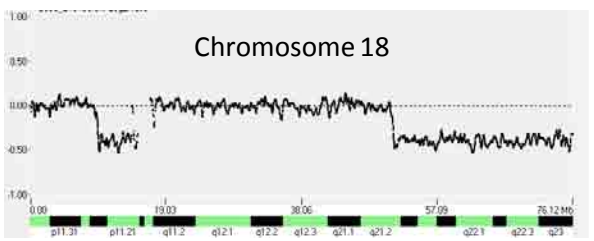
Chromosome 18

Figure 4.5: q-PCR validation of gene copy number changes on chromosome 8 in C666-1.

(A) The figure displays the genomic copy number trace of C666-1 on chromosome 8. The locations of the genes FGF20, KIAA1967, CLU, NRG1 and CYP7A1 are indicated by arrows.

(B) The copy number analysis software calculated these genomic regions respectively as having a copy number of 4, 1, 1, 4 and 2 (purple columns). Genomic q-PCR validation of the copy number within these regions gave values of, respectively, 4.8, 1.2, 1.1, 4.4 and 2.0 (blue columns).

A

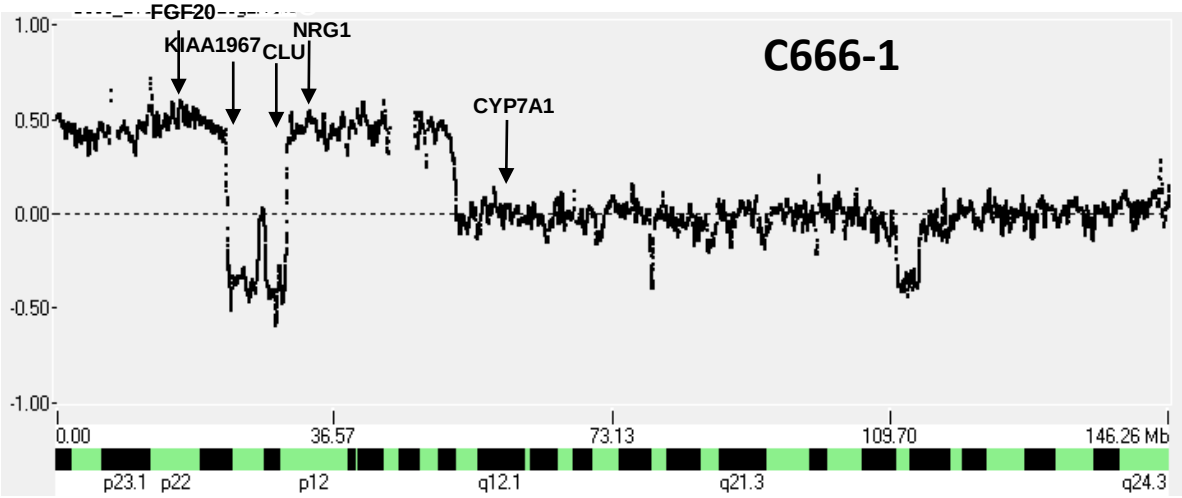
FGF20
KIAA1967
CLU
NRG1
CYP7A1
C666-1
1.00
0.50
0.00
-0.50
-1.00
0.00
36.57
73.13
109.70
146.26 Mb
p23.1
p22
p12
q12.1
q21.3
q24.3

B

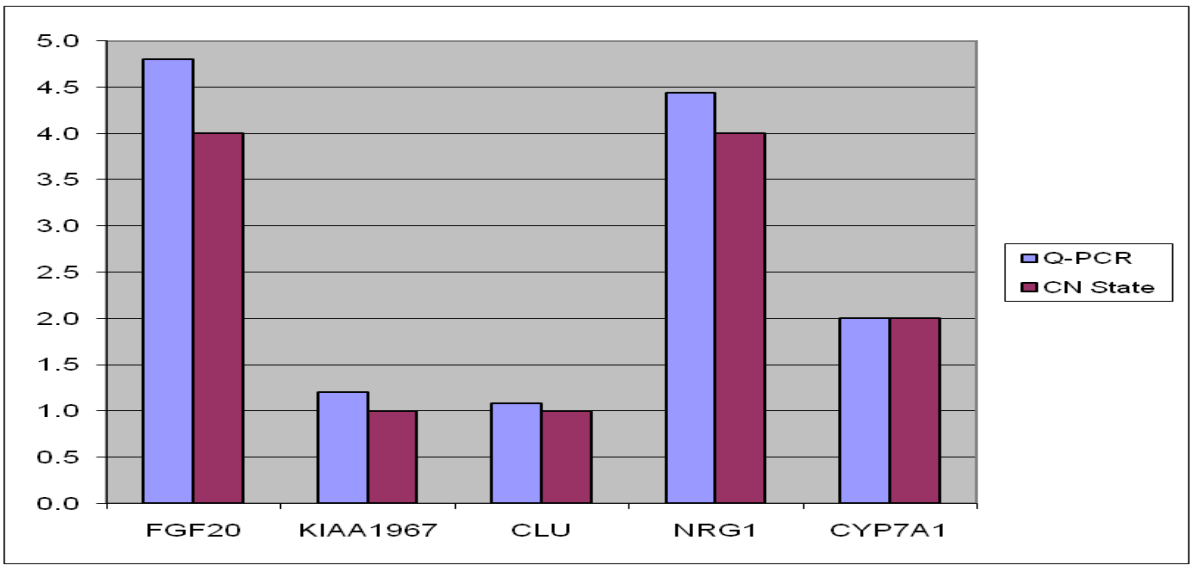
5.0
4.5
4.0
3.5
3.0
2.5
2.0
1.5
1.0
0.5
0.0
FGF20
KIAA1967
CLU
NRG1
CYP7A1
Q-PCR
CN State

array, this gene was used as a reference gene when determining the copy number of other genes of interest by q-PCR analyses.

4.5.3 Small copy number changes

The 500K SNP array analysis takes advantage of its enhanced resolution and delineates more precise physical boundaries of chromosomal breakpoints in NPC. As a result, a number of substantially smaller regions of copy number changes have been identified. Although both the extensive and smaller chromosomal abnormalities are supposed to be critical for NPC pathogenesis, the smaller aberrations allow us more easily to pinpoint the genes involved. Especially, those common minimum regions of chromosomal loss or gain often contain genes that may play important roles in the process of cancer development. By integrating the Human Genome (Build 35, hg17) and DNA copy number data obtained from SNP array analyses, the genes encoded in the smaller regions of genetic alterations are defined. Some of the genes are well-known TSGs or oncogenes already identified previously in NPC or other types of tumour, whereas others have not been reported before but might be potential NPC-related genes. On this basis, the minimal segments of genetic copy number changes and genes included are summarised in Table 4.2. Here, we will draw attention to these small genetic changes. Q-PCR data are used to validate the copy number changes of genes located in the corresponding loci. In addition, the copy number data were analysed in the context of their expression at the RNA level determined by expression array analysis. Some of them were also analysed at the protein level by IHC staining.

Table 4.2: Small regions of copy number change and the genes included.

SMALL LOSSES					
Chromosomal Locus	**Physical position**		**Minimum Common Loss**	**Number Showing Loss**	**Genes Within Minimum Region**
	Start	**Stop**			
3p14.2	59964552	61028019	1.06Mb	12	FHIT
4q13.1	63804596	66196603	2.40Mb	1	SRD5A2L2, EPHA5
5q14.1	77358197	80545692	3.19Mb	9	22 genes including THBS4, MSH3, RASGRF2
5q31.1-31.2	133726836	135799356	2.07Mb	7	24 genes including PITX1, CXCL14, TGFBI
5q11.2	50425128	54143484	3.72Mb	3	12 genes including ITGA2
6q23.3	136679431	138220854	1.54Mb	3	MAP7, MAP3K5, PEX7, IL20R1, IFNGR1, OLIG3, TNFAIP3
8p21.3-p12	22533530	27843228	5.31Mb	3	44 genes including TNFRSF10B, CLU
9p21.3	21717208	22014351	297kb	12	MTAP, CDKN2A, CDKN2B
9p23-p22.3	13606431	14329236	723kb	7	NFIB
14q11.2-q12	21631939	23934069	2.30Mb	7	58 genes including TINF2
1p13.1 – p12	117391884	118686724	1.29Mb	1	TTF2, TRIM45, VTCN1, MAN1A2, FAM46C, GDAP2, WDR3, SPAG17
1q25.3	181280422	183870395	2.59Mb	2	LAMC2, NMNAT2, SMG7, NCF2, RGL1, APOBEC4, GLT25D2, C1orf19,21,25,26, EDEM3, FAM129A, RNF2, IVNS1ABP
8q23.1-q23.3	110401143	113408633	3.01Mb	1	77 genes including PKHD1L1, EBAG9, GOLSYN, KCNV1
12p13.2-p12.3	11853840	15065706	3.21Mb	1	35 genes including CDKN1B
SMALL AMPLIFICATION					
8p11.22-11.21	39740721	42425970	2.69Mb	1	INDOL1, C8orf4, ZMAT4, SFRP1, GOLGA7, GINS4, AGPAT6, ANK1, MYST3, AP3M2, PLAT, IKBKB, POLB, DKK4
SMALL GAINS					
1q41-q42.11	220828751	222157313	1.33Mb	7	9 genes including AIDA, SUSD4 and TP53BP2
17q11.2	25273428	25728007	455kb	2	EFCAB5, CCDC55, SLC6A4, BLMH, TMIGD1

Chromosome 3

12 out of 15 NPC samples showed extensive loss of chromosome 3p. Three samples (MKAV, MMAH and C666-1) did not follow this pattern. Uniquely, C666-1 displayed only a 1.06Mb homozygous deletion at 3p14.2 and this region appeared to be diploid in only three samples (MKAV, MMAH, and 235326) (Figure 4.6 A). A well-known TSG, FHIT, is located in this small region. We designed a q-PCR primer/probe set specific for the FHIT deleted locus and confirmed the copy number predicted by SNP array in 8 samples (Figure 4.6 B). Deletion of 3p14.2 and inactivation of FHIT has been frequently observed in NPC tumours (introduced in Section 1.4.2.1), whereas our SNP array delineating the finer boundary of deletion at this minimal locus further suggests that FHIT is a critical TSG whose aberration might contribute to NPC development and progression. However, functional investigation of this gene is required for understanding its particular role in carcinogenesis.

Chromosome 4

A 2.4Mb region of loss at 4q13 containing two genes called SRD5A2L2 and EPHA5 (ephrinA5) was observed in only one sample (XY8) (Figure 4.7). The function of SRD5A2L is poorly understood so far, whereas a recent study of ephrinA5 in breast cancer reveals that the expression of ephrinA5 was significantly decreased in breast cancers compared to their normal control (Fu *et al.*, 2009), indicating its potential TSG function. In our expression array data, ephrinA5 was called “absent” by GCOS in most of the NPC tumour and normal epithelial samples and therefore changes in expression could not be determined.

Figure 4.6: Small deletions on chromosome 3p.

(A) Extensive deletions were found in most of the NPC biopsies. C666-1 displayed only a 1.06Mb deletion at 3p14.2. This is labelled by black lines and arrows. This region was diploid in only three samples (MKAV, MMAH, and 235326). The tumour suppressor gene FHIT is within this small deletion.

(B) Comparison of DNA copy number in the FHIT gene locus identified by SNP array analysis (purple columns) and q-PCR analysis (blue columns) in 9 samples.

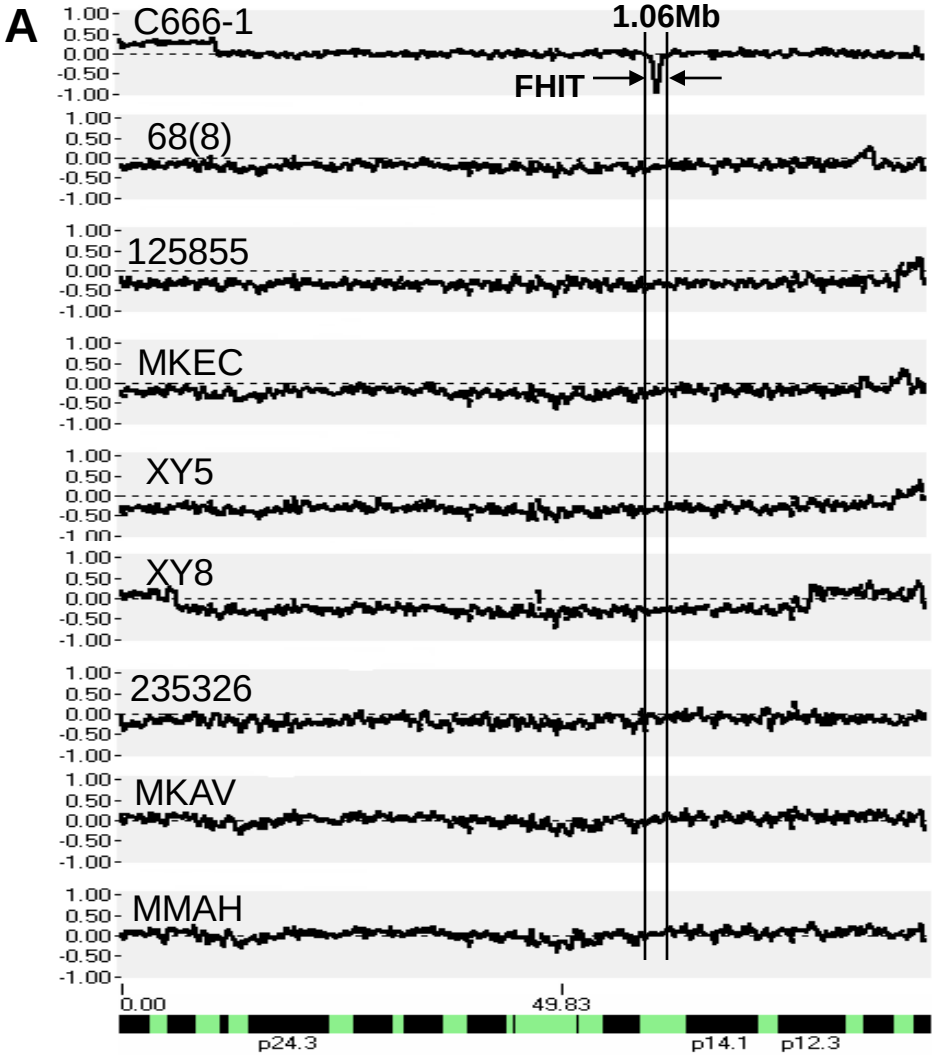
A
C666-1
1.06Mb
FHIT
68(8)
125855
MKEC
XY5
XY8
235326
MKAV
MMAH
1.00
0.50
0.00
-0.50
-1.00
0.00
49.83
p24.3
p14.1
p12.3

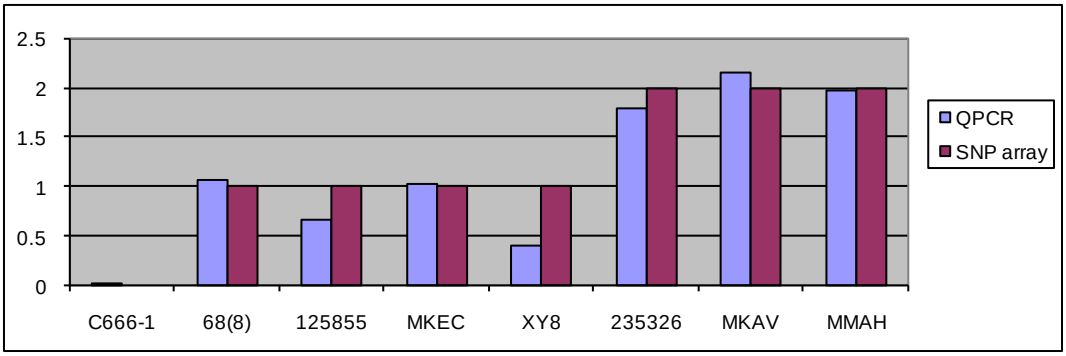
B
2.5
2
1.5
1
0.5
0
C666-1
68(8)
125855
MKEC
XY8
235326
MKAV
MMAH
QPCR
SNP array

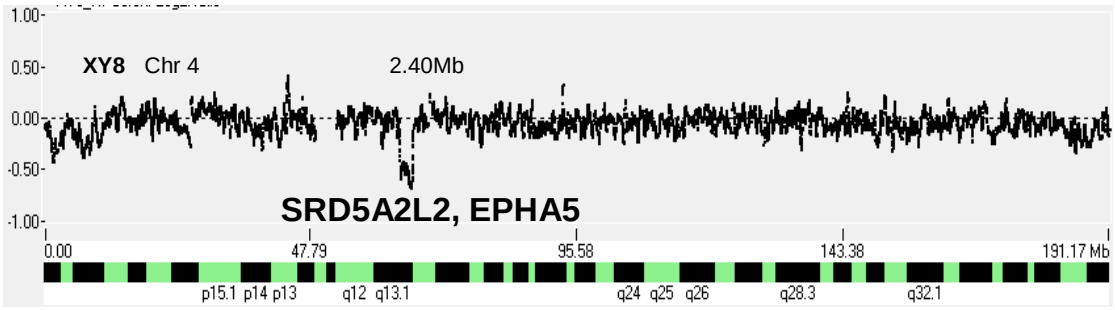

Figure 4.7: Small deletion on chromosome 4. A 2.40Mb region of loss at 4q13 containing two genes called SRD5A2L2 and ephrinA5 (EPHA5) was found in one sample (XY8).

Chromosome 5

C666-1 contained two regions of loss on chromosome 5. The first deletion, a 3.19 Mb region at 5q14.1 was also within larger regions of loss in a further 8 samples (173570, 235326, MMAH, MKEC, XY5, XY8, XY16, XY23) and encodes 22 genes, including RASGRF2, MSH3 and THBS4 (Figure 4.8 A), whose reduced expression has been associated with tumourigenesis. RASGRF2 was found to be down-expressed in human non-small cell lung cancer (Chen *et al.*, 2006), but the precise function of this gene remains to be elucidated. MSH3 is a mismatch repair gene, genetic alterations such as LOH in cancer have been reported before (Benachenhou *et al.*, 1999), and down-regulation of MSH3 was observed in bladder cancer compared to their normal counterparts (Kawakami *et al.*, 2004). In the expression array data, MSH3 was shown to be down-regulated at the RNA level in 38% (6/16) tumours of which four are haploid samples (C666-1, 173570, XY8, XY23) and two are diploid (68(8) and MDIG) (Figure 4.8B, upper, left panel). IHC staining in paired NPC tumour and normal epithelial tissue array revealed MSH3 expression was reduced in 83.3% (15/18) tumours (Figure 4.8B, upper, right panel).

The second deletion is a region of 2.07Mb, at 5q31.1-31.2, and this region was also encompassed by larger deletions in 6 more samples (68(8), 173570, MKEC, MMAH, XY8 and XY6). 24 genes including PITX1, CXCL14 and TGFBI are within this deletion (Figure 4.8A). PITX1 was recently identified as a tumour suppressor gene, inhibition of which induces the RAS pathway and tumourigenicity (Kolfschoten *et al.*, 2005), whereas expression of PITX1 leads to cell-cycle arrest and apoptosis by transcriptional activation of p53 (Liu & Lobie, 2007). Reduced expression of PITX1

Figure 4.8: Small deletions at 5q14.1 and 5q31.1-31.2.

(A) C666-1 exhibits two small regions of loss on chromosome 5. Deletion 1, located at 5q14.1 is labelled between two black arrows and contains the genes RASGRF2, MSH3 and THBS4. Deletion 2 is at 5q31.1-31.2 and includes the genes PITX1, CXCL14 and TGFBI.

(B) MSH3 expression was analysed using expression arrays and IHC. The upper left panel shows normalised expression array intensities for the 4 normal samples (grey) and 15 NPCs plus C666-1 (red), whilst the upper right panel shows the IHC scoring results from the tissue arrays (normal, grey: tumour, red). The bottom panels show examples of IHC staining in NPC tumour (T) and normal epithelial cells (N). At the RNA and protein levels respectively, MSH3 is downregulated in 6/16 (38%) and 15/18 (83%) samples. Copy number analysis at the MSH3 locus showed four of the six downregulated samples (173570, XY8, C666-1 and XY23) to be haploid (red arrows), whilst the other two (MDIG and 68(8)) were diploid (green arrows). Three more haploid samples (MKEC, XY5 and MMAH) (black arrows) did not appear to be downregulated at the RNA level.

(C) The figure shows normalised expression array intensities for the 4 normal samples (grey) and 15 NPCs plus C666-1 (red). At the RNA level, PITX1 is down-regulated in all the tumours (left panel), and CXCL14 is down-regulated in 75% (12/16) tumours (right panel).

(D) TGFBI expression was analysed using expression arrays and IHC. At the RNA and protein levels respectively, TGFBI is upregulated in 10/16 (63%) and 7/13 (54%) samples. Haploid samples are indicated by red arrows.

A

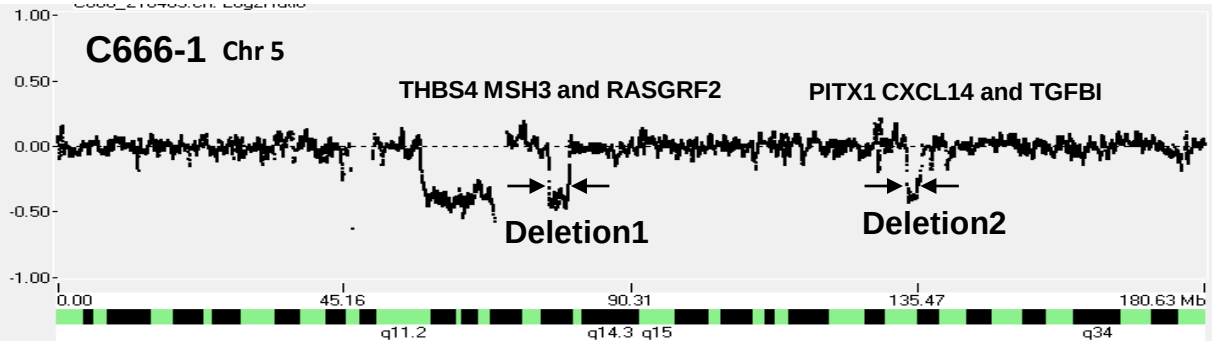
C666-1 Chr 5
THBS4 MSH3 and RASGRF2
PITX1 CXCL14 and TGFBI
Deletion1
Deletion2
1.00
0.50
0.00
-0.50
-1.00
0.00
45.16
90.31
135.47
180.63 Mb
q11.2
q14.3 q15
q34

B

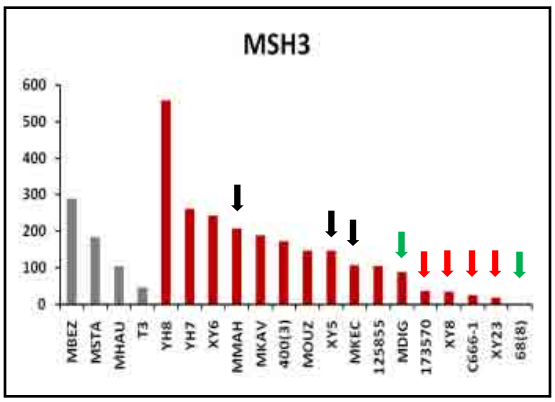
MSH3
600
500
400
300
200
100
0
MBEZ
MSTA
MHAU
T3
YH8
YH7
XY6
MMAH
MKAV
400(3)
MOUZ
XY5
MKEC
125855
MDIG
173570
XY8
C666-1
XY23
68(8)

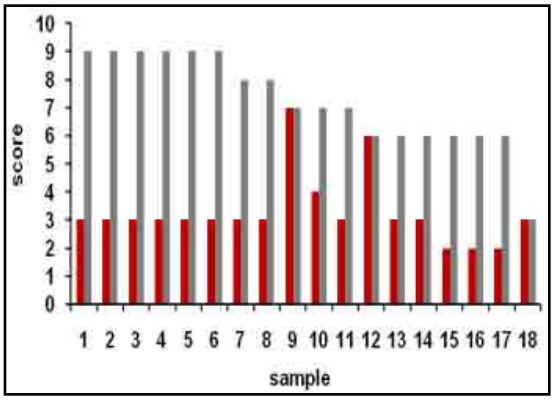
score
10
9
8
7
6
5
4
3
2
1
0
1 2 3 4 5 6 7 8 9 10 11 12 13 14 15 16 17 18
sample

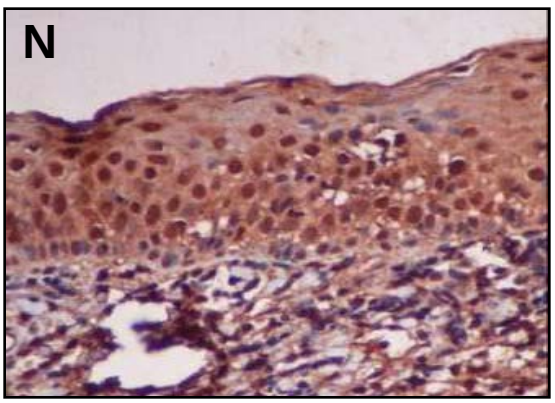
N

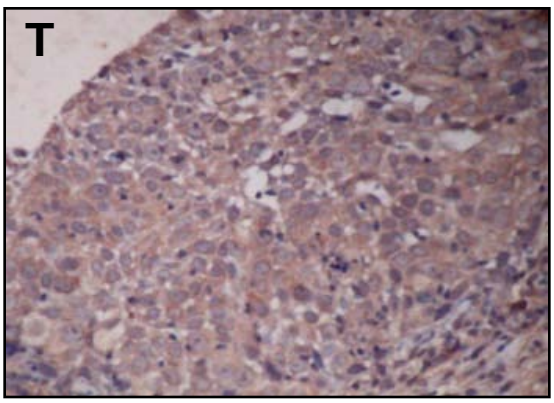
T

C

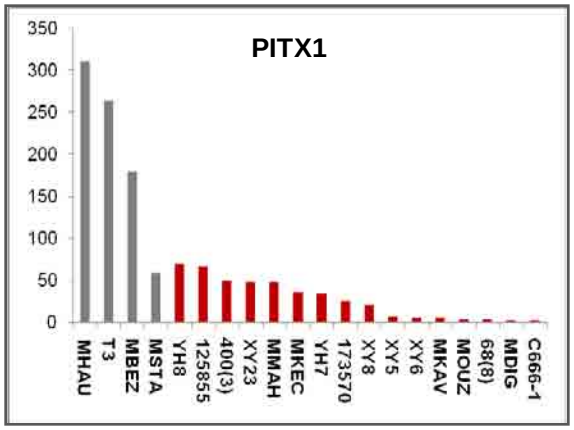
PITX1
350
300
250
200
150
100
50
0
MHAU
T3
MBEZ
MSTA
YH8
125855
400(3)
XY23
MMAH
MKEC
YH7
173570
XY8
XY5
XY6
MKAV
MOUZ
68(8)
MDIG
C666-1

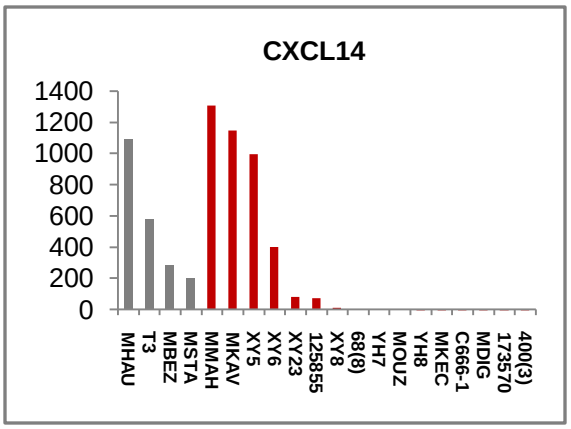
CXCL14
1400
1200
1000
800
600
400
200
0
MHAU
T3
MBEZ
MSTA
MMAH
MKAV
XY5
XY6
XY23
125855
XY8
68(8)
YH7
MOUZ
YH8
MKEC
C666-1
MDIG
173570
400(3)

D

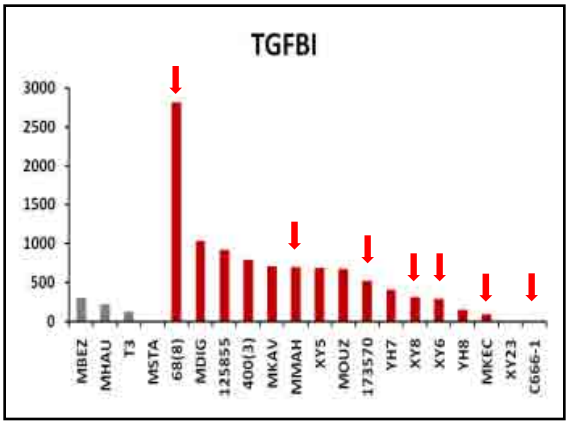
TGFBI
3000
2500
2000
1500
1000
500
0
MBEZ
MHAU
T3
MSTA
68(8)
MDIG
125855
400(3)
MKAV
MMAH
XY5
MOUZ
173570
YH7
XY8
XY6
YH8
MKEC
XY23
C666-1

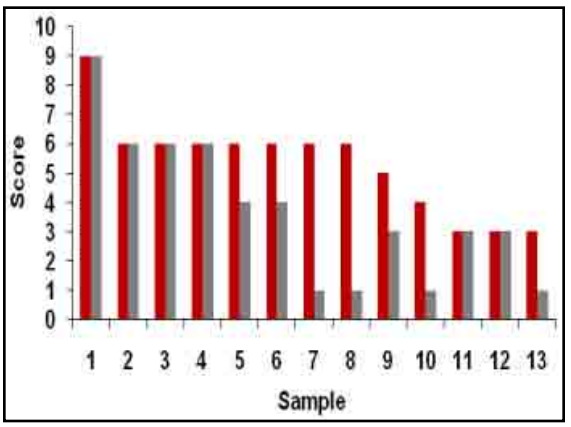
Score
10
9
8
7
6
5
4
3
2
1
0
1
2
3
4
5
6
7
8
9
10
11
12
13
Sample

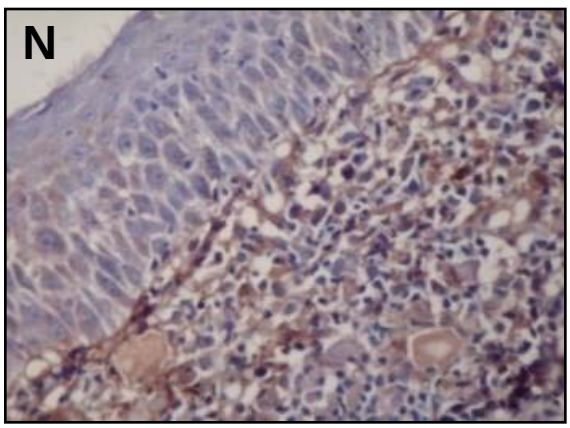
N

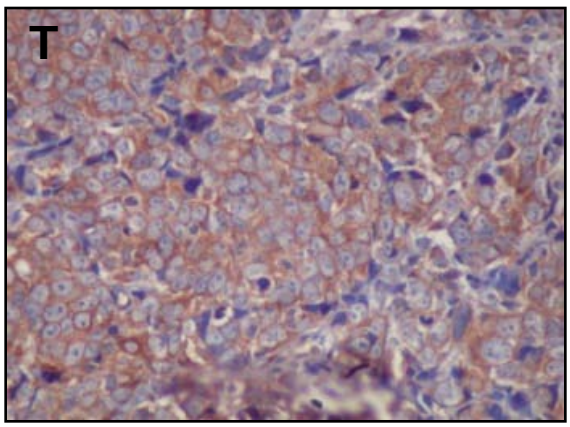
T

has been observed in oesophageal carcinoma (Lord *et al.*, 2005), gastric cancer (Chen *et al.*, 2008), prostate and bladder cancers (Kolfschoten et al., 2005). CXCL14 is a chemokine, and loss of CXCL14 expression was found in tongue squamous cell carcinoma (Shellenberger *et al.*, 2004). The expression of CXCL14 has been shown to suppress tumour growth in oral carcinoma and prostate cancer (Schwarze *et al.*, 2005; Ozawa *et al.*, 2006). In the expression data, PITX1 was down-regulated in all the tumours (Figure 4.8 C, left panel) and CXCL14 was found to be down-regulated in 75% (12/16) tumours (Figure 4.8 C, right panel). However, TGFBI, although being single copy in a number of samples, was up-regulated in 63% (10/16) tumours (Figure 4.8 D, upper left panel). IHC staining revealed that the expression of this gene was increased in 54% (7/13) tumours at the protein level (Figure 4.8 D, upper right panel). TGFBI expression is induced by transforming growth factor-beta and acts to inhibit cell adhesion. The expression and function of TGFBI in cancers appears to be context dependent. Loss of TGFBI expression has been reported in breast cancer (Calaf *et al.*, 2008) as well as lung cancer (Zhao *et al.*, 2006), and correlates with tumour formation and progression. However, in colon cancer, TGFBI was overexpressed and was associated with increased metastatic potential and poor patient prognosis (Ma *et al.*, 2008).

Another locus, a 3.72 Mb loss at 5q11.2 was observed in MOUZ (Figure 4.9 A), and this segment was also included within larger deletions of samples 173570 and MKEC. 58 genes including ITGA2 are encoded in this region. ITGA2 was down-regulated at the RNA level in 81% (13/16) tumours (Figure 4.9 B, upper left panel). This was further confirmed by IHC staining as reduced protein expression in 78% (14/18) tumours (Figure 4.9 B, upper right panel). ITGA2 belongs to the integrin alpha chain

Figure 4.9: Small deletions at 5q11.2.

(A) A 3.72 Mb region of loss at 5q11.2 in sample MOUZ is labelled between two black arrows. The gene ITGA2 is encoded in this region.

(B) The expression of integrin alpha 2 (ITGA2) was analysed by expression array and IHC. The upper left panel shows normalised expression array intensities for the 4 normal samples (grey) and 15 NPCs plus C666-1 (red), whilst the upper right panel shows the IHC scoring results from the tissue arrays (normal, grey: tumour, red). The bottom panel shows examples of IHC staining in NPC tumour (T) and normal epithelial cells (N). At the RNA and protein levels respectively, ITGA2 is downregulated in 13/16 (81%) and 14/18 (78%) samples. Haploid samples are indicated by red arrows.

A

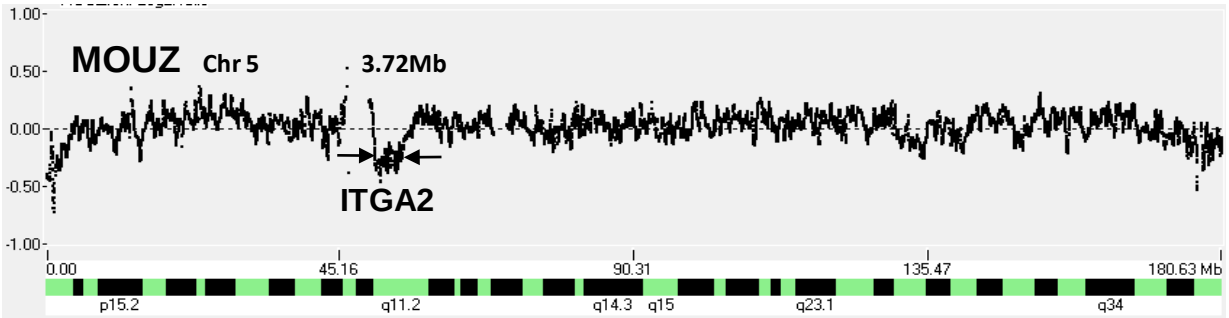
MOUZ
Chr 5
3.72Mb
ITGA2
1.00
0.50
0.00
-0.50
-1.00
0.00
45.16
90.31
135.47
180.63 Mb
p15.2
q11.2
q14.3
q15
q23.1
q34

B

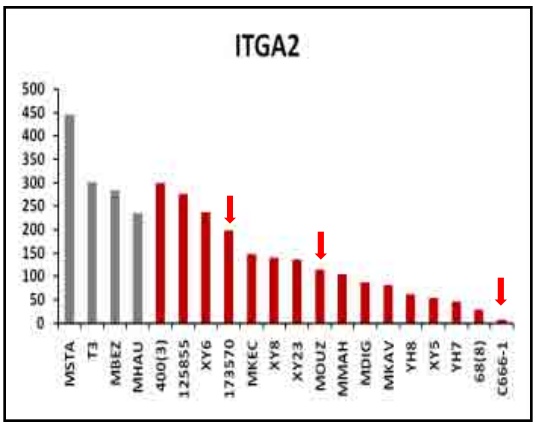
ITGA2
500
450
400
350
300
250
200
150
100
50
0
MSTA
T3
MBEZ
MHAU
400(3)
125855
XY6
173570
MKEC
XY8
XY23
MOUZ
MMAH
MDIG
MKAV
YH8
XY5
YH7
68(8)
C666-1

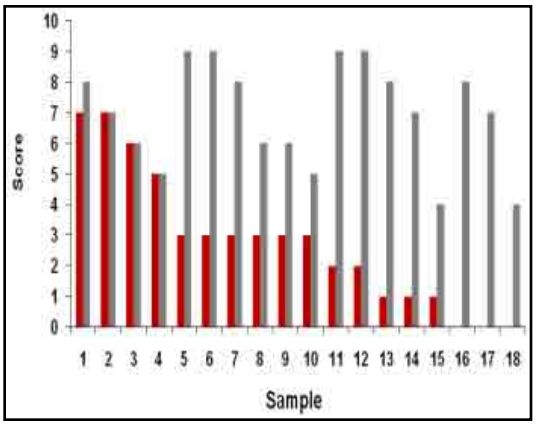
Score
10
9
8
7
6
5
4
3
2
1
0
1 2 3 4 5 6 7 8 9 10 11 12 13 14 15 16 17 18
Sample

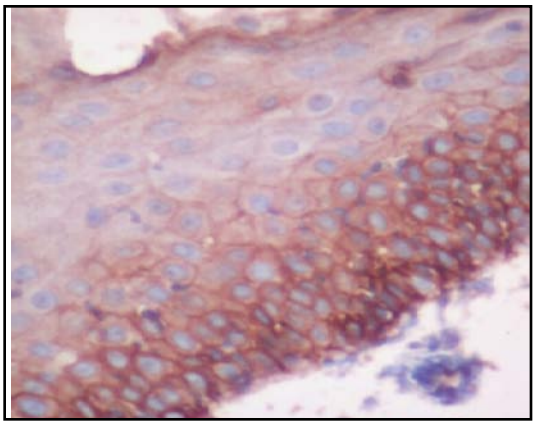

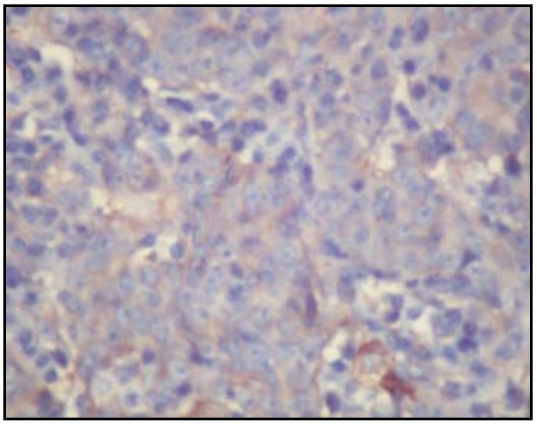

family that is involved in cell adhesion and also participates in cell-surface mediated signalling. Reduction of ITGA2 expression was previously reported to be related to cell immortalisation and malignant progression in oesophageal keratinocytes (Sashiyama *et al.*, 2002).

Chromosome 6

Two samples (C666-1, XY5) showed a 1.54Mb region of loss at 6q23.3, while sample MDIG showed a big deletion in 6q including the loss of 6q23.3. 7 genes (MAP7, MAP3K5, PEX7, IL20RA, IFNGR1, OLIG3, TNFAIP3) are included in this small deletion (Figure 4.10A). q-PCR validations for MAP3K5 and IL20RA confirmed the copy number predicted by SNP array (Figure 4.10B). Among the above 7 genes, TNFAIP3 is considered to be a potential NPC-associated oncogene (Section 1.4.3). Expression data revealed that MAP7 was down-regulated in 94% (15/16) tumours at the RNA level (Figure 4.10C). Although the function of MAP7 in cancers is still unclear, it is predominantly expressed in cells of epithelial origin and is thought to be involved in microtubule dynamics, which is essential for cell polarisation and differentiation (Suzuki *et al.*, 2003).

Chromosome 8

On chromosome 8, both copy number loss and gain have been observed in the C666-1 cell line. Two regions of loss are included in C666-1 cell line. One is a 3.01 Mb loss at 8q23.1 – q23.3 that is described later. Another is a 7.6 Mb region of loss at 8p21.3-p12 that is partially overlapped by deletions in samples XY5 and MMAH. The common region of loss (5.31 Mb) in all three contains 44 genes including the gene CLU (clusterin) (Figure 4.11A). Copy number loss of CLU in C666-1 was confirmed

Figure 4.10: **Deletions on chromosome 6.**

(A) Samples C666-1, XY5 and MDIG showed a minimal 1.5Mb common region of loss at 6q23.3 as the region labelled with black lines and arrows. Genes MAP7, MAP3K5, PEX7, IL20RA, IFNGR1, OLIG3 and TNFAIP3 are included in this small deletion.

(B) Comparison of DNA copy number in NPC tumours at the MAP3K5 and IL20RA loci predicted by SNP array data (purple columns) and q-PCR analysis (blue columns).

(C) Normalised expression array intensities for MAP7 in the 4 normal samples (grey) and 15 NPCs plus C666-1 (red) shows MAP7 is down-regulated in 94% (15/16) tumours.

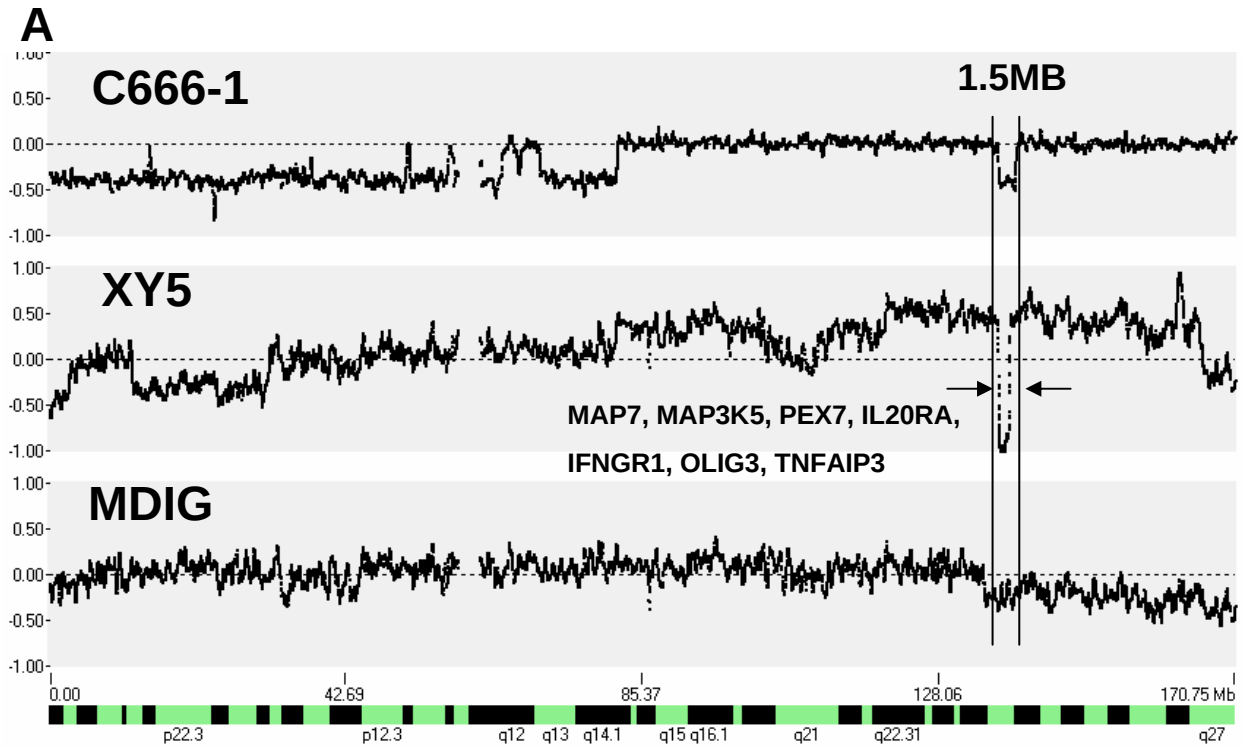
A
C666-1
1.5MB
XY5
MAP7, MAP3K5, PEX7, IL20RA,
IFNGR1, OLIG3, TNFAIP3
MDIG
0.00
42.69
85.37
128.06
170.75 Mb
p22.3
p12.3
q12
q13
q14.1
q15 q16.1
q21
q22.31
q27

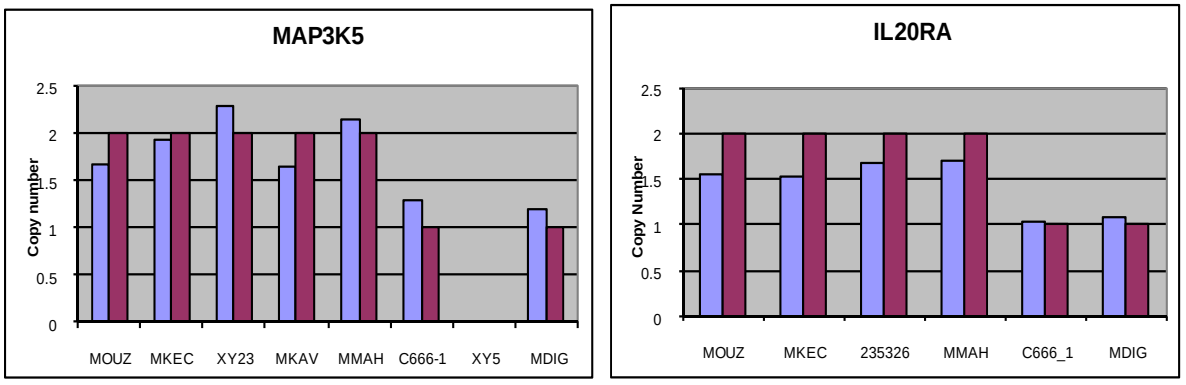
B
MAP3K5
Copy number
MOUZ
MKEC
XY23
MKAV
MMAH
C666-1
XY5
MDIG
IL20RA
Copy Number
MOUZ
MKEC
235326
MMAH
C666_1
MDIG

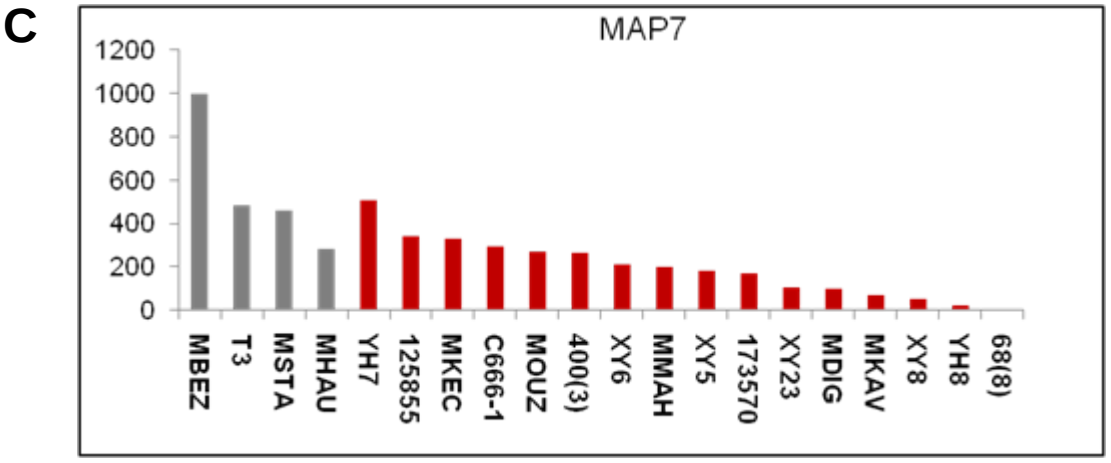
C
MAP7
MBEZ
T3
MSTA
MHAU
YH7
125855
MKEC
C666-1
MOUZ
400(3)
XY6
MMAH
XY5
173570
XY23
MDIG
MKAV
XY8
YH8
68(8)

by qPCR analysis (see Figure 4.5B). Expression array data revealed that CLU was down-regulated in all 16 NPCs (Figure 4.11B). In addition, IHC staining in tumour and normal samples showed down-expression of clusterin at the protein level in 100% (13/13) NPCs (Figure 4.11B). CLU is a multivalent glycoprotein with ubiquitous tissue distribution and appears to be involved in several basic biological events including cell death, apoptosis, and tumour progression. CLU has been shown to be downregulated during prostate cancer onset and progression, and its upregulation inhibits DNA synthesis and cell cycle progression of immortalised human prostate epithelial cells (Bettuzzi *et al.*, 2002; Caccamo *et al.*, 2003).

A 2.69 Mb minimal overlapping region of gain at 8p11.22 – 11.21 was found in 7 samples (173570, C666, MKAV, MKEC, MMAH, XY8 and XY16). Sample 173570 exhibited the minimum region of change (Figure 4.12A). The Affymetrix copy number algorithm defines copy number state only up to a maximum of ≥4 and therefore q-PCR analysis at the IKBKB locus was used to confirm the copy number gain in this sample. This suggested that this region was actually amplified to 8-9 copies (Figure 4.12B). This is the only example of an amplification (5 or more copies), rather than a gain, that is found in the cases under study. In expression array data the relative mRNA levels of the genes encoded in this amplified region were visualised using dChip software, which revealed that the majority of genes throughout this region have a higher expression level in the amplified sample (173570) but were relatively unchanged in samples with two or three copies (Figure 4.12C).

Figure 4.11: Small deletions at 8p21.3-p12.

(A) C666-1 exhibits two small regions of loss, a 7.6Mb region of loss at 8p21.3-p12 in which the gene CLU is encoded as labelled between two black arrows, and a 3.01Mb loss at 8q23.1 – q23.3.

(B) The expression of CLU was analysed with expression array and IHC. The upper left panel shows normalised expression array intensities for the 4 normal samples (grey) and 15 NPCs plus C666-1 (red), whilst the upper right panel shows the IHC scoring results from the tissue arrays (normal, grey: tumour, red). The bottom panel shows examples of IHC staining in NPC tumour (T) and normal epithelial cells (N). At the RNA and protein levels respectively, CLU expression is downregulated in 16/16 (100%) and 13/13 (100%) samples. Haploid samples are indicated by red arrows.

A

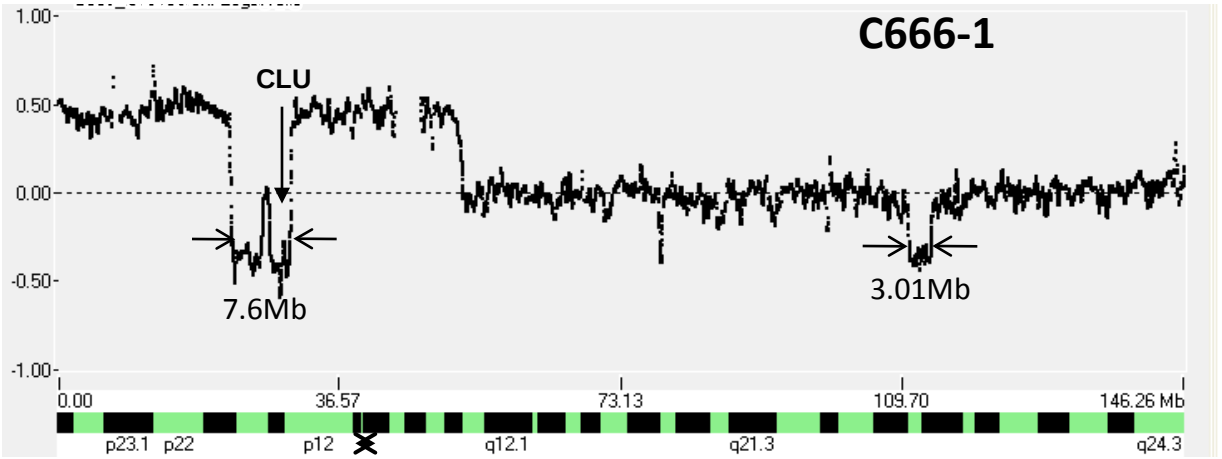
C666-1
CLU
1.00
0.50
0.00
-0.50
-1.00
7.6Mb
3.01Mb
0.00
36.57
73.13
109.70
146.26 Mb
p23.1
p22
p12
q12.1
q21.3
q24.3

B

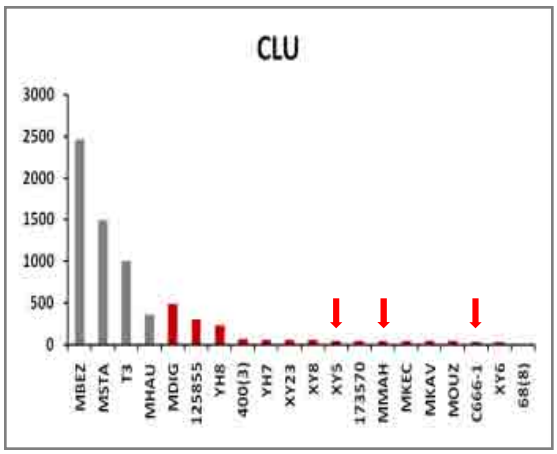
CLU
3000
2500
2000
1500
1000
500
0
MBEZ
MSTA
T3
MHAU
MDIG
125855
YH8
400(3)
YH7
XY23
XY8
XY5
173570
MMAH
MKEC
MKAV
MOUZ
C666-1
XY6
68(8)

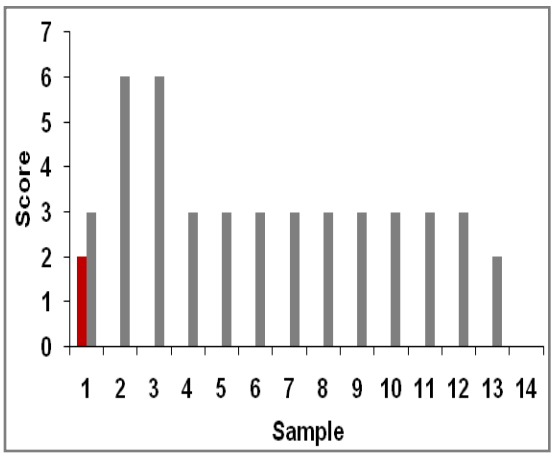
Score
7
6
5
4
3
2
1
0
1 2 3 4 5 6 7 8 9 10 11 12 13 14
Sample

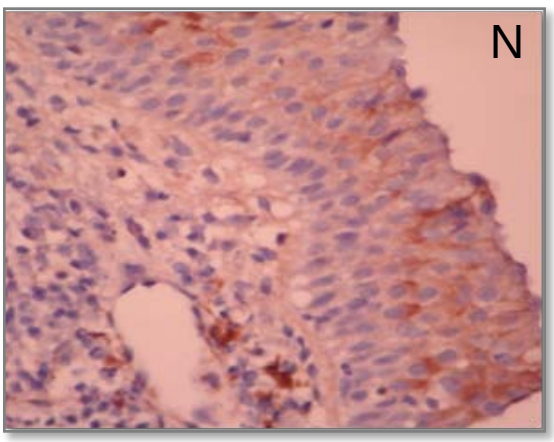
N

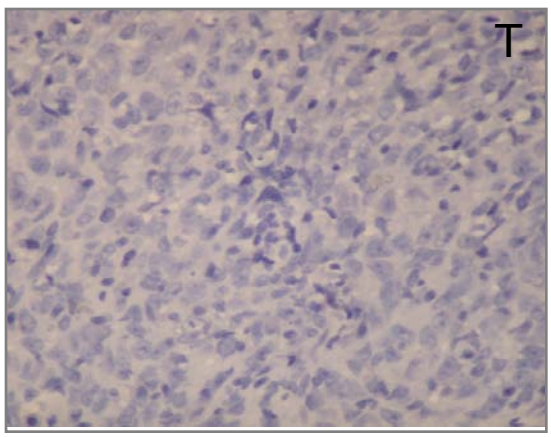
T

Figure 4.12: Amplification on chromosome 8.

(A) High-level amplification detected by SNP array at 8p11.22 – 11.21 in sample 173570. The amplicon size is approximately 2.69 Mb.

(B) The copy numbers of gene IKBKB calculated by SNP array are 2, 3 and 4 in sample XY23, C666-1 cells and 173570, respectively (purple columns), whereas they are 1.7, 3.6 and 8.7 as measured by q-PCR (blue columns).

(C) Heatmap of the relative expression levels of the genes found within the 8p11.22 – 11.21 amplified region of tumour 173570. The samples appear in columns with the 4 normal samples on the left whilst the individual genes within the amplified region form the rows. The relative expression level of each gene across all samples is indicated by colour with increasing expression being represented by the intensity of red and downregulation by the intensity of blue. No change is white. The brackets at the bottom indicate tumour samples with genome copy numbers of 2 or 3 throughout this region. Almost all genes in tumour 173570 are highly expressed as indicated by the intense red colour.

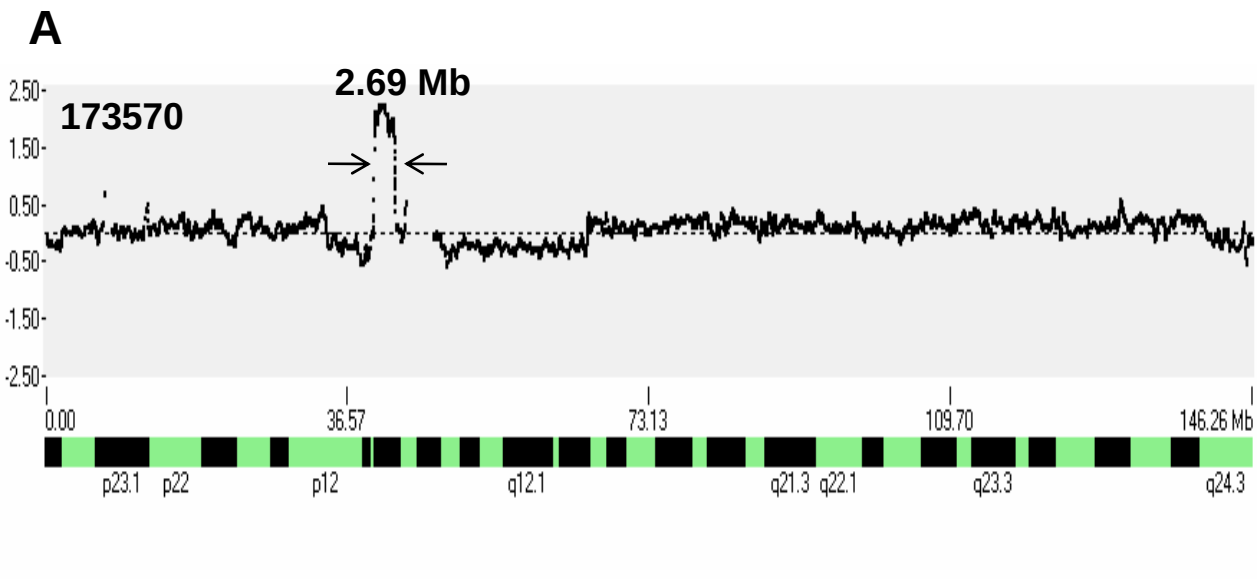
A
2.69 Mb
173570
2.50
1.50
0.50
-0.50
-1.50
-2.50
0.00
36.57
73.13
109.70
146.26 Mb
p23.1
p22
p12
q12.1
q21.3
q22.1
q23.3
q24.3

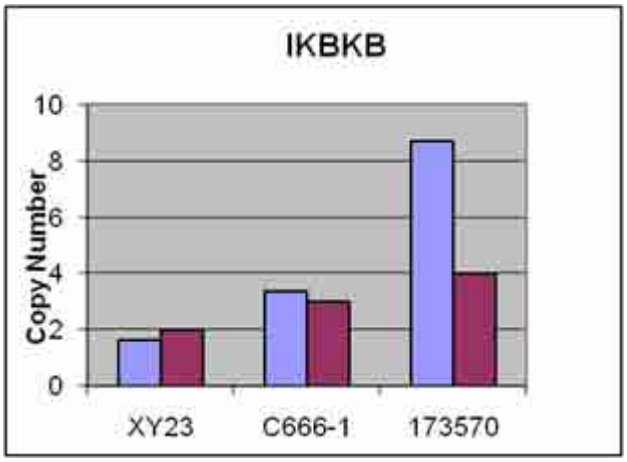
B
IKBKB
Copy Number
10
8
6
4
2
0
XY23
C666-1
173570

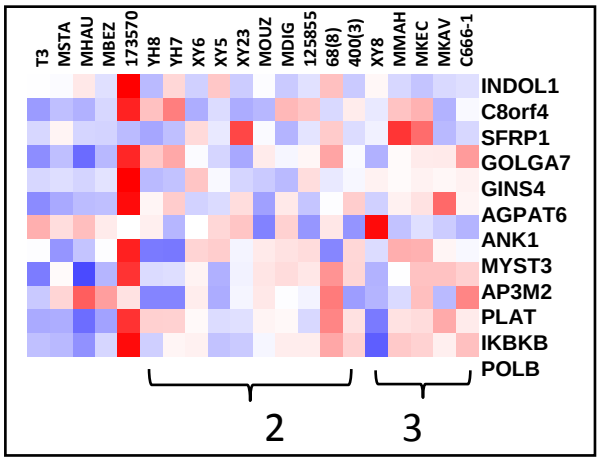
C
T3
MSTA
MHAU
MBEZ
173570
YH8
YH7
XY6
XY5
XY23
MOUZ
MDIG
125855
68(8)
400(3)
XY8
MMAH
MKEC
MKAV
C666-1
INDOL1
C8orf4
SFRP1
GOLGA7
GINS4
AGPAT6
ANK1
MYST3
AP3M2
PLAT
IKBKB
POLB
2
3

Chromosome 9

Loss of the 9p21.3 region was found in 12/15 (80%) of samples. The deletions in 5 samples (XY6, XY8, MMAH, 125855, and XY5) were relatively small (Figure 4.13A). The minimal overlapping region of loss was approximately 300Kb and contained the genes MTAP, CDKN2A and CDKN2B. Q-PCR validation was performed at the CDKN2A locus on 7 samples and confirmed the array-predicted copy number change (Figure 4.13B). Loss of 9p21 has been frequently detected in NPC tumours (see Section 1.4.2.1), and the SNP array data mapped the minimum deletion to 9p21.3 locus containing only three genes. This further suggests that aberrations of the genes involved are critical for NPC carcinogenesis. As described in Chapter 1, CDKN2A and CDKN2B are considered to be important NPC-associated TSGs and their functions have been extensively investigated. In expression array data, although expression in the normal samples was somewhat variable (being called "present" in only 3 of the 4), it was expressed at low levels in several tumours, being called "absent" in 7/16 (44%). Moreover, a relatively low level of expression was observed in the samples showing small deletions (Figure 4.13C). Although the function of the co-deleted gene (MTAP) has not been investigated in NPC, it has been shown to be downregulated in a number of cancers and contributes to carcinogenesis (Christopher *et al.*, 2002; Hustinx *et al.*, 2005; Hellerbrand *et al.*, 2006).

Chromosome 14

On chromosome 14, a 2.3 Mb deletion at 14q11.2-q12 in MOUZ (Figure 4.14A) was also lost in 6 more samples. This segment contains 58 genes of which TINF2, a component of the shelterin complex, was downregulated in all samples.

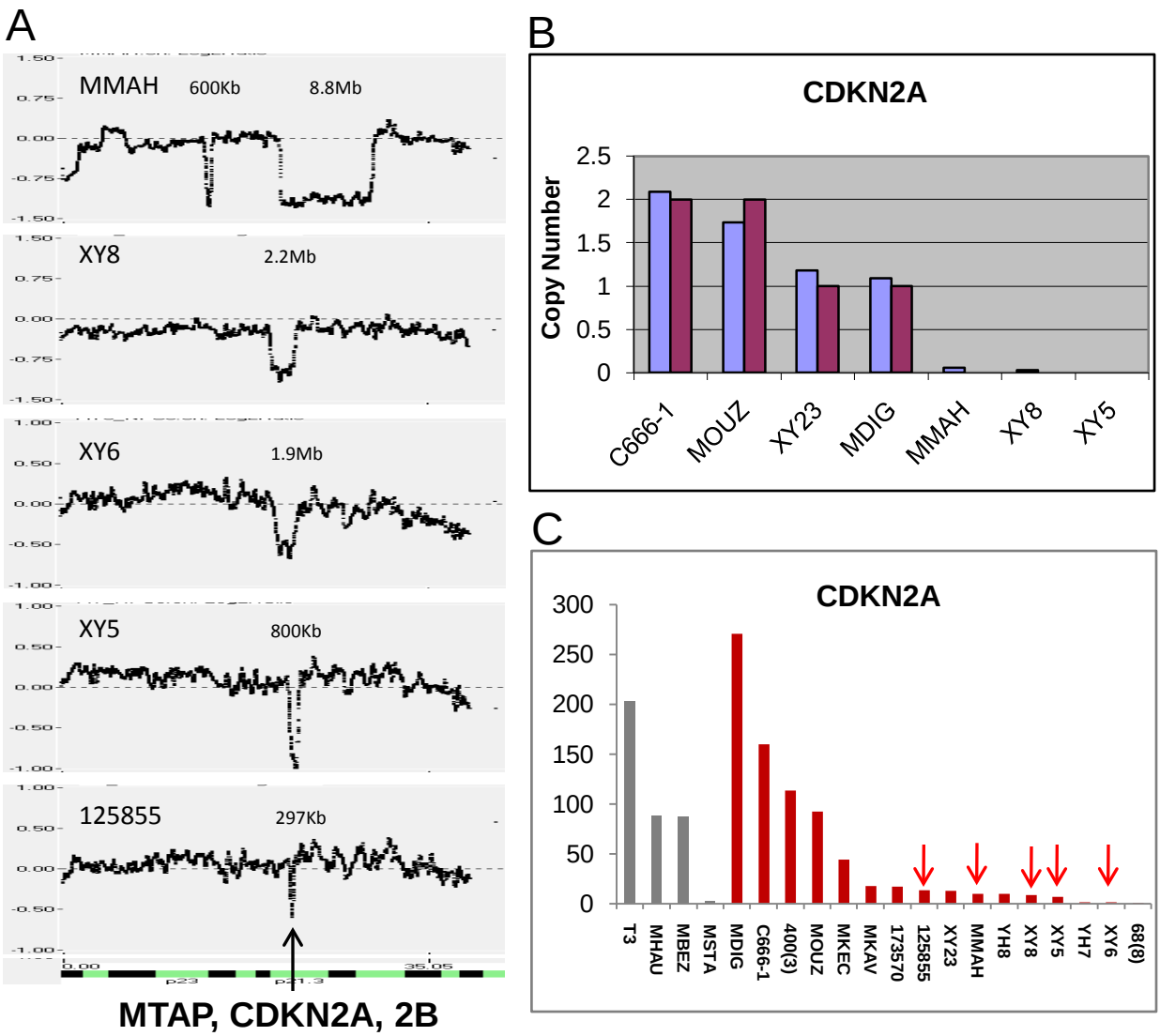

Figure 4.13: **Deletions on chromosome 9p.**

(A) Sample XY6, XY8, MMAH, 125855 and XY5 show a minimal overlapping region of loss at 9p21.3. The minimum deletion is approximately 300Kb and contains the genes MTAP, CDKN2A and CDKN2B.

(B) Comparison of DNA copy number at the CDKN2A locus identified by SNP array data (purple columns) and q-PCR analysis (blue columns) in 7 samples.

(C) CDKN2A expression at the RNA level in the 4 normal samples (grey) and 15 NPCs plus C666-1 (red) is presented using normalised expression array intensities. Samples that showed deletion of 9p21.3 are indicated by red arrows.

Downregulation of TINF2 has been associated with telomere maintenance in gastric cancer cells (Yamada *et al.*, 2002), and reorganisation of this gene is associated with the control of cell proliferation in mammary epithelial cells (Kaminker *et al.*, 2005). In expression array data, TINF2 expression appeared to be downregulated in all the NPCs (Figure 4.14B).

Other small regions of copy number change

In addition to the regions described above, there are some other small regions of copy number loss or gain. Although these genetic changes were not detected or significant in previous data, our data suggest that they might have been missed by the older methodology or important in only a minority of samples. These include a 1.29 Mb deletion at 1p13.1 – p12 in MMAH, an overlapping 2.59 Mb loss at 1q25.3 in two samples (XY6, MKEC) and four additional small changes in the C666-1 cell line. Of the four deletions in the C666-1 cell line, the first, a 1.33 Mb gain at 1q41 – q42.11 was part of larger gains in 6 more tumours. The second region, a 3.01 Mb single copy segment at 8q23.1 – q23.3 was uniquely lost in C666-1 but part of large gains in several other samples. The third region, 3.21 Mb at 12p13.2 – p12.3 formed another locus that was single copy in C666-1, but which was duplicated in a number of tumour samples. The fourth additional small change observed in C666-1 was a 455 kb gain at 17q11.2 that was also duplicated in one other tumour. These small genetic changes and the genes involved are shown in Table 4.2.

4.5.4 LOH analysis

9 tumour samples and C666-1 showed extensive regions of homozygosity (uniparental disomy, UPD). These were distributed among the majority of

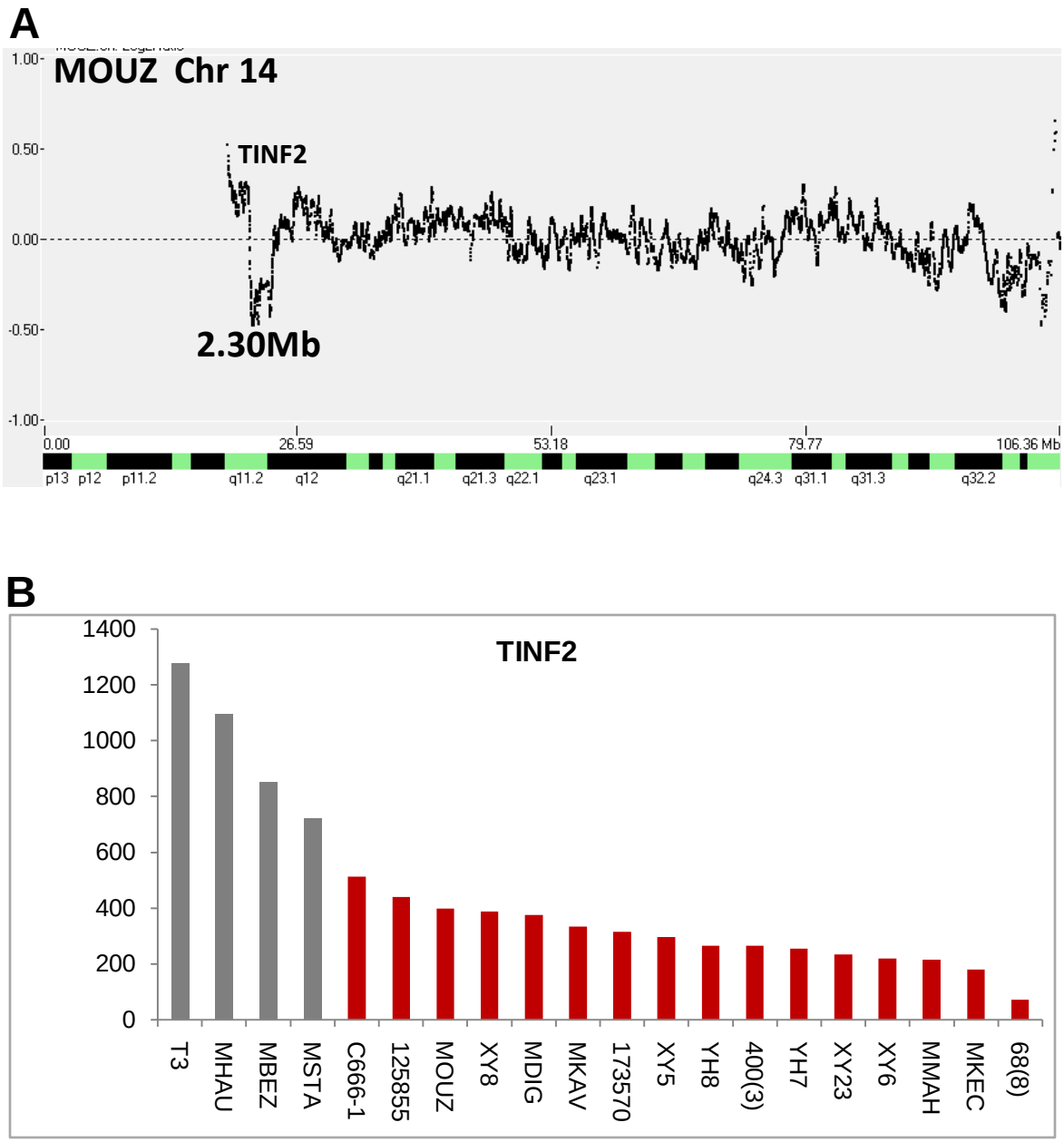

Figure 4.14: Deletion at 14q11.2-q12.

(A) Sample MOUZ shows a small region of loss at 14q11.2-q12, which is approximately 2.30Mb and contains 58 genes including TINF2.

(B) TINF2 expression at the RNA level in the 4 normal samples (grey) and 15 NPCs plus C666-1 (red) is presented using normalised expression array intensities. It appears to be downregulated in all the NPCs compared to normal controls.

chromosomes (chromosomes 1, 2, 4, 5, 6, 7, 8, 9, 11, 12, 13, 14, 15, 16, 17, 18 and 20; Figure 4.15). Chromosome 6 was completely homozygous in 3 samples whilst a substantial portion of 6q was homozygous in a fourth sample. Chromosome 9 showed regions of UPD in four samples. Putative tumour suppressor genes GAS1, SYK, GADD45G and DAPK1 are located in the overlapping small region of UPD at 9q21-22 in three samples.

4.6 Relationship of chromosomal copy number to level of gene expression

In the above sections, we introduced several potential NPC tumour-associated genes that are involved in small regions of loss or gain. Their copy number change was analysed in the context of gene expression level. This reveals that in some cases, gene up- or down- regulation is associated with regions of gain or loss, but in others, it is not the case. For instance, TGFBI is within a deletion at 5q31.1-31.2, but its expression was found to be upregulated at both the RNA and protein levels.

In addition, our expression array data identified a number of tumour-related genes (Chapter 3). 13 samples from which both copy number and expression data were available (cell line C666-1 and 12 biopsies, see Table 2.1) were examined for copy number status at the loci of each of the putative tumour-associated genes, and the data are summarised in Tables 3.1 – 3.3. This revealed that in the oncogene list some genes such as PIK3CA, EGFR and SKIL might be activated by DNA copy number gain in NPC since previous studies and our data taken together show that more than 20% of NPC tumours are duplicated (Hui *et al*., 2002; Sheu *et al*., 2009). However for the majority of genes increased transcript levels are not a consequence of DNA copy

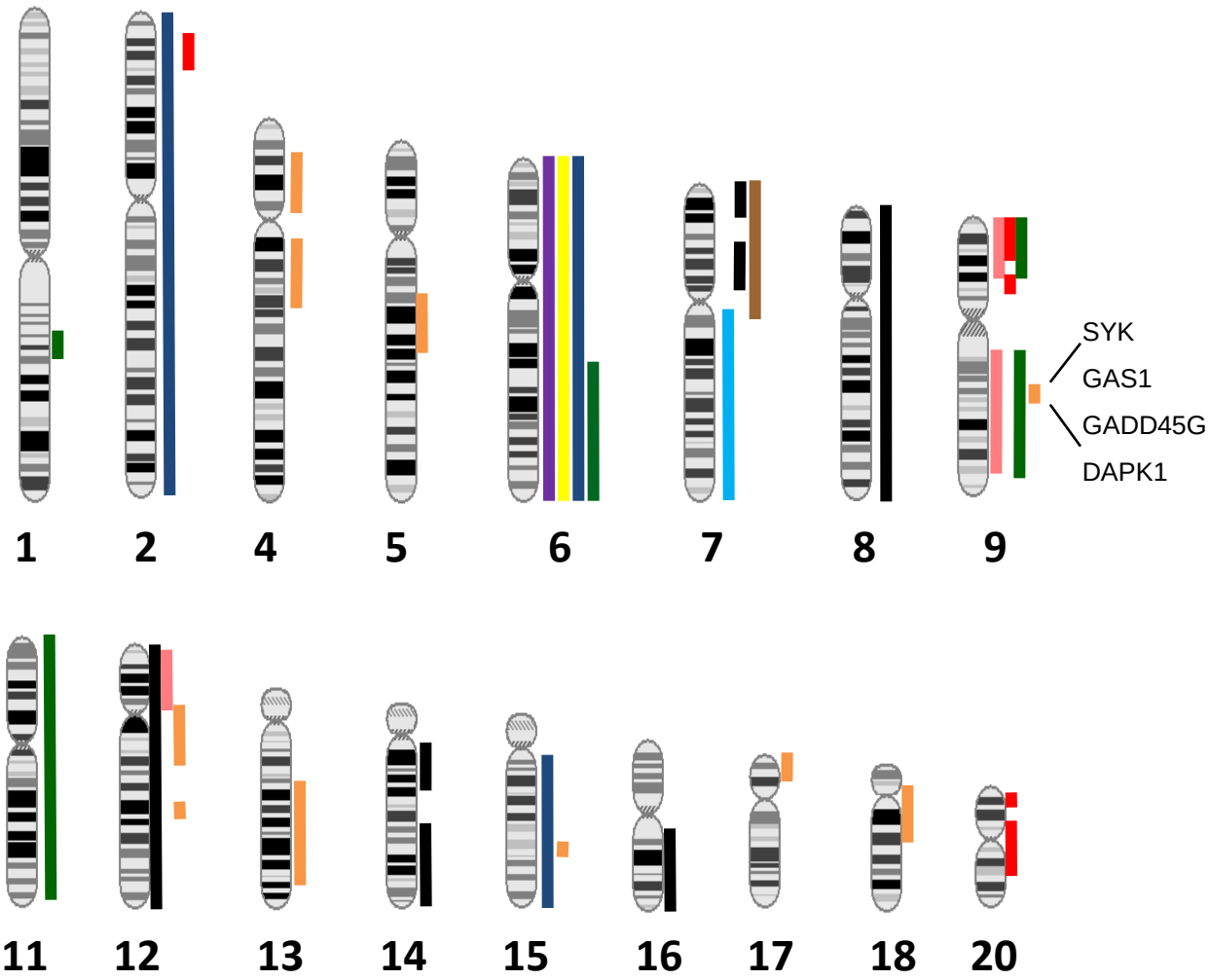

Figure 4.15: Regions of uniparental disomy. The coloured bars alongside the ideograms indicate homozygous diploid regions. Different samples are identified by individual colours. Chromosomes 6 and 9 show most frequent UPD. Genes GAS1, SYK, GADD45G and DAPK1 are located in the minimal overlapping region of UPD on chromosome 9q in three samples (as indicated).

number gain since it is not a frequent event at their respective loci. Conversely, a number of upregulated genes showed chromosomal loss. For example, enhanced expressions of single-copy oncogenes (e.g. RAF1, RAB5A, THRB, CTNNB1 and WNT5A on chromosome 3p) are observed. A similar phenomenon was also observed in the TSGs list. Although the down-regulation of some candidate TSGs appeared to be associated with copy number loss, e.g. SFN and BRD7 which were both downregulated in 100% of tumours and single copy in 60% and 53% of tumours respectively, the expression of many candidate TSGs did not correlate with copy number loss. Some TSGs, e.g. CEACAM1, DLG1, KLK11, showed downregulation in 100% of NPC tumours but no copy number loss, whilst for others e.g. EPAS1, S100A2, frequent copy number gains were detected.

To ascertain further whether there was any consistent correlation between up- or down-regulation of the genes of interest (genes involved in small regions of loss or gain, and families of tumour-related genes) and genomic copy number changes, the relationship between expression level and copy number status was further analysed in the 13 NPC samples for each gene in these two groups (Table 4.2, and Tables 3.1-3.3). This reveals that in the genes involved in small regions of loss or gain, 62.4% of instances of copy number loss is associated with gene down-expression, whereas only 25% of copy number gain correlates with gene up-expression. On the contrary, in about 50% of instances of copy number gain, gene down-expression was observed (Table 4.3 A). A similar phenomenon is also found in the tumour-related genes (Table 4.3 B).

Table 4.3: The relationship between copy number and expression changes.

A. Genes involved in small regions of loss or gain

	DOWNREGULATED	NO CHANGE	UPREGULATED
COPY LOSS	62.4%	24.3%	13.4%
(202)	(126)	(49)	(27)
COPY NEUTRAL	40.6%	29.2%	30.2%
(281)	(114)	(82)	(85)
COPY GAIN	50.0%	25.0%	25.0%
(24)	(12)	(6)	(6)

B. Tumour-related genes

	DOWNREGULATED	NO CHANGE	UPREGULATED
COPY LOSS	64.1%	21.5%	14.4%
(535)	(343)	(115)	(77)
COPY NEUTRAL	51.9%	23.9%	24.3%
(1899)	(985)	(453)	(461)
COPY GAIN	40.8%	24.8%	34.4%
(218)	(89)	(54)	(75)

The 13 samples from which both copy number and expression data were available (cell line C666-1 and 12 biopsies, see Table 1) were examined for copy number status at the locus of each gene that is called "present" by GCOS in all four normals in the two groups (A: Table 4.2, B: Tables 3.1-3.3). Copy number was scored as "loss" (0 – 1 copy, top row), "neutral" (2 copies, middle row) or "gain" (>2 copies, bottom row). Gene expression was classified as "downregulated" (fold change≥ -1.5, left column), "no change" (fold change -1.4 – 1.4, middle column) or "upregulated" (fold change≥ 1.5, right column). The numbers in parentheses indicate the number of instances of the given condition whilst the percentage figures represent the proportions of downregulated, unchanged or upregulated genes in each of the three copy-number classes.

4.7 Discussion

In the present study, we identified multiple regions of chromosomal loss, gain, and LOH using a panel of 14 NPC biopsies and one NPC cell line C666-1. A number of potential tumour-associated genes involved in the altered regions were implicated. The copy number changes predicted by SNP array were verified using an independent method based on q-PCR and reveals that our SNP array analysis is both sensitive and specific.

We determined the EBV status of the NPC samples. All samples except MMAH were EBV positive. After review of the histological morphology of this sample by an experienced NPC pathologist it was confirmed to be undifferentiated NPC. There is thought to be near 100% EBV positivity in undifferentiated NPC, but we failed to confirm the presence of the virus in tumour MMAH even when using the most sensitive way of EBV detection i.e. detecting the amplified BamHI-W region. This suggests that this sample might be an example of a relatively rare, EBV negative, undifferentiated NPC.

NPC tissues are especially heterogeneous with an extensive lymphocytic infiltrate surrounding the tumour cells. Previous studies have shown that the quality of the data obtained from SNP arrays is highly dependent on tumour purity. Up to 20% of contamination with non-neoplastic cells should be acceptable for the detection of genomic abnormalities, whereas more than 30% of contamination will result in a significant reduction of the sensitivity of the analysis (Lindblad-Toh *et al.*, 2000; Huang *et al.*, 2004; Zhao *et al.*, 2004). Tissue microdissection enables the collection

of purified populations of NPC tumour cells. However, a DNA amplification step is needed in order to obtain sufficient DNA from microdissected cells. The preliminary data from 10K SNP arrays confirmed (at more than 99% concordance) the fidelity of amplified DNA by comparison of amplified and unamplified DNA derived from C666-1 cells, as well as DNA sequence analysis of the LMP1 region. But in 500K SNP arrays, the amplified DNA showed some artefactual genetic changes (e.g. isolated, ~200kb regions of genetic copy number loss or gain across the chromosome and deletion at the chromosomal termini). Thus, when analysing the SNP array data, we filtered out 300kb or less small genetic changes as well as losses close to chromosomal termini.

In our SNP array data, the most frequent deletions were observed in chromosomes 3p, 5q, 9p and q, 13q, 14q, 16p and q. Frequent gains were observed in chromosome 1q, 3q, 8p and q, 12p and q, which is general agreement with previous studies obtained from CGH analysis (Chen *et al.*, 1999; Hui *et al.*, 1999; Fang *et al.*, 2001; Wong *et al.*, 2003).

However, it is worthy to note that the genetic changes in the C666-1 cell line obtained by SNP array analysis are somewhat different from those described previously (see Section 3.5.2). This line was originally described in 1999 and chromosomal aberrations were examined using conventional CGH where gains of 7q and 8q, and losses of 6pter-q12, 11q14-qter, 14q23-qter, 16q and 18q21-qter were found (Cheung *et al.*, 1999). Our data additionally identified several smaller regions of copy number loss or gain, which might have been missed by the previous studies since they used a

detection technique with much lower resolution. Whilst the discrepancy in some extensive regions of genetic changes detected by their study and ours might be partly due to cell allelic variation as a consequence of long-period passage and different condition in culture. In addition, a closer examination of the earlier data revealed hints of some of the changes that were observed in our data (e.g. gains of 8pter-p22, 8p12-q12 and 16pter-q12). Although these were not significant in the earlier work, it could suggest that the original population was heterogeneous and that some of the previously minor components are now in the majority.

Our methodology had high resolution and additionally identified several novel small regions of copy number loss, gain and LOH which might have been overlooked by conventional methods. We identified a 2.4 Mb loss at chromosome 4q13 that contained two genes, SRD5A2L2 and ephrinA5 (EPHA5). Since this deletion was detected in only one sample, it might suggest that this deletion is important in only a small proportion of NPC tumours. Deletions on chromosome 5q have not been frequently observed in previous studies, whereas we detected 3 small deletions including 5q14.1, 5q31.1-31.2 and 5q11.2. Among them, 9/15 (60%) loss of 5q14.1 and 7/15 (47%) loss of 5q31.1-31.2 was observed in our samples. Several genes encoded in these regions (e.g. THBS4, MSH3, RASGRF2 PITX1, CXCL14 and TGFBI) are found to have tumour suppressor potential, suggesting that these deletions might be critical for carcinogenesis. Further functional investigation of these genes in NPC might provide new insight to its pathogenesis. Although another deletion on chromosome 5, deletion of 5q31.1-31.2, was observed in only three samples, one of the genes encoded in this region was ITGA2, whose reduction was previously

reported to be associated with cell immortalisation and malignant progression (see Section 4.5.3).

Small gains are not detected as frequently as small deletions in our SNP array data. High-copy number at 8p11.22 – 11.21 in one sample was identified by SNP array and confirmed by q-PCR as having 8-9 copies. This is the only example of an amplification (5 or more copies) observed in our data. 14 genes have been implicated in this amplification. This amplified region has been also noted in breast cancer where several putative oncogenes were defined and found to be overexpressed including genes GOLGA7, MYST3 and AP3M2 that are also implicated in our data (Gelsi-Boyer *et al.*, 2005). Although their functions in NPC are still unclear, the notable amplification may indicate their potential relevance to the oncogenic process. Recent investigations demonstrate that two novel regions of gain at 11q13.1-13.3 and 12p13.3 have been detected in more than 50% of NPC tumour samples (see Section 1.4.2.2). However, in our data, gain of 11q13.1-13.3 is rarely observed, whereas gain of 12p13.3 is mostly detected within an extensive region of gain on chromosome 12p.

Our study integrated expression data with DNA copy number data in the same NPC tumour samples, thus allowing an exploration of the relationship between chromosomal copy number and gene expression in the genes that are potentially important in tumourigenesis. It is generally considered that gene copy number loss or gain is one of the mechanisms resulting in reduced or increased gene expression level. In our data, it is probably true in some cases, and a good example was shown in chromosome 8p11.22 – 11.21 in which several genes encoded were unambiguously upregulated in a single tumour that exhibited amplification. However, some cases do

not seem to follow this concept. A number of tumour-associated genes that showed down- or up-regulation in NPC tumours did not definitely display copy number loss or gain. Conversely, the upregulated genes exhibited chromosome loss and down-regulated genes showed chromosome gain. For instance, chromosome 3p which has been reported to be frequently deleted in NPC tumours (Hui *et al.*, 1999; Chan *et al.*, 2000; Chien *et al.*, 2001) were single copy in 80% (12/15) of our samples, and a number of TSGs are located here. Nevertheless, several putative oncogenes are also found in these monosomic regions (e.g. RAF1, RAB5A, THRB, CTNNB1 and WNT5A on chromosome 3p), which were found to be up-regulated in over half of NPC tumours in expression array data.

When the relationship between expression level and copy number status was examined in the 13 NPC samples for each tumour associated gene (Table 4.2, and Tables 3.1-3.3), it revealed that although in 60% of instances of copy number loss appeared to be associated with gene down-expression. However, in more than 40% of instances of copy number gain, gene expression was downregulated (Tables 4.3 A and B). Thus, with regard to this analysis, it seems to have a tendency that copy number loss correlates with gene down-regulation, whereas copy number gain is not associated with gene up-regulation. However, for the individual genes, the concept that gene up- or down-expression is driven by gene copy number gain or loss might be overestimated or oversimplified, at least in NPC tumours. The gene expression changes in NPC might be caused by more complicated mechanisms such as mutation, methylation or regulated by some key factors during the tumour biology process.

SNP array data can integrate copy number data with LOH status, so as to identify UPD regions (copy neutral LOH). Several UPD regions have been identified in our data and are found in a number of chromosomes. The most frequently involved are chromosomes 6 and 9. Although in previous studies LOH of chromosome 9p was considered to be a frequent event, LOH of 9q has not been mentioned before. However, in our data, a small minimal overlapping region of UPD at 9q was observed in three samples, indicating that this UPD region may be a non-random event in NPC tumours. Putative tumour suppressor genes SYK, GAS1, DAPK1 and GADD45G are found to be encoded in this small UPD region. It has been considered that a UPD region often harbours genes targeted by somatic mutation. To understand whether these genes are mutated in NPC, sequence analysis in these three samples is needed.

In summary, we detected a number of allelic imbalances (including copy number changes, LOH and UPD) in NPC tumours by using high density SNP arrays. The altered fragments are narrowed in a minimal boundary, which makes it possible to identify critical NPC-associated genes and provides more clues for understanding the mechanisms of NPC pathogenesis. The integrated analysis of SNP array data and expression data suggested that frequently there is no direct or strong correlation between gene chromosome abnormalities and expression changes. Other mechanisms may be involved such as abnormal signalling pathways that could regulate gene expression.

CHAPTER 5

Dysregulated signalling pathways

5.1 Introduction

In common with other tumours, the complex process of NPC tumour formation has been distilled to a series of stochastic events that occur gradually in the tumour development and progression and are required for tumour cell growth and survival. These include the ability to resist growth inhibitory factors, and to facilitate proliferation, invasiveness and metastasis. These functions are obtained not only from genetic alterations such as activation of oncogenes or inactivation of tumour suppressor genes, but also from altered production of, or responsiveness to, the components and functional target genes of multiple signal transduction pathways that normally control cellular homeostasis. Thus, NPC tumourigenesis can be viewed as a disruption of these pathways through genetic, epigenetic or somatic alterations. To determine novel hypotheses on the most relevant pathways engaged in the pathogenesis of NPC, the differentially expressed genes identified from expression array data by RP analysis were examined using the FatiGO program (Al-Shahrour *et al.*, 2004) and KEGG database (Kanehisa *et al.*, 2002). This revealed a substantial enhancement in the expression of genes involved in several signalling pathways including the TGF-β/activin, Wnt/β-catenin and Hedgehog (Hh) pathways that were differentially regulated in NPC tumours compared to normal control epithelia.

Expression profiles of NPC in previous studies have discovered dysregulation of the TGF-β and Wnt/β-catenin pathways in NPC tumours (Sriuranpong *et al.*, 2004; Shi *et al.*, 2006; Zeng *et al.*, 2007). Data presented here confirm and extend these findings.

As was mentioned in Section 1.4.4.1, dysregulation of the NF-κB signalling pathway is critical for NPC tumourigenesis. In previous studies this pathway has been more extensively investigated. Thus, it is not considered here although our data show this pathway to be abnormally regulated in our NPC samples. Activation of the Hh pathway has been reported in several other types of cancer (Bailey *et al.*, 2009; Kasper *et al.*, 2009; Zhao *et al.*, 2009), whereas it has not been investigated thus far in NPC. Our findings could provide a new insight to the mechanism of NPC development. To validate the accuracy of array predictions, some up- and down-regulated gene components involved in these signalling pathways were validated either at the transcriptional level by PCR and q-RT-PCR or at the protein level by IHC staining.

5.2 The TGF-β signalling pathway

The TGF-β superfamily members and TGF-β signal transduction were described in detail in Section 1.4.4.2. Like other cell signalling pathways, the activities of the TGF-β signalling pathway are closely related to the gene status and expression levels of their components. Alterations in the expression of TGF-β family members are associated with a number of human malignancies (Diaz-Chavez *et al.*, 2008; Kapral *et al.*, 2008; Langenskiold *et al.*, 2008). In NPC tumours, although previous gene expression profiling revealed that a small number of genes involved in the TGF-β pathway were deregulated (Zeng *et al.*, 2007), the expression patterns of the family members in this particular tumour still remain elusive due to the limited studies.

5.2.1 Dysregulation of the TGF-β signalling pathway in NPC

The significantly differentially regulated genes identified from expression array data by RP analysis were examined for groups of functionally related proteins by the FatiGO program (Al-Shahrour *et al.*, 2004) and protein interaction networks of signalling pathways using the KEGG database (Kanehisa *et al.*, 2002). Figure 5.1 generated through this analysis presents a schematic model for the main components involved in this pathway. Table 5.1 presents the fold change and statistical significance of the individual genes included in the TGF-β pathway as revealed by RP analysis. This showed that a number of TGF-β family members including ligands (BMP2, INHBA), receptors (TGFBR1, TGFBR2, ACVR1, BMPR1A and BMPR2), SMADs (SMAD1, 2, 4, 5 and 7) and a number of target genes (e.g. TGFBI, SKIL) were generally upregulated in NPC tumours. Although some genes were not regarded as being significantly changed following RP analysis, they are either important components in this pathway (e.g. TGFβ1) or found to be upregulated in several NPCs when analysed using GCOS and the rules that were employed in the previous chapters (e.g. SERPINE1). These are also included in Table 5.1. To validate the reliability of the array data, the protein expression of several differentially regulated genes was examined by IHC staining in NPC tumour and normal control tissue arrays as well as in frozen sections from the same biopsies that had been used for array analysis (see below).

5.2.1.1 TGF-β family ligands

Elevated expression of TGF-β family ligands could enhance signal transduction through the sustained activation of SMAD signalling. In our expression array data, the expression levels of ligands BMP2 and activin A (inhibin-βA homodimers), showed

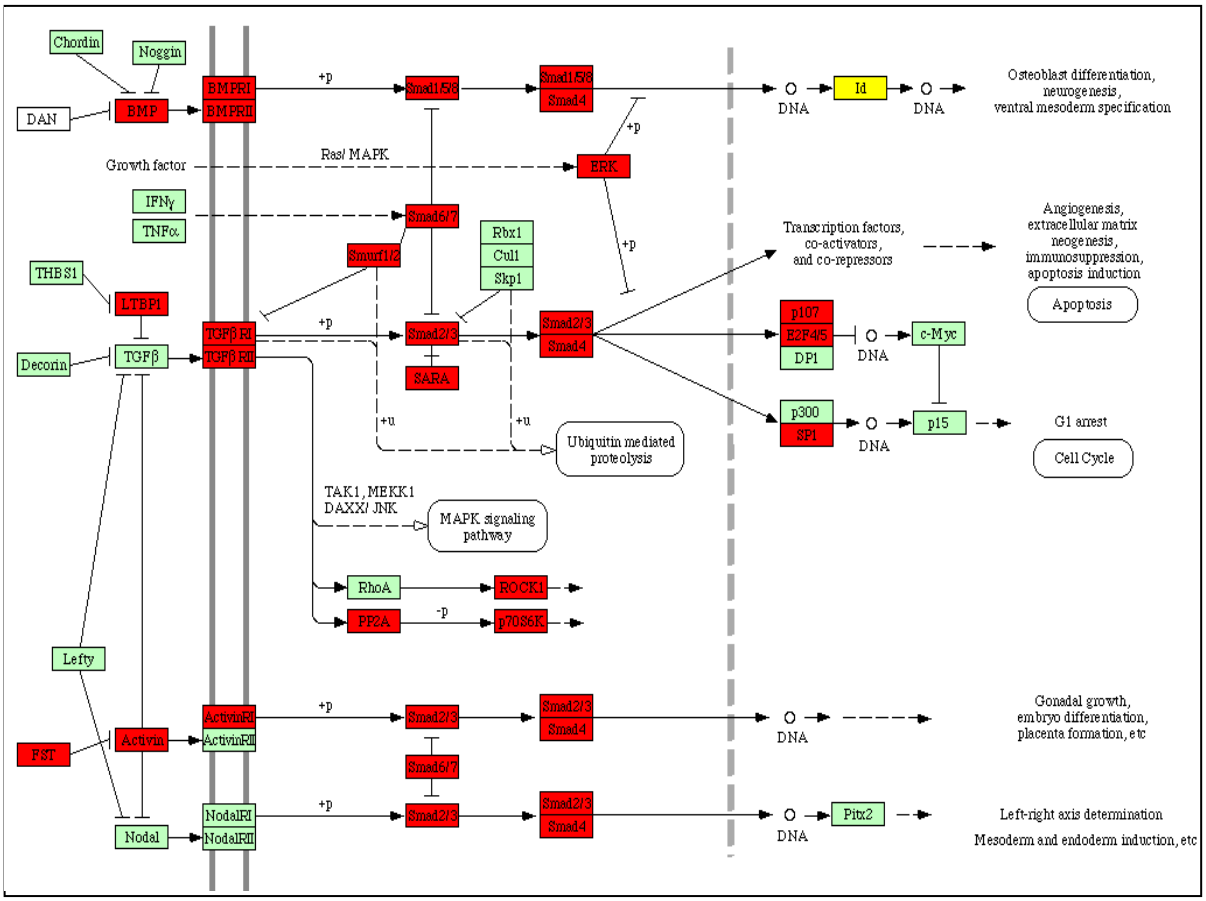

Figure 5.1: A number of genes involved in the TGF-β signalling pathway are dysregulated in NPC. The significantly differentially regulated genes identified from expression array data by RP analysis were examined using the FatiGO program and KEGG database. The figure generated through this analysis represents a schematic model of the main components involved in the TGF-β signalling pathway. A number of genes involved in this pathway ranging from ligands, receptors, Smads and target genes are generally upregulated as shown by the red boxes, whereas ID1 appears to be downregulated in NPC tumours (yellow box). The green boxes indicate genes whose expression was not significantly changed.

Table 5.1: Differentially regulated genes involved in the TGF-β signalling pathway.

Gene Symbol	Name	p value (t)	FC (overall)	FC (C666-1)
TGF-β ligands				
TGFB1	transforming growth factor, beta 1		A	
TGFB2	transforming growth factor, beta 2		A	
TGFB3	transforming growth factor, beta 3		A	
INHBA	inhibin, beta A	0.0028	2.8	-1.6
INHBB	inhibin, beta B (activin AB beta polypeptide)		A	
BMP2	bone morphogenetic protein 2	0.0014	2.4	4.6
TGF-β receptors				
TGFBR1	transforming growth factor, beta receptor I (activin A receptor type II-like kinase, 53kDa)	0.0013	3.7	2.9
TGFBR2	transforming growth factor, beta receptor II (70/80kDa)	0.057	2.1	A
ACVR1	activin A receptor, type I	0.0000082	5.2	5.9
ACVR1B	activin A receptor, type IB	0.0023	2.9	1.0
ACVR2B	activin A receptor, type IIB	NS		
BMPR1A	bone morphogenetic protein receptor, type IA	0.0028	4.0	7.3
BMPR2	bone morphogenetic protein receptor, type II (serine/threonine kinase)	0.0000003	5.8	2.7
TGF-β antagonists				
FST	follistatin	0.21	2.0	14.2
SMAD transducers				
SMAD1	SMAD family member 1	0.00073	5.1	3.5
SMAD2	SMAD family member 2	0.000057	3.5	5.7
SMAD3	SMAD family member 3	NS	1.3	-1.2
SMAD4	SMAD family member 4	0.00016	3.2	2.3
SMAD5	SMAD family member 5	0.13	2.4	-1.8
SMAD7	SMAD family member 7	0.0030	4.4	6.1
Protein Phosphatases				
PPP2R2A	protein phosphatase 2 (formerly 2A), regulatory subunit B, alpha isoform	0.15	2.0	1.0
PPP2R1B	protein phosphatase 2 (formerly 2A), regulatory subunit A, beta isoform	0.0018	1.9	2.7
PPP2R3C	protein phosphatase 2 (formerly 2A), regulatory subunit B'', gamma	0.025	3.5	9.6
PPP2R5E	protein phosphatase 2, regulatory subunit B', epsilon isoform	0.0086	3.5	10.1
PPP2CB	protein phosphatase 2 (formerly 2A), catalytic subunit, beta isoform	0.020	2.8	6.2
PPA1	pyrophosphatase (inorganic) 1	0.0098	2.0	3.7

PTPRK	protein tyrosine phosphatase, receptor type, K	0.11	4.3	3.9
Protein kinases				
RPS6KB1	ribosomal protein S6 kinase, 70kDa, polypeptide 1	0.012	2.5	5.5
ROCK1	Rho-associated, coiled-coil containing protein kinase 1	0.0013	2.2	3.2
MAPK1	mitogen-activated protein kinase 1	0.0045	2.4	2.2
MAPK6	mitogen-activated protein kinase 6	0.023	2.1	1.9
MAP3K7	mitogen-activated protein kinase kinase kinase 7	0.000087	4.4	4.3
Transcription factors				
SMURF2	SMAD specific E3 ubiquitin protein ligase 2	0.17	3.1	5.4
LTBP1	latent transforming growth factor beta binding protein 1	0.000065	4.7	7.8
E2F5	E2F transcription factor 5, p130-binding	0.00086	2.8	5.7
SP1	Sp1 transcription factor	0.016	1.9	-1.4
WWP1	WW domain containing E3 ubiquitin protein ligase 1	0.024	3.7	3.4
ZFYVE16	zinc finger, FYVE domain containing 16	0.0019	3.2	1.4
TGF-β targets				
TGFBI	transforming growth factor, beta-induced, 68kDa	0.023	2.0	A
ITGB6	integrin, beta 6	0.16	2.0	-5.6
SKIL	SKI-like oncogene	0.0000038	5.4	1.8
SERPINE1	serpin peptidase inhibitor, clade E (nexin, plasminogen activator inhibitor type 1), member 1	NS	1.7	-1.2
NEDD9	neural precursor cell expressed, developmentally down-regulated 9	0.0076	4.6	-2.0
COL4A1	collagen, type IV, alpha 1	0.0013	10.5	6.8
NET1	neuroepithelial cell transforming gene 1	0.053	2.4	4.4
CLDN1	Claudin 1	0.011	2.7	A
JUN	jun oncogene	0.0066	4.9	13.4
ID2	inhibitor of DNA binding 2, dominant negative helix-loop-helix protein	0.21	1.8	8.2
BTG1	B-cell translocation gene 1, anti-proliferative	0.028	14.2	9.3
SGK1	serum/glucocorticoid regulated kinase 1	0.047	2.0	1.4
RNF111	ring finger protein 111	0.0027	4.2	9.9
COPS5	COP9 constitutive photomorphogenic homolog subunit 5 (Arabidopsis)	0.14	1.8	3.1
SOX4	SRY (sex determining region Y)-box 4	0.0014	14.3	8.8

GATA3	GATA binding protein 3	0.0020	2.7	1.0
ID1	inhibitor of DNA binding 1, dominant negative helix-loop-helix protein	0.020	-3.7	-2.2
RUNX1	runt-related transcription factor 1 (acute myeloid leukemia 1; aml1 oncogene)	0.0044	-2.5	-3.3
ELK3	ELK3, ETS-domain protein (SRF accessory protein 2)	0.12	-2.6	1.0
HES1	hairy and enhancer of split 1, (Drosophila)	0.000028	-5.7	-3.7
LEFTY2	left-right determination factor 2	NS	-1.6	-1.4

“FC” indicates fold change determined by comparing the 4 normal samples with both the whole tumour set (overall) and with cell line C666-1 alone (C666-1)

“A” indicates that expression was called “absent” by GCOS.

“NS” indicates not significantly changed

The red boxes indicate genes whose expression change in C666-l is in the opposite direction to that in the whole tumour set. The yellow boxes indicate genes whose expression level in C666-1 is relatively unchanged.

more than 2-fold upregulation in tumour samples compared to normal control epithelia. Increased expression of activin A has been observed in lung adenocarcinoma tissue where its over-expression was associated with cell proliferation (Seder *et al.*, 2009). Conversely, the main member of the canonical TGF-β pathway ligands, TGF-β1, was called "absent" in both tumour and normal controls by GCOS analysis. TGF-β can regulate the growth of cancer cells in an autocrine or paracrine fashion. The tumour development and progression are controlled by the synergistic interplay of cancer cells and activated stroma. Although the tumour cells do not appear to make TGF-β1 themselves, they could still respond to TGF-β1 secreted from the surrounding stromal cells (Yue & Mulder, 2001; Tobin *et al.*, 2002).

5.2.1.2 TGF-β family receptors

TGF-β family receptors couple extracellular ligands to the SMADs and are essential for the activation of entire pathways. In the expression array data, several TGF-β family receptors (BMPR1A, BMPR2, TGFBR1, TGFBR2, and ACVR1) were found to be upregulated in NPC tumours compared to control normal epithelia. TGFBR1 and TGFBR2 are TGF-β type I and type II receptors, respectively. In the array data, TGFBR2 showed 2-fold upregulation in NPC tumours using RP analysis. However, when TGFBR2 expression was analysed using the GCOS rules, 6 samples showed upregulation compared to controls. IHC staining for this gene product in matched NPC and normal nasal epithelial (NP) samples revealed over-expression of TGFBR2 protein in 65.4% (17/26) of NPC tumours (Figure 5.2 A). Another TGF-β receptor, TGFBR1, exhibited 3.7-fold upregulation at the RNA level in RP analysis. GCOS analysis revealed that TGFBR1 was upregulated in 75% (12/16) NPCs. IHC staining of TGFBR1 was performed in frozen sections from the same sample used for

Figure 5.2: Expression array intensities and immunohistochemical staining on NPC and nasopharyngeal epithelial (NP) samples reveals differential regulation at both the RNA and the protein levels for genes TGFBR2, SMAD7 and SERPINE1.

The left panels show normalised expression array intensities for the 4 normal samples (grey) and 15 NPCs plus C666-1 (red). The centre panels show examples of immunohistochemical staining on NPC and NP tissue samples. The right panels show the immunohistochemical scoring results from the tissue arrays (normal, grey: tumour, red). At the RNA and protein levels respectively, (A) TGFBR2 is upregulated in 6/16 (37.5.5%) and in 65.4% (17/26) samples, and positive TGFBR2 staining is predominantly observed in the cytoplasm and membrane. (B) SMAD7 is upregulated in 69% (11/16) and 60% (21/35) samples, and positive SMAD7 staining is predominantly observed in the cytoplasm; (C) SERPINE1 is upregulated in 37.5% (6/16, YH7, MKEC, 125855, XY6, 400(3) and XY5) and 53.6% (15/28) samples, and positive SERPINE1 staining is predominantly observed in the cytoplasm and membrane.

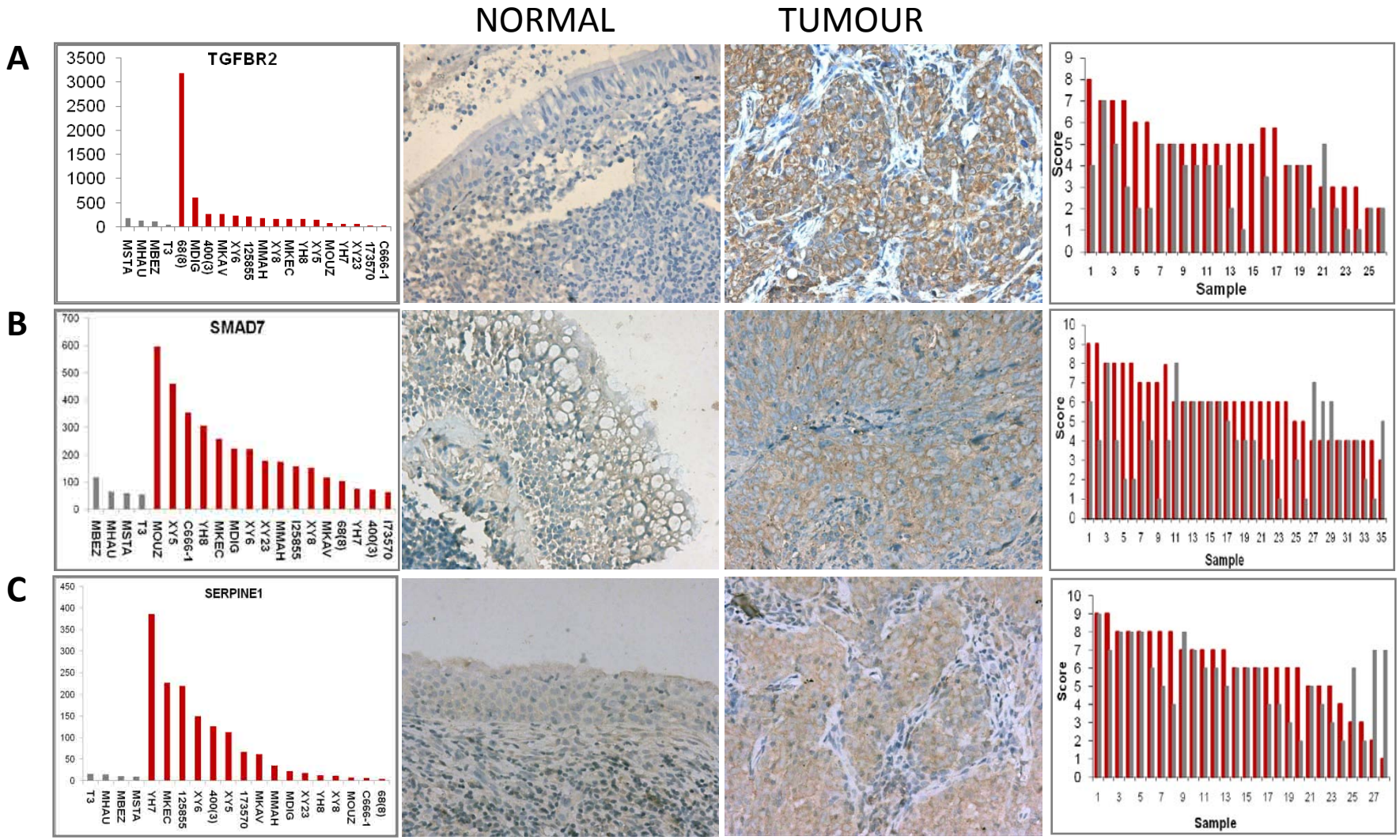
NORMAL
TUMOUR
A
TGFBR2
3500
3000
2500
2000
1500
1000
500
0
MSTA
MHAU
MBEZ
T3
68(8)
MDIG
400(3)
MKAV
XY6
125855
MMAH
XY8
MKEC
XY5
YH8
MOUZ
YH7
XY23
173570
C666-1
Score
Sample
B
SMAD7
700
600
500
400
300
200
100
0
MBEZ
MHAU
MSTA
T3
MOUZ
XY5
C666-1
YH8
MKEC
MDIG
XY6
XY23
MMAH
I25855
XY8
MKAV
68(8)
YH7
400(3)
I73570
Score
Sample
C
SERPINE1
450
400
350
300
250
200
150
100
50
0
T3
MHAU
MBEZ
MSTA
YH7
MKEC
125855
XY6
400(3)
XY5
173570
MKAV
MMAH
MDIG
XY23
YH8
XY8
MOUZ
C666-1
68(8)
Score
Sample

Figure 5.3: Expression array intensities and immunohistochemical staining on frozen samples reveals differential regulation at both the RNA and protein levels of genes involved in the TGF-β signalling pathway.

IHC staining of genes (TGFBR1, SMAD2, BTG1, ID1 and SP1) was performed on the same frozen samples used for array analysis. The left and middle panels show examples of immunohistochemical staining in normal and tumour samples, whilst the right panels show the normalised expression array signal intensities for the 4 normal samples (grey) and 15 NPCs plus C666-1 (brown).

(A) At the RNA level, TGFBR1 is upregulated in 75% (12/16) of NPC samples. At the protein level, the tumour sample MKEC (high array intensity) shows intense cytosolic staining of TGFBR1, whereas in the normal sample MSTA (low array intensity) TGFBR1 protein expression is not detectable.

(B) At the RNA level, SMAD2 is upregulated in 81% (13/16) of NPC tumours. Tumour MMAH (high array intensity) shows strong cytosolic expression of SMAD2 protein whereas normal MHAU (low array intensity) shows very weak expression of SMAD2.

(C) At the RNA level BTG1 is upregulated in 93% (15/16) of NPC tumours. Tumour MDIG (high array intensity) shows strong cytosolic expression of BTG1 protein whereas normal MHAU (low array intensity) shows weak expression of BTG1.

(D) At the RNA level ID1 is downregulated in 81% (13/16) of NPC tumours. Tumour MMAH (low array intensity) shows weak expression of ID1 protein whereas normal MHAU (high array intensity) shows strong cytosolic expression of ID1.

(E) At the RNA level SP1 is upregulated in 69% (11/16) of NPC tumours. Tumour MMAH (high array intensity) shows strong nuclear expression of SP1 protein whereas normal MHAU (low array intensity) shows weak expression of SP1.

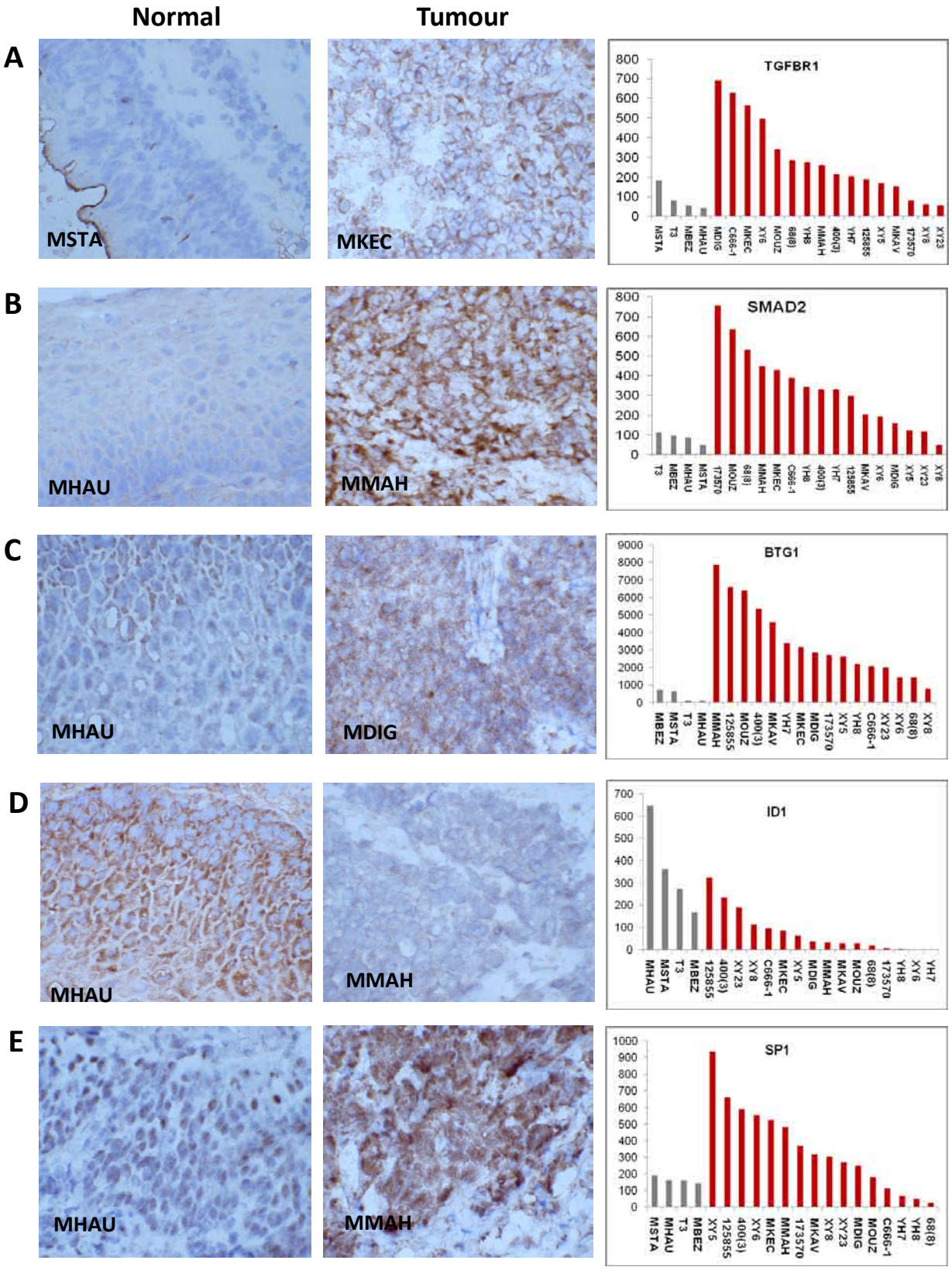
Normal
Tumour
A
MSTA
MKEC
TGFBR1
B
MHAU
MMAH
SMAD2
C
MHAU
MDIG
BTG1
D
MHAU
MMAH
ID1
E
MHAU
MMAH
SP1

array analysis, and the results confirmed the array prediction as shown in Figure 5.3A. A recent publication indicated that reduced expression of TGFBR1 may contribute to decreased risk of developing pancreatic cancer (Adrian *et al.*, 2009), findings which support the notion that over-expressed TGFBR1 can act as a tumour promoting factor.

5.2.1.3 TGF-β family SMAD signalling

As mediators of TGF-β signalling, the SMADs play central roles in signal transduction and transcriptional regulation of this pathway. The array data revealed that expression of most of the SMADs including SMAD1, 2, 4, 5 and 7 was upregulated in NPC. SMAD4, as a common-mediator SMAD, is a link between receptor SMADs and downstream effectors. Inactivation of SMAD4 has been frequently observed in pancreatic and colorectal cancer and is associated with malignant progression (Miyaki & Kuroki, 2003; Bardeesy *et al.*, 2006), whereas in a subset of advanced pancreatic tumours, intact SMAD4 induces TGF-β-dependent cell proliferation (Bardeesy *et al.*, 2006). Activation of SMAD2 is essential for TGF-β and activin signal transduction. RP analysis estimated 3.5-fold upregulation of SMAD2 expression in NPC. With GCOS analysis, it was shown to be upregulated in 81% (13/16) NPCs. IHC staining for this gene in frozen sections verified the array predictions (Figure 5.3B). SMAD7 is an inhibitory SMAD for TGF-β and activin signalling, as it binds to type I receptors and interferes with the phosphorylation of the receptor SMADs, SMAD2 and 3. Transcription of inhibitory SMAD7 mRNA is induced by TGF-β stimulation and acts as an autoregulatory negative feedback signal for TGF-β and activin signal transduction (Nakao *et al.*, 1997). In RP analysis, this gene showed 4.4-fold upregulation in NPC, whereas GCOS analysis revealed that it was upregulated in 69% (11/16) samples. The protein level of SMAD7 in NPC

tumour and normal epithelial tissue was determined by IHC staining, and the results showed that 60% (21/35) of NPC tumours displayed increased expression of SMAD7 compared to normal nasal epithelia (Figure 5.2 B).

5.2.1.4 TGF-β family target genes

TGF-β family members exert a variety of biological effects by modulating the transcriptional responses of a number of target genes (Levy & Hill, 2005). TGF-β and activin utilise the same set of SMADs (SMAD2, 3 and 4) for signal transduction. Comparative expression profiling of cell lines overexpressing constitutively active type I TGF-β or activin receptors revealed that they modulate similar transcriptional responses (Ryu & Kern, 2003). BMP signalling utilises different pathway-restricted SMADs (SMAD1/5/8), and its targets might be somewhat different (Miyazono *et al.*, 2005). A number of well-known TGF-β family target genes were found to be upregulated in our expression array data. These included TGFBI, a TGF-β-responsive gene (Thapa *et al.*, 2007), that was described in Chapter 4. This gene was found to be located in chromosome 5q31.1-31.2, a small region of loss. Transcripts of TGFBI were elevated 2 fold and GCOS analysis and IHC data revealed that its expression was increased in 63% (10/16) and 54% (7/13) NPC tumours at the RNA and protein level, respectively. SKIL, an oncogene that was introduced in Chapter 3, showed 5.4-fold upregulation in NPC by RP analysis. Another well-established TGF-β-responsive gene (Kortlever *et al.*, 2008), plasminogen activator inhibitor-1 (PAI1), also called SERPINE1, although not identified by RP analysis, was found to be absent in 4 normal controls while present in about 37.5% (6/16) of NPCs. The protein expression of SERPINE1 was examined by IHC staining in tissue arrays, where protein upregulation was observed in 53.6% (15/28) of NPC tumours (Figure 5.2 C). RP

analysis revealed that another TGF-β target gene, BTG1, was upregulated 14.2-fold in NPCs. By GCOS analysis it was found to be upregulated in 93% (15/16) NPCs. IHC staining of BTG1 in the frozen NPC tumour confirmed its upregulation relative to normal control epithelium (Figure 5.3C). Overexpression of BTG1 has been demonstrated to promote cell migration and play an important role in angiogenesis (Iwai *et al.*, 2004). In addition to the transcriptional upregulation, a small number of TGF-β target genes were down-regulated in NPC tumours. ID1, which plays an important role in the inhibition of cell differentiation and growth arrest was firstly found to be a direct target for BMP signalling (Miyazono & Miyazawa, 2002). Although ID1 expression is induced by BMP signalling, it has been reported that the level of its expression is suppressed in response to canonical TGF-β signalling in epithelial cells (Ling *et al.*, 2002). RP analysis identified a 3.7-fold downregulation of ID1 transcripts in NPC tumours. GCOS analysis confirmed downregulation of ID1 in 81% (13/16) of NPC tumours. IHC staining of frozen sections from the same samples used for array analysis further confirmed that ID1 protein was reduced in NPC compared to normal epithelia (Figure 5.3D).

5.2.2 Dysregulation of TGF-β signalling in the C666-1 cell line

As mentioned in chapter 3, a sample correlation analysis revealed that the C666-1 cell line had an overall expression pattern very similar to that of the majority of NPC tumour biopsies. To analyse the similarity in the expression of individual genes in C666-1 cells and NPC tumour biopsies further, a comparison of gene expression between C666-1 and the 4 normal biopsies was carried out. The array-determined fold changes determined by comparing the 4 normal samples with both the whole tumour set and with cell line C666-1 alone are shown in Table 5.1. In the majority of cases,

accounting for 74% (40/54) of genes, C666-1 follows the overall pattern of up- or down-regulation but some genes do not follow the average trend (the fold changes for these genes are highlighted in the table). For example activin, TGFBR2 and ITGB6 are predicted to be down-regulated in C666-1 whereas they were estimated to be upregulated in NPCs by RP analysis.

Since the sample correlation analysis also indicates that tonsillar epithelial cells appear to be a good model for normal nasopharyngeal epithelial cells, they were used as a normal control to examine the reliability of array predictions in C666-1 cells. The mRNA derived from C666-1 cells and cultured primary tonsillar epithelial cells were used for RT-PCR and qRT-PCR analysis. Downregulation of TGFBR2, TGFBI and upregulation of SMAD2 were verified by RT-PCR (Figure 5.4), findings which are consistent with previous results that demonstrated the absence of TGFBR2 and TGFBI expression in C666-1 (Wood *et al.*, 2007). In addition, qRT-PCR analyses confirmed the upregulation of BMP2, MAPK1, and E2F5, and downregulation of NEDD9, HES1 and ID1 in C666-1 cells (Figure 5.5). Since GCOS called CLDN1 expression as “absent” in C666-1 cells, its fold change could not be accurately estimated. In agreement with the array data, CLDN1 expression was undetectable in the qRT-PCR analysis.

5.3 The Wnt signalling pathway

5.3.1 The Wnt/β-catenin pathway and cancer

The Wnt signalling pathway and its signal transduction were introduced in detail in Section 1.4.4.3. The activation of the Wnt canonical signalling pathway ultimately leads to the stabilisation and accumulation of β-catenin in the nucleus of cells.

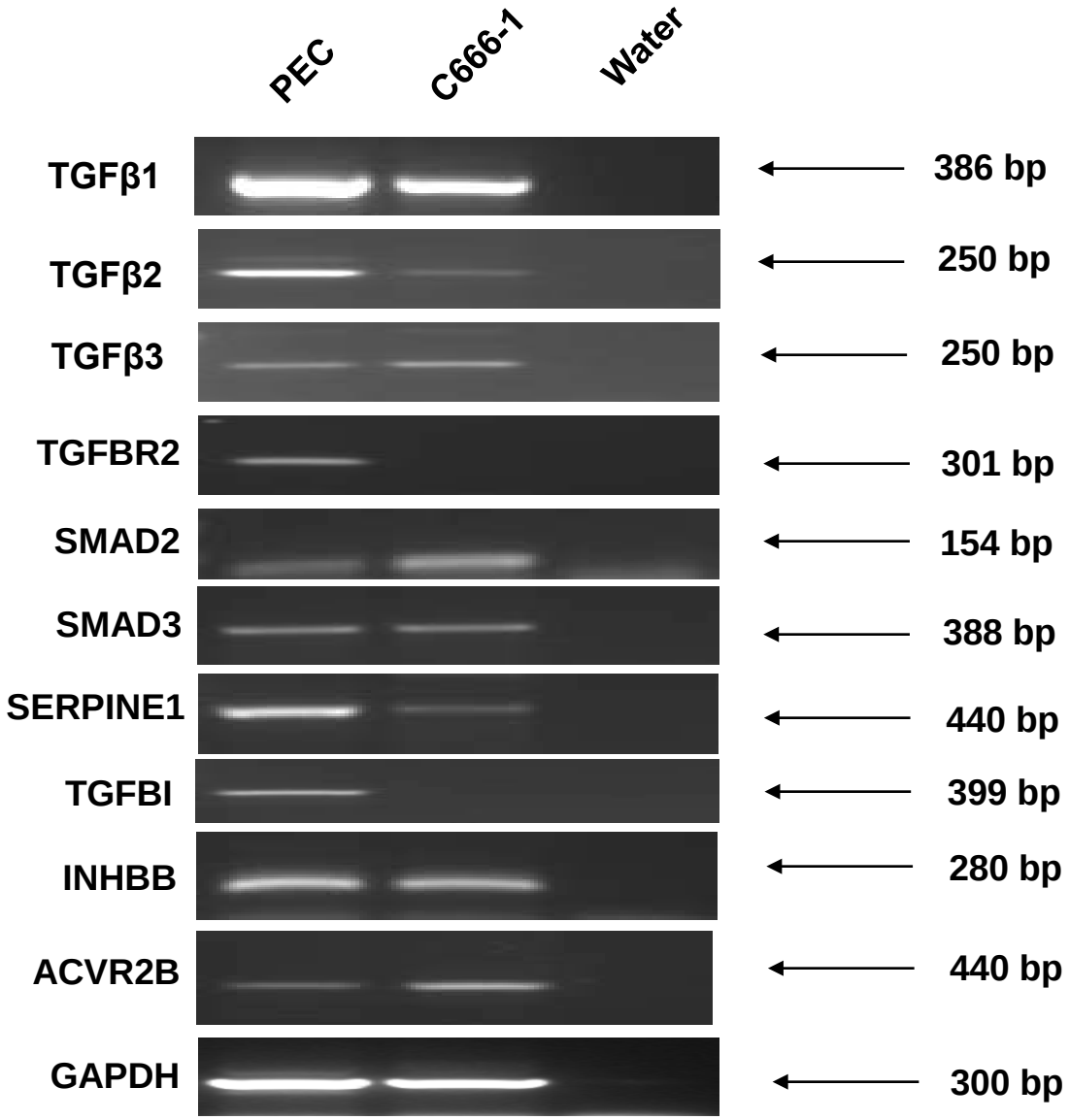

Figure 5.4: Expression levels of TGF-β family members in C666-1 cells determined by RT-PCR. RNA was extracted from C666-1 and cultured primary tonsillar epithelial cells (PEC). Following cDNA synthesis, the expression of TGF-β family genes was analysed by RT-PCR. The PCR products were viewed by agarose gel electrophoresis. RT-PCR for the housekeeping gene GAPDH was utilised as an internal control to confirm equal RNA input into each PCR reaction. Compared to control primary tonsillar epithelial cells, the downregulation of TGFBR2, TGFBI, and upregulation of SMAD2 are observed in C666-1 cells.

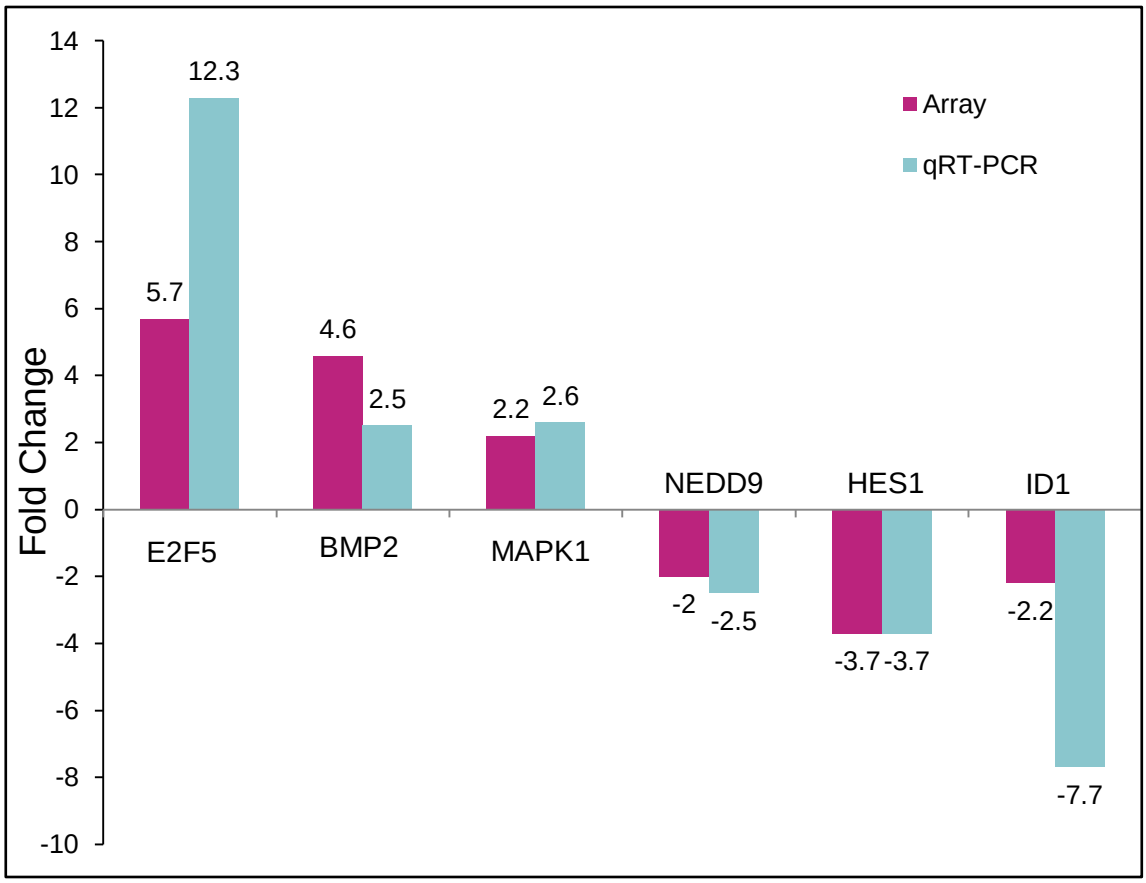

Figure 5.5: Validation of expression array data for C666-1 by qRT-PCR analyses. Three biological replicates of RNA were extracted from C666-1 and cultured primary tonsillar epithelial cells (PEC). Following cDNA synthesis, the expression of TGF-β family genes (E2F5, BMP2, MAPK1, NEDD9, HES1, and ID1) were analysed by qRT-PCR. Each assay on each sample was performed in triplicate. The mean fold change of RNA expression in C666-1 cells relative to PEC were determined by using the housekeeping gene GAPDH as an internal control. The fold change determined by both array (purple bars) and qRT-PCR (blue bars) are in the same direction (upregulation of E2F5, BMP2 and MAPK1, downregulation of NEDD9, HES1, and ID1).

Nuclear β-catenin plays critical roles in tumourigenesis by enhancing the expression of a number of functional genes. The aberrant activation of the Wnt/β-catenin pathway has been associated with various human cancers, including colorectal cancer (Hadjihannas *et al.*, 2006), prostate cancer (Verras & Sun, 2006), liver cancer (Monga, 2009), and NPC (Zeng *et al.*, 2007).

A distinct feature of the activated Wnt/β-catenin pathway in cancers is the mutation of key signalling components. Any mutational inactivation of pathway negative regulators (eg, APC, AXIN and GSK3β) and aberrant activation of positive regulators (eg, CTNNB1) through mutation could cause abnormal activation of this pathway. A large number of tumour types have been described with mutations in APC or CTNNB1 (β-catenin), and occasionally mutations in AXIN or other components have also been documented. Colorectal cancer is the most notable tumour with mutations in genes included in the Wnt/β-catenin pathway. More than 90% of colorectal cancer showed abnormal activating mutations of Wnt/β-catenin signalling, approximately 80% of them carrying APC mutations and more than 10% containing gain-of-function mutations in CTNNB1 (Groden *et al.*, 1991; Miyaki *et al.*, 1999; Schneikert & Behrens, 2007). Gastric carcinoma is another common cancer with a high number of mutations in APC (76%) (Lee *et al.*, 2002)) and CTNNB1 (26%) (Clements *et al.*, 2002). Whereas AXIN1 mutation has been observed in hepatocellular carcinoma (Satoh *et al.*, 2000) and prostate carcinoma (Yardy *et al.*, 2009).

In addition to the frequent observation of mutations in components of the Wnt/β-catenin signalling in cancers, the aberrant expression of genes involved in this pathway is also a common event. Increasingly altered nuclear accumulation of

CTNNB1 has been found to be associated with advanced gastric cancer (Ougolkov *et al.*, 2000). Reduced APC protein expression has been detected in primary breast cancer (Ho *et al.*, 1999). Increased expression of CTNNB1 and GSK3β and reduced APC expression have been observed in ovarian carcinoma compared to normal ovary (Rask *et al.*, 2003). Several publications have investigated the relationship of gene mutation and aberrant expression in cancers. In some cases, the mutational inactivation of AXIN1, APC or activation of CTNNB1 did closely correlate with their aberrant expression. For instance, in ovarian carcinoma, all the cases with mutation of CTNNB1 showed nuclear CTNNB1 protein expression (Wright *et al.*, 1999). The nuclear expression level of CTNNB1 was significantly higher in colorectal tumours with APC mutations compared to tumours with wild type APC (Dimberg *et al.*, 2001). But in others, it suggests that the mutations and abnormal expression might be independent events activating the Wnt/β-catenin signalling pathway and contributing to tumourigenesis (Cui *et al.*, 2003; Austinat *et al.*, 2008; Tanahashi *et al.*, 2008).

5.3.2 Dysregulation of the Wnt signalling pathway in NPC

Although the precise function of the Wnt signalling pathway in NPC is not fully understood, several lines of evidence indicate that Wnt signalling plays roles in NPC development. Gene expression profile revealed dysregulation of a number of components involved in Wnt signalling (Shi *et al.*, 2006; Zeng *et al.*, 2007). Wnt inhibitory factor1 (WIF1) is frequently silenced, and the finding that ectopic expression of WIF1 inhibits tumour cell colony formation underscores a possible role for WIF1 silencing in NPC pathogenesis (Lin *et al.*, 2006; Chan *et al.*, 2007). In agreement with previous findings, our array data revealed a substantial enhancement of several Wnt signalling components in NPC including ligands (WNT5A and

WNT10B), receptors (FZDs and LRP), signalling adapters (DVL3), transcription factors (CTTNB1, LEF and TCF) and targets (JUN and CCND2), whereas a key negative regulator, APC, was significantly down-regulated (Figure 5.6 and Table 5.2).

The upregulation of WNT5A and CTNNB1 was verified at the protein level in tissue arrays by IHC staining (Section 3.5.1 and 3.5.5). The IHC data revealed that 43.5% of NPC tumours showed upregulation of WNT5A compared to adjacent normal epithelia. WNT5A can engage both the canonical (β-catenin, TCF/LEF) and non-canonical Wnt signalling pathways (Rac/JAK/NLK). This signalling is context-dependent based on the expression of its downstream targets, for example, WNT5A engagement of FZD5 activates the canonical pathway (Katoh & Katoh, 2007). In the expression array, FZD5 expression was upregulated 2.4-fold in NPC, which indicates that activating Wnt signalling in NPC might be initiated from the interaction of WNT5A and FZD5. Upregulation of WNT5A has been frequently detected in cancers, and its upregulation has been suggested to enhance tumour cell migration, proliferation and invasiveness (Ripka *et al.*, 2007). CTNNB1 is the key mediator of canonical Wnt signalling. IHC data showed CTNNB1 was over-expressed in 33.3% (6/18) of NPC (Section 3.5.5). Although CTNNB1 mutation has been frequently observed in gastric and colorectal cancer (see above section), mutation of CTNNB1 is rarely observed in NPC tumours (Li *et al.*, 2004). Therefore, the increased CTNNB1 expression in NPC might be a consequence of Wnt signalling activation or mutational inactivation of other components.

Our expression array revealed that down-regulation of Wnt signalling components in NPC is not a frequent event. However, the destruction complex component, APC,

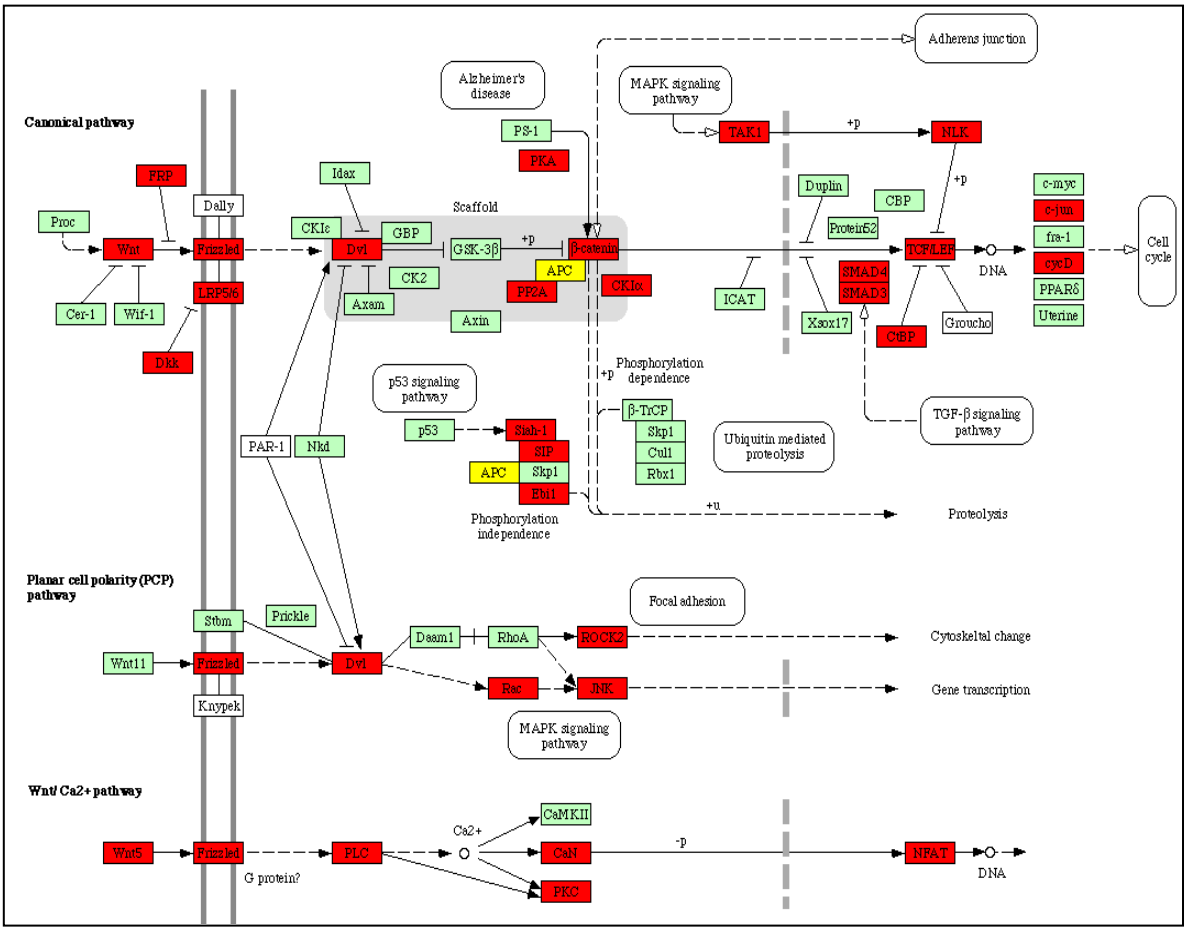

Figure 5.6: A number of genes involved in Wnt signalling are dysregulated in NPC. The significantly differentially regulated genes identified by RP analysis of expression array data were examined using the FatiGO program and KEGG database. The figure generated through this analysis represents a schematic model of the main components involved in the Wnt signalling pathway. A number of genes involved in the Wnt signalling pathway ranging from ligands, receptors, transcription factors and target genes are generally upregulated as shown by the red boxes, whereas APC appears to be downregulated in NPC tumours (yellow box). The green boxes indicate genes whose expression was not significantly changed.

Table 5.2: Differentially regulated genes involved in the Wnt signalling pathway.

Gene Symbol	Name	p value (t)	FC (overall)	FC (C666-1)
Wnt Ligands				
WNT10B	wingless-type MMTV integration site family, member 10B	0.0057	2.2	2.2
WNT5A	wingless-type MMTV integration site family, member 5A	0.067	1.8	4.1
Wnt antagonists				
DKK1	dickkopf homolog 1 (Xenopus laevis)	0.010	2.1	1.3
SFRP1	secreted frizzled-related protein 1	0.062	2.0	-1.2
Wnt Receptors				
FZD7	frizzled homolog 7 (Drosophila)	0.000001	27.8	65.4
FZD6	frizzled homolog 6 (Drosophila)	0.022	4.0	4.8
FZD1	frizzled homolog 1 (Drosophila)	0.00087	2.5	1.9
FZD5	frizzled homolog 5 (Drosophila)	0.0018	2.4	2.8
Signalling adapter				
DVL3	dishevelled, dsh homolog 3 (Drosophila)	0.00047	3.1	4.8
Signal transduction				
AKT3	v-akt murine thymoma viral oncogene homolog 3 (protein kinase B, gamma)	0.00037	5.5	19.5
AKT2	v-akt murine thymoma viral oncogene homolog 2	0.032	2.2	1.5
APC	adenomatous polyposis coli	0.18	-4.0	-3.1
MAP kinases				
MAP3K7	mitogen-activated protein kinase kinase kinase 7	0.000087	4.4	4.3
MAPK8	mitogen-activated protein kinase 8	0.00017	2.7	6.4
MAPK9	mitogen-activated protein kinase 9	0.0065	2.3	9.9
Protein Phosphatases				
PPP2R3C	protein phosphatase 2 (formerly 2A), regulatory subunit B'', gamma	0.025	3.5	9.6
PPP2R5E	protein phosphatase 2, regulatory subunit B', epsilon isoform	0.0086	3.5	10.1
PPP3R1	protein phosphatase 3 (formerly 2B), regulatory subunit B, alpha isoform	0.011	3.1	9.9
PPP3CB	protein phosphatase 3 (formerly 2B), catalytic subunit, beta isoform	0.0016	2.9	4.6
PPP2CB	protein phosphatase 2 (formerly 2A), catalytic subunit, beta isoform	0.020	2.8	6.2
PPP3CA	protein phosphatase 3 (formerly 2B), catalytic subunit, alpha isoform	0.035	2.5	1.9
PPP2R2A	protein phosphatase 2 (formerly 2A), regulatory subunit B, alpha isoform	0.15	2.0	1.0
PPP2R1B	protein phosphatase 2 (formerly 2A), regulatory subunit A, beta isoform	0.0019	1.9	2.7
Protein kinases				

PRKAR2B	protein kinase, cAMP-dependent, regulatory, type II, beta	0.050	3.4	25.2
PRKAB2	protein kinase, AMP-activated, beta 2 non-catalytic subunit	0.0018	2.2	2.1
PRKCA	protein kinase C, alpha	0.056	2.1	1.0
PRKCI	protein kinase C, iota	0.15	2.0	2.2
NLK	nemo-like kinase	0.10	1.9	1.9
PRKCZ	protein kinase C, zeta	0.017	-2.8	-2.1
Ubiquination				
SIAH1	Seven in absentia homolog 1 (Drosophila)	0.000096	2.3	5.5
BTRC	beta-transducin repeat containing	0.00023	-1.8	-1.9
Miscellaneous				
CACYBP	calcyclin binding protein	0.00011	4.7	5.0
Rho GTPases				
CDC42EP3	CDC42 effector protein (Rho GTPase binding) 3	0.000033	3.1	6.0
ROCK2	Rho-associated, coiled-coil containing protein kinase 2	0.020	2.2	4.6
Transcription factors				
LEF1	lymphoid enhancer-binding factor 1	0.00028	4.8	6.2
TCF3	transcription factor 3 (E2A immunoglobulin enhancer binding factors E12/E47)	0.015	3.2	3.5
CTNNB1	catenin (cadherin-associated protein), beta 1, 88kDa	0.058	2.5	2.4
NFATC2IP	nuclear factor of activated T-cells, cytoplasmic, calcineurin-dependent 2 interacting protein	0.000012	6.1	6.4
NFAT5	nuclear factor of activated T-cells 5, tonicity-responsive	0.0015	2.2	2.1
NFATC2	Nuclear factor of activated T-cells, cytoplasmic, calcineurin-dependent 2	0.022	1.9	4.2
Wnt targets				
CCND2	cyclin D2	0.0023	4.8	8.0
JUN	jun oncogene	0.0066	4.9	13.4

“FC” indicates fold change determined by comparing the 4 normal samples with both the whole tumour set (overall) and with cell line C666-1 alone (C666-1).

The yellow boxes indicate genes whose expression level in C666-1 is relatively unchanged.

showed an overall 4-fold downregulation by RP analysis and reduced expression in all the NPCs by GCOS analysis. IHC staining of our tissue array revealed that 46.2% (6/13) of NPCs had reduced APC protein expression (Figure 5.7). Although reduced APC expression has been reported in a number of tumour types (Ho *et al.*, 1999; Chen *et al.*, 2005; Song & Zhang, 2009), the expression pattern of this gene has not been reported in NPC. In theory, inactivation of APC could result in the stabilisation of CTNNB1 and contribute to activation of Wnt signalling.

5.3.3 Dysregulation of Wnt signalling in the C666-1 cell line

To analyse further the similarity in the expression of individual Wnt family members in C666-1 cells and in the whole tumour set, a comparison of gene expression between C666-1 and the 4 normal biopsies was carried out. The array-determined fold changes determined by comparing the 4 normal samples with both the whole tumour set and with cell line C666-1 alone are shown in Table 5.2. Relative expression levels of all genes except DKK1, CLDN1 and SFRP1 in C666-1 showed the same direction for their up- or down-regulation as the average level in the whole tumour set.

5.4 The Hedgehog (Hh) signalling pathway

In addition to the dysregulation of TGF-β and Wnt signalling in our NPC tumour samples, many components of the Hh signalling pathway were also found to be dysregulated. The Hh pathway is essential for mammalian development, with components acting as morphogens, growth factors and survival factors (Ingham & McMahon, 2001; Goetz *et al.*, 2002). The dysregulation of the Hh pathway has been

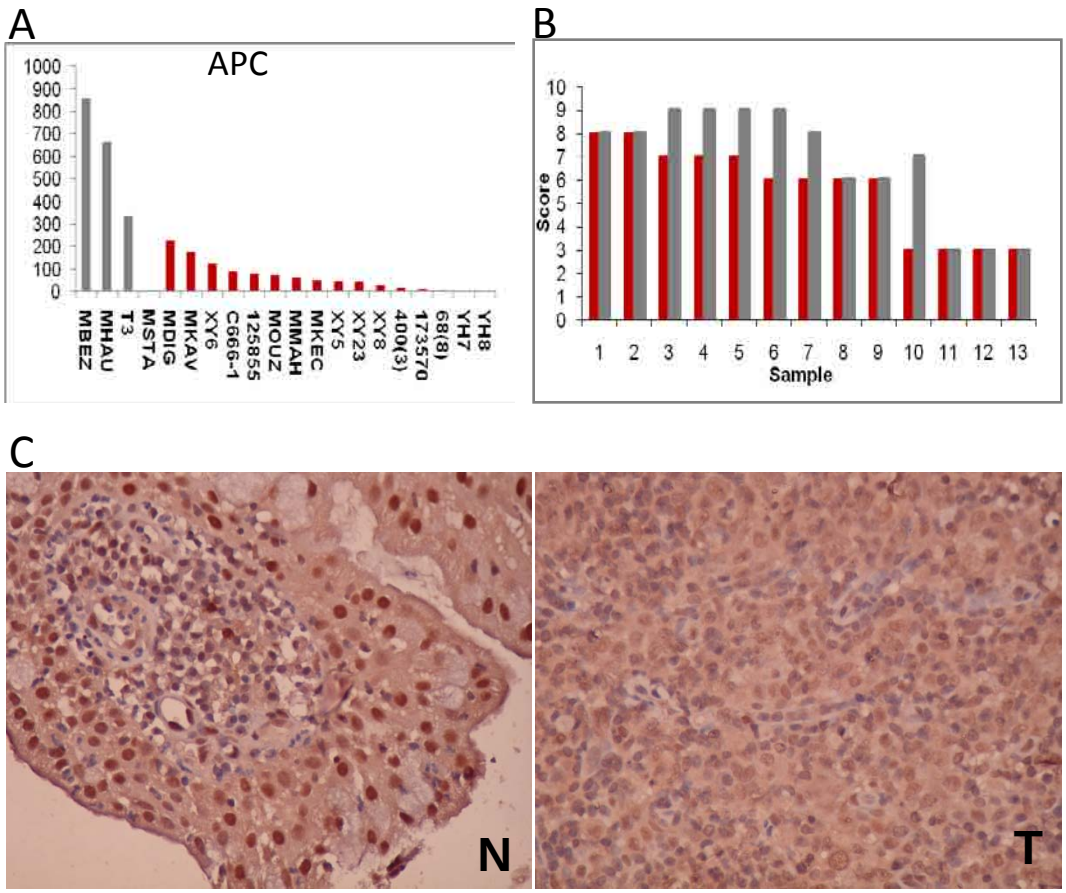

Figure 5.7: APC expression is downregulated in NPC at both the RNA and protein level. APC expression was analysed with expression array and IHC data. Panel A shows normalised expression array intensities for the 4 normal samples (grey) and 15 NPCs plus C666-1 (red), whilst panel B shows the IHC scoring results from the tissue arrays (normal, grey: tumour, red). Panel C shows examples of IHC staining in NPC tumour (T) and normal epithelial cells (N). At the RNA and protein levels respectively, APC is downregulated in 16/16 (100%) and 46.2% (6/13) samples. Positive APC staining is predominantly observed in the nucleus. Normal epithelial cells (N) show intense APC protein expression, whereas tumour cells (T) show weak APC expression.

implicated in several cancers (Kayed *et al.*, 2004; Wang *et al.*, 2006; Lee *et al.*, 2007), however its dysregulation has not been reported in NPC.

5.4.1 Hh signal transduction

In mammals, the Hh family members consist of Sonic Hh (SHH), Indian and Desert Hh. Hh binding to its receptor Patched 1 (PTCH1) initiates Hh signalling. PTCH1 functions as a negative regulator in this pathway. In the absence of Hh ligands, PTCH1 blocks Smoothened (SMO) activity by preventing its localisation to the cell surface. The amount of Hh available to bind PTCH1 is tightly controlled by Hh-binding proteins (HIP) and Growth arrest-specific gene (GAS1). In addition to being a signalling receptor, PTCH1 is also an Hh target and is frequently used as an indicator of Hh activation. The upregulation of PTCH1 sequesters hedgehog and suppresses its spread. Thus, the activity of Hh signalling is affected by the balance between the concentrations of Hh and PTCH1 (Chen & Struhl, 1996). When Hh is present, the activity of SMO is derepressed. The activated SMO regulates transcriptional factors, GLI family (GLI1, 2 and 3), which are responsible for modulating a number of Hh target genes (Jiang & Hui, 2008). GLI1 and 2 are thought to be activators for Hh targets whereas GLI3 is considered to act mainly as a repressor (Ruiz i Altaba, 1999). Suppressor of fused (SUFU) acts as a key negative regulator in the Hh pathway. SUFU binds GLI transcription factors, preventing them from activating Hh target genes (Evangelista *et al.*, 2006; Cheng & Yue, 2008). The target genes of Hh signalling include PTCH1, the Wnt family and Bone Morphogenic Proteins (BMPs), members of the TGF-β superfamily (Cohen, 2003), which have been introduced earlier.

5.4.2 Dysregulation of Hh signalling components in NPC

The expression array data revealed that a number of genes involved in Hh signalling were upregulated in NPC relative to control normal epithelia (Figure 5.8 and Table 5.3). These included the Hh signalling receptor (PTCH1), pathway inhibitors (GAS1 and RAB23), several protein kinases, Hh pathway mediators and regulators, transcription factor (GLI3) and a number of Hh target genes (i.e., FOXM1, CCND2, BMI1 and BCL-2) whose abnormal expression has been associated with cell cycle progression, proliferation and apoptosis. Conversely, a few genes were found to be down-regulated in NPC. These included the Hh pathway inhibitor (SUFU), and transcription factor (GLI2). The array-determined fold changes determined by comparing the 4 normal samples with both the whole tumour set and with cell line C666-1 alone are also shown in Table 5.3. This reveals that in the majority of cases, C666-1 followed the same direction for the up- or down-regulation of genes involved in Hh pathway.

SHH is the major ligand of the Hh pathway. Although it was called by GCOS as "absent" in both the normal and tumour samples, except for sample XY6 (Figure 5.9 A, upper panel), in a preliminary IHC staining experiment, it appeared to be upregulated in NPC tumour cells compared to tonsil epithelial cells (Figure 5.9 A, middle and bottom panel). PTCH1 is a crucial receptor and target of this pathway. It was shown to be upregulated in 50% (8/16) NPCs in GCOS analysis (Figure 5.9 B, upper panel), and a preliminary IHC staining data for PTCH1 showed that it was upregulated in NPC tumour cells (Figure 5.9 B, middle and bottom panels).

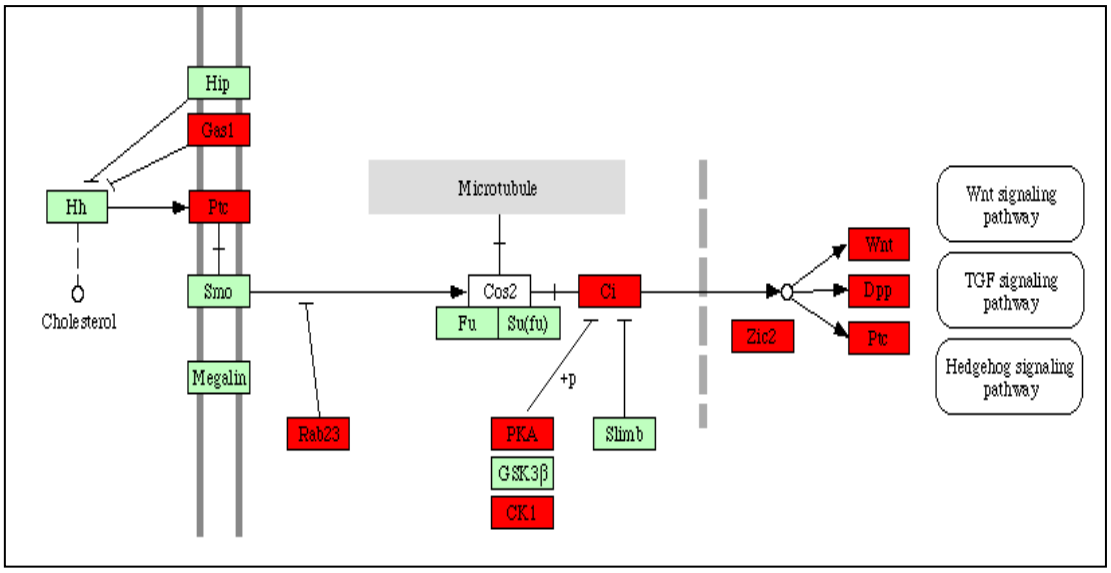

Figure 5.8: A number of genes involved in Hh signalling are dysregulated in NPC. The significantly differentially regulated genes identified by RP analysis of expression array data were examined using the FatiGO program and KEGG database. The figure generated through this analysis represents a schematic model of the main components involved in the Hh signalling pathway. A number of genes involved in this signalling pathway ranging from ligands, receptors, transcription factors and target genes are generally upregulated as shown by the red boxes. The green boxes indicate genes whose expression was not significantly changed.

Table 5.3: Differentially regulated genes involved in Hh signalling.

Gene Symbol	Name	p value (t)	FC (overall)	FC (C666-1)
Hh receptor				
PTCH1	patched homolog 1 (Drosophila)	0.013	3.3	6.6
Hh antagonists				
SUFU	suppressor of fused homolog (Drosophila)	NS	-1.7	-1.7
GAS1	growth arrest-specific 1	0.18	1.7	2.3
RAB23	RAB23, member RAS oncogene family	0.0011	2.3	1.2
Protein kinases				
CSNK1A1	Casein kinase 1, alpha 1	0.049	2.5	2.8
PRKACB	protein kinase, cAMP-dependent, catalytic, beta	0.0046	2.9	-2.0
DYRK1A	dual-specificity tyrosine-(Y)-phosphorylation regulated kinase 1A	0.064	2.8	5.3
Signalling mediator and regulator				
DZIP1	DAZ interacting protein 1	NS	1.7	1.0
FBXW11	F-box and WD-40 domain protein 11	NS	1.5	1.6
KIF4A	kinesin family member 4A	NS	3.3	5.0
ZIC2	Zic family member 2 (odd-paired homolog, Drosophila)	0.00024	2.9	8.4
Transcription factors				
GLI2	GLI-Kruppel family member GLI2	NS	-1.4	-1.7
GLI3	GLI-Kruppel family member GLI3	0.025	2.1	2.3
Hh targets				
PTCH1	patched homolog 1 (Drosophila)	0.013	3.3	6.6
BMP2	bone morphogenetic protein 2	0.0014	2.4	4.6
FOXM1	forkhead box M1	0.099	2.0	2.6
BMI1	B lymphoma Mo-MLV insertion region (mouse)	0.12	2.1	8.6
BCL2	B-cell CLL/lymphoma 2	0.0000033	30.4	7.4
SFRP1	secreted frizzled-related protein 1	0.55	2.0	-1.1
CCND2	cyclin D2	0.0023	4.8	8.0

"FC" indicates fold change determined by comparing the 4 normal samples with both the whole tumour set (overall) and with cell line C666-1 alone (C666-1)

"NS" indicates not significantly changed.

The red boxes indicate genes whose expression change in C666-l is in the opposite direction to that in the whole tumour set. The yellow boxes indicate genes whose expression level in C666-1 is relatively unchanged.

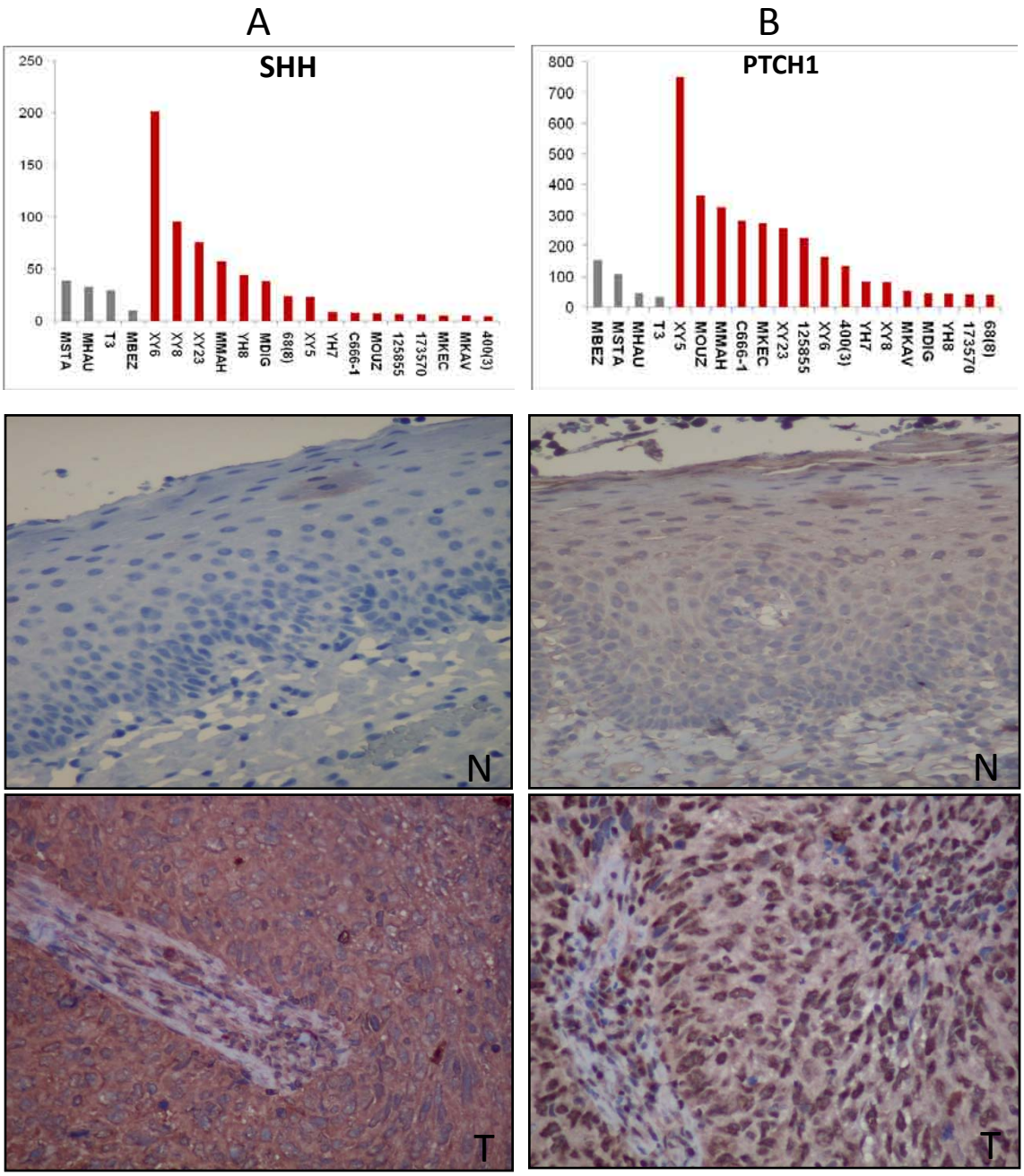

Figure 5.9: Expression array intensities and immunohistochemical staining for genes SHH and PTCH1 on NPC and tonsil epithelial sample. The upper panels show normalised expression array intensities for the 4 normal samples (grey) and 15 NPCs plus C666-1 (red). The middle and bottom panels show examples of a preliminary immunohistochemical staining on tonsil epithelial and NPC tissue. (A) SHH is present in one NPC tumour (XY6) but absent in other NPCs and normal controls at the RNA level. At the protein level, SHH shows intense cytoplasmic staining in NPC tumour cells but is absent in tonsil epithelial cells. (B) PTCH1 is upregulated in 50% (8/16) NPCs at the RNA level. At the protein level, it shows strong nuclear staining in NPC tumour cells but is weak in tonsil epithelial cells.

5.5 Discussion

To identify cell signalling pathways whose activity was dysregulated in NPC, the differentially regulated genes identified from expression array data by RP analysis were examined in the FatiGO program and KEGG database. This revealed that several signalling pathways including TGF-β/activin, Wnt/β-catenin and Hedgehog (Hh) signalling pathways were differentially regulated in NPC compared to normal nasopharyngeal epithelia. The dysregulation of several gene components involved in these pathways predicted by array analysis were validated at the protein or RNA levels by IHC staining, RT-PCR and qRT-PCR, respectively.

In the expression array data, a large number of components involved in TGF-β signalling were found to be upregulated in NPC including TGF-β family ligands, receptors, SMADs and targets, findings which indicate that TGF-β signalling is abnormally activated in NPC. We know that activation of the TGF-β family is initiated through ligand binding to receptors, however, in the array data the expression of canonical TGF-β ligands, TGF-β1, 2 and 3 was estimated to be absent in NPC tumours. How can the pathway be activated without ligand stimulation? One possible mechanism is that the NPC tumour cells do not make TGF-β ligands themselves, but respond to TGF-β produced by the surrounding stroma (see Section 5.2.1.1). Increased expression of TGF-β in the surrounding stroma of head and neck cancer has been reported (Rosenthal *et al.*, 2004). To verify this hypothesis, an expression study of TGF-β in NPC and its surrounding stroma is required. Although expression of the canonical TGF-β ligands appears to be absent in NPC, expression of the TGF-β family member, activin, is upregulated in NPC. As both canonical TGFβ and non-

canonical activin signalling utilise the same SMADs and modulate a similar set of target genes (see Section 5.2.1.4), it is possible that the differential transcriptional levels of some TGF-β family members were abnormally regulated due to activin rather than TGF-β signalling. TGFBR2 has been reported to be mutated and/or downregulated in a number of tumours (Munoz *et al.*, 2006; Xu *et al.*, 2007; Biswas *et al.*, 2008). Transfection of dominant negative TGFBR2 into mice accelerates tumourigenesis and contributes to tumour development (Pu *et al.*, 2009), whereas high levels of expression can reportedly enhance TGF-β signal transduction and increase the specificity of its biological effect (Rojas *et al.*, 2009). In our expression array data, the RP analysis revealed 2.1-fold upregulation of TGFBR2 expression in NPCs, with IHC staining confirming upregulation of TGFBR2 at the protein level in NPC tumours. This observation supports the notion that chronic activation rather than disruption of the TGF-β pathway is a consistent feature in NPC tumours.

The subcellular localisation of SMAD2 to the nucleus is an indication of transcriptionally active SMAD2 and is essential for activation of the SMAD-dependent TGF-β signalling pathway. IHC staining of SMAD2 in frozen NPC shows a predominantly cytoplasmic localisation in tumour cells. To examine further an active form of SMAD2 in NPC, it would be helpful to use a phosphorylated SMAD2 antibody for IHC staining.

Our expression array, IHC and q-PCR data revealed that ID1 expression was downregulated in both the NPC biopsies and cell line C666-1. It has been suggested that ID1 expression is suppressed by TGF-β signalling in some cancers (Ling *et al.*, 2002; Damdinsuren *et al.*, 2006), findings which are consistent with our result

demonstrating activation of TGF-β signalling and downregulation of ID1 expression in NPC. However, this result disagrees with previous findings in which ID1 expression was observed to be upregulated in NPC (Wang *et al.*, 2002). The opposing results may be due to different sample sets being used in their study and ours. Actually, the sample size used in their study is relatively small (only 5 NPC samples). To further confirm the expression status of ID1 in NPC, the sample number needs to be increased.

In addition to activation of the TGF-β signalling pathway, the Wnt signalling pathway was also found to be aberrantly activated in NPC. Expression array and IHC data demonstrated that the putative Wnt target, CTNNB1 was upregulated at both the transcriptional and protein level in NPC. In response to Wnt signalling, CTNNB1 becomes stabilised and enters the nucleus to modulate cellular gene expression. Therefore, CTNNB1 nuclear accumulation is usually considered to be an important indicator of the activation of canonical Wnt signalling. Although increased nuclear expression of CTNNB1 has been frequently found in tumours, our CTNNB1 staining in NPC was predominantly observed in the cytoplasm and membrane rather than in the nucleus. Actually, there is no consensus on the mechanism by which CTNNB1 travels between cytoplasm and nucleus. In many cases, the activation of Wnt signalling causes an overall rise in CTNNB1 protein without clear nuclear preference. This indicates that CTNNB1 nuclear import is independent of nuclear localisation (Clevers, 2006). In addition, the increased cytosolic localisation of CTNNB1 has previously been noticed in NPC (Zeng *et al.*, 2007).

Although a large number of Wnt signalling-related genes were upregulated in NPC, the tumour suppressor gene APC was found to be down-regulated. Numerous studies attest to the importance of APC silencing in the activation of Wnt signalling responses in carcinomas. APC has most frequently been observed in the cytoplasm of cells, whereas in our IHC staining, APC was predominantly localised in the cell nucleus of normal epithelium. Nuclear APC staining has also been observed previously. In the nucleus APC can bind to CTNNB1 and export it to the cytoplasm for degradation (Henderson, 2000). The reduced APC level will decrease CTNNB1 degradation, and the activated CTNNB1 is essential for activation of Wnt signalling.

The expression array data in the context of signalling pathway analysis also revealed dysregulation of the Hh pathway in NPC. Although the majority of components were upregulated in NPC, the critical pathway antagonist, SUFU, which suppresses the Hh pathway at the transcriptional level by binding to GLI proteins (Cheng & Bishop, 2002; Di Marcotullio *et al.*, 2004; Barnfield *et al.*, 2005), appeared to be downregulated in NPC despite the RP analysis not scoring its expression as significantly changed. Another antagonist, GAS1, that was identified as a putative TSG in our genetic analysis (Section 4.5.4) and has been demonstrated to inhibit cell growth and induce apoptosis (Dominguez-Monzon *et al.*, 2009), was found to be upregulated in NPC tumours. GAS1 is probably induced in NPC as part of a negative feedback loop to limit SHH signalling and can therefore be used as a readout for Hh activation.

A link between 17p deletion and abnormal activation of Hh signalling has been suggested in medulloblastoma. This study observed frequent chromosome 17p

deletion of a region carrying several genes (KCTD11, TP53, HIC1 and MNT whose dysregulation interferes with the Hh signalling cascades, ranging from GLI1, to target genes CCNDs, BCL-2 and Myc (De Smaele *et al.*, 2004; Ferretti *et al.*, 2005). In Chapter 4, we introduced the genetic changes of NPC and observed deletions of 17p11.2 - pter in 50% of NPC, which indicate that the aberrant Hh signalling in NPC might be driven by the deletion of chromosome 17p. When the expression level of genes involved in the chromosome 17 deletion (KCTD11, TP53, HIC1 and MNT) was examined using RP analysis, it estimated them to be not significantly changed. With GCOS analysis, only MNT appeared to be downregulated in about 50% of NPCs compared to normal controls, the other three (KCTD11, TP53 and HIC1) were not. This suggests that activation of the Hh pathway in NPC does not seem to be linked to dysregulation of genes involved in deletion of chromosome 17p.

Although considered to be a negative regulator in the Hh signalling pathway, GLI3 was found to be upregulated in our NPC tumour samples. Unlike GLI1 and 2, which function as transcriptional activators, GLI3 appears to function as a transcriptional repressor. Although evidence for a GLI3 activator form is weak, some studies have suggested this possibility, with GLI3 serving to regulate the expression of GLI1 through binding to the GLI1 promoter (Dai *et al.*, 1999). As overexpression of GLI3 has been shown to induce cell migration and angiogenesis (Renault *et al.*, 2009), our findings suggest that Hh induction of GLI3 may contribute to disease pathogenesis.

In spite of the observation of the activation of transcriptional factors and target genes of the Hh pathway as well as repression of pathway antagonists, the Hh ligands were scored as absent in our NPC tumour samples. It has been reported previously that the

Hh pathway can be activated in the absence of Hh ligands, with both TGFβ and activated Ras mutations simulating GLI expression and activity (Dennler *et al.*, 2007; Stecca *et al.*, 2007). This finding suggests a model where Hh ligands or other growth factors produced by adjacent stromal tissue act in a paracrine manner to activate the Hh signalling pathway (Yauch *et al.*, 2008).

The C666-1 cell line is the only cell line used in our array analysis. This is the only EBV-positive NPC cell line available and is therefore considered to be more like an NPC tumour than are other NPC lines. To investigate whether C666-1 behaves as a real tumour in the transcriptional expression of individual genes, the array-predicted fold changes were determined by comparing the 4 normal samples with both the whole tumour set and with cell line C666-1 alone. The comparison revealed that C666-1 exhibited a similar expression pattern for the majority of signalling pathway-related genes (see Table 5.1-5.3). This indicates that C666-1 approximates a real tumour and can be viewed as a good tumour model. However, a few genes do not follow the overall expression trend, for example, activin, TGFBR2, ITGB6, NEDD9 and CLDN1 are predicted to be downregulated in C666-1 whereas they appear to be upregulated in tumour samples. The observation of this phenomenon is not surprising considering that each gene has its own particular expression pattern in any one sample, whereas RP analysis can only produce a fold change by comparing the whole sample set. Actually, when the data were analysed with GCOS, it was shown even in the authentic NPC biopsies that individual gene expression could be upregulated in some samples but downregulated in others. For example, although RP analysis revealed that TGFBR2 expression was upregulated 2.1-fold, with GCOS analysis, it was shown to

be upregulated in 6 NPC tumours. Therefore, from this viewpoint, C666-1 is not unique and some of the tumour samples also behave in the same way.

Although different cell signalling pathways utilise distinct signal transduction pathways and perform different functions in tumourigenesis, emerging data suggest that crosstalk among TGF-β, Wnt and Hh signalling pathways cooperate and contribute to cancer development and progression. The crosstalk between TGF-β and Wnt has been suggested to occur at multiple levels. For example, TGF-β can induce CTNNB1 nuclear accumulation in a SMAD7-dependent manner in prostate cancer (Edlund *et al.*, 2005). In the nucleus, the SMADs and CTNNB1/LEF synergistically regulate a set of shared genes (Labbe *et al.*, 2000). SHH can induce TGF-β ligand production and TGFBR1 expression, which is essential for an invasive phenotype of gastric cancer cells (Yoo *et al.*, 2008). Wnt signalling can stimulate the expression of Hh pathway activator, GLI1, which contributes to the proliferation of colorectal cancer cells (Noubissi *et al.*, 2009). NPC pathogenesis is a highly complex process, and the disruption of various signalling pathways is most likely involved. Here, we have focused on the dysregulation of the TGF-β, Wnt and Hh signalling pathways with regard to the substantial enhancement of the components included in these three pathways. Our knowledge about the molecular nature of these pathways and their interactions is still limited in NPC. Since the expression pattern of C666-1 is very similar to NPC biopsies in the context of signalling pathway analysis, it could be used as a model to investigate the role of dysregulation of these signalling pathways in NPC tumourigenesis.

CHAPTER 6

In vitro investigation of signalling pathways in NPC cells

6.1 Introduction

The TGF-β signalling pathway has been widely investigated in cancers. It plays an important role in epithelial tumour progression by acting both as a tumour suppressor at earlier stages of tumourigenesis and as a tumour promoter at later, more advanced stages of tumour progression (Bachman & Park, 2005; Massague, 2008). Activin is a member of the TGF-β superfamily. The critical role of the activin signalling pathway in cancer has drawn attention only more recently. It has been demonstrated to be involved in cell proliferation, differentiation, apoptosis, metabolism, homeostasis, immune response and wound repair (Risbridger *et al.*, 2001; Chen *et al.*, 2006). The Hh pathway has a typical role in mammalian development and in recent years has been found to be abnormally activated in cancers (Berman *et al.*, 2003; Thayer *et al.*, 2003; Yauch *et al.*, 2008). As was introduced in chapter 5, a number of genes implicated in the TGF-β pathway (including the canonical TGF-β and activin pathways) and Hh pathway were generally upregulated in NPC tumours compared to normal nasopharyngeal epithelia (Tables 5.1 and 5.3), which suggests that these pathways might have a tumour promoting effect on the process of carcinogenesis. However, their precise function in NPC still remains to be elucidated. The present study is a preliminary investigation into the potential role of these signalling pathways in NPC carcinogenesis.

To address this question, two cell lines were used: the EBV-positive NPC cell line C666-1 and the telomerase immortalised oral keratinocyte cell line OKF6 tert-1. Since

investigation of the signalling pathways *in vivo* revealed that C666-1 exhibited a similar gene expression pattern as that of NPC biopsies (see Section 5.2.2), this cell line probably harbours the same dysregulated cell signalling pathways common to authentic NPC tumours and therefore it was used as a model for NPC tumours. OKF6 tert-1 has been demonstrated to be responsive to TGFβ1-mediated pathway activation (Peng *et al.*, 2006). Thus, this line is considered to be a good control line. The preliminary data obtained so far reveal that activin A but not TGF-β1 induces TGF-β responsive genes in C666-1 cells, indicating that the activin pathway is intact but that the TGF-β pathway is not. Both activin A and TGF-β1 induce cell cycle arrest at G2/M phase in the OKF tert-1 cell line but not in the C666-1 line. In addition, investigation of the Hh pathway in C666-1 cells reveals that this pathway is intact and seems to be activated.

6.2 TGF-β and activin signalling pathways

6.2.1 Determination of the integrity of the TGF-β and activin signalling pathways in the C666-1 line

To characterise the responsiveness of C666-1 and OKF6 tert-1 cells to TGF-β and activin signals, a TGF-β and activin-responsive reporter gene construct, SERPINE1 luciferase reporter (p3TP-luciferase) was used. C666-1 and OKF6 tert-1 cells were transiently transfected with p3TP-luciferase and a plasmid expressing Renilla luciferase, as described in section 2.10. After serum starvation for 5 hours to remove the presence of any serum-derived cytokines, cells were treated with serial dilutions of activin A or TGF-β1 for 16 hours. SERPINE1 promoter activity was examined and normalised to Renilla luciferase readings to control for transfection efficiency. A

representative set of histograms from three independent experiments are shown in Figure 6.1.

Both C666-1 and OKF6 tert-1 cells showed increased luciferase reporter activity in a dose dependent manner after treatment with activin A, indicating the presence of an intact activin signalling pathway in both types of cells. The OKF6 tert-1 cells responded to activin A (50ng/ml) by a 3.4-fold upregulation relative to control (Figure 6.1 B2), whilst the C666-1 cells showed 11.6-fold upregulation (Figure 6.1A). This indicates that C666-1 cells have a stronger response to activin A stimulation than do OKF6 tert-1 cells. However C666-1 cells did not respond to TGF-β1 stimulation (Figure 6.1A), whereas OKF6 tert-1 cells exhibited a dose-dependent increase, with the highest response (9.8-fold) following stimulation with only 0.5ng/ml of TGF-β1 (Figure 6.1 B1) This indicates that TGF-β signalling is intact in OKF6 tert-1 cells but not in C666-1 cells. Previous studies and our work (Section 5.2.2) demonstrated that C666-1 cells lack TGFBR2 expression, which most likely explains why the cells are unresponsive to TGF-β.

To further confirm the integrity of the signalling pathways, the Smad-binding element luciferase reporter (CAGA12-luciferase) was also transfected into C666-1 and OKF6 tert-1 cells. Similarly, activin A upregulated the CAGA12 reporter in both cell types in a dose-dependent manner, with the strongest responses being 33.8-fold upregulation in C666-1 (Figure 6.2A) and 11.2-fold upregulation in OKF6 tert-1 cells (Figure 6.2 B2) to 50ng/ml of activin A. This provides further evidence in support of an intact activin response in C666-1 cells. Again, C666-1 cells did not respond to TGF-β1 (Figure 6.2A), whilst OKF6 tert-1 cells exhibited a strong response in a dose-

Figure 6.1: Activin A but not TGF-β1 induces the TGF-β-responsive, SERPINE1 reporter activity in C666-1 cells.

(A) The columns show the relative activity of SERPINE1 luciferase (p3TP) in C666-1 without stimulation or after stimulation with a serial dilution of TGF-β1 or activin A. No increase in reporter activity is observed after TGF-β1 stimulation, whereas an increase in a dose dependent manner is observed after activin A stimulation.

(B) The columns show the relative activity of p3TP in OKF6 tert-1 cells after stimulation with a serial dilution of TGF-β1 (B1) or activin A (B2). A dose-dependent increase in p3TP activity is observed after stimulation.

Reporter assays were performed in biological and technical triplicate, and error bars indicate SD from three replicates of a representative experiment.

A

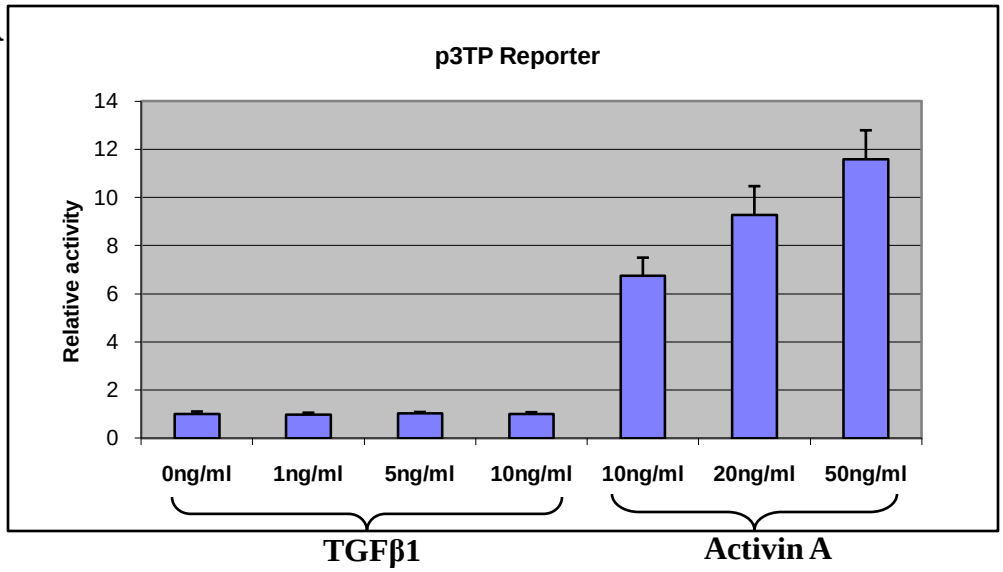
p3TP Reporter
Relative activity
14
12
10
8
6
4
2
0
0ng/ml
1ng/ml
5ng/ml
10ng/ml
10ng/ml
20ng/ml
50ng/ml
TGFβ1
Activin A

B1

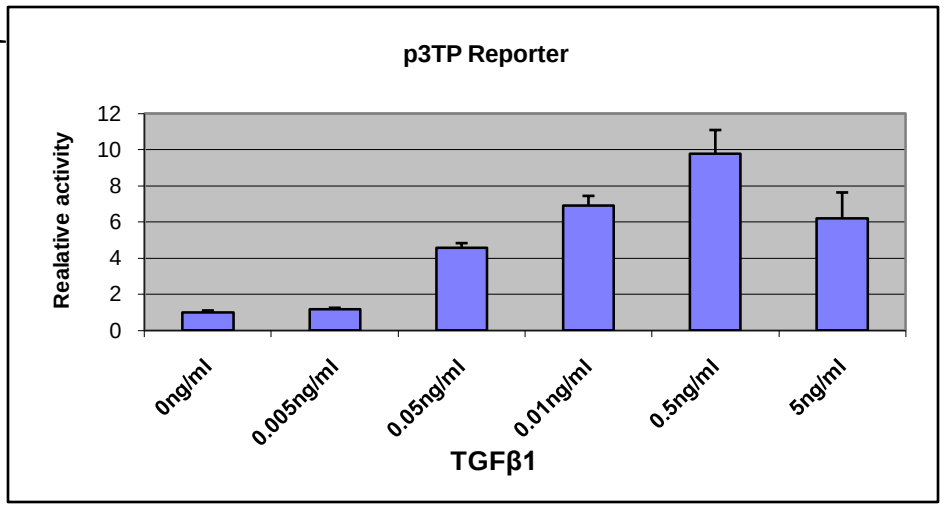
p3TP Reporter
Realative activity
12
10
8
6
4
2
0
0ng/ml
0.005ng/ml
0.05ng/ml
0.01ng/ml
0.5ng/ml
5ng/ml
TGFβ1

B2

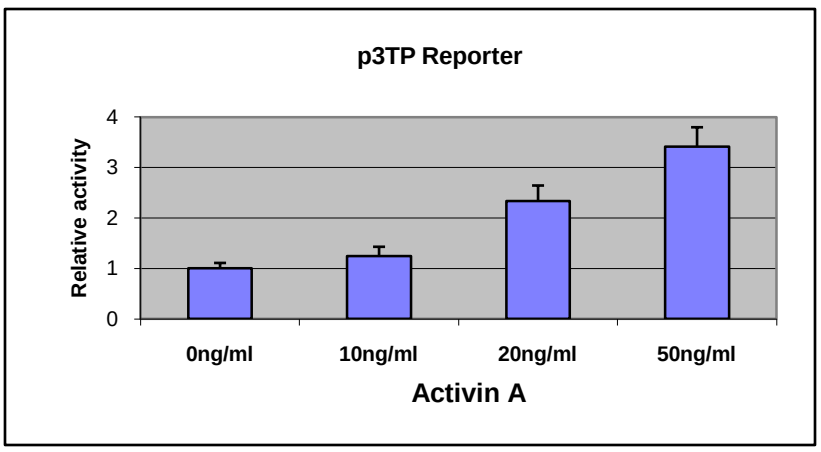
p3TP Reporter
Relative activity
4
3
2
1
0
0ng/ml
10ng/ml
20ng/ml
50ng/ml
Activin A

Figure 6.2: Activin A but not TGF-β1 induces SMAD-responsive reporter activity in C666-1 cells.

(A) The columns show the relative activity of SMAD-responsive, CAGA12 luciferase in C666-1 cells without stimulation or after stimulation with a serial dilution of TGF-β1 or activin A. No increase in reporter activity is observed after TGF-β1 stimulation, whereas an increase in a dose dependent manner is observed after activin A stimulation.

(B) The columns show the relative CAGA12 luciferase activity in OKF6 tert-1 cells after stimulation with a serial dilution of TGF-β1 (B1) or activin A (B2). A dose-dependent increase in CAGA12 luciferase activity is observed after stimulation.

A

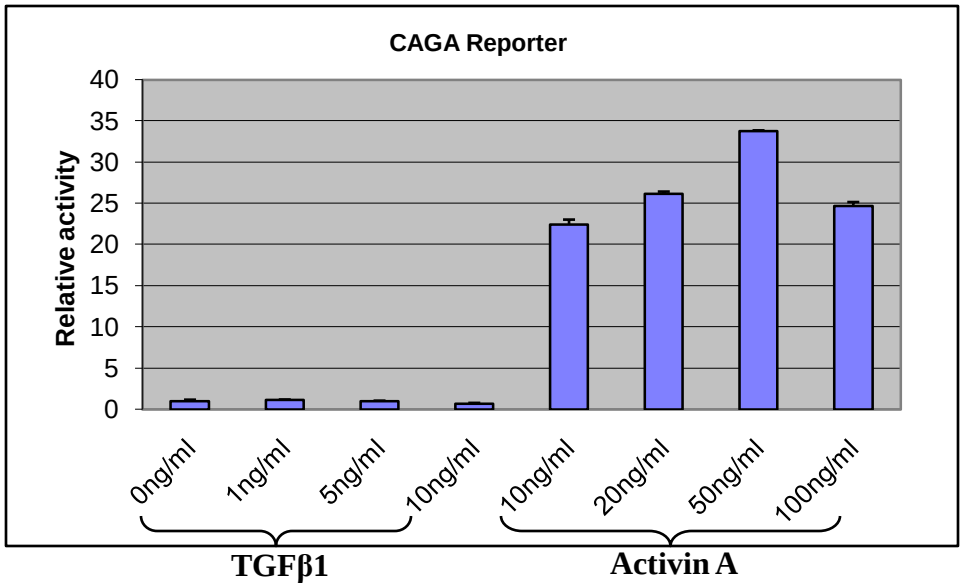
CAGA Reporter
Relative activity
40
35
30
25
20
15
10
5
0
0ng/ml
1ng/ml
5ng/ml
10ng/ml
10ng/ml
20ng/ml
50ng/ml
100ng/ml
TGFβ1
Activin A

B1

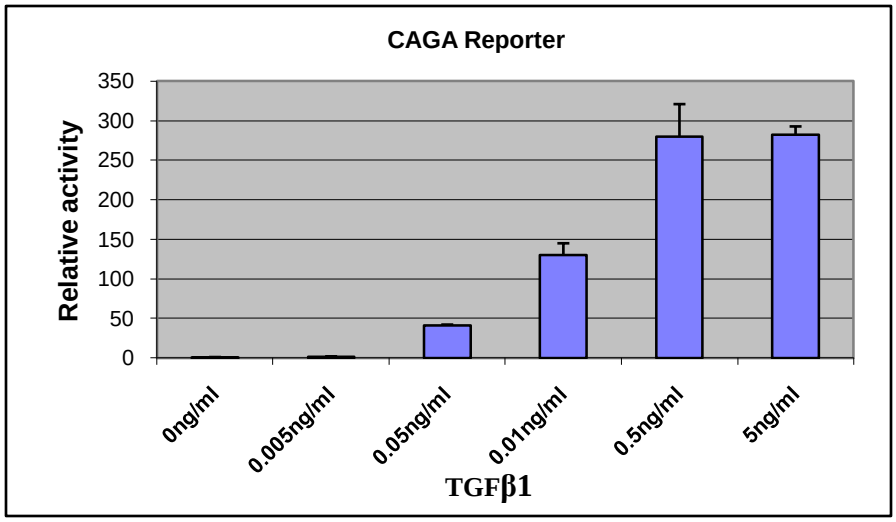
CAGA Reporter
Relative activity
350
300
250
200
150
100
50
0
0ng/ml
0.005ng/ml
0.05ng/ml
0.01ng/ml
0.5ng/ml
5ng/ml
TGFβ1

B2

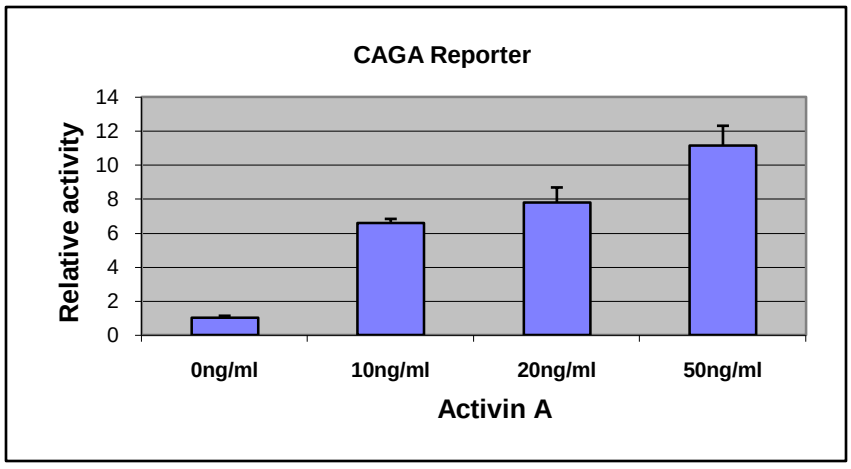
CAGA Reporter
Relative activity
14
12
10
8
6
4
2
0
0ng/ml
10ng/ml
20ng/ml
50ng/ml
Activin A

dependent manner (Figure 6.2 B1). This result once more suggests that the TGF-β pathway is not intact in C666-1 cells.

6.2.2 Analysis of gene expression levels impacted by TGF-β and activin signalling

To determine whether downstream targets of TGF-β and activin signalling were activated or altered by TGF-β and activin A stimulation, C666-1 and control cells were treated with TGF-β1 (10ng/ml) or activin A (100ng/ml) and harvested at varying time points. The total cell lysates were analysed for the expression level of known TGF-β–responsive genes using immunoblotting.

As was described in Section 1.4.4.2, both the activation of TGF-β and activin signalling can induce phosphorylation of SMAD2 and SMAD3. Immunoblotting using an antibody against the phosphorylated form of SMAD2 (p-SMAD2) revealed the presence of p-SMAD2 in C666-1 cells after activin A stimulation. The highest level of p-SMAD2 was observed after 1-hour and appeared to be slightly attenuated after that. However p-SMAD2 protein was not detected in C666-1 cells following treatment with TGF-β1 (Figure 6.3A). Control cells showed a basal p-SMAD2 level and also an increased expression after treatment with both TGF-β1 and activin A (Figure 6.3B).

SERPINE1 (PAI-1) has been identified to be a target of both TGF-β1 and activin signalling (Ryu & Kern, 2003). Immunoblotting for this protein revealed the presence of SERPINE1 expression in C666-1 after 4-hours of treatment with activin A and the strongest expression was found after 6 hours (Figure 6.3A). TGF-β1 did not induce

Figure 6.3: Activin A but not TGF-β1 induces phosphorylation of SMAD2 and upregulation of SERPINE1 and p21 in C666-1.

In response to stimulation with TGF-β1（10ng/ml）or activin A (100ng/ml), the expression levels for p-SMAD2, SERPINE1 and p21 protein in C666-1 cells (A) and OKF6 tert-1 cells (B) are displayed. β-actin is used as a loading control. Phosphorylation of SMAD2 and upregulation of SERPINE1 and p21 expression are observed in C666-1 cells after activin A stimulation, whereas no response is observed after TGF-β1 stimulation (A).

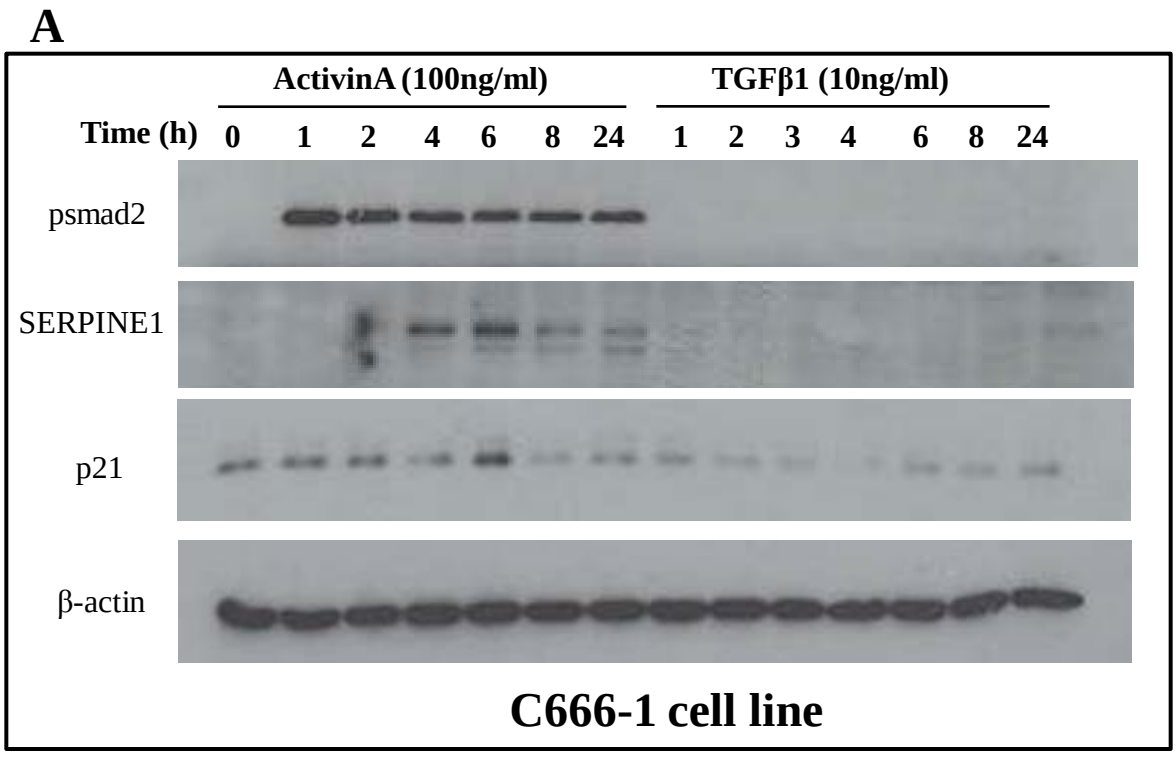
A
ActivinA (100ng/ml)
TGFβ1 (10ng/ml)
Time (h)
0 1 2 4 6 8 24
1 2 3 4 6 8 24
psmad2
SERPINE1
p21
β-actin
C666-1 cell line

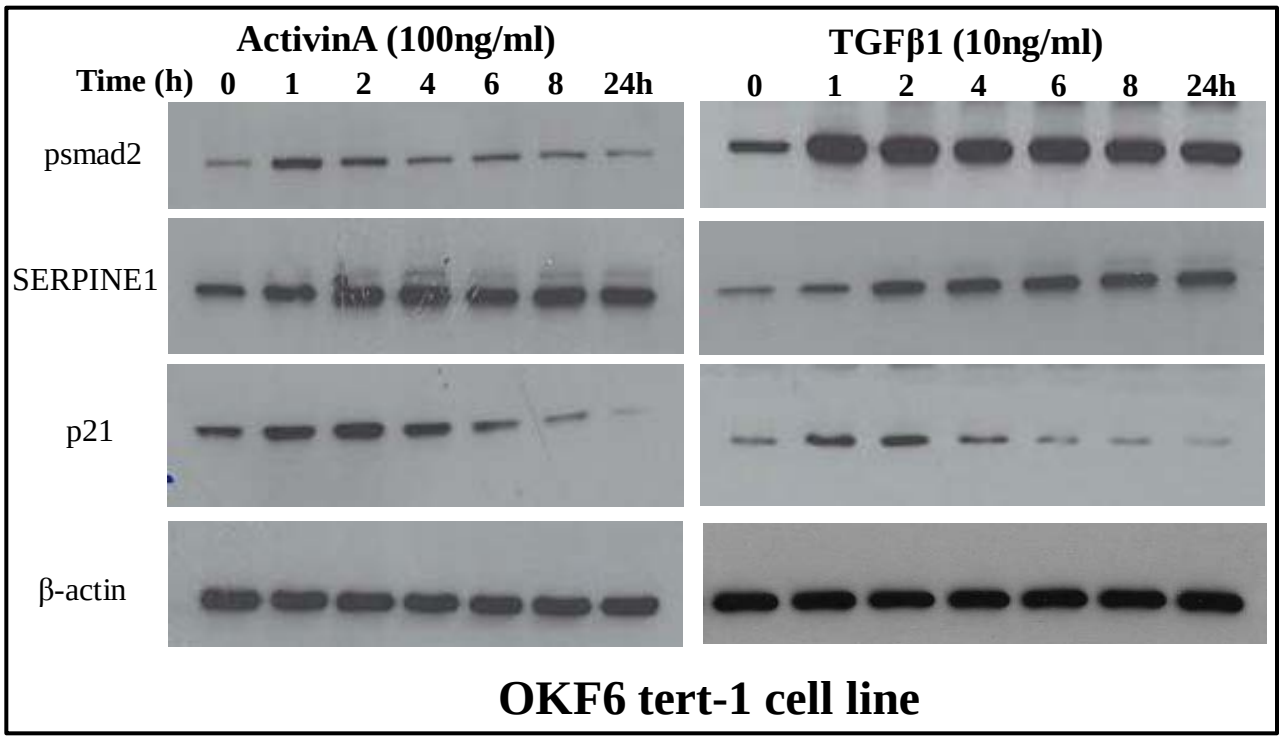
B
ActivinA (100ng/ml)
TGFβ1 (10ng/ml)
Time (h)
0 1 2 4 6 8 24h
0 1 2 4 6 8 24h
psmad2
SERPINE1
p21
β-actin
OKF6 tert-1 cell line

SERPINE1 expression. OKF6 tert-1 cells showed basal expression of SERPINE1, whereas the strongest accumulation was observed after 2 hours of TGF-β1 or activin A stimulation (Figure 6.3B).

P21 is the product of the CDKN1A gene. It is a cyclin kinase inhibitor that is also responsive to TGF-β1 and activin signalling (Ryu & Kern, 2003) and has been demonstrated to play an important role in TGF-β-induced growth inhibition (Yoo *et al.*, 1999; Bachman *et al.*, 2004; Nakamura *et al.*, 2009). In response to activin A stimulation, p21 expression was induced in C666-1 cells 6-hours after treatment, but induction of p21 was not observed after treatment with TGF-β1 (Figure 6.3A). The strongest induction of p21 was detected in OKF6 tert-1 cells after 2-hours of treatment with TGF-β1 or activin A (Figure 6.3B).

6.2.3 Analysis of cell cycle progression impacted by activin A or TGF-β1

The activin and TGF-β signalling pathways have been shown to disturb cell cycle progression and inhibit tumour growth in several types of cells (Iavarone & Massague, 1997; Yamato *et al.*, 1997; Yoo *et al.*, 1999; Burdette *et al.*, 2005). To investigate the effect of these pathways on cell cycle progression of C666-1 cells, the OKF tert-1 and C666-1 cells were treated with or without activin A (100ng/ml) or TGF-β1 (10ng/ml) for 5 days, stained with propidium iodide and analysed by flow cytometry (see Section 2.11). Compared to untreated cells (control), the OKF6 tert-1 cells treated with either activin A or TGF-β1 showed an increased cell population in G2/M phase (4.4% vs. 10.0% and 12.2%, respectively). However, no difference of cell-cycle distribution was observed in activin A or TGF-β1 treated C666-1 cells compared to

the control (Figure 6.4). This reveals that whilst both activin A and TGF-β1 induce cell cycle arrest at G2/M phase in the OKF tert-1 cell line neither influence cell cycle progression in the C666-1 line. These data suggest that whilst C666-1 cells are capable of responding to activin, they are refractory to activin-mediated growth inhibition.

6.3 Hh signalling pathway

6.3.1 Determination of the integrity of the Hh signalling pathway in C666-1 cells

To determine the integrity of the Hh pathway in C666-1 cells, C666-1 and OKF6 tert1 cells were transfected with an Hh responsive reporter (8xGLI1 luciferase), or pGL2 basic reporter as a control, and a Renilla plasmid. 24 hours after transfection, cells were treated with or without a SHH ligand (2µg/ml) for 16 hours. GLI1 reporter activity was measured and normalised to Renilla luciferase readings. Compared to OKF6 tert-1 cells, GLI1 reporter was significantly higher in C666-1 cells. Furthermore, whilst reporter activity could be stimulated in OKF6 tert-1 cells in response to SHH treatment (Figure 6.5), SHH treatment had only marginal affects on GLI reporter activity in C666-1 cells (Figure 6.5). This indicates that the Hh pathway is constitutively active in C666-1 cells.

6.3.2 Examination of the expression of Hh pathway components at the protein level

To examine the expression level of components involved in the Hh pathway, C666-1 and OKF tert-1 cells were grown *in situ* for 24 hours, and then examined for SMO, PTCH1 and GLI1 expression using a two-step immunofluorescence (IF) staining

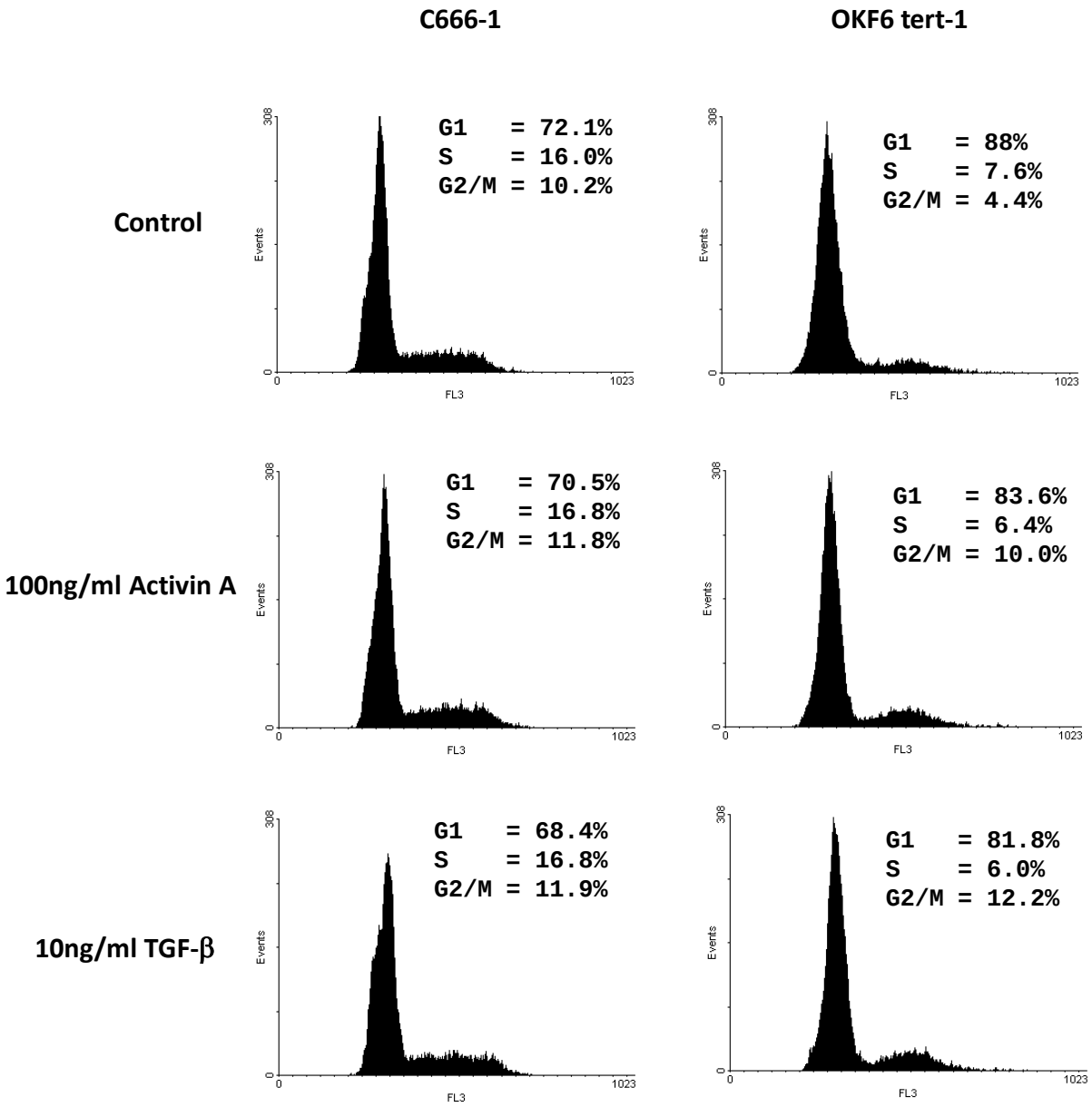

Figure 6.4: Both activin A and TGF-β1 induce cell cycle arrest at G2/M phase in OKF6 tert-1 cell line but not in C666-1 line. Cell-cycle distributions of C666-1 and OKF6 tert-1 in three phases are represented by the figures and percentages. Compared to untreated cells (control), C666-1 cells treated with either activin A or TGF-β1 shows no difference in cell-cycle distribution (left panels), whereas compare to the control, both activin A and TGF-β1 treated OKF6 tert-1 cells show an increased cell population at G2/M phase (right panels).

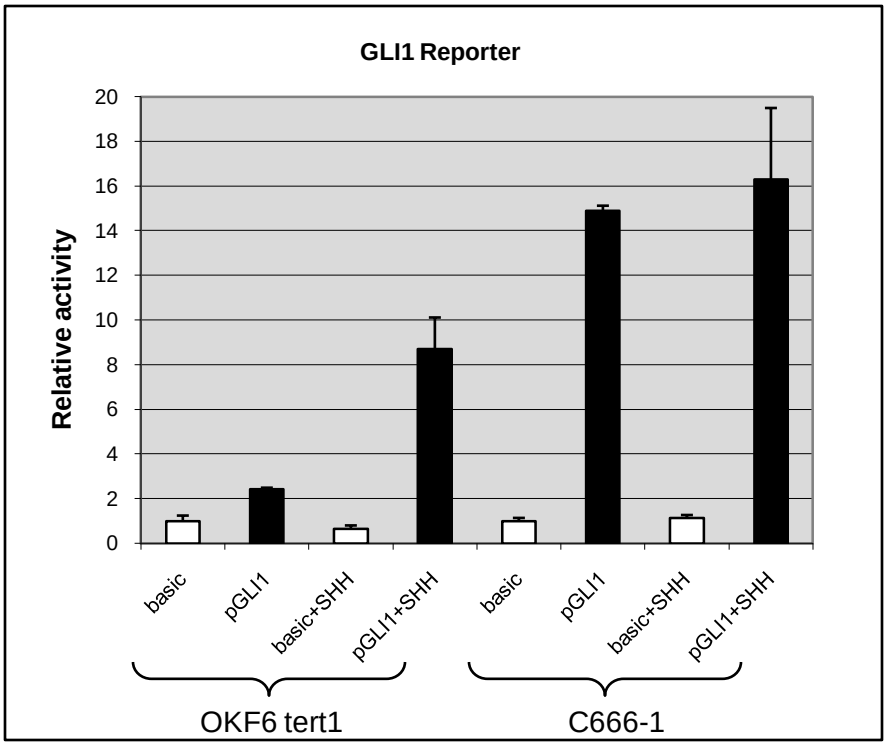

Figure 6.5: SHH induces the activity of the Hh responsive reporter, GLI1 luciferase in C666-1 cells. The columns show the relative activity of Hh-responsive, GLI1 luciferase in C666-1 cells without stimulation or after stimulation with SHH (2µg/ml). Compared to the basal level (open columns), an increase in reporter activity is observed in cells transfected with GLI1 reporter, and the responses are slightly elevated after treatment with SHH (black columns).

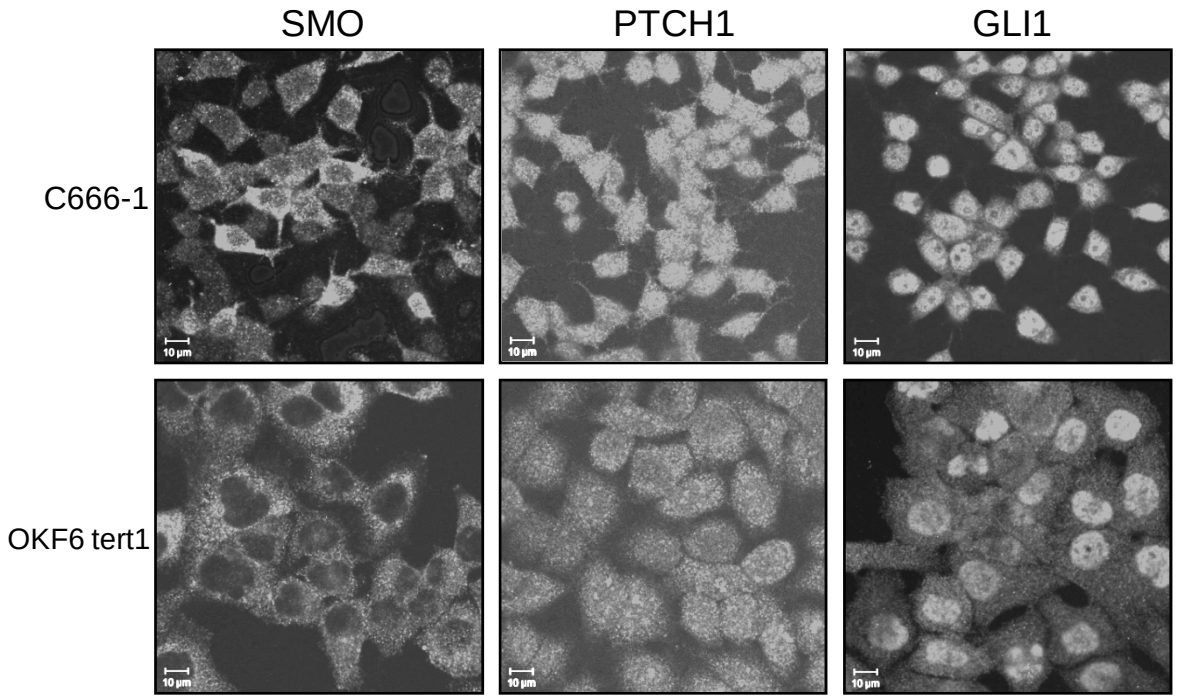

Figure 6.6: Immunofluorescence staining reveals higher protein levels of Hh pathway components SMO, PTCH1 and GLI1 in C666-1. The expression of SMO, PTCH1 and GLI1 in C666-1 (upper panels) and OKF6 tert-1 cells (bottom panels) are shown. C666-1 cells show higher levels of SMO (cytoplasm), PTCH1 (cytoplasm) and GLI1 (nucleus) expression.

technique as described in section 2.7. Compared to OKF6 tert-1 cells, C666-1 cells showed significantly higher expression levels of SMO, PTCH1 and GLI1 (Figure 6.6). Localisation of SMO to the cell surface is essential for initiation of Hh pathway signalling. GLI1 is an activator for modulating Hh target genes, for example, PTCH1 (Jiang & Hui, 2008). Therefore, higher expression of these proteins indicates activation of the Hh pathway in C666-1 cells.

6.4 Discussion

The present work forms the beginning of a study into the functions of the canonical TGF-β, activin and Hh pathways in NPC pathogenesis. To address this question, the integrity of the pathways was first investigated by using TGF-β responsive genes and suggested that in the C666-1 line the activin signalling pathway is intact but the TGF-β pathway is not. This was confirmed by immunoblotting which showed that activin A but not TGF-β1 could induce SMAD2 phosphorylation and upregulate the expression of the TGF-β responsive genes, SERPINE1 and p21 in C666-1 cells. The defects of the TGF-β pathway in C666-1 are most likely caused by loss of TGFBR2, which when bound to TGF-β ligands is important for pathway activation (see Section 1.4.4.2). In addition, C666-1 cells transiently transfected with a TGFBR2 expression plasmid have been shown to become responsive to TGF-β signalling (unpublished work in our group, Date *et al*). Previous studies demonstrated that loss of functional TGFBR2 in cancers results in insensitivity to TGF-β-mediated cell growth inhibition or apoptosis (Fukuda *et al.*, 2006; Pu *et al.*, 2009), which contributes to malignant transformation at an early step of tumourigenesis and that it can occur through mutation or transcriptional repression of the TGFBR2 gene (Park *et al.*, 1994; Hahm,

1999). A recent study reveals that induction of p21 expression is associated with a high level of TGFBR2 expression (Rojas *et al.*, 2009).

Although the canonical TGF-β pathway has been widely studied in cancers, the function of the activin pathway in cancers is relatively poorly understood despite its roles in proliferation, apoptosis and carcinogenesis having been reported (Chen *et al.*, 2006). Activin and TGF-β share the same receptor binding properties and their receptors phosphorylate and activate the same SMADs (SMAD2 and SMAD3). Therefore, it is possible that they may have some common biological functions in carcinogenesis. Although this concept still remains to be elucidated, it has been shown that activin and TGF-β induce a similar set of gene responses that have been implicated in the control of cell growth and tumourigenesis (Schnepp & Hua, 2003; Deacu *et al.*, 2004). These responsive genes include SERPINE1 and p21 that were shown to be upregulated in C666-1 after treatment with activin A (Figure 6.3).

P21 is a well-established cyclin-dependent kinase inhibitor that mediates cell cycle arrest at G1 phase resulting in cell growth inhibition. An investigation in a model of breast cancer reveals that activin A upregulated the expression of cyclin kinase inhibitors, p21 and p27, and mediated growth inhibition and cell cycle arrest (Burdette *et al.*, 2005). However, a recent publication reported that activin A was overexpressed in lung cancer and that this was associated with cell proliferation and poor survival (Seder *et al.*, 2009). These observations indicate that the activin pathway may have complicated functions in cancers and, like TGF-β, can function as either a tumour promoter or a tumour suppressor.

To investigate the function of the TGF-β and activin pathways in C666-1 cells, cell cycle analysis of activin A and TGF-β1 treated cells was performed. The preliminary data reveal that although OKF6 tert-1 cells were arrested at G2/M phase after treatment with either activin A or TGF-β1, the C666-1 cells were not. It has been demonstrated that the TGF-β signalling pathway is not intact in the C666-1 cell line. Thus, it is not surprising that this cell line does not respond to TGF-β1-induced cell cycle arrest. However, although the activin signalling pathway is intact, the C666-1 line also appears to resist activin A-induced cell cycle arrest. Although activin signalling mediates cell cycle progression mainly through activation of the SMAD-dependent pathway, the SMAD-independent pathways such as p38 MAPK also appear critical (Cocolakis *et al.*, 2001; Chen *et al.*, 2006). For example, activation of p38 MAPK has been shown to be required for activin A-induced cell cycle arrest in breast cancer cell lines. The finding that P38 MAPK activity appears to be suppressed in EBV infected cells including C666-1 (Lo *et al.*, 2006) suggests that engagement of SMAD-independent signalling pathways are defective in this cell line..

In the expression array data (Table 5.1), activin A was found to be upregulated in NPC biopsies, whereas it was absent in C666-1 cells. This raises some interesting questions. For example, how do C666-1 cells exhibit similar expression patterns of TGF-β responsive genes as authentic NPC tumours in the absence of TGFBR2 and activin A expression? Do other pathways crosstalk with these two pathways in C666-1 cells? What precise functions do the TGF-β and activin pathways exert in NPC cancer cells? Do they have similar effects in C666-1? If the defects of the TGF-β pathway in C666-1 are repaired, do the TGF-β and activin pathways synergistically

act as tumour promoters or suppressors in cells? To answer these questions, further functional investigations in C666-1 cells are required.

Using the Hh responsive reporter, GLI1 luciferase, the preliminary data reveal that the Hh pathway is intact in C666-1. Moreover, the expression of the Hh pathway components SMO, PTCH1 and GLI1 was shown to be at a higher level in C666-1 cells compared to the non-malignant OKF6 tert-1 cells, indicating chronic activation of the Hh pathway in C666-1 cells. However, expression array data showed that the SHH transcript was called by GCOS as "absent" in C666-1 cells (Section 5.4.2), in this context, how is the Hh pathway activated in this line? Studies show that TGF-β and Ras can stimulate GLI activity in epithelial cells in a Hh-independent manner resulting in activation of its downstream targets (Dennler *et al.*, 2007). A recent study has also revealed that Wnt signalling can stimulate expression of the Hh pathway activator, GLI1, in colorectal cancer (Noubissi *et al.*, 2009). This might also apply to NPC cells since both the TGF-β and Wnt signalling pathways are generally activated in C666-1 cells (Table 5.2). However it is also possible that other pathways or viral components are involved in regulation of this pathway.

The preliminary data obtained so far from the pathways analysis provide a basis for further study. Since the integrity of the activin, TGF-β and Hh signalling pathways have been determined in C666-1, this line can be used as an *in vitro* model for further functional investigation of these signalling pathways.

CHAPTER 7

General discussion and future work

NPC is a highly malignant tumour arising from the epithelial lining of the nasopharynx. Although the molecular basis of NPC pathogenesis is still unclear, it has been suggested that it is a multistep process. EBV infection, environmental and inherited components are considered to be three major factors for carcinogenesis (Tao & Chan, 2007). During the development and progression of this disease, multiple somatic genetic aberrations are accumulated, along with the effects of environmental factors and EBV infection, synergistically acting together and disrupting normal cellular functions and multiple signalling pathways (Lo & Huang, 2002). The aim of this thesis was to identify and correlate chromosomal copy number changes with abnormal cellular gene expression, and to examine dysregulation of signalling pathways in NPC in an attempt to understand the molecular basis of this disease.

The examination of cellular gene expression in NPC tumours and normal nasopharyngeal epithelial cells revealed perturbations in a large number of genes that are implicated in the process of tumourigenesis. These genes have been found to be included in a variety of functional groups (Chapter 3) and signalling pathways (Chapter 5) that have been frequently associated with tumourigenesis.

As was introduced in Chapter 1, previous genetic and expression analysis characterised a number of NPC-associated oncogenes and TSGs. When these genes were examined in our tumour-related gene lists (Tables 3.1-3.3), we found that some of them are included but some are not. For example, several putative oncogenes

identified by previous studies (e.g. MYCL1, PIK3CA, SKIL, TP63, BCL2, EGFR, TNFAIP3, BIRC3, MET, and BMI1) were also found to be upregulated in our NPC sample set, but a few previously characterised oncogenes e.g. CCND1, LTβR, GPR160, EVI1, were not. In addition some, e.g. FGF3, were called by GCOS as absent in both tumours and normals so that their expression level could not be compared (Tables 3.1 and 3.3). Similarly, several well- established TSGs, e.g. RARB, GSTP1, CDH1, BRD7 and PTEN, were found to be downregulated in our samples. However, others e.g. ZYMND10, MLH1, RBL2, THY1 and ATM were not included because their expression was called by GCOS as absent in both tumours and normals or present in less than 4 normals. The discrepancy between our data and previous publications might be caused by the different sample sets used in the respective studies. Although a number of oncogenes and tumour suppressor genes appear to be universally differentially expressed, the majority seem to be important in only a fraction of cases. Therefore, different studies that use different sample sets may reveal incompletely congruent data. This is also true when we analyse gene expression in the context of signalling pathways. The majority of genes' up- or down- expression is consistent with previous data (e.g. upregulation of WNT5A, FZD7, and CTNNB1). However, there are a few exceptions e.g. WIF-1 that has been shown to be downregulated in NPC cell lines (Lin *et al.*, 2006) but was called by GCOS as absent in both tumours and normals and ID1 that has been previously reported to be upregulated but was downregulated in our samples (Tables 5.1 and 5.2).

Although our expression array analysis identified such a big list of up- or down-regulated genes, it is not clear how many - or how few - are required for tumourigenesis. A further examination of the expression of these genes in each tumour revealed that the mean number of oncogenes upregulated in each cancer was

93 (range 40 – 120), whilst the mean number of TSGs downregulated in each tumour was 109 (range 90 – 135). It is clear that each tumour is an individual, possessing its own set of up- or down-regulated tumour-associated genes, drawn in various combinations from an extensive list. Functional characterisation of putative tumour suppressor genes using cell lines or animal models reveals dramatic effects on tumour cell growth in response to the perturbation of expression of just a single TSG (Wang *et al.*, 1999; Chow *et al.*, 2004; Cheung *et al.*, 2008). On the other hand, functional silencing the expression of a single oncogene reveals significant induction of apoptosis or inhibition of proliferation in tumour cells (Friboulet *et al.*, 2008; Qin *et al.*, 2008; Or *et al.*, 2010). Considering these data alongside the current observations that reveal downregulation of over 100 TSGs and upregulation of over 90 oncogenes per tumour emphasises the magnitude of the loss of proliferative control in NPC. The identification of them paves the way for a number of further investigations. For example, the individual oncogenes and TSGs might have their particular function in carcinogenesis, therefore, knockdown, overexpression or methylation analysis of individual up- or down-regulated genes in NPC cells would be helpful to find some critical genes and understand their particular roles.

Meanwhile, the SNP array data identified a number of chromosomal abnormalities in NPCs. The extensive regions of loss or gain found in our analysis are consistent with previous findings (Table 4.1). One study with conventional CGH and aCGH analysis suggests that Mediterranean NPCs have higher frequencies of gains at 1q and losses at 13q (Rodriguez *et al.*, 2005). Considering the samples used in our SNP array analysis are derived from both Mediterranean areas (5 NPCs) and Southern China (9 NPCs), chromosomal changes at 1q and 13q were closely examined between both sample sets.

It reveals a higher 13q loss in Mediterranean NPCs than in Chinese NPCs (80% (4/5) vs. 33.3% (3/9)). However, no significant difference in 1q gain was observed (40% (2/5) vs. 44.4% (4/9)). This discrepancy is not surprising considering that the sample size performed in this comparison is relatively small, whereas Rodriguez *et al* drew their conclusion by comparing 6 independent studies.

In addition to some extensive regions of chromosomal aberrations, compared to previous findings the present work observed several discrete, minimal regions of chromosomal changes by taking advantage of the high-resolution of these arrays (see Section 4.5.3). The genes involved in the critical regions of genetic changes have also been recognised. For example, genes PITX1, CXCL14, TGFBI CLU, TINF2, ITGA2 and MSH3 were observed within the small deletions, and genes GAS1, SYK, DAPK1 and GADD45G were found to be located in the minimal region of UPD at 9q21.32 – q22.2. The majority of these have been shown to be involved in the process of tumourigenesis (see Section 4.5.4). To investigate their importance in carcinogenesis, mutational or methylation analysis of some genes in NPC biopsies might provide an important clue.

The relationship between cellular gene expression and DNA copy number in NPC tumours was analysed in the genes involved in small regions of loss or gain and the lists of tumour-related genes. This revealed that the direct copy number/expression link applies in about 60% of the instances of copy number loss/down-expression and less than 35% of instances of copy number gain/up-expression that were examined (Table 4.3). This result indicates that the up- or down- regulation of gene expression in NPC might not be a direct consequence of DNA copy number gain or loss. NPC

tumour cells seem to upregulate or downregulate the expression of many such genes irrespective of the underlying gene copy number. Especially, copy number gain, up to about 4 copies, is not generally associated with upregulation of expression but amplification appears to be (e.g. amplification at 8p11.22 – 11.21). Actually, more complicated mechanisms might be involved in the process of regulation in gene expression. For example, the expression of some genes might be tightly controlled by cellular regulators of particular signalling pathways.

It is worthy to note that our copy number data were generated by comparing amplified DNA with unamplified reference DNA, which could introduce potential confounding artefactual copy number variants that are caused by the DNA amplification procedure. Since these artefacts have been shown to be relatively small and isolated or that they comprise losses close to chromosome termini, such changes were filtered out (Section 4.2). In addition, whether large or small, the regions of chromosomal abnormalities described in our SNP array data are more than 1MB, which are not likely to be amplification artefacts. Moreover, Q-PCR data for several genes encoded in the loci of loss or gain verified the fidelity of our copy number data. However, when the copy number data are analysed in relation to the tumour-related gene lists, it is possibly problematic since the regions that the majority of genes are involved are small. One study (Pugh *et al.*, 2008) compared copy number data of amplified and unamplified DNA in 500K SNP arrays and suggested that many amplification artefacts are reproducible and that up to around 700 artefacts were generated, a number that is consistent with our estimates when comparing amplified and unamplified C666-1 DNA. The total size of the amplification artefacts was 21.97Mb or about 0.7% of the total genome. Therefore we suggest that these artefacts would make only a small

difference to the outcome of our analysis since, in the highly unlikely event that every one of the 700 artefacts was in a mRNA-encoding region, this would affect only about 0.7% of the transcripts that are assayed on the U133Plus2 array, assuming equal distribution. Nevertheless we are currently processing a number of amplified, normal DNA samples on 500K arrays in order to generate a bioinformatic correction factor that will enable a more robust analysis to be performed.

When the expression array data were analysed for signalling pathways, a number of pathways were found to be dysregulated. Especially, the expression of numerous components involved in the TGF-β, Wnt and Hedgehog signalling pathways were differentially regulated. This suggests that the disruptions of these pathways are critical for NPC pathogenesis. Nonetheless, their precise functions remain to be elucidated.

It has been suggested that EBV latent genes can modulate cellular gene expression in NPC tumours (Raab-Traub, 2002). For example, EBNA1 has been shown to repress the TGF-β1-induced target gene transcription in tumour cells of nasopharyngeal origin (Wood *et al.*, 2007), whereas LMP1 expression upregulates downstream targets of the TGF-β signalling pathway in MDCK cells (unpublished work, Laverick *et al*). This reveals that individual viral genes have different or even opposing effects on the TGF-β signalling pathway, which might raise the question as to what and how does coexpression of the EBV latent genes impact on the expression and function of this signalling pathway in authentic NPC tumours since both EBNA1 and LMP1 are expressed in NPCs? Our pathway analysis showed that the TGF-β signalling pathway was universally activated in NPCs (Table 5.1). The authentic NPC tumour exhibits

much more complicated cellular and viral components. Therefore, competition for the viral genes interaction between cellular coactivators and corepressors may be more complicated in determining the outcome of the TGF-β signalling pathway, and the balance may shift depending on the relative levels of these viral proteins and on signalling inputs that affect their activities. Moreover, the activity of other pathways or other factors may also involve and influence the outcome of the TGF-β response. This applies not only to the TGF-β signalling pathway but has also been observed in other pathways, for example, the NF-κB signalling pathway. NF-κB was shown to be inhibited by EBNA1 in NPC cells (Valentine *et al.*, 2010), whilst it was activated by LMP1 (Liu *et al.*, 2009). Although not discussed, our data showed that several components of this pathway were upregulated and confirmed that it was activated in NPC.

In the context of the interaction between expression of viral and cellular genes, determining the EBV gene expression pattern in microdissected samples will enable us to monitor the pattern of EBV gene expression alongside any cellular gene changes we observe. In addition, the present work mainly focused on analysis of NPC tumour cells. However a common feature in NPC is the existence of an extensive lymphoid infiltrate surrounding the tumour cells. The interaction between tumour cells and their microenvironment is critical to the initiation, progression and maintenance of cancer (Gourzones *et al.*, 2009). Therefore, a global analysis of cellular gene expression to include this reactive component could identify novel receptor-ligand pairs, including chemokines and their receptors that mediate the interaction between reactive cells and tumour cells. This would allow us to have a more global view on the mechanisms of NPC development and progression.

The C666-1 cell line was the only cell line used in the present study. Sample correlation analysis as well as pathway studies revealed that the gene expression pattern of the C666-1 cell line approximates to that of authentic NPC biopsies. Thus, it is considered to be a good tumour model. *In vitro* investigation of the pathways in C666-1 cells may provide a better understanding of cellular mechanisms of NPC tumourigenesis. The preliminary data from pathway analyses suggest that the activin and hedgehog pathways are intact in C666-1 cells while the canonical TGF-β pathway is not. Cell cycle analysis reveals that both activin A and TGF-β1 induce cell cycle arrest at G2/M phase in OKF tert-1 cells but not in C666-1 cells. The data obtained so far provide a basis for further investigation. Since loss of TGFBR2 expression in C666-1 was observed (See section 5.2.2), restoration of TGFBR2 expression in C666-1 by constructing a C666-1 derivative cell line that stably expresses TGFBR2 would be essential for functional investigation of the TGF-β pathway in this line. Since it appears that the C666-1 cell line is resistant to both activin A and TGF-β1 induced cell cycle arrest, do the activin or TGF-β signalling pathways have any effect on the tumour growth or proliferation of this NPC line? What precise functions and by what mechanism do these pathways exert in C666-1? To answer this questions, C666-1 cells with or without TGFBR2 expression can be analysed further for cell cycle, proliferation, cell motility and invasiveness, after treatment with TGF-β1 or activin A, or they can be analysed for other signalling pathways (e.g. Hedgehog, and Wnt pathways) that might be involved in crosstalking with the TGF-β pathway. In addition, since the Wnt pathway was generally activated in NPCs, the functional investigation in C666-1 cells *in vitro* might be also important for understanding of NPC pathogenesis. This is an ongoing study in our group.

REFERENCES

Abdollah S, Macias-Silva M, Tsukazaki T, Hayashi H, Attisano L & Wrana JL (1997) TbetaRI phosphorylation of Smad2 on Ser465 and Ser467 is required for Smad2-Smad4 complex formation and signaling. *J Biol Chem* **272**, 27678-27685.

Adrian K, Strouch MJ, Zeng Q, Barron MR, Cheon EC, Honasoge A, Xu Y, Phukan S, Sadim M, Bentrem DJ, Pasche B & Grippo PJ (2009) Tgfbr1 haploinsufficiency inhibits the development of murine mutant Kras-induced pancreatic precancer. *Cancer Res* **69**, 9169-9174.

Agathanggelou A, Dallol A, Zochbauer-Muller S, Morrissey C, Honorio S, Hesson L, Martinsson T, Fong KM, Kuo MJ, Yuen PW, Maher ER, Minna JD & Latif F (2003) Epigenetic inactivation of the candidate 3p21.3 suppressor gene BLU in human cancers. *Oncogene* **22**, 1580-1588.

Ai MD, Li LL, Zhao XR, Wu Y, Gong JP & Cao Y (2005) Regulation of survivin and CDK4 by Epstein-Barr virus encoded latent membrane protein 1 in nasopharyngeal carcinoma cell lines. *Cell Res* **15**, 777-784.

Al-Sarraf M, LeBlanc M, Giri PG, Fu KK, Cooper J, Vuong T, Forastiere AA, Adams G, Sakr WA, Schuller DE & Ensley JF (1998) Chemoradiotherapy versus radiotherapy in patients with advanced nasopharyngeal cancer: phase III randomized Intergroup study 0099. *J Clin Oncol* **16**, 1310-1317.

Al-Shahrour F, Diaz-Uriarte R & Dopazo J (2004) FatiGO: a web tool for finding significant associations of Gene Ontology terms with groups of genes. *Bioinformatics* **20**, 578-580.

Allen MD, Young LS & Dawson CW (2005) The Epstein-Barr virus-encoded LMP2A and LMP2B proteins promote epithelial cell spreading and motility. *J Virol* **79**, 1789-1802.

Andersson-Anvret M, Forsby N, Klein G, Henle W & Biorklund A (1979) Relationship between the Epstein-Barr virus genome and nasopharyngeal carcinoma in Caucasian patients. *Int J Cancer* **23**, 762-767.

Ang EZ, Nguyen HT, Sim HL, Putti TC & Lim LH (2009) Annexin-1 regulates growth arrest induced by high levels of estrogen in MCF-7 breast cancer cells. *Mol Cancer Res* **7**, 266-274.

Armstrong AP, Miller RE, Jones JC, Zhang J, Keller ET & Dougall WC (2008) RANKL acts directly on RANK-expressing prostate tumor cells and mediates migration and expression of tumor metastasis genes. *Prostate* **68**, 92-104.

Armstrong RW, Imrey PB, Lye MS, Armstrong MJ, Yu MC & Sani S (2000) Nasopharyngeal carcinoma in Malaysian Chinese: occupational exposures to particles, formaldehyde and heat. *Int J Epidemiol* **29**, 991-998.

Arrand JR, Walsh-Arrand JE & Rymo L (1983) Cytoplasmic RNA from normal and malignant human cells shows homology to the DNAs of Epstein-Barr virus and human adenoviruses. *Embo J* **2**, 1673-1683.

Austinat M, Dunsch R, Wittekind C, Tannapfel A, Gebhardt R & Gaunitz F (2008) Correlation between beta-catenin mutations and expression of Wnt-signaling target genes in hepatocellular carcinoma. *Mol Cancer* **7**, 21.

Ayadi W, Karray-Hakim H, Khabir A, Feki L, Charfi S, Boudawara T, Ghorbel A, Daoud J, Frikha M, Busson P & Hammami A (2008) Aberrant methylation of p16, DLEC1, BLU and E-cadherin gene promoters in nasopharyngeal carcinoma biopsies from Tunisian patients. *Anticancer Res* **28**, 2161-2167.

Baba Y, Tsukuda M, Mochimatsu I, Furukawa S, Kagata H, Satake K, Koshika S, Nakatani Y, Hara M, Kato Y & Nagashima Y (2001) Reduced expression of p16 and p27 proteins in nasopharyngeal carcinoma. *Cancer Detect Prev* **25**, 414-419.

Bachman KE, Blair BG, Brenner K, Bardelli A, Arena S, Zhou S, Hicks J, De Marzo AM, Argani P & Park BH (2004) p21(WAF1/CIP1) mediates the growth response to TGF-beta in human epithelial cells. *Cancer Biol Ther* **3**, 221-225.

Bachman KE & Park BH (2005) Duel nature of TGF-beta signaling: tumor suppressor vs. tumor promoter. *Current Opinion in Oncology* **17**, 49-54.

Baer R, Bankier AT, Biggin MD, Deininger PL, Farrell PJ, Gibson TJ, Hatfull G, Hudson GS, Satchwell SC & Seguin C (1984) DNA sequence and expression of the B95-8 Epstein-Barr virus genome. *Nature* **310**, 207-211.

Bailey JM, Mohr AM & Hollingsworth MA (2009) Sonic hedgehog paracrine signaling regulates metastasis and lymphangiogenesis in pancreatic cancer. *Oncogene* **28**, 3513-3525.

Balmain A, Gray J & Ponder B (2003) The genetics and genomics of cancer. *Nat Genet* **33 Suppl**, 238-244.

Bardeesy N, Cheng KH, Berger JH, Chu GC, Pahler J, Olson P, Hezel AF, Horner J, Lauwers GY, Hanahan D & DePinho RA (2006) Smad4 is dispensable for normal pancreas development yet critical in progression and tumor biology of pancreas cancer. *Genes Dev* **20**, 3130-3146.

Barletta JM, Kingma DW, Ling Y, Charache P, Mann RB & Ambinder RF (1993) Rapid in situ hybridization for the diagnosis of latent Epstein-Barr virus infection. *Mol Cell Probes* **7**, 105-109.

Barnfield PC, Zhang X, Thanabalasingham V, Yoshida M & Hui CC (2005) Negative regulation of Gli1 and Gli2 activator function by Suppressor of fused through multiple mechanisms. *Differentiation* **73**, 397-405.

Baumforth KR, Young LS, Flavell KJ, Constandinou C & Murray PG (1999) The Epstein-Barr virus and its association with human cancers. *Mol Pathol* **52**, 307-322.

Benachenhou N, Guiral S, Gorska-Flipot I, Labuda D & Sinnett D (1999) Frequent loss of heterozygosity at the DNA mismatch-repair loci hMLH1 and hMSH3 in sporadic breast cancer. *Br J Cancer* **79**, 1012-1017.

Berman DM, Karhadkar SS, Maitra A, Montes De Oca R, Gerstenblith MR, Briggs K, Parker AR, Shimada Y, Eshleman JR, Watkins DN & Beachy PA (2003) Widespread requirement for Hedgehog ligand stimulation in growth of digestive tract tumours. *Nature* **425**, 846-851.

Bernheim A, Rousselet G, Massaad L, Busson P & Tursz T (1993) Cytogenetic studies in three xenografted nasopharyngeal carcinomas. *Cancer Genet Cytogenet* **66**, 11-15.

Bettuzzi S, Scorcioni F, Astancolle S, Davalli P, Scaltriti M & Corti A (2002) Clusterin (SGP-2) transient overexpression decreases proliferation rate of SV40-immortalized human prostate epithelial cells by slowing down cell cycle progression. *Oncogene* **21**, 4328-4334.

Biswas S, Trobridge P, Romero-Gallo J, Billheimer D, Myeroff LL, Willson JK, Markowitz SD & Grady WM (2008) Mutational inactivation of TGFBR2 in microsatellite unstable colon cancer arises from the cooperation of genomic instability and the clonal outgrowth of transforming growth factor beta resistant cells. *Genes Chromosomes Cancer* **47**, 95-106.

Bose S, Yap LF, Fung M, Starzcynski J, Saleh A, Morgan S, Dawson C, Chukwuma MB, Maina E, Buettner M, Wei W, Arrand J, Lim PV, Young LS, Teo SH, Stankovic T, Woodman CB & Murray PG (2009) The ATM tumour suppressor gene is down-regulated in EBV-associated nasopharyngeal carcinoma. *J Pathol* **217**, 345-352.

Botstein D & Risch N (2003) Discovering genotypes underlying human phenotypes: past successes for mendelian disease, future approaches for complex disease. *Nat Genet* **33 Suppl**, 228-237.

Breitling R, Armengaud P, Amtmann A & Herzyk P (2004) Rank products: a simple, yet powerful, new method to detect differentially regulated genes in replicated microarray experiments. *FEBS Lett* **573**, 83-92.

Brooks L, Yao QY, Rickinson AB & Young LS (1992) Epstein-Barr virus latent gene transcription in nasopharyngeal carcinoma cells: coexpression of EBNA1, LMP1, and LMP2 transcripts. *J Virol* **66**, 2689-2697.

Buell P (1974) The effect of migration on the risk of nasopharyngeal cancer among Chinese. *Cancer Res* **34**, 1189-1191.

Burdette JE, Jeruss JS, Kurley SJ, Lee EJ & Woodruff TK (2005) Activin A mediates growth inhibition and cell cycle arrest through Smads in human breast cancer cells. *Cancer Res* **65**, 7968-7975.

Burgos JS (2005) Involvement of the Epstein-Barr virus in the nasopharyngeal carcinoma pathogenesis. *Med Oncol* **22**, 113-121.

Busson P, Ganem G, Flores P, Mugneret F, Clausse B, Caillou B, Braham K, Wakasugi H, Lipinski M & Tursz T (1988) Establishment and characterization of three transplantable EBV-containing nasopharyngeal carcinomas. *Int J Cancer* **42**, 599-606.

Busson P, Keryer C, Ooka T & Corbex M (2004) EBV-associated nasopharyngeal carcinomas: from epidemiology to virus-targeting strategies. *Trends Microbiol* **12**, 356-360.

Busson P, McCoy R, Sadler R, Gilligan K, Tursz T & Raab-Traub N (1992) Consistent transcription of the Epstein-Barr virus LMP2 gene in nasopharyngeal carcinoma. *J Virol* **66**, 3257-3262.

Caccamo AE, Scaltriti M, Caporali A, D'Arca D, Scorcioni F, Candiano G, Mangiola M & Bettuzzi S (2003) Nuclear translocation of a clusterin isoform is associated with induction of anoikis in SV40-immortalized human prostate epithelial cells. *Ann N Y Acad Sci* **1010**, 514-519.

Calaf GM, Echiburu-Chau C, Zhao YL & Hei TK (2008) BigH3 protein expression as a marker for breast cancer. *Int J Mol Med* **21**, 561-568.

Cao Q, Yu J, Dhanasekaran SM, Kim JH, Mani RS, Tomlins SA, Mehra R, Laxman B, Cao X, Yu J, Kleer CG, Varambally S & Chinnaiyan AM (2008) Repression of E-cadherin by the polycomb group protein EZH2 in cancer. *Oncogene* **27**, 7274-7284.

Chan AS, To KF, Lo KW, Ding M, Li X, Johnson P & Huang DP (2002) Frequent chromosome 9p losses in histologically normal nasopharyngeal epithelia from southern Chinese. *Int J Cancer* **102**, 300-303.

Chan AS, To KF, Lo KW, Mak KF, Pak W, Chiu B, Tse GM, Ding M, Li X, Lee JC & Huang DP (2000) High frequency of chromosome 3p deletion in histologically normal nasopharyngeal epithelia from southern Chinese. *Cancer Res* **60**, 5365-5370.

Chan SL, Cui Y, van Hasselt A, Li H, Srivastava G, Jin H, Ng KM, Wang Y, Lee KY, Tsao GS, Zhong S, Robertson KD, Rha SY, Chan AT & Tao Q (2007) The

tumor suppressor Wnt inhibitory factor 1 is frequently methylated in nasopharyngeal and esophageal carcinomas. *Lab Invest* **87**, 644-650.

Chang CM, Yu KJ, Mbulaiteye SM, Hildesheim A & Bhatia K (2009) The extent of genetic diversity of Epstein-Barr virus and its geographic and disease patterns: a need for reappraisal. *Virus Res* **143**, 209-221.

Chang ET & Adami HO (2006) The enigmatic epidemiology of nasopharyngeal carcinoma. *Cancer Epidemiol Biomarkers Prev* **15**, 1765-1777.

Chen H, Suzuki M, Nakamura Y, Ohira M, Ando S, Iida T, Nakajima T, Nakagawara A & Kimura H (2006) Aberrant methylation of RASGRF2 and RASSF1A in human non-small cell lung cancer. *Oncol Rep* **15**, 1281-1285.

Chen J, Hu CF, Hou JH, Shao Q, Yan LX, Zhu XF, Zeng YX & Shao JY (2010) Epstein-Barr virus encoded latent membrane protein 1 regulates mTOR signaling pathway genes which predict poor prognosis of nasopharyngeal carcinoma. *J Transl Med* **8**, 30.

Chen J, Rocken C, Lofton-Day C, Schulz HU, Muller O, Kutzner N, Malfertheiner P & Ebert MP (2005) Molecular analysis of APC promoter methylation and protein expression in colorectal cancer metastasis. *Carcinogenesis* **26**, 37-43.

Chen MK, Lai JC, Chang CC, Chang JH, Chang YJ & Chen HC (2008) Prognostic impact of bcl-2 expression on advanced nasopharyngeal carcinoma. *Head Neck* **30**, 1052-1057.

Chen MK, Yang SF, Lai JC, Yeh KT, Yang JS, Chen LS & Chen HC (2009) Expression of bcl-2 correlates with poor prognosis and modulates migration of nasopharyngeal carcinoma cells. *Clin Chim Acta* **411**, 400-405.

Chen Y & Chen C (2008) DNA copy number variation and loss of heterozygosity in relation to recurrence of and survival from head and neck squamous cell carcinoma: a review. *Head Neck* **30**, 1361-1383.

Chen Y & Struhl G (1996) Dual roles for patched in sequestering and transducing Hedgehog. *Cell* **87**, 553-563.

Chen YG, Wang Q, Lin SL, Chang CD, Chuang J & Ying SY (2006) Activin signaling and its role in regulation of cell proliferation, apoptosis, and carcinogenesis. *Exp Biol Med (Maywood)* **231**, 534-544.

Chen YJ, Ko JY, Chen PJ, Shu CH, Hsu MT, Tsai SF & Lin CH (1999) Chromosomal aberrations in nasopharyngeal carcinoma analyzed by comparative genomic hybridization. *Genes Chromosomes Cancer* **25**, 169-175.

Chen YJ, Wu CY, Chang CC, Ma CJ, Li MC & Chen CM (2008) Nuclear Kruppel-like factor 4 expression is associated with human skin squamous cell carcinoma progression and metastasis. *Cancer Biol Ther* **7**, 777-782.

Chen YN, Chen H, Xu Y, Zhang X & Luo Y (2008) Expression of pituitary homeobox 1 gene in human gastric carcinogenesis and its clinicopathological significance. *World J Gastroenterol* **14**, 292-297.

Cheng SY & Bishop JM (2002) Suppressor of Fused represses Gli-mediated transcription by recruiting the SAP18-mSin3 corepressor complex. *Proc Natl Acad Sci U S A* **99**, 5442-5447.

Cheng SY & Yue S (2008) Role and regulation of human tumor suppressor SUFU in Hedgehog signaling. *Adv Cancer Res* **101**, 29-43.

Cheng Y, Chakrabarti R, Garcia-Barcelo M, Ha TJ, Srivatsan ES, Stanbridge EJ & Lung ML (2002) Mapping of nasopharyngeal carcinoma tumor-suppressive activity to a 1.8-megabase region of chromosome band 11q13. *Genes Chromosomes Cancer* **34**, 97-103.

Cheng Y, Ko JM, Lung HL, Lo PH, Stanbridge EJ & Lung ML (2003) Monochromosome transfer provides functional evidence for growth-suppressive genes on chromosome 14 in nasopharyngeal carcinoma. *Genes Chromosomes Cancer* **37**, 359-368.

Cheng Y, Poulos NE, Lung ML, Hampton G, Ou B, Lerman MI & Stanbridge EJ (1998) Functional evidence for a nasopharyngeal carcinoma tumor suppressor gene that maps at chromosome 3p21.3. *Proc Natl Acad Sci U S A* **95**, 3042-3047.

Cheng YJ, Hildesheim A, Hsu MM, Chen IH, Brinton LA, Levine PH, Chen CJ & Yang CS (1999) Cigarette smoking, alcohol consumption and risk of nasopharyngeal carcinoma in Taiwan. *Cancer Causes Control* **10**, 201-207.

Cheung AK, Lung HL, Hung SC, Law EW, Cheng Y, Yau WL, Bangarusamy DK, Miller LD, Liu ET, Shao JY, Kou CW, Chua D, Zabarovsky ER, Tsao SW, Stanbridge EJ & Lung ML (2008) Functional analysis of a cell cycle-associated, tumor-suppressive gene, protein tyrosine phosphatase receptor type G, in nasopharyngeal carcinoma. *Cancer Res* **68**, 8137-8145.

Cheung ST, Huang DP, Hui AB, Lo KW, Ko CW, Tsang YS, Wong N, Whitney BM & Lee JC (1999) Nasopharyngeal carcinoma cell line (C666-1) consistently harbouring Epstein-Barr virus. *Int J Cancer* **83**, 121-126.

Chiang CT, Chu WK, Chow SE & Chen JK (2009) Overexpression of delta Np63 in a human nasopharyngeal carcinoma cell line downregulates CKIs and enhances cell proliferation. *J Cell Physiol* **219**, 117-122.

Chien G, Yuen PW, Kwong D & Kwong YL (2001) Comparative genomic hybridization analysis of nasopharygeal carcinoma: consistent patterns of genetic aberrations and clinicopathological correlations. *Cancer Genet Cytogenet* **126**, 63-67.

Cho EY, Hildesheim A, Chen CJ, Hsu MM, Chen IH, Mittl BF, Levine PH, Liu MY, Chen JY, Brinton LA, Cheng YJ & Yang CS (2003) Nasopharyngeal carcinoma and genetic polymorphisms of DNA repair enzymes XRCC1 and hOGG1. *Cancer Epidemiol Biomarkers Prev* **12**, 1100-1104.

Chou J, Lin YC, Kim J, You L, Xu Z, He B & Jablons DM (2008) Nasopharyngeal carcinoma--review of the molecular mechanisms of tumorigenesis. *Head Neck* **30**, 946-963.

Chow LS, Lo KW, Kwong J, To KF, Tsang KS, Lam CW, Dammann R & Huang DP (2004) RASSF1A is a target tumor suppressor from 3p21.3 in nasopharyngeal carcinoma. *Int J Cancer* **109**, 839-847.

Christopher SA, Diegelman P, Porter CW & Kruger WD (2002) Methylthioadenosine phosphorylase, a gene frequently codeleted with p16(cdkN2a/ARF), acts as a tumor suppressor in a breast cancer cell line. *Cancer Res* **62**, 6639-6644.

Clements WM, Wang J, Sarnaik A, Kim OJ, MacDonald J, Fenoglio-Preiser C, Groden J & Lowy AM (2002) beta-Catenin mutation is a frequent cause of Wnt pathway activation in gastric cancer. *Cancer Res* **62**, 3503-3506.

Clevers H (2006) Wnt/beta-catenin signaling in development and disease. *Cell* **127**, 469-480.

Cocolakis E, Lemay S, Ali S & Lebrun JJ (2001) The p38 MAPK pathway is required for cell growth inhibition of human breast cancer cells in response to activin. *J Biol Chem* **276**, 18430-18436.

Codd JD, Salisbury JR, Packham G & Nicholson LJ (1999) A20 RNA expression is associated with undifferentiated nasopharyngeal carcinoma and poorly differentiated head and neck squamous cell carcinoma. *J Pathol* **187**, 549-555.

Cohen JI (2003) Benign and malignant Epstein-Barr virus-associated B-cell lymphoproliferative diseases. *Semin Hematol* **40**, 116-123.

Cohen MM, Jr. (2003) The hedgehog signaling network. *Am J Med Genet A* **123A**, 5-28.

Crook T, Nicholls JM, Brooks L, O'Nions J & Allday MJ (2000) High level expression of deltaN-p63: a mechanism for the inactivation of p53 in undifferentiated nasopharyngeal carcinoma (NPC)? *Oncogene* **19**, 3439-3444.

Cui J, Zhou X, Liu Y, Tang Z & Romeih M (2003) Wnt signaling in hepatocellular carcinoma: analysis of mutation and expression of beta-catenin, T-cell factor-4 and glycogen synthase kinase 3-beta genes. *J Gastroenterol Hepatol* **18**, 280-287.

Cui L, Xu LY, Shen ZY, Tao Q, Gao SY, Lv Z, Du ZP, Fang WK & Li EM (2008) NGALR is overexpressed and regulated by hypomethylation in esophageal squamous cell carcinoma. *Clin Cancer Res* **14**, 7674-7681.

Cvitkovic E, Bachouchi M, Boussen H, Busson P, Rousselet G, Mahjoubi R, Flores P, Tursz T, Armand JP & Azli N (1993) Leukemoid reaction, bone marrow invasion, fever of unknown origin, and metastatic pattern in the natural history of advanced undifferentiated carcinoma of nasopharyngeal type: a review of 255 consecutive cases. *J Clin Oncol* **11**, 2434-2442.

Dai P, Akimaru H, Tanaka Y, Maekawa T, Nakafuku M & Ishii S (1999) Sonic Hedgehog-induced activation of the Gli1 promoter is mediated by GLI3. *J Biol Chem* **274**, 8143-8152.

Daikoku T, Kudoh A, Fujita M, Sugaya Y, Isomura H, Shirata N & Tsurumi T (2005) Architecture of replication compartments formed during Epstein-Barr virus lytic replication. *J Virol* **79**, 3409-3418.

Dambaugh T, Hennessy K, Chamnankit L & Kieff E (1984) U2 region of Epstein-Barr virus DNA may encode Epstein-Barr nuclear antigen 2. *Proc Natl Acad Sci U S A* **81**, 7632-7636.

Damdinsuren B, Nagano H, Kondo M, Natsag J, Hanada H, Nakamura M, Wada H, Kato H, Marubashi S, Miyamoto A, Takeda Y, Umeshita K, Dono K & Monden M (2006) TGF-beta1-induced cell growth arrest and partial differentiation is related to the suppression of Id1 in human hepatoma cells. *Oncol Rep* **15**, 401-408.

Daoud J, Toumi N, Bouaziz M, Ghorbel A, Jlidi R, Drira MM & Frikha M (2003) Nasopharyngeal carcinoma in childhood and adolescence: analysis of a series of 32 patients treated with combined chemotherapy and radiotherapy. *Eur J Cancer* **39**, 2349-2354.

Dawson CW, Eliopoulos AG, Blake SM, Barker R & Young LS (2000) Identification of functional differences between prototype Epstein-Barr virus-encoded LMP1 and a nasopharyngeal carcinoma-derived LMP1 in human epithelial cells. *Virology* **272**, 204-217.

Dawson CW, Rickinson AB & Young LS (1990) Epstein-Barr virus latent membrane protein inhibits human epithelial cell differentiation. *Nature* **344**, 777-780.

de Nigris F, Sica V, Herrmann J, Condorelli G, Chade AR, Tajana G, Lerman A, Lerman LO & Napoli C (2003) c-Myc oncoprotein: cell cycle-related events and new therapeutic challenges in cancer and cardiovascular diseases. *Cell Cycle* **2**, 325-328.

De Smaele E, Di Marcotullio L, Ferretti E, Screpanti I, Alesse E & Gulino A (2004) Chromosome 17p deletion in human medulloblastoma: a missing checkpoint in the Hedgehog pathway. *Cell Cycle* **3**, 1263-1266.

Deacu E, Mori Y, Sato F, Yin J, Olaru A, Sterian A, Xu Y, Wang S, Schulmann K, Berki A, Kan T, Abraham JM & Meltzer SJ (2004) Activin type II receptor restoration in ACVR2-deficient colon cancer cells induces transforming growth factor-beta response pathway genes. *Cancer Res* **64**, 7690-7696.

Deng L, Jing N, Tan G, Zhou M, Zhan F, Xie Y, Cao L & Li G (1998) A common region of allelic loss on chromosome region 3p25.3-26.3 in nasopharyngeal carcinoma. *Genes Chromosomes Cancer* **23**, 21-25.

Deng L, Yang J, Zhao XR, Deng XY, Zeng L, Gu HH, Tang M & Cao Y (2003) Cells in G2/M phase increased in human nasopharyngeal carcinoma cell line by EBV-LMP1 through activation of NF-kappaB and AP-1. *Cell Res* **13**, 187-194.

Deng YF, Tian F, Lu YD, Chen ZC, Xie DH, Yang XM & Shao XY (2001) Mutation and abnormal expression of the fragile histidine triad gene in nasopharyngeal carcinoma. *Laryngoscope* **111**, 1589-1592.

Deng YF, Zhou DN & Lu YD (2010) Allelic imbalance and abnormal expression of FHIT in endemic nasopharyngeal carcinoma: association with clinicopathological features. *Eur Arch Otorhinolaryngo*l, DOI 10.1007/s00405-010-1301-4.

Dennler S, Andre J, Alexaki I, Li A, Magnaldo T, ten Dijke P, Wang XJ, Verrecchia F & Mauviel A (2007) Induction of sonic hedgehog mediators by transforming growth factor-beta: Smad3-dependent activation of Gli2 and Gli1 expression in vitro and in vivo. *Cancer Res* **67**, 6981-6986.

Derynck R, Akhurst RJ & Balmain A (2001) TGF-beta signaling in tumor suppression and cancer progression. *Nat Genet* **29**, 117-129.

Di Marcotullio L, Ferretti E, De Smaele E, Screpanti I & Gulino A (2006) Suppressors of hedgehog signaling: Linking aberrant development of neural progenitors and tumorigenesis. *Mol Neurobiol* **34**, 193-204.

Diaz-Chavez J, Hernandez-Pando R, Lambert PF & Gariglio P (2008) Down-regulation of transforming growth factor-beta type II receptor (TGF-betaRII) protein and mRNA expression in cervical cancer. *Mol Cancer* **7**, 3.

Dickens P, Srivastava G, Loke SL, Chan CW & Liu YT (1992) Epstein-Barr virus DNA in nasopharyngeal carcinomas from Chinese patients in Hong Kong. *J Clin Pathol* **45**, 396-397.

Dimberg J, Hugander A, Sirsjo A & Soderkvist P (2001) Enhanced expression of cyclooxygenase-2 and nuclear beta-catenin are related to mutations in the APC gene in human colorectal cancer. *Anticancer Res* **21**, 911-915.

Ding L, Li LL, Yang J, Tao YG, Ye M, Shi Y, Tang M, Yi W, Li XL, Gong JP & Cao Y (2005) Epstein-Barr virus encoded latent membrane protein 1 modulates nuclear translocation of telomerase reverse transcriptase protein by activating nuclear factor-kappaB p65 in human nasopharyngeal carcinoma cells. *Int J Biochem Cell Biol* **37**, 1881-1889.

Dominguez-Monzon G, Benitez JA, Vergara P, Lorenzana R & Segovia J (2009) Gas1 inhibits cell proliferation and induces apoptosis of human primary gliomas in the absence of Shh. *Int J Dev Neurosci* **27**, 305-313.

Douma S, Van Laar T, Zevenhoven J, Meuwissen R, Van Garderen E & Peeper DS (2004) Suppression of anoikis and induction of metastasis by the neurotrophic receptor TrkB. *Nature* **430**, 1034-1039.

Druck T, Hadaczek P, Fu TB, Ohta M, Siprashvili Z, Baffa R, Negrini M, Kastury K, Veronese ML, Rosen D, Rothstein J, McCue P, Cotticelli MG, Inoue H, Croce CM & Huebner K (1997) Structure and expression of the human FHIT gene in normal and tumor cells. *Cancer Res* **57**, 504-512.

Dutt A & Beroukhim R (2007) Single nucleotide polymorphism array analysis of cancer. *Curr Opin Oncol* **19**, 43-49.

Edlund S, Lee SY, Grimsby S, Zhang S, Aspenstrom P, Heldin CH & Landstrom M (2005) Interaction between Smad7 and beta-catenin: importance for transforming growth factor beta-induced apoptosis. *Mol Cell Biol* **25**, 1475-1488.

Edmiston JS, Yeudall WA, Chung TD & Lebman DA (2005) Inability of transforming growth factor-beta to cause SnoN degradation leads to resistance to transforming growth factor-beta-induced growth arrest in esophageal cancer cells. *Cancer Res* **65**, 4782-4788.

Edwards RH, Seillier-Moiseiwitsch F & Raab-Traub N (1999) Signature amino acid changes in latent membrane protein 1 distinguish Epstein-Barr virus strains. *Virology* **261**, 79-95.

Ellenrieder V, Hendler SF, Ruhland C, Boeck W, Adler G & Gress TM (2001) TGF-beta-induced invasiveness of pancreatic cancer cells is mediated by matrix metalloproteinase-2 and the urokinase plasminogen activator system. *Int J Cancer* **93**, 204-211.

Ellouz R, Cammoun M, Attia RB & Bahi J (1978) Nasopharyngeal carcinoma in children and adolescents in Tunisia: clinical aspects and the paraneoplastic syndrome. *IARC Sci Publ*, 115-129.

Engel E (1980) A new genetic concept: uniparental disomy and its potential effect, isodisomy. *Am J Med Genet* **6**, 137-143.

Epstein MA, Achong BG & Barr YM (1964) Virus Particles in Cultured Lymphoblasts from Burkitt's Lymphoma. *Lancet* **1**, 702-703.

Evangelista M, Tian H & de Sauvage FJ (2006) The hedgehog signaling pathway in cancer. *Clin Cancer Res* **12**, 5924-5928.

Fan CS, Wong N, Leung SF, To KF, Lo KW, Lee SW, Mok TS, Johnson PJ & Huang DP (2000) Frequent c-myc and Int-2 overrepresentations in nasopharyngeal carcinoma. *Hum Pathol* **31**, 169-178.

Fang Y, Guan X, Guo Y, Sham J, Deng M, Liang Q, Li H, Zhang H, Zhou H & Trent J (2001) Analysis of genetic alterations in primary nasopharyngeal carcinoma by comparative genomic hybridization. *Genes Chromosomes Cancer* **30**, 254-260.

Faqing T, Zhi H, Liqun Y, Min T, Huanhua G, Xiyun D & Ya C (2005) Epstein-Barr virus LMP1 initiates cell proliferation and apoptosis inhibition via regulating expression of Survivin in nasopharyngeal carcinoma. *Exp Oncol* **27**, 96-101.

Fendri A, Khabir A, Hadhri-Guiga B, Sellami-Boudawara T, Ghorbel A, Daoud J, Frikha M, Jlidi R, Gargouri A & Mokdad-Gargouri R (2008) Overexpression of COX-2 and LMP1 are correlated with lymph node in Tunisian NPC patients. *Oral Oncol* **44**, 710-715.

Fendri A, Khabir A, Mnejja W, Sellami-Boudawara T, Daoud J, Frikha M, Ghorbel A, Gargouri A & Mokdad-Gargouri R (2009) PIK3CA amplification is predictive of poor prognosis in Tunisian patients with nasopharyngeal carcinoma. *Cancer Sci* **100**, 2034-2039.

Fendri A, Kontos CK, Khabir A, Mokdad-Gargouri R, Ardavanis A & Scorilas A (2010) Quantitative analysis of BCL2 mRNA expression in nasopharyngeal carcinoma: an unfavorable and independent prognostic factor. *Tumour Biol* [Epub ahead of print].

Ferretti E, De Smaele E, Di Marcotullio L, Screpanti I & Gulino A (2005) Hedgehog checkpoints in medulloblastoma: the chromosome 17p deletion paradigm. *Trends Mol Med* **11**, 537-545.

Fingeroth JD, Diamond ME, Sage DR, Hayman J & Yates JL (1999) CD21-Dependent infection of an epithelial cell line, 293, by Epstein-Barr virus. *J Virol* **73**, 2115-2125.

Forrester E, Chytil A, Bierie B, Aakre M, Gorska AE, Sharif-Afshar AR, Muller WJ & Moses HL (2005) Effect of conditional knockout of the type II TGF-beta receptor gene in mammary epithelia on mammary gland development and polyomavirus middle T antigen induced tumor formation and metastasis. *Cancer Res* **65**, 2296-2302.

Foster KW, Frost AR, McKie-Bell P, Lin CY, Engler JA, Grizzle WE & Ruppert JM (2000) Increase of GKLF messenger RNA and protein expression during progression of breast cancer. *Cancer Res* **60**, 6488-6495.

Foster KW, Ren S, Louro ID, Lobo-Ruppert SM, McKie-Bell P, Grizzle W, Hayes MR, Broker TR, Chow LT & Ruppert JM (1999) Oncogene expression cloning by retroviral transduction of adenovirus E1A-immortalized rat kidney RK3E cells: transformation of a host with epithelial features by c-MYC and the zinc finger protein GKLF. *Cell Growth Differ* **10**, 423-434.

Frangou P, Buettner M & Niedobitek G (2005) Epstein-Barr virus (EBV) infection in epithelial cells in vivo: rare detection of EBV replication in tongue mucosa but not in salivary glands. *J Infect Dis* **191**, 238-242.

Friboulet L, Pioche-Durieu C, Rodriguez S, Valent A, Souquere S, Ripoche H, Khabir A, Tsao SW, Bosq J, Lo KW & Busson P (2008) Recurrent overexpression of c-IAP2 in EBV-associated nasopharyngeal carcinomas: critical role in resistance to Toll-like receptor 3-mediated apoptosis. *Neoplasia* **10**, 1183-1194.

Friedman JM, Liang G, Liu CC, Wolff EM, Tsai YC, Ye W, Zhou X & Jones PA (2009) The putative tumor suppressor microRNA-101 modulates the cancer epigenome by repressing the polycomb group protein EZH2. *Cancer Res* **69**, 2623-2629.

Fries KL, Miller WE & Raab-Traub N (1996) Epstein-Barr virus latent membrane protein 1 blocks p53-mediated apoptosis through the induction of the A20 gene. *J Virol* **70**, 8653-8659.

Fu DY, Wang ZM, Wang BL, Chen L, Yang WT, Shen ZZ, Huang W & Shao ZM (2009) Frequent epigenetic inactivation of the receptor tyrosine kinase EphA5 by promoter methylation in human breast cancer. *Hum Pathol* **41**, 48-58.

Fukuda M, Kurosaki H & Sairenji T (2006) Loss of functional transforming growth factor (TGF)-beta type II receptor results in insensitivity to TGF-beta1-mediated apoptosis and Epstein-Barr virus reactivation. *J Med Virol* **78**, 1456-1464.

Fung LF, Lo AK, Yuen PW, Liu Y, Wang XH & Tsao SW (2000) Differential gene expression in nasopharyngeal carcinoma cells. *Life Sci* **67**, 923-936.

Gabriel SB, Schaffner SF, Nguyen H, Moore JM, Roy J, Blumenstiel B, Higgins J, DeFelice M, Lochner A, Faggart M, Liu-Cordero SN, Rotimi C, Adeyemo A, Cooper R, Ward R, Lander ES, Daly MJ & Altshuler D (2002) The structure of haplotype blocks in the human genome. *Science* **296**, 2225-2229.

Gallicchio L, Matanoski G, Tao XG, Chen L, Lam TK, Boyd K, Robinson KA, Balick L, Mickelson S, Caulfield LE, Herman JG, Guallar E & Alberg AJ (2006) Adulthood consumption of preserved and nonpreserved vegetables and

the risk of nasopharyngeal carcinoma: a systematic review. *Int J Cancer* **119**, 1125-1135.

Garcia Pedrero JM, Fernandez MP, Morgan RO, Herrero Zapatero A, Gonzalez MV, Suarez Nieto C & Rodrigo JP (2004) Annexin A1 down-regulation in head and neck cancer is associated with epithelial differentiation status. *Am J Pathol* **164**, 73-79.

Gardina PJ, Lo KC, Lee W, Cowell JK & Turpaz Y (2008) Ploidy status and copy number aberrations in primary glioblastomas defined by integrated analysis of allelic ratios, signal ratios and loss of heterozygosity using 500K SNP Mapping Arrays. *BMC Genomics* **9**, 489.

Garrett-Sinha LA, Eberspaecher H, Seldin MF & de Crombrugghe B (1996) A gene for a novel zinc-finger protein expressed in differentiated epithelial cells and transiently in certain mesenchymal cells. *J Biol Chem* **271**, 31384-31390.

Gelsi-Boyer V, Orsetti B, Cervera N, Finetti P, Sircoulomb F, Rouge C, Lasorsa L, Letessier A, Ginestier C, Monville F, Esteyries S, Adelaide J, Esterni B, Henry C, Ethier SP, Bibeau F, Mozziconacci MJ, Charafe-Jauffret E, Jacquemier J, Bertucci F, Birnbaum D, Theillet C & Chaffanet M (2005) Comprehensive profiling of 8p11-12 amplification in breast cancer. *Mol Cancer Res* **3**, 655-667.

Giles RH, van Es JH & Clevers H (2003) Caught up in a Wnt storm: Wnt signaling in cancer. *Biochim Biophys Acta* **1653**, 1-24.

Goetz JA, Suber LM, Zeng X & Robbins DJ (2002) Sonic Hedgehog as a mediator of long-range signaling. *Bioessays* **24**, 157-165.

Gourzones C, Klibi J, Friboulet L, Jlidi R & Busson P (2009) Cellular Interactions in Nasopharyngeal Carcinomas. In *Nasopharyngeal carcinoma* [P Busson, editor], in press.

Groden J, Thliveris A, Samowitz W, Carlson M, Gelbert L, Albertsen H, Joslyn G, Stevens J, Spirio L & Robertson M (1991) Identification and characterization of the familial adenomatous polyposis coli gene. *Cell* **66**, 589-600.

Gulley ML, Amin MB, Nicholls JM, Banks PM, Ayala AG, Srigley JR, Eagan PA & Ro JY (1995) Epstein-Barr virus is detected in undifferentiated nasopharyngeal carcinoma but not in lymphoepithelioma-like carcinoma of the urinary bladder. *Hum Pathol* **26**, 1207-1214.

Gullo C, Low WK & Teoh G (2008) Association of Epstein-Barr virus with nasopharyngeal carcinoma and current status of development of cancer-derived cell lines. *Ann Acad Med Singapore* **37**, 769-777.

Gunnarsson R, Staaf J, Jansson M, Ottesen AM, Goransson H, Liljedahl U, Ralfkiaer U, Mansouri M, Buhl AM, Smedby KE, Hjalgrim H, Syvanen AC, Borg A, Isaksson A, Jurlander J, Juliusson G & Rosenquist R (2008) Screening for copy-number alterations and loss of heterozygosity in chronic lymphocytic leukemia--a comparative study of four differently designed, high resolution microarray platforms. *Genes Chromosomes Cancer* **47**, 697-711.

Guo C, Pan ZG, Li DJ, Yun JP, Zheng MZ, Hu ZY, Cheng LZ & Zeng YX (2006) The expression of p63 is associated with the differential stage in nasopharyngeal carcinoma and EBV infection. *J Transl Med* **4**, 23.

Hadjihannas MV, Bruckner M, Jerchow B, Birchmeier W, Dietmaier W & Behrens J (2006) Aberrant Wnt/beta-catenin signaling can induce chromosomal instability in colon cancer. *Proc Natl Acad Sci U S A* **103**, 10747-10752.

Hahm KB (1999) Repression of the gene encoding the TGF-beta type II receptor is a major target of the EWS-FLI1 oncoprotein. *Nat Genet* **23**, 222-227.

Hanahan D & Weinberg RA (2000) The hallmarks of cancer. *Cell* **100**, 57-70.

Hannon GJ & Beach D (1994) p15INK4B is a potential effector of TGF-beta-induced cell cycle arrest. *Nature* **371**, 257-261.

Hartsough MT & Mulder KM (1997) Transforming growth factor-beta signaling in epithelial cells. *Pharmacol Ther* **75**, 21-41.

Hasanuzzaman M, Kutner R, Agha-Mohammadi S, Reiser J & Sehgal I (2007) A doxycycline-inducible urokinase receptor (uPAR) upregulates uPAR activities including resistance to anoikis in human prostate cancer cell lines. *Mol Cancer* **6**, 34.

Hata A, Lagna G, Massague J & Hemmati-Brivanlou A (1998) Smad6 inhibits BMP/Smad1 signaling by specifically competing with the Smad4 tumor suppressor. *Genes Dev* **12**, 186-197.

Hatzivassiliou E & Mosialos G (2002) Cellular signaling pathways engaged by the Epstein-Barr virus transforming protein LMP1. *Front Biosci* **7**, 319-329.

Heldin CH, Miyazono K & ten Dijke P (1997) TGF-beta signalling from cell membrane to nucleus through SMAD proteins. *Nature* **390**, 465-471.

Hellerbrand C, Muhlbauer M, Wallner S, Schuierer M, Behrmann I, Bataille F, Weiss T, Scholmerich J & Bosserhoff AK (2006) Promoter-hypermethylation is causing functional relevant downregulation of methylthioadenosine phosphorylase (MTAP) expression in hepatocellular carcinoma. *Carcinogenesis* **27**, 64-72.

Henderson BR (2000) Nuclear-cytoplasmic shuttling of APC regulates beta-catenin subcellular localization and turnover. *Nat Cell Biol* **2**, 653-660.

Henle G & Henle W (1966) Immunofluorescence in cells derived from Burkitt's lymphoma. *J Bacteriol* **91**, 1248-1256.

Henle G & Henle W (1976) Epstein-Barr virus-specific IgA serum antibodies as an outstanding feature of nasopharyngeal carcinoma. *Int J Cancer* **17**, 1-7.

Henle G, Henle W & Diehl V (1968) Relation of Burkitt's tumor-associated herpes-ytpe virus to infectious mononucleosis. *Proc Natl Acad Sci U S A* **59**, 94-101.

Henle W, Diehl V, Kohn G, Zur Hausen H & Henle G (1967) Herpes-type virus and chromosome marker in normal leukocytes after growth with irradiated Burkitt cells. *Science* **157**, 1064-1065.

Heussinger N, Buttner M, Ott G, Brachtel E, Pilch BZ, Kremmer E & Niedobitek G (2004) Expression of the Epstein-Barr virus (EBV)-encoded latent membrane protein 2A (LMP2A) in EBV-associated nasopharyngeal carcinoma. *J Pathol* **203**, 696-699.

Heymann MF, Riet A, Le Goff B, Battaglia S, Paineau J & Heymann D (2008) OPG, RANK and RANK ligand expression in thyroid lesions. *Regul Pept* **148**, 46-53.

Hildesheim A, Anderson LM, Chen CJ, Cheng YJ, Brinton LA, Daly AK, Reed CD, Chen IH, Caporaso NE, Hsu MM, Chen JY, Idle JR, Hoover RN, Yang CS & Chhabra SK (1997) CYP2E1 genetic polymorphisms and risk of nasopharyngeal carcinoma in Taiwan. *J Natl Cancer Inst* **89**, 1207-1212.

Hill CE, Harris SB, Culler EE, Zimring JC, Nolte FS & Caliendo AM (2006) Performance characteristics of two real-time PCR assays for the quantification of Epstein-Barr virus DNA. *Am J Clin Pathol* **125**, 665-671.

Ho KY, Kalle WH, Lo TH, Lam WY & Tang CM (1999) Reduced expression of APC and DCC gene protein in breast cancer. *Histopathology* **35**, 249-256.

Hockenbery D, Nunez G, Milliman C, Schreiber RD & Korsmeyer SJ (1990) Bcl-2 is an inner mitochondrial membrane protein that blocks programmed cell death. *Nature* **348**, 334-336.

Hoe SL, Lee ES, Khoo AS & Peh SC (2009) Lack of Rb2/p130 genetic alteration in Malaysian nasopharyngeal carcinoma. *Malays J Pathol* **31**, 53-56.

Hoe SL & Sam CK (2006) Mutational analysis of p53 and RB2/p130 genes in Malaysian nasopharyngeal carcinoma samples: a preliminary report. *Malays J Pathol* **28**, 35-39.

Horikawa T, Sheen TS, Takeshita H, Sato H, Furukawa M & Yoshizaki T (2001) Induction of c-Met proto-oncogene by Epstein-Barr virus latent membrane protein-1 and the correlation with cervical lymph node metastasis of nasopharyngeal carcinoma. *Am J Pathol* **159**, 27-33.

Horikawa T, Yoshizaki T, Sheen TS, Lee SY & Furukawa M (2000) Association of latent membrane protein 1 and matrix metalloproteinase 9 with metastasis in nasopharyngeal carcinoma. *Cancer* **89**, 715-723.

Hu LF, Chen F, Zhen QF, Zhang YW, Luo Y, Zheng X, Winberg G, Ernberg I & Klein G (1995) Differences in the growth pattern and clinical course of EBV-LMP1 expressing and non-expressing nasopharyngeal carcinomas. *Eur J Cancer* **31A**, 658-660.

Hu LF, Eiriksdottir G, Lebedeva T, Kholodniouk I, Alimov A, Chen F, Luo Y, Zabarovsky ER, Ingvarsson S, Klein G & Ernberg I (1996) Loss of heterozygosity on chromosome arm 3p in nasopharyngeal carcinoma. *Genes Chromosomes Cancer* **17**, 118-126.

Hu LF, Qiu QH, Fu SM, Sun D, Magnusson K, He B, Lindblom A & Ernberg I (2008) A genome-wide scan suggests a susceptibility locus on 5p 13 for nasopharyngeal carcinoma. *Eur J Hum Genet* **16**, 343-349.

Hu ZY, Zhu XF, Zhong ZD, Sun J, Wang J, Yang D & Zeng YX (2008) ApoG2, a novel inhibitor of antiapoptotic Bcl-2 family proteins, induces apoptosis and suppresses tumor growth in nasopharyngeal carcinoma xenografts. *Int J Cancer* **123**, 2418-2429.

Huang DP, Ho JH, Chan WK, Lau WH & Lui M (1989) Cytogenetics of undifferentiated nasopharyngeal carcinoma xenografts from southern Chinese. *Int J Cancer* **43**, 936-939.

Huang DP, Lo KW, Choi PH, Ng AY, Tsao SY, Yiu GK & Lee JC (1991) Loss of heterozygosity on the short arm of chromosome 3 in nasopharyngeal carcinoma. *Cancer Genet Cytogenet* **54**, 91-99.

Huang DP, Lo KW, van Hasselt CA, Woo JK, Choi PH, Leung SF, Cheung ST, Cairns P, Sidransky D & Lee JC (1994) A region of homozygous deletion on chromosome 9p21-22 in primary nasopharyngeal carcinoma. *Cancer Res* **54**, 4003-4006.

Huang GW, Mo WN, Kuang GQ, Nong HT, Wei MY, Sunagawa M & Kosugi T (2001) Expression of p16, nm23-H1, E-cadherin, and CD44 gene products and their significance in nasopharyngeal carcinoma. *Laryngoscope* **111**, 1465-1471.

Huang H & He X (2008) Wnt/beta-catenin signaling: new (and old) players and new insights. *Curr Opin Cell Biol* **20**, 119-125.

Huang J, Wei W, Zhang J, Liu G, Bignell GR, Stratton MR, Futreal PA, Wooster R, Jones KW & Shapero MH (2004) Whole genome DNA copy number changes identified by high density oligonucleotide arrays. *Hum Genomics* **1**, 287-299.

Hui AB, Lo KW, Chan SY, Kwong J, Chan AS & Huang DP (2002) Absence of SDHD mutations in primary nasopharyngeal carcinomas. *Int J Cancer* **97**, 875-877.

Hui AB, Lo KW, Kwong J, Lam EC, Chan SY, Chow LS, Chan AS, Teo PM & Huang DP (2003) Epigenetic inactivation of TSLC1 gene in nasopharyngeal carcinoma. *Mol Carcinog* **38**, 170-178.

Hui AB, Lo KW, Leung SF, Choi PH, Fong Y, Lee JC & Huang DP (1996) Loss of heterozygosity on the long arm of chromosome 11 in nasopharyngeal carcinoma. *Cancer Res* **56**, 3225-3229.

Hui AB, Lo KW, Leung SF, Teo P, Fung MK, To KF, Wong N, Choi PH, Lee JC & Huang DP (1999) Detection of recurrent chromosomal gains and losses in primary nasopharyngeal carcinoma by comparative genomic hybridisation. *Int J Cancer* **82**, 498-503.

Hui AB, Lo KW, Teo PM, To KF & Huang DP (2002) Genome wide detection of oncogene amplifications in nasopharyngeal carcinoma by array based comparative genomic hybridization. *Int J Oncol* **20**, 467-473.

Hui AB, Or YY, Takano H, Tsang RK, To KF, Guan XY, Sham JS, Hung KW, Lam CN, van Hasselt CA, Kuo WL, Gray JW, Huang DP & Lo KW (2005) Array-based comparative genomic hybridization analysis identified cyclin D1 as a target oncogene at 11q13.3 in nasopharyngeal carcinoma. *Cancer Res* **65**, 8125-8133.

Hui EP, Leung SF, Au JS, Zee B, Tung S, Chua D, Sze WM, Law CK, Leung TW & Chan AT (2004) Lung metastasis alone in nasopharyngeal carcinoma: a relatively favorable prognostic group. A study by the Hong Kong Nasopharyngeal Carcinoma Study Group. *Cancer* **101**, 300-306.

Hummerich L, Muller R, Hess J, Kokocinski F, Hahn M, Furstenberger G, Mauch C, Lichter P & Angel P (2006) Identification of novel tumour-associated genes differentially expressed in the process of squamous cell cancer development. *Oncogene* **25**, 111-121.

Hustinx SR, Leoni LM, Yeo CJ, Brown PN, Goggins M, Kern SE, Hruban RH & Maitra A (2005) Concordant loss of MTAP and p16/CDKN2A expression in pancreatic intraepithelial neoplasia: evidence of homozygous deletion in a noninvasive precursor lesion. *Mod Pathol* **18**, 959-963.

Hwang CF, Cho CL, Huang CC, Wang JS, Shih YL, Su CY & Chang HW (2002) Loss of cyclin D1 and p16 expression correlates with local recurrence in nasopharyngeal carcinoma following radiotherapy. *Ann Oncol* **13**, 1246-1251.

Hwang YC, Lu TY, Huang DY, Kuo YS, Kao CF, Yeh NH, Wu HC & Lin CT (2009) NOLC1, an enhancer of nasopharyngeal carcinoma progression, is essential for TP53 to regulate MDM2 expression. *Am J Pathol* **175**, 342-354.

Iavarone A & Massague J (1997) Repression of the CDK activator Cdc25A and cell-cycle arrest by cytokine TGF-beta in cells lacking the CDK inhibitor p15. *Nature* **387**, 417-422.

Imai S, Nishikawa J & Takada K (1998) Cell-to-cell contact as an efficient mode of Epstein-Barr virus infection of diverse human epithelial cells. *J Virol* **72**, 4371-4378.

Ingham PW & McMahon AP (2001) Hedgehog signaling in animal development: paradigms and principles. *Genes Dev* **15**, 3059-3087.

Inokuchi J, Lau A, Tyson DR & Ornstein DK (2009) Loss of annexin A1 disrupts normal prostate glandular structure by inducing autocrine IL-6 signaling. *Carcinogenesis* **30**, 1082-1088.

Irizarry RA, Hobbs B, Collin F, Beazer-Barclay YD, Antonellis KJ, Scherf U & Speed TP (2003) Exploration, normalization, and summaries of high density oligonucleotide array probe level data. *Biostatistics* **4**, 249-264.

Iwai K, Hirata K, Ishida T, Takeuchi S, Hirase T, Rikitake Y, Kojima Y, Inoue N, Kawashima S & Yokoyama M (2004) An anti-proliferative gene BTG1 regulates angiogenesis in vitro. *Biochem Biophys Res Commun* **316**, 628-635.

Jia WH, Pan QH, Qin HD, Xu YF, Shen GP, Chen L, Chen LZ, Feng QS, Hong MH, Zeng YX & Shugart YY (2009) A case-control and a family-based association study revealing an association between CYP2E1 polymorphisms and nasopharyngeal carcinoma risk in Cantonese. *Carcinogenesis* **30**, 2031-2036.

Jiang J & Hui CC (2008) Hedgehog signaling in development and cancer. *Dev Cell* **15**, 801-812.

Jones RJ, Smith LJ, Dawson CW, Haigh T, Blake NW & Young LS (2003) Epstein-Barr virus nuclear antigen 1 (EBNA1) induced cytotoxicity in epithelial cells is associated with EBNA1 degradation and processing. *Virology* **313**, 663-676.

Joseph AM, Babcock GJ & Thorley-Lawson DA (2000) Cells expressing the Epstein-Barr virus growth program are present in and restricted to the naive B-cell subset of healthy tonsils. *J Virol* **74**, 9964-9971.

Kallioniemi A (2008) CGH microarrays and cancer. *Curr Opin Biotechnol* **19**, 36-40.

Kallioniemi A, Kallioniemi OP, Sudar D, Rutovitz D, Gray JW, Waldman F & Pinkel D (1992) Comparative genomic hybridization for molecular cytogenetic analysis of solid tumors. *Science* **258**, 818-821.

Kaminker P, Plachot C, Kim SH, Chung P, Crippen D, Petersen OW, Bissell MJ, Campisi J & Lelievre SA (2005) Higher-order nuclear organization in growth arrest of human mammary epithelial cells: a novel role for telomere-associated protein TIN2. *J Cell Sci* **118**, 1321-1330.

Kanehisa M, Goto S, Kawashima S & Nakaya A (2002) The KEGG databases at GenomeNet. *Nucleic Acids Res* **30**, 42-46.

Kapral M, Strzalka B, Kowalczyk M, Jurzak M, Mazurek U, Gierek T, Paluch J, Markowski J, Swiatkowska L & Weglarz L (2008) Transforming growth factor beta isoforms (TGF-beta1, TGF-beta2, TGF-beta3) messenger RNA expression in laryngeal cancer. *Am J Otolaryngol* **29**, 233-237.

Karajannis MA, Hummel M, Anagnostopoulos I & Stein H (1997) Strict lymphotropism of Epstein-Barr virus during acute infectious mononucleosis in nonimmunocompromised individuals. *Blood* **89**, 2856-2862.

Kasper M, Jaks V, Fiaschi M & Toftgard R (2009) Hedgehog signalling in breast cancer. *Carcinogenesis* **30**, 903-911.

Kassambara A, Klein B & Moreaux J (2009) MMSET is overexpressed in cancers: link with tumor aggressiveness. *Biochem Biophys Res Commun* **379**, 840-845.

Katoh M & Katoh M (2007) STAT3-induced WNT5A signaling loop in embryonic stem cells, adult normal tissues, chronic persistent inflammation, rheumatoid arthritis and cancer (Review). *Int J Mol Med* **19**, 273-278.

Katz JP, Perreault N, Goldstein BG, Lee CS, Labosky PA, Yang VW & Kaestner KH (2002) The zinc-finger transcription factor Klf4 is required for terminal differentiation of goblet cells in the colon. *Development* **129**, 2619-2628.

Kawakami T, Shiina H, Igawa M, Deguchi M, Nakajima K, Ogishima T, Tokizane T, Urakami S, Enokida H, Miura K, Ishii N, Kane CJ, Carroll PR & Dahiya R (2004) Inactivation of the hMSH3 mismatch repair gene in bladder cancer. *Biochem Biophys Res Commun* **325**, 934-942.

Kayed H, Kleeff J, Keleg S, Guo J, Ketterer K, Berberat PO, Giese N, Esposito I, Giese T, Buchler MW & Friess H (2004) Indian hedgehog signaling pathway: expression and regulation in pancreatic cancer. *Int J Cancer* **110**, 668-676.

Khabir A, Karray H, Rodriguez S, Rose M, Daoud J, Frikha M, Boudawara T, Middeldorp J, Jlidi R & Busson P (2005) EBV latent membrane protein 1 abundance correlates with patient age but not with metastatic behavior in north African nasopharyngeal carcinomas. *Virol J* **2**, 39.

Kleer CG, Cao Q, Varambally S, Shen R, Ota I, Tomlins SA, Ghosh D, Sewalt RG, Otte AP, Hayes DF, Sabel MS, Livant D, Weiss SJ, Rubin MA & Chinnaiyan AM (2003) EZH2 is a marker of aggressive breast cancer and promotes neoplastic transformation of breast epithelial cells. *Proc Natl Acad Sci U S A* **100**, 11606-11611.

Kloth JN, Oosting J, van Wezel T, Szuhai K, Knijnenburg J, Gorter A, Kenter GG, Fleuren GJ & Jordanova ES (2007) Combined array-comparative genomic hybridization and single-nucleotide polymorphism-loss of heterozygosity analysis reveals complex genetic alterations in cervical cancer. *BMC Genomics* **8**, 53.

Knox PG, Li QX, Rickinson AB & Young LS (1996) In vitro production of stable Epstein-Barr virus-positive epithelial cell clones which resemble the virus:cell interaction observed in nasopharyngeal carcinoma. *Virology* **215**, 40-50.

Knudson AG, Jr. (1971) Mutation and cancer: statistical study of retinoblastoma. *Proc Natl Acad Sci U S A* **68**, 820-823.

Ko JY, Lee TC, Hsiao CF, Lin GL, Yen SH, Chen KY, Hsiung CA, Chen PJ, Hsu MM & Jou YS (2002) Definition of three minimal deleted regions by comprehensive allelotyping and mutational screening of FHIT,p16(INK4A), and p19(ARF) genes in nasopharyngeal carcinoma. *Cancer* **94**, 1987-1996.

Kolfschoten IG, van Leeuwen B, Berns K, Mullenders J, Beijersbergen RL, Bernards R, Voorhoeve PM & Agami R (2005) A genetic screen identifies PITX1 as a suppressor of RAS activity and tumorigenicity. *Cell* **121**, 849-858.

Kortlever RM, Nijwening JH & Bernards R (2008) Transforming growth factor-beta requires its target plasminogen activator inhibitor-1 for cytostatic activity. *J Biol Chem* **283**, 24308-24313.

Kwong J, Chow LS, Wong AY, Hung WK, Chung GT, To KF, Chan FL, Daigo Y, Nakamura Y, Huang DP & Lo KW (2007) Epigenetic inactivation of the deleted in lung and esophageal cancer 1 gene in nasopharyngeal carcinoma. *Genes Chromosomes Cancer* **46**, 171-180.

Kwong J, Lo KW, To KF, Teo PM, Johnson PJ & Huang DP (2002) Promoter hypermethylation of multiple genes in nasopharyngeal carcinoma. *Clin Cancer Res* **8**, 131-137.

Labbe E, Letamendia A & Attisano L (2000) Association of Smads with lymphoid enhancer binding factor 1/T cell-specific factor mediates cooperative signaling by the transforming growth factor-beta and wnt pathways. *Proc Natl Acad Sci U S A* **97**, 8358-8363.

Laherty CD, Hu HM, Opipari AW, Wang F & Dixit VM (1992) The Epstein-Barr virus LMP1 gene product induces A20 zinc finger protein expression by activating nuclear factor kappa B. *J Biol Chem* **267**, 24157-24160.

Laiho M, DeCaprio JA, Ludlow JW, Livingston DM & Massague J (1990) Growth inhibition by TGF-beta linked to suppression of retinoblastoma protein phosphorylation. *Cell* **62**, 175-185.

Langenskiold M, Holmdahl L, Falk P, Angenete E & Ivarsson ML (2008) Increased TGF-beta 1 protein expression in patients with advanced colorectal cancer. *J Surg Oncol* **97**, 409-415.

Lee CH, Fang CY, Sheu JJ, Chang Y, Takada K & Chen JY (2008) Amplicons on chromosome 3 contain oncogenes induced by recurrent exposure to 12-O-tetradecanoylphorbol-13-acetate and sodium n-butyrate and Epstein-Barr virus reactivation in a nasopharyngeal carcinoma cell line. *Cancer Genet Cytogenet* **185**, 1-10.

Lee DC, Chua DT, Wei WI, Sham JS & Lau AS (2007) Induction of matrix metalloproteinases by Epstein-Barr virus latent membrane protein 1 isolated from nasopharyngeal carcinoma. *Biomed Pharmacother* **61**, 520-526.

Lee HJ, Lee EK, Lee KJ, Hong SW, Yoon Y & Kim JS (2006) Ectopic expression of neutrophil gelatinase-associated lipocalin suppresses the invasion and liver metastasis of colon cancer cells. *Int J Cancer* **118**, 2490-2497.

Lee JH, Abraham SC, Kim HS, Nam JH, Choi C, Lee MC, Park CS, Juhng SW, Rashid A, Hamilton SR & Wu TT (2002) Inverse relationship between APC gene mutation in gastric adenomas and development of adenocarcinoma. *Am J Pathol* **161**, 611-618.

Lee SY, Han HS, Lee KY, Hwang TS, Kim JH, Sung IK, Park HS, Jin CJ & Choi KW (2007) Sonic hedgehog expression in gastric cancer and gastric adenoma. *Oncol Rep* **17**, 1051-1055.

Lee YC, Hwang YC, Chen KC, Lin YS, Huang DY, Huang TW, Kao CY, Wu HC, Lin CT & Huang CY (2007) Effect of Epstein-Barr virus infection on global gene expression in nasopharyngeal carcinoma. *Funct Integr Genomics* **7**, 79-93.

Lennette ET, Winberg G, Yadav M, Enblad G & Klein G (1995) Antibodies to LMP2A/2B in EBV-carrying malignancies. *Eur J Cancer* **31A**, 1875-1878.

Leris AC, Roberts TR, Jiang WG, Newbold RF & Mokbel K (2005) WNT5A expression in human breast cancer. *Anticancer Res* **25**, 731-734.

Lerman MI & Minna JD (2000) The 630-kb lung cancer homozygous deletion region on human chromosome 3p21.3: identification and evaluation of the resident candidate tumor suppressor genes. The International Lung Cancer Chromosome 3p21.3 Tumor Suppressor Gene Consortium. *Cancer Res* **60**, 6116-6133.

Levy L & Hill CS (2005) Smad4 dependency defines two classes of transforming growth factor beta (TGF-beta) target genes and distinguishes TGF-beta-induced epithelial-mesenchymal transition from its antiproliferative and migratory responses. *Mol Cell Biol* **25**, 8108-8125.

Li C & Wong WH (2001) Model-based analysis of oligonucleotide arrays: expression index computation and outlier detection. *Proc Natl Acad Sci U S A* **98**, 31-36.

Li HM, Man C, Jin Y, Deng W, Yip YL, Feng HC, Cheung YC, Lo KW, Meltzer PS, Wu ZG, Kwong YL, Yuen AP & Tsao SW (2006) Molecular and cytogenetic changes involved in the immortalization of nasopharyngeal epithelial cells by telomerase. *Int J Cancer* **119**, 1567-1576.

Li J, Yin C, Okamoto H, Mushlin H, Balgley BM, Lee CS, Yuan K, Ikejiri B, Glasker S, Vortmeyer AO, Oldfield EH, Weil RJ & Zhuang Z (2008) Identification of a novel proliferation-related protein, WHSC1 4a, in human gliomas. *Neuro Oncol* **10**, 45-51.

Li J, Zhang XS, Xie D, Deng HX, Gao YF, Chen QY, Huang WL, Masucci MG & Zeng YX (2007) Expression of immune-related molecules in primary EBV-positive Chinese nasopharyngeal carcinoma: associated with latent membrane protein 1 (LMP1) expression. *Cancer Biol Ther* **6**, 1997-2004.

Li JM, Hu PP, Shen X, Yu Y & Wang XF (1997) E2F4-RB and E2F4-p107 complexes suppress gene expression by transforming growth factor beta through E2F binding sites. *Proc Natl Acad Sci U S A* **94**, 4948-4953.

Li QX, Young LS, Niedobitek G, Dawson CW, Birkenbach M, Wang F & Rickinson AB (1992) Epstein-Barr virus infection and replication in a human epithelial cell system. *Nature* **356**, 347-350.

Li W, Ray RM, Gao DL, Fitzgibbons ED, Seixas NS, Camp JE, Wernli KJ, Astrakianakis G, Feng Z, Thomas DB & Checkoway H (2006) Occupational risk factors for nasopharyngeal cancer among female textile workers in Shanghai, China. *Occup Environ Med* **63**, 39-44.

Li X, Wang E, Zhao YD, Ren JQ, Jin P, Yao KT & Marincola FM (2006) Chromosomal imbalances in nasopharyngeal carcinoma: a meta-analysis of comparative genomic hybridization results. *J Transl Med* **4**, 4.

Li Z, Ren Y, Lin SX, Liang YJ & Liang HZ (2004) Association of E-cadherin and beta-catenin with metastasis in nasopharyngeal carcinoma. *Chin Med J (Engl)* **117**, 1232-1239.

Lin D, Watahiki A, Bayani J, Zhang F, Liu L, Ling V, Sadar MD, English J, Fazli L, So A, Gout PW, Gleave M, Squire JA & Wang YZ (2008) ASAP1, a gene at 8q24, is associated with prostate cancer metastasis. *Cancer Res* **68**, 4352-4359.

Lin HS, Berry GJ, Sun Z & Fee WE, Jr. (2006) Cyclin D1 and p16 expression in recurrent nasopharyngeal carcinoma. *World J Surg Oncol* **4**, 62.

Lin LJ, Asaoka Y, Tada M, Sanada M, Nannya Y, Tanaka Y, Tateishi K, Ohta M, Seto M, Sasahira N, Tada M, Kawabe T, Zheng CQ, Kanai F, Ogawa S & Omata M (2008) Integrated analysis of copy number alterations and loss of heterozygosity in human pancreatic cancer using a high-resolution, single nucleotide polymorphism array. *Oncology* **75**, 102-112.

Lin SY, Tsang NM, Kao SC, Hsieh YL, Chen YP, Tsai CS, Kuo TT, Hao SP, Chen IH & Hong JH (2001) Presence of Epstein-Barr virus latent membrane protein 1 gene in the nasopharyngeal swabs from patients with nasopharyngeal carcinoma. *Head Neck* **23**, 194-200.

Lin YC, You L, Xu Z, He B, Mikami I, Thung E, Chou J, Kuchenbecker K, Kim J, Raz D, Yang CT, Chen JK & Jablons DM (2006) Wnt signaling activation and WIF-1 silencing in nasopharyngeal cancer cell lines. *Biochem Biophys Res Commun* **341**, 635-640.

Lindblad-Toh K, Tanenbaum DM, Daly MJ, Winchester E, Lui WO, Villapakkam A, Stanton SE, Larsson C, Hudson TJ, Johnson BE, Lander ES & Meyerson M (2000) Loss-of-heterozygosity analysis of small-cell lung carcinomas using single-nucleotide polymorphism arrays. *Nat Biotechnol* **18**, 1001-1005.

Ling MT, Wang X, Tsao SW & Wong YC (2002) Down-regulation of Id-1 expression is associated with TGF beta 1-induced growth arrest in prostate epithelial cells. *Biochim Biophys Acta* **1570**, 145-152.

Liu DX & Lobie PE (2007) Transcriptional activation of p53 by Pitx1. *Cell Death Differ* **14**, 1893-1907.

Liu H, Zheng H, Duan Z, Hu D, Li M, Liu S, Li Z, Deng X, Wang Z, Tang M, Shi Y, Yi W & Cao Y (2009) LMP1-augmented kappa intron enhancer activity contributes to upregulation expression of Ig kappa light chain via NF-kappaB and AP-1 pathways in nasopharyngeal carcinoma cells. *Mol Cancer* **8**, 92.

Liu MZ, Xie D, Mai SJ, Tong ZT, Shao JY, Fu YS, Xia WJ, Kung HF, Guan XY & Zeng YX (2008) Overexpression of AIB1 in nasopharyngeal carcinomas correlates closely with advanced tumor stage. *Am J Clin Pathol* **129**, 728-734.

Liu SC, Jen YM, Jiang SS, Chang JL, Hsiung CA, Wang CH & Juang JL (2009) G(alpha)12-mediated pathway promotes invasiveness of nasopharyngeal carcinoma by modulating actin cytoskeleton reorganization. *Cancer Res* **69**, 6122-6130.

Liu XQ, Chen HK, Zhang XS, Pan ZG, Li A, Feng QS, Long QX, Wang XZ & Zeng YX (2003) Alterations of BLU, a candidate tumor suppressor gene on chromosome 3p21.3, in human nasopharyngeal carcinoma. *Int J Cancer* **106**, 60-65.

Liu ZQ, Tian YQ, Hu YF, Li XL, Ma FR & Li GY (2009) Alteration of gene expression during nasopharyngeal carcinogenesis revealed by oligonucleotide microarray after microdissection of tumor tissue and normal epithelia from nasopharynx. *Chin Med J (Engl)* **122**, 437-443.

Lo AK, Lo KW, Tsao SW, Wong HL, Hui JW, To KF, Hayward DS, Chui YL, Lau YL, Takada K & Huang DP (2006) Epstein-Barr virus infection alters cellular signal cascades in human nasopharyngeal epithelial cells. *Neoplasia* **8**, 173-180.

Lo KW, Chung G.T and Lo, K. F (2008) Acquired genetic and epigenetic alterations in nasopharyngral carcinoma. In *Nasopharyngeal carcinoma* [P Busson, editor], in press.

Lo KW & Huang DP (2002) Genetic and epigenetic changes in nasopharyngeal carcinoma. *Semin Cancer Biol* **12**, 451-462.

Lo KW, Huang DP & Lau KM (1995) p16 gene alterations in nasopharyngeal carcinoma. *Cancer Res* **55**, 2039-2043.

Lo KW, Kwong J, Hui AB, Chan SY, To KF, Chan AS, Chow LS, Teo PM, Johnson PJ & Huang DP (2001) High frequency of promoter hypermethylation of RASSF1A in nasopharyngeal carcinoma. *Cancer Res* **61**, 3877-3881.

Lo KW, Teo PM, Hui AB, To KF, Tsang YS, Chan SY, Mak KF, Lee JC & Huang DP (2000) High resolution allelotype of microdissected primary nasopharyngeal carcinoma. *Cancer Res* **60**, 3348-3353.

Lo KW, Tsang YS, Kwong J, To KF, Teo PM & Huang DP (2002) Promoter hypermethylation of the EDNRB gene in nasopharyngeal carcinoma. *Int J Cancer* **98**, 651-655.

Lo YM, Chan AT, Chan LY, Leung SF, Lam CW, Huang DP & Johnson PJ (2000) Molecular prognostication of nasopharyngeal carcinoma by quantitative analysis of circulating Epstein-Barr virus DNA. *Cancer Res* **60**, 6878-6881.

Logan CY & Nusse R (2004) The Wnt signaling pathway in development and disease. *Annu Rev Cell Dev Biol* **20**, 781-810.

Longnecker R (2000) Epstein-Barr virus latency: LMP2, a regulator or means for Epstein-Barr virus persistence? *Adv Cancer Res* **79**, 175-200.

Lord RV, Brabender J, Wickramasinghe K, DeMeester SR, Holscher A, Schneider PM, Danenberg PV & DeMeester TR (2005) Increased CDX2 and decreased PITX1 homeobox gene expression in Barrett's esophagus and Barrett's-associated adenocarcinoma. *Surgery* **138**, 924-931.

Lu CC, Chen JC, Jin YT, Yang HB, Chan SH & Tsai ST (2003) Genetic susceptibility to nasopharyngeal carcinoma within the HLA-A locus in Taiwanese. *Int J Cancer* **103**, 745-751.

Lu CC, Chen JC, Tsai ST, Jin YT, Tsai JC, Chan SH & Su IJ (2005) Nasopharyngeal carcinoma-susceptibility locus is localized to a 132 kb segment containing HLA-A using high-resolution microsatellite mapping. *Int J Cancer* **115**, 742-746.

Lu J, Chua HH, Chen SY, Chen JY & Tsai CH (2003) Regulation of matrix metalloproteinase-1 by Epstein-Barr virus proteins. *Cancer Res* **63**, 256-262.

Lu QL, Elia G, Lucas S & Thomas JA (1993) Bcl-2 proto-oncogene expression in Epstein-Barr-virus-associated nasopharyngeal carcinoma. *Int J Cancer* **53**, 29-35.

Lu SJ, Day NE, Degos L, Lepage V, Wang PC, Chan SH, Simons M, McKnight B, Easton D & Zeng Y. (1990) Linkage of a nasopharyngeal carcinoma susceptibility locus to the HLA region. *Nature* **346**, 470-471.

Lung HL, Bangarusamy DK, Xie D, Cheung AK, Cheng Y, Kumaran MK, Miller L, Liu ET, Guan XY, Sham JS, Fang Y, Li L, Wang N, Protopopov AI, Zabarovsky ER, Tsao SW, Stanbridge EJ & Lung ML (2005) THY1 is a candidate tumour suppressor gene with decreased expression in metastatic nasopharyngeal carcinoma. *Oncogene* **24**, 6525-6532.

Lung HL, Cheng Y, Kumaran MK, Liu ET, Murakami Y, Chan CY, Yau WL, Ko JM, Stanbridge EJ & Lung ML (2004) Fine mapping of the 11q22-23 tumor suppressive region and involvement of TSLC1 in nasopharyngeal carcinoma. *Int J Cancer* **112**, 628-635.

Lung HL, Cheung AK, Cheng Y, Kwong FM, Lo PH, Law EW, Chua D, Zabarovsky ER, Wang N, Tsao SW, Stanbridge EJ & Lung ML (2009) Functional characterization of THY1 as a tumor suppressor gene with antiinvasive activity in nasopharyngeal carcinoma. *Int J Cancer* **127**, 304-312.

Lung HL, Cheung AK, Xie D, Cheng Y, Kwong FM, Murakami Y, Guan XY, Sham JS, Chua D, Protopopov AI, Zabarovsky ER, Tsao SW, Stanbridge EJ & Lung ML (2006) TSLC1 is a tumor suppressor gene associated with metastasis in nasopharyngeal carcinoma. *Cancer Res* **66**, 9385-9392.

Lung HL, Lo CC, Wong CC, Cheung AK, Cheong KF, Wong N, Kwong FM, Chan KC, Law EW, Tsao SW, Chua D, Sham JS, Cheng Y, Stanbridge EJ, Robertson GP & Lung ML (2008) Identification of tumor suppressive activity by irradiation microcell-mediated chromosome transfer and involvement of alpha B-crystallin in nasopharyngeal carcinoma. *Int J Cancer* **122**, 1288-1296.

Lung HL, Lo PH, Xie D, Apte SS, Cheung AK, Cheng Y, Law EW, Chua D, Zeng YX, Tsao SW, Stanbridge EJ & Lung ML (2008) Characterization of a novel epigenetically-silenced, growth-suppressive gene, ADAMTS9, and its association with lymph node metastases in nasopharyngeal carcinoma. *Int J Cancer* **123**, 401-408.

Ma BB & Chan AT (2006) Systemic treatment strategies and therapeutic monitoring for advanced nasopharyngeal carcinoma. *Expert Rev Anticancer Ther* **6**, 383-394.

Ma C, Rong Y, Radiloff DR, Datto MB, Centeno B, Bao S, Cheng AW, Lin F, Jiang S, Yeatman TJ & Wang XF (2008) Extracellular matrix protein betaig-h3/TGFBI promotes metastasis of colon cancer by enhancing cell extravasation. *Genes Dev* **22**, 308-321.

Mainou BA & Raab-Traub N (2006) LMP1 strain variants: biological and molecular properties. *J Virol* **80**, 6458-6468.

Makitie AA, MacMillan C, Ho J, Shi W, Lee A, O'Sullivan B, Payne D, Pintilie M, Cummings B, Waldron J, Warde P, Irish J, Brown D, Gilbert R, Gullane P, Liu FF & Kamel-Reid S (2003) Loss of p16 expression has prognostic significance in human nasopharyngeal carcinoma. *Clin Cancer Res* **9**, 2177-2184.

Man C, Rosa J, Lee LT, Lee VH, Chow BK, Lo KW, Doxsey S, Wu ZG, Kwong YL, Jin DY, Cheung AL & Tsao SW (2007) Latent membrane protein 1 suppresses RASSF1A expression, disrupts microtubule structures and induces chromosomal aberrations in human epithelial cells. *Oncogene* **26**, 3069-3080.

Mao B, Wu W, Li Y, Hoppe D, Stannek P, Glinka A & Niehrs C (2001) LDL-receptor-related protein 6 is a receptor for Dickkopf proteins. *Nature* **411**, 321-325.

Marinari B, Moretti F, Botti E, Giustizieri ML, Descargues P, Giunta A, Stolfi C, Ballaro C, Papoutsaki M, Alema S, Monteleone G, Chimenti S, Karin M & Costanzo A (2008) The tumor suppressor activity of IKKalpha in stratified epithelia is exerted in part via the TGF-beta antiproliferative pathway. *Proc Natl Acad Sci U S A* **105**, 17091-17096.

Markowitz SD & Roberts AB (1996) Tumor suppressor activity of the TGF-beta pathway in human cancers. *Cytokine Growth Factor Rev* **7**, 93-102.

Marks JE, Phillips JL & Menck HR (1998) The National Cancer Data Base report on the relationship of race and national origin to the histology of nasopharyngeal carcinoma. *Cancer* **83**, 582-588.

Martin JM, Veis D, Korsmeyer SJ & Sugden B (1993) Latent membrane protein of Epstein-Barr virus induces cellular phenotypes independently of expression of Bcl-2. *J Virol* **67**, 5269-5278.

Massague J (1998) TGF-beta signal transduction. *Annu Rev Biochem* **67**, 753-791.

Massague J (2008) TGFbeta in Cancer. *Cell* **134**, 215-230.

Massague J & Chen YG (2000) Controlling TGF-beta signaling. *Genes Dev* **14**, 627-644.

McCarroll SA, Kuruvilla FG, Korn JM, Cawley S, Nemesh J, Wysoker A, Shapero MH, de Bakker PI, Maller JB, Kirby A, Elliott AL, Parkin M, Hubbell E, Webster T, Mei R, Veitch J, Collins PJ, Handsaker R, Lincoln S, Nizzari M, Blume J, Jones KW, Rava R, Daly MJ, Gabriel SB & Altshuler D (2008) Integrated detection and population-genetic analysis of SNPs and copy number variation. *Nat Genet* **40**, 1166-1174.

Mei YP, Zhou JM, Wang Y, Huang H, Deng R, Feng GK, Zeng YX & Zhu XF (2007) Silencing of LMP1 induces cell cycle arrest and enhances chemosensitivity through inhibition of AKT signaling pathway in EBV-positive nasopharyngeal carcinoma cells. *Cell Cycle* **6**, 1379-1385.

Micheau C, Boussen H, Klijanienko J, Cvitkovic E, Stosic S, Schwaab G, Eschwege F & Armand JP (1987) Bone marrow biopsies in patients with undifferentiated carcinoma of the nasopharyngeal type. *Cancer* **60**, 2459-2464.

Miller WE, Edwards RH, Walling DM & Raab-Traub N (1994) Sequence variation in the Epstein-Barr virus latent membrane protein 1. *J Gen Virol* **75**, 2729-2740.

Mitelman F, Mertens F & Johansson B (1997) A breakpoint map of recurrent chromosomal rearrangements in human neoplasia. *Nat Genet* **15**, 417-474.

Miyaki M, Iijima T, Kimura J, Yasuno M, Mori T, Hayashi Y, Koike M, Shitara N, Iwama T & Kuroki T (1999) Frequent mutation of beta-catenin and APC genes in primary colorectal tumors from patients with hereditary nonpolyposis colorectal cancer. *Cancer Res* **59**, 4506-4509.

Miyaki M & Kuroki T (2003) Role of Smad4 (DPC4) inactivation in human cancer. *Biochem Biophys Res Commun* **306**, 799-804.

Miyazono K, Maeda S & Imamura T (2005) BMP receptor signaling: transcriptional targets, regulation of signals, and signaling cross-talk. *Cytokine Growth Factor Rev* **16**, 251-263.

Miyazono K & Miyazawa K (2002) Id: a target of BMP signaling. *Sci STKE* **2002**, pe40.

Monga SP (2009) Role of Wnt/beta-catenin signaling in liver metabolism and cancer. *Int J Biochem Cell Biol*, DOI:10.1016/j.biocel.2009.09.001.

Moniaux N, Chakraborty S, Yalniz M, Gonzalez J, Shostrom VK, Standop J, Lele SM, Ouellette M, Pour PM, Sasson AR, Brand RE, Hollingsworth MA, Jain M & Batra SK (2008) Early diagnosis of pancreatic cancer: neutrophil gelatinase-associated lipocalin as a marker of pancreatic intraepithelial neoplasia. *Br J Cancer* **98**, 1540-1547.

Morgan DG, Niederman JC, Miller G, Smith HW & Dowaliby JM (1979) Site of Epstein-Barr virus replication in the oropharynx. *Lancet* **2**, 1154-1157.

Moses HL & Serra R (1996) Regulation of differentiation by TGF-beta. *Curr Opin Genet Dev* **6**, 581-586.

Munoz NM, Upton M, Rojas A, Washington MK, Lin L, Chytil A, Sozmen EG, Madison BB, Pozzi A, Moon RT, Moses HL & Grady WM (2006) Transforming growth factor beta receptor type II inactivation induces the malignant transformation of intestinal neoplasms initiated by Apc mutation. *Cancer Res* **66**, 9837-9844.

Murono S, Inoue H, Tanabe T, Joab I, Yoshizaki T, Furukawa M & Pagano JS (2001) Induction of cyclooxygenase-2 by Epstein-Barr virus latent membrane protein 1 is involved in vascular endothelial growth factor production in nasopharyngeal carcinoma cells. *Proc Natl Acad Sci U S A* **98**, 6905-6910.

Murono S, Yoshizaki T, Park CS & Furukawa M (1999) Association of Epstein-Barr virus infection with p53 protein accumulation but not bcl-2 protein in nasopharyngeal carcinoma. *Histopathology* **34**, 432-438.

Murono S, Yoshizaki T, Tanaka S, Takeshita H, Park CS & Furukawa M (1997) Detection of Epstein-Barr virus in nasopharyngeal carcinoma by in situ hybridization and polymerase chain reaction. *Laryngoscope* **107**, 523-526.

Mutirangura A, Pornthanakasem W, Sriuranpong V, Supiyaphun P & Voravud N (1998) Loss of heterozygosity on chromosome 14 in nasopharyngeal carcinoma. *Int J Cancer* **78**, 153-156.

Nagamine M, Takahara M, Kishibe K, Nagato T, Ishii H, Bandoh N, Ogino T & Harabuchi Y (2007) Sequence variations of Epstein-Barr virus LMP1 gene in nasal NK/T-cell lymphoma. *Virus Genes* **34**, 47-54.

Naidoo R & Chetty R (1998) The application of microsatellites in molecular pathology. *Pathol Oncol Res* **4**, 310-315.

Nakamura S, Kamakura T & Ookura T (2009) Tongue epithelial KT-1 cell-cycle arrest by TGF-beta associated with induction of p21(Cip1) and p15 (Ink4b). *Cytotechnology* **61**, 109-116.

Nakao A, Afrakhte M, Moren A, Nakayama T, Christian JL, Heuchel R, Itoh S, Kawabata M, Heldin NE, Heldin CH & ten Dijke P (1997) Identification of Smad7, a TGFbeta-inducible antagonist of TGF-beta signalling. *Nature* **389**, 631-635.

Nam JM, McLaughlin JK & Blot WJ (1992) Cigarette smoking, alcohol, and nasopharyngeal carcinoma: a case-control study among U.S. whites. *J Natl Cancer Inst* **84**, 619-622.

Nazar-Stewart V, Vaughan TL, Burt RD, Chen C, Berwick M & Swanson GM (1999) Glutathione S-transferase M1 and susceptibility to nasopharyngeal carcinoma. *Cancer Epidemiol Biomarkers Prev* **8**, 547-551.

Nemerow GR, Mold C, Schwend VK, Tollefson V & Cooper NR (1987) Identification of gp350 as the viral glycoprotein mediating attachment of Epstein-Barr virus (EBV) to the EBV/C3d receptor of B cells: sequence homology of gp350 and C3 complement fragment C3d. *J Virol* **61**, 1416-1420.

Nicholls J & Niedobitek G (2008) Histopathological Diagnosis of Nasopharyngeal Carcinoma‑Looking beyond the Blue Book. In *Nasopharyngeal carcinoma* [P Busson, editor], in press.

Nicholls JM, Agathanggelou A, Fung K, Zeng X & Niedobitek G (1997) The association of squamous cell carcinomas of the nasopharynx with Epstein-Barr virus shows geographical variation reminiscent of Burkitt's lymphoma. *J Pathol* **183**, 164-168.

Niedobitek G, Agathanggelou A, Rowe M, Jones EL, Jones DB, Turyaguma P, Oryema J, Wright DH & Young LS (1995) Heterogeneous expression of Epstein-Barr virus latent proteins in endemic Burkitt's lymphoma. *Blood* **86**, 659-665.

Niedobitek G, Agathanggelou A, Steven N & Young LS (2000) Epstein-Barr virus (EBV) in infectious mononucleosis: detection of the virus in tonsillar B lymphocytes but not in desquamated oropharyngeal epithelial cells. *Mol Pathol* **53**, 37-42.

Niedobitek G, Hamilton-Dutoit S, Herbst H, Finn T, Vetner M, Pallesen G & Stein H (1989) Identification of Epstein-Barr virus-infected cells in tonsils of acute infectious mononucleosis by in situ hybridization. *Hum Pathol* **20**, 796-799.

Nitta T, Chiba A, Yamamoto N & Yamaoka S (2004) Lack of cytotoxic property in a variant of Epstein-Barr virus latent membrane protein-1 isolated from nasopharyngeal carcinoma. *Cell Signal* **16**, 1071-1081.

Noubissi FK, Goswami S, Sanek NA, Kawakami K, Minamoto T, Moser A, Grinblat Y & Spiegelman VS (2009) Wnt signaling stimulates transcriptional outcome of the Hedgehog pathway by stabilizing GLI1 mRNA. *Cancer Res* **69**, 8572-8578.

O'Neil JD, Owen TJ, Wood VH, Date KL, Valentine R, Chukwuma MB, Arrand JR, Dawson CW & Young LS (2008) Epstein-Barr virus-encoded EBNA1 modulates the AP-1 transcription factor pathway in nasopharyngeal carcinoma cells and enhances angiogenesis in vitro. *J Gen Virol* **89**, 2833-2842.

Or YY, Chung GT, To KF, Chow C, Choy KW, Tong CY, Leung AW, Hui AB, Tsao SW, Ng HK, Yip TT, Busson P & Lo KW (2010) Identification of a novel 12p13.3 amplicon in nasopharyngeal carcinoma. *J Pathol* **220**, 97-107.

Or YY, Hui AB, Tam KY, Huang DP & Lo KW (2005) Characterization of chromosome 3q and 12q amplicons in nasopharyngeal carcinoma cell lines. *Int J Oncol* **26**, 49-56.

Ougolkov A, Mai M, Takahashi Y, Omote K, Bilim V, Shimizu A & Minamoto T (2000) Altered expression of beta-catenin and c-erbB-2 in early gastric cancer. *J Exp Clin Cancer Res* **19**, 349-355.

Owen TJ, O'Neil JD, Dawson CW, Hu C, Chen X, Yao Y, Wood VH, Mitchell LE, White RJ, Young LS & Arrand JR (2010) Epstein-Barr virus-encoded EBNA1 enhances RNA polymerase III-dependent EBER expression through induction of EBER-associated cellular transcription factors. *Mol Cancer* **9**, 241-256.

Ozawa S, Kato Y, Komori R, Maehata Y, Kubota E & Hata R (2006) BRAK/CXCL14 expression suppresses tumor growth in vivo in human oral carcinoma cells. *Biochem Biophys Res Commun* **348**, 406-412.

Paez JG, Lin M, Beroukhim R, Lee JC, Zhao X, Richter DJ, Gabriel S, Herman P, Sasaki H, Altshuler D, Li C, Meyerson M & Sellers WR (2004) Genome coverage and sequence fidelity of phi29 polymerase-based multiple strand displacement whole genome amplification. *Nucleic Acids Res* **32**, e71.

Pan X, Urban AE, Palejev D, Schulz V, Grubert F, Hu Y, Snyder M & Weissman SM (2008) A procedure for highly specific, sensitive, and unbiased whole-genome amplification. *Proc Natl Acad Sci U S A* **105**, 15499-15504.

Park K, Kim SJ, Bang YJ, Park JG, Kim NK, Roberts AB & Sporn MB (1994) Genetic changes in the transforming growth factor beta (TGF-beta) type II receptor gene in human gastric cancer cells: correlation with sensitivity to growth inhibition by TGF-beta. *Proc Natl Acad Sci U S A* **91**, 8772-8776.

Pathmanathan R, Prasad U, Chandrika G, Sadler R, Flynn K & Raab-Traub N (1995) Undifferentiated, nonkeratinizing, and squamous cell carcinoma of the nasopharynx. Variants of Epstein-Barr virus-infected neoplasia. *Am J Pathol* **146**, 1355-1367.

Pathmanathan R, Prasad U, Sadler R, Flynn K & Raab-Traub N (1995) Clonal proliferations of cells infected with Epstein-Barr virus in preinvasive lesions related to nasopharyngeal carcinoma. *N Engl J Med* **333**, 693-698.

Pegtel DM, Subramanian A, Sheen TS, Tsai CH, Golub TR & Thorley-Lawson DA (2005) Epstein-Barr-virus-encoded LMP2A induces primary epithelial cell migration and invasion: possible role in nasopharyngeal carcinoma metastasis. *J Virol* **79**, 15430-15442.

Peng C, Liu HY, Zhou M, Zhang LM, Li XL, Shen SR & Li GY (2007) BRD7 suppresses the growth of Nasopharyngeal Carcinoma cells (HNE1) through negatively regulating beta-catenin and ERK pathways. *Mol Cell Biochem* **303**, 141-149.

Peng D, Ren CP, Yi HM, Zhou L, Yang XY, Li H & Yao KT (2006) Genetic and epigenetic alterations of DLC-1, a candidate tumor suppressor gene, in nasopharyngeal carcinoma. *Acta Biochim Biophys Sin (Shanghai)* **38**, 349-355.

Peng H, Shintani S, Kim Y & Wong DT (2006) Loss of p12CDK2-AP1 expression in human oral squamous cell carcinoma with disrupted transforming growth factor-beta-Smad signaling pathway. *Neoplasia* **8**, 1028-1036.

Peng H, Zhao T & Yao KT (2003) Expression of RASSF1A gene in nasopharyngeal carcinoma. *Di Yi Jun Yi Da Xue Xue Bao* **23**, 673-676.

Petrella A, Festa M, Ercolino SF, Zerilli M, Stassi G, Solito E & Parente L (2006) Annexin-1 downregulation in thyroid cancer correlates to the degree of tumor differentiation. *Cancer Biol Ther* **5**, 643-647.

Pierce DF, Jr., Gorska AE, Chytil A, Meise KS, Page DL, Coffey RJ, Jr. & Moses HL (1995) Mammary tumor suppression by transforming growth factor beta 1 transgene expression. *Proc Natl Acad Sci U S A* **92**, 4254-4258.

Poirier S, Bouvier G, Malaveille C, Ohshima H, Shao YM, Hubert A, Zeng Y, de The G & Bartsch H (1989) Volatile nitrosamine levels and genotoxicity of food samples from high-risk areas for nasopharyngeal carcinoma before and after nitrosation. *Int J Cancer* **44**, 1088-1094.

Ponder BA (2001) Cancer genetics. *Nature* **411**, 336-341.

Pot I & Bonni S (2008) SnoN in TGF-beta signaling and cancer biology. *Curr Mol Med* **8**, 319-328.

Presneau N, Manderson EN & Tonin PN (2003) The quest for a tumor suppressor gene phenotype. *Curr Mol Med* **3**, 605-629.

Pu H, Collazo J, Jones E, Gayheart D, Sakamoto S, Vogt A, Mitchell B & Kyprianou N (2009) Dysfunctional transforming growth factor-beta receptor II accelerates prostate tumorigenesis in the TRAMP mouse model. *Cancer Res* **69**, 7366-7374.

Pugh TJ, Delaney AD, Farnoud N, Flibotte S, Griffith M, Li HI, Qian H, Farinha P, Gascoyne RD & Marra MA (2008) Impact of whole genome amplification on analysis of copy number variants. *Nucleic Acids Res* **36**, e80.

Purdie KJ, Lambert SR, Teh MT, Chaplin T, Molloy G, Raghavan M, Kelsell DP, Leigh IM, Harwood CA, Proby CM & Young BD (2007) Allelic imbalances and microdeletions affecting the PTPRD gene in cutaneous squamous cell carcinomas detected using single nucleotide polymorphism microarray analysis. *Genes Chromosomes Cancer* **46**, 661-669.

Qian CN, Guo X, Cao B, Kort EJ, Lee CC, Chen J, Wang LM, Mai WY, Min HQ, Hong MH, Vande Woude GF, Resau JH & Teh BT (2002) Met protein expression level correlates with survival in patients with late-stage nasopharyngeal carcinoma. *Cancer Res* **62**, 589-596.

Qin L, Zhang X, Zhang L, Feng Y, Weng GX, Li MZ, Kong QL, Qian CN, Zeng YX, Zeng MS, Liao DF & Song LB (2008) Downregulation of BMI-1 enhances 5-fluorouracil-induced apoptosis in nasopharyngeal carcinoma cells. *Biochem Biophys Res Commun* **371**, 531-535.

Qiu GH, Tan LK, Loh KS, Lim CY, Srivastava G, Tsai ST, Tsao SW & Tao Q (2004) The candidate tumor suppressor gene BLU, located at the commonly deleted region 3p21.3, is an E2F-regulated, stress-responsive gene and inactivated by both epigenetic and genetic mechanisms in nasopharyngeal carcinoma. *Oncogene* **23**, 4793-4806.

Raab-Traub N (2002) Epstein-Barr virus in the pathogenesis of NPC. *Semin Cancer Biol* **12**, 431-441.

Rask K, Nilsson A, Brannstrom M, Carlsson P, Hellberg P, Janson PO, Hedin L & Sundfeldt K (2003) Wnt-signalling pathway in ovarian epithelial tumours: increased expression of beta-catenin and GSK3beta. *Br J Cancer* **89**, 1298-1304.

Renault MA, Roncalli J, Tongers J, Misener S, Thorne T, Jujo K, Ito A, Clarke T, Fung C, Millay M, Kamide C, Scarpelli A, Klyachko E & Losordo DW (2009) The Hedgehog transcription factor Gli3 modulates angiogenesis. *Circ Res* **105**, 818-826.

Reynolds GM, Billingham LJ, Gray LJ, Flavell JR, Najafipour S, Crocker J, Nelson P, Young LS & Murray PG (2002) Interleukin 6 expression by Hodgkin/Reed-Sternberg cells is associated with the presence of 'B' symptoms and failure to achieve complete remission in patients with advanced Hodgkin's disease. *Br J Haematol* **118**, 195-201.

Ripka S, Konig A, Buchholz M, Wagner M, Sipos B, Kloppel G, Downward J, Gress T & Michl P (2007) WNT5A--target of CUTL1 and potent modulator of tumor cell migration and invasion in pancreatic cancer. *Carcinogenesis* **28**, 1178-1187.

Risbridger GP, Schmitt JF & Robertson DM (2001) Activins and inhibins in endocrine and other tumors. *Endocr Rev* **22**, 836-858.

Rodrigo JP, Garcia-Pedrero JM, Fernandez MP, Morgan RO, Suarez C & Herrero A (2005) Annexin A1 expression in nasopharyngeal carcinoma correlates with squamous differentiation. *Am J Rhinol* **19**, 483-487.

Rodriguez S, Khabir A, Keryer C, Perrot C, Drira M, Ghorbel A, Jlidi R, Bernheim A, Valent A & Busson P (2005) Conventional and array-based comparative genomic hybridization analysis of nasopharyngeal carcinomas from the Mediterranean area. *Cancer Genet Cytogenet* **157**, 140-147.

Rojas A, Padidam M, Cress D & Grady WM (2009) TGF-beta receptor levels regulate the specificity of signaling pathway activation and biological effects of TGF-beta. *Biochim Biophys Acta* **1793**, 1165-1173.

Rosenthal E, McCrory A, Talbert M, Young G, Murphy-Ullrich J & Gladson C (2004) Elevated expression of TGF-beta1 in head and neck cancer-associated fibroblasts. *Mol Carcinog* **40**, 116-121.

Rowe M, Rowe DT, Gregory CD, Young LS, Farrell PJ, Rupani H & Rickinson AB (1987) Differences in B cell growth phenotype reflect novel patterns of Epstein-Barr virus latent gene expression in Burkitt's lymphoma cells. *Embo J* **6**, 2743-2751.

Ruiz i Altaba A (1999) Gli proteins and Hedgehog signaling: development and cancer. *Trends Genet* **15**, 418-425.

Russo G, Zegar C & Giordano A (2003) Advantages and limitations of microarray technology in human cancer. *Oncogene* **22**, 6497-6507.

Ryu B & Kern SE (2003) The essential similarity of TGFbeta and activin receptor transcriptional responses in cancer cells. *Cancer Biol Ther* **2**, 164-170.

Sabe H, Hashimoto S, Morishige M, Ogawa E, Hashimoto A, Nam JM, Miura K, Yano H & Onodera Y (2009) The EGFR-GEP100-Arf6-AMAP1 signaling pathway specific to breast cancer invasion and metastasis. *Traffic* **10**, 982-993.

Saechan V, Mori A, Mitarnun W, Settheetham-Ishida W & Ishida T (2006) Analysis of LMP1 variants of EBV in Southern Thailand: evidence for strain-associated T-cell tropism and pathogenicity. *J Clin Virol* **36**, 119-125.

Saitoh T, Mine T & Katoh M (2002) Frequent up-regulation of WNT5A mRNA in primary gastric cancer. *Int J Mol Med* **9**, 515-519.

Sam CK, Brooks LA, Niedobitek G, Young LS, Prasad U & Rickinson AB (1993) Analysis of Epstein-Barr virus infection in nasopharyngeal biopsies from a group at high risk of nasopharyngeal carcinoma. *Int J Cancer* **53**, 957-962.

Sample J, Young L, Martin B, Chatman T, Kieff E, Rickinson A & Kieff E (1990) Epstein-Barr virus types 1 and 2 differ in their EBNA-3A, EBNA-3B, and EBNA-3C genes. *J Virol* **64**, 4084-4092.

Sarac S, Akyol MU, Kanbur B, Poyraz A, Akyol G, Yilmaz T & Sungur A (2001) Bcl-2 and LMP1 expression in nasopharyngeal carcinomas. *Am J Otolaryngol* **22**, 377-382.

Sashiyama H, Shino Y, Sakao S, Shimada H, Kobayashi S, Ochiai T & Shirasawa H (2002) Alteration of integrin expression relates to malignant progression of human papillomavirus-immortalized esophageal keratinocytes. *Cancer Lett* **177**, 21-28.

Satoh S, Daigo Y, Furukawa Y, Kato T, Miwa N, Nishiwaki T, Kawasoe T, Ishiguro H, Fujita M, Tokino T, Sasaki Y, Imaoka S, Murata M, Shimano T, Yamaoka Y & Nakamura Y (2000) AXIN1 mutations in hepatocellular carcinomas, and growth suppression in cancer cells by virus-mediated transfer of AXIN1. *Nat Genet* **24**, 245-250.

Schneikert J & Behrens J (2007) The canonical Wnt signalling pathway and its APC partner in colon cancer development. *Gut* **56**, 417-425.

Schnepp R & Hua X (2003) A tumor-suppressing duo: TGFbeta and activin modulate a similar transcriptome. *Cancer Biol Ther* **2**, 171-172.

Scholle F, Bendt KM & Raab-Traub N (2000) Epstein-Barr virus LMP2A transforms epithelial cells, inhibits cell differentiation, and activates Akt. *J Virol* **74**, 10681-10689.

Schwarze SR, Luo J, Isaacs WB & Jarrard DF (2005) Modulation of CXCL14 (BRAK) expression in prostate cancer. *Prostate* **64**, 67-74.

Seder CW, Hartojo W, Lin L, Silvers AL, Wang Z, Thomas DG, Giordano TJ, Chen G, Chang AC, Orringer MB & Beer DG (2009) Upregulated INHBA expression may promote cell proliferation and is associated with poor survival in lung adenocarcinoma. *Neoplasia* **11**, 388-396.

Segre JA, Bauer C & Fuchs E (1999) Klf4 is a transcription factor required for establishing the barrier function of the skin. *Nat Genet* **22**, 356-360.

Sengupta S, den Boon JA, Chen IH, Newton MA, Dahl DB, Chen M, Cheng YJ, Westra WH, Chen CJ, Hildesheim A, Sugden B & Ahlquist P (2006) Genome-wide expression profiling reveals EBV-associated inhibition of MHC class I expression in nasopharyngeal carcinoma. *Cancer Res* **66**, 7999-8006.

Shair KH, Schnegg CI & Raab-Traub N (2009) Epstein-Barr virus latent membrane protein-1 effects on junctional plakoglobin and induction of a cadherin switch. *Cancer Res* **69**, 5734-5742.

Sham JS & Choy D (1990) Prognostic factors of nasopharyngeal carcinoma: a review of 759 patients. *Br J Radiol* **63**, 51-58.

Shanmugaratnam K & Sobin LH (1993) The World Health Organization histological classification of tumours of the upper respiratory tract and ear. A commentary on the second edition. *Cancer* **71**, 2689-2697.

Shannon-Lowe CD, Neuhierl B, Baldwin G, Rickinson AB & Delecluse HJ (2006) Resting B cells as a transfer vehicle for Epstein-Barr virus infection of epithelial cells. *Proc Natl Acad Sci U S A* **103**, 7065-7070.

Shao J, Li Y, Wu Q, Liang X, Yu X, Huang L, Hou J, Huang X, Ernberg I, Hu LF & Zeng Y (2002) High frequency loss of heterozygosity on the long arms of chromosomes 13 and 14 in nasopharyngeal carcinoma in Southern China. *Chin Med J (Engl)* **115**, 571-575.

Shao JY, Ernberg I, Biberfeld P, Heiden T, Zeng YX & Hu LF (2004) Epstein-Barr virus LMP1 status in relation to apoptosis, p53 expression and leucocyte infiltration in nasopharyngeal carcinoma. *Anticancer Res* **24**, 2309-2318.

Shao JY, Huang XM, Yu XJ, Huang LX, Wu QL, Xia JC, Wang HY, Feng QS, Ren ZF, Ernberg I, Hu LF & Zeng YX (2001) Loss of heterozygosity and its correlation with clinical outcome and Epstein-Barr virus infection in nasopharyngeal carcinoma. *Anticancer Res* **21**, 3021-3029.

Shao YM, Poirier S, Ohshima H, Malaveille C, Zeng Y, de The G & Bartsch H (1988) Epstein-Barr virus activation in Raji cells by extracts of preserved food from high risk areas for nasopharyngeal carcinoma. *Carcinogenesis* **9**, 1455-1457.

Shapiro IM & Volsky DJ (1983) Infection of normal human epithelial cells by Epstein-Barr virus. *Science* **219**, 1225-1228.

Shellenberger TD, Wang M, Gujrati M, Jayakumar A, Strieter RM, Burdick MD, Ioannides CG, Efferson CL, El-Naggar AK, Roberts D, Clayman GL & Frederick MJ (2004) BRAK/CXCL14 is a potent inhibitor of angiogenesis and a chemotactic factor for immature dendritic cells. *Cancer Res* **64**, 8262-8270.

Shen D, Nooraie F, Elshimali Y, Lonsberry V, He J, Bose S, Chia D, Seligson D, Chang HR & Goodglick L (2006) Decreased expression of annexin A1 is correlated with breast cancer development and progression as determined by a tissue microarray analysis. *Hum Pathol* **37**, 1583-1591.

Sherr CJ (2001) Parsing Ink4a/Arf: "pure" p16-null mice. *Cell* **106**, 531-534.

Sheu JJ, Lee CH, Ko JY, Tsao GS, Wu CC, Fang CY, Tsai FJ, Hua CH, Chen CL & Chen JY (2009) Chromosome 3p12.3-p14.2 and 3q26.2-q26.32 are genomic markers for prognosis of advanced nasopharyngeal carcinoma. *Cancer Epidemiol Biomarkers Prev* **18**, 2709-2716.

Sheu LF, Chen A, Meng CL, Ho KC, Lee WH, Leu FJ & Chao CF (1996) Enhanced malignant progression of nasopharyngeal carcinoma cells mediated by the expression of Epstein-Barr nuclear antigen 1 in vivo. *J Pathol* **180**, 243-248.

Sheu LF, Chen A, Meng CL, Ho KC, Lin FG & Lee WH (1997) Analysis of bcl-2 expression in normal, inflamed, dysplastic nasopharyngeal epithelia, and nasopharyngeal carcinoma: association with p53 expression. *Hum Pathol* **28**, 556-562.

Shi B, Liang J, Yang X, Wang Y, Zhao Y, Wu H, Sun L, Zhang Y, Chen Y, Li R, Zhang Y, Hong M & Shang Y (2007) Integration of estrogen and Wnt signaling circuits by the polycomb group protein EZH2 in breast cancer cells. *Mol Cell Biol* **27**, 5105-5119.

Shi W, Bastianutto C, Li A, Perez-Ordonez B, Ng R, Chow KY, Zhang W, Jurisica I, Lo KW, Bayley A, Kim J, O'Sullivan B, Siu L, Chen E & Liu FF (2006) Multiple dysregulated pathways in nasopharyngeal carcinoma revealed by gene expression profiling. *Int J Cancer* **119**, 2467-2475.

Shi Y, Tian Y, Zhou YQ, Ju JY, Qu L, Chen SL, Xiang ZG, Liu Y & Zhu LP (2007) Inhibition of malignant activities of nasopharyngeal carcinoma cells with high expression of CD44 by siRNA. *Oncol Rep* **18**, 397-403.

Shields JM, Christy RJ & Yang VW (1996) Identification and characterization of a gene encoding a gut-enriched Kruppel-like factor expressed during growth arrest. *J Biol Chem* **271**, 20009-20017.

Shih-Hsin Wu L (2006) Construction of evolutionary tree models for nasopharyngeal carcinoma using comparative genomic hybridization data. *Cancer Genet Cytogenet* **168**, 105-108.

Shivakumar L, Minna J, Sakamaki T, Pestell R & White MA (2002) The RASSF1A tumor suppressor blocks cell cycle progression and inhibits cyclin D1 accumulation. *Mol Cell Biol* **22**, 4309-4318.

Slots J, Saygun I, Sabeti M & Kubar A (2006) Epstein-Barr virus in oral diseases. *J Periodontal Res* **41**, 235-244.

Solomon E, Borrow J & Goddard AD (1991) Chromosome aberrations and cancer. *Science* **254**, 1153-1160.

Song LB, Li J, Liao WT, Feng Y, Yu CP, Hu LJ, Kong QL, Xu LH, Zhang X, Liu WL, Li MZ, Zhang L, Kang TB, Fu LW, Huang WL, Xia YF, Tsao SW, Li M, Band V, Band H, Shi QH, Zeng YX & Zeng MS (2009) The polycomb group protein Bmi-1 represses the tumor suppressor PTEN and induces epithelial-mesenchymal transition in human nasopharyngeal epithelial cells. *J Clin Invest* **119**, 3626-3636.

Song LB, Zeng MS, Liao WT, Zhang L, Mo HY, Liu WL, Shao JY, Wu QL, Li MZ, Xia YF, Fu LW, Huang WL, Dimri GP, Band V & Zeng YX (2006) Bmi-1 is a novel molecular marker of nasopharyngeal carcinoma progression and immortalizes primary human nasopharyngeal epithelial cells. *Cancer Res* **66**, 6225-6232.

Song Y & Zhang C (2009) Hydralazine inhibits human cervical cancer cell growth in vitro in association with APC demethylation and re-expression. *Cancer Chemother Pharmacol* **63**, 605-613.

Sriuranpong V, Mutirangura A, Gillespie JW, Patel V, Amornphimoltham P, Molinolo AA, Kerekhanjanarong V, Supanakorn S, Supiyaphun P, Rangdaeng S, Voravud N & Gutkind JS (2004) Global gene expression profile of nasopharyngeal carcinoma by laser capture microdissection and complementary DNA microarrays. *Clin Cancer Res* **10**, 4944-4958.

Stecca B, Mas C, Clement V, Zbinden M, Correa R, Piguet V, Beermann F & Ruiz IAA (2007) Melanomas require HEDGEHOG-GLI signaling regulated by interactions between GLI1 and the RAS-MEK/AKT pathways. *Proc Natl Acad Sci U S A* **104**, 5895-5900.

Stevens SJ, Verkuijlen SA, Hariwiyanto B, Harijadi, Paramita DK, Fachiroh J, Adham M, Tan IB, Haryana SM & Middeldorp JM (2006) Noninvasive diagnosis of nasopharyngeal carcinoma: nasopharyngeal brushings reveal high Epstein-Barr virus DNA load and carcinoma-specific viral BARF1 mRNA. *Int J Cancer* **119**, 608-614.

Su B, Xiang B, Wang L, Cao L, Xiao L, Li X, Li X, Wu M & Li G (2010) Profiling and comparing transcription factors activated in non-metastatic and metastatic nasopharyngeal carcinoma cells. *J Cell Biochem* **109**, 173-183.

Sung NS, Edwards RH, Seillier-Moiseiwitsch F, Perkins AG, Zeng Y & Raab-Traub N (1998) Epstein-Barr virus strain variation in nasopharyngeal carcinoma from the endemic and non-endemic regions of China. *Int J Cancer* **76**, 207-215.

Sung NS, Zeng Y & Raab-Traub N (2000) Alterations on chromosome 3 in endemic and nonendemic nasopharyngeal carcinoma. *Int J Cancer* **86**, 244-250.

Suva ML, Riggi N, Janiszewska M, Radovanovic I, Provero P, Stehle JC, Baumer K, Le Bitoux MA, Marino D, Cironi L, Marquez VE, Clement V & Stamenkovic I (2009) EZH2 is essential for glioblastoma cancer stem cell maintenance. *Cancer Res* **69**, 9211-9218.

Suzuki M, Hirao A & Mizuno A (2003) Microtubule-associated [corrected] protein 7 increases the membrane expression of transient receptor potential vanilloid 4 (TRPV4). *J Biol Chem* **278**, 51448-51453.

Tanahashi J, Daa T, Yada N, Kashima K, Kondoh Y & Yokoyama S (2008) Mutational analysis of Wnt signaling molecules in ameloblastoma with aberrant nuclear expression of beta-catenin. *J Oral Pathol Med* **37**, 565-570.

Tang B, Vu M, Booker T, Santner SJ, Miller FR, Anver MR & Wakefield LM (2003) TGF-beta switches from tumor suppressor to prometastatic factor in a model of breast cancer progression. *J Clin Invest* **112**, 1116-1124.

Tang KF, Chan SH, Loh KS, Chong SM, Wang D, Yeoh KH & Hu H (1999) Increased production of interferon-gamma by tumour infiltrating T lymphocytes in nasopharyngeal carcinoma: indicative of an activated status. *Cancer Lett* **140**, 93-98.

Tao Q & Chan AT (2007) Nasopharyngeal carcinoma: molecular pathogenesis and therapeutic developments. *Expert Rev Mol Med* **9**, 1-24.

Tao Y, Bidault F, Bosq J & Bourhis J (2008) Distant metastasis of undifferentiated carcinoma of nasopharyngeal type. *Onkologie* **31**, 574-575.

Tatsumi E & Purtilo DT (1986) Epstein-Barr virus (EBV) and X-linked lymphoproliferative syndrome (XLP). *AIDS Res* **2 Suppl 1**, S109-113.

Thapa N, Lee BH & Kim IS (2007) TGFBIp/betaig-h3 protein: a versatile matrix molecule induced by TGF-beta. *Int J Biochem Cell Biol* **39**, 2183-2194.

Thayer SP, di Magliano MP, Heiser PW, Nielsen CM, Roberts DJ, Lauwers GY, Qi YP, Gysin S, Fernandez-del Castillo C, Yajnik V, Antoniu B, McMahon M,

Warshaw AL & Hebrok M (2003) Hedgehog is an early and late mediator of pancreatic cancer tumorigenesis. *Nature* **425**, 851-856.

Thorley-Lawson DA (2005) EBV the prototypical human tumor virus--just how bad is it? *J Allergy Clin Immunol* **116**, 251-261.

Tiwawech D, Srivatanakul P, Karalak A & Ishida T (2008) Association between EBNA2 and LMP1 subtypes of Epstein-Barr virus and nasopharyngeal carcinoma in Thais. *J Clin Virol* **42**, 1-6.

Tobin SW, Douville K, Benbow U, Brinckerhoff CE, Memoli VA & Arrick BA (2002) Consequences of altered TGF-beta expression and responsiveness in breast cancer: evidence for autocrine and paracrine effects. *Oncogene* **21**, 108-118.

Tong Z, Wu X, Ovcharenko D, Zhu J, Chen CS & Kehrer JP (2005) Neutrophil gelatinase-associated lipocalin as a survival factor. *Biochem J* **391**, 441-448.

Trask BJ (1991) Fluorescence in situ hybridization: applications in cytogenetics and gene mapping. *Trends Genet* **7**, 149-154.

Tsai CN, Tsai CL, Tse KP, Chang HY & Chang YS (2002) The Epstein-Barr virus oncogene product, latent membrane protein 1, induces the downregulation of E-cadherin gene expression via activation of DNA methyltransferases. *Proc Natl Acad Sci U S A* **99**, 10084-10089.

Tsang YS, Lo KW, Leung SF, Choi PH, Fong Y, Lee JC & Huang DP (1999) Two distinct regions of deletion on chromosome 13q in primary nasopharyngeal carcinoma. *Int J Cancer* **83**, 305-308.

Tsao SW, Tramoutanis G, Dawson CW, Lo AK & Huang DP (2002) The significance of LMP1 expression in nasopharyngeal carcinoma. *Semin Cancer Biol* **12**, 473-487.

Tsuji A, Wakisaka N, Kondo S, Murono S, Furukawa M & Yoshizaki T (2008) Induction of receptor for advanced glycation end products by EBV latent membrane protein 1 and its correlation with angiogenesis and cervical lymph node metastasis in nasopharyngeal carcinoma. *Clin Cancer Res* **14**, 5368-5375.

Tsurumi T, Fujita M & Kudoh A (2005) Latent and lytic Epstein-Barr virus replication strategies. *Rev Med Virol* **15**, 3-15.

Tuna M, Knuutila S & Mills GB (2009) Uniparental disomy in cancer. *Trends Mol Med* **15**, 120-128.

Valentine R, Dawson CW, Hu C, Shah KM, Owen TJ, Date KL, Maia SP, Shao J, Arrand JR, Young LS & O'Neil JD (2010) Epstein-Barr virus-encoded EBNA1 inhibits the canonical NF-kappaB pathway in carcinoma cells by inhibiting IKK phosphorylation. *Mol Cancer* **9**, 1.

van Leenders GJ, Dukers D, Hessels D, van den Kieboom SW, Hulsbergen CA, Witjes JA, Otte AP, Meijer CJ & Raaphorst FM (2007) Polycomb-group oncogenes EZH2, BMI1, and RING1 are overexpressed in prostate cancer with adverse pathologic and clinical features. *Eur Urol* **52**, 455-463.

Varambally S, Dhanasekaran SM, Zhou M, Barrette TR, Kumar-Sinha C, Sanda MG, Ghosh D, Pienta KJ, Sewalt RG, Otte AP, Rubin MA & Chinnaiyan AM (2002) The polycomb group protein EZH2 is involved in progression of prostate cancer. *Nature* **419**, 624-629.

Veeman MT, Axelrod JD & Moon RT (2003) A second canon. Functions and mechanisms of beta-catenin-independent Wnt signaling. *Dev Cell* **5**, 367-377.

Verma A, Kambhampati S, Parmar S & Platanias LC (2003) Jak family of kinases in cancer. *Cancer Metastasis Rev* **22**, 423-434.

Verras M & Sun Z (2006) Roles and regulation of Wnt signaling and beta-catenin in prostate cancer. *Cancer Lett* **237**, 22-32.

Vos MD, Ellis CA, Bell A, Birrer MJ & Clark GJ (2000) Ras uses the novel tumor suppressor RASSF1 as an effector to mediate apoptosis. *J Biol Chem* **275**, 35669-35672.

Wang D, Liebowitz D & Kieff E (1985) An EBV membrane protein expressed in immortalized lymphocytes transforms established rodent cells. *Cell* **43**, 831-840.

Wang GL, Lo KW, Tsang KS, Chung NY, Tsang YS, Cheung ST, Lee JC & Huang DP (1999) Inhibiting tumorigenic potential by restoration of p16 in nasopharyngeal carcinoma. *Br J Cancer* **81**, 1122-1126.

Wang J, Sun L, Myeroff L, Wang X, Gentry LE, Yang J, Liang J, Zborowska E, Markowitz S & Willson JK. (1995) Demonstration that mutation of the type II transforming growth factor beta receptor inactivates its tumor suppressor activity in replication error-positive colon carcinoma cells. *J Biol Chem* **270**, 22044-22049.

Wang LH, Choi YL, Hua XY, Shin YK, Song YJ, Youn SJ, Yun HY, Park SM, Kim WJ, Kim HJ, Choi JS & Kim SH (2006) Increased expression of sonic hedgehog and altered methylation of its promoter region in gastric cancer and its related lesions. *Mod Pathol* **19**, 675-683.

Wang Q, Li M, Wang Y, Zhang Y, Jin S, Xie G, Liu Z, Wang S, Zhang H, Shen L & Ge H (2008) RNA interference targeting CML66, a novel tumor antigen, inhibits proliferation, invasion and metastasis of HeLa cells. *Cancer Lett* **269**, 127-138.

Wang X, Xu K, Ling MT, Wong YC, Feng HC, Nicholls J & Tsao SW (2002) Evidence of increased Id-1 expression and its role in cell proliferation in nasopharyngeal carcinoma cells. *Mol Carcinog* **35**, 42-49.

Wei L, Xue T, Wang J, Chen B, Lei Y, Huang Y, Wang H & Xin X (2009) Roles of clusterin in progression, chemoresistance and metastasis of human ovarian cancer. *Int J Cancer* **125**, 791-806.

Wei WI & Sham JS (2005) Nasopharyngeal carcinoma. *Lancet* **365**, 2041-2054.

Weinberg RA (1991) Tumor suppressor genes. *Science* **254**, 1138-1146.

Wong KK, Tsang YT, Shen J, Cheng RS, Chang YM, Man TK & Lau CC (2004) Allelic imbalance analysis by high-density single-nucleotide polymorphic allele (SNP) array with whole genome amplified DNA. *Nucleic Acids Res* **32**, e69.

Wong N, Hui AB, Fan B, Lo KW, Pang E, Leung SF, Huang DP & Johnson PJ (2003a) Molecular cytogenetic characterization of nasopharyngeal carcinoma cell lines and xenografts by comparative genomic hybridization and spectral karyotyping. *Cancer Genet Cytogenet* **140**, 124-132.

Wong TS, Kwong DL, Sham J, Wei WI, Kwong YL & Yuen AP (2005) Elevation of plasma osteopontin level in patients with undifferentiated nasopharyngeal carcinoma. *Eur J Surg Oncol* **31**, 555-558.

Wong TS, Tang KC, Kwong DL, Sham JS, Wei WI, Kwong YL & Yuen AP (2003) Differential gene methylation in undifferentiated nasopharyngeal carcinoma. *Int J Oncol* **22**, 869-874.

Wood VH, O'Neil JD, Wei W, Stewart SE, Dawson CW & Young LS (2007) Epstein-Barr virus-encoded EBNA1 regulates cellular gene transcription and modulates the STAT1 and TGFbeta signaling pathways. *Oncogene* **26**, 4135-4147.

Wright K, Wilson P, Morland S, Campbell I, Walsh M, Hurst T, Ward B, Cummings M & Chenevix-Trench G (1999) beta-catenin mutation and expression

analysis in ovarian cancer: exon 3 mutations and nuclear translocation in 16% of endometrioid tumours. *Int J Cancer* **82**, 625-629.

Wu TC, Mann RB, Epstein JI, MacMahon E, Lee WA, Charache P, Hayward SD, Kurman RJ, Hayward GS & Ambinder RF (1991) Abundant expression of EBER1 small nuclear RNA in nasopharyngeal carcinoma. A morphologically distinctive target for detection of Epstein-Barr virus in formalin-fixed paraffin-embedded carcinoma specimens. *Am J Pathol* **138**, 1461-1469.

Xie L, Xu L, He Z, Zhou W, Wang L, Zhang L, Lan K, Ren C, Liu W & Yao K (2000) Identification of differentially expressed genes in nasopharyngeal carcinoma by means of the Atlas human cancer cDNA expression array. *J Cancer Res Clin Oncol* **126**, 400-406.

Xie LQ, Bian LJ, Li Z, Li Y, Li ZX & Li B (2010) Altered Expression of E-cadherin by Hepatocyte Growth Factor and Effect on the Prognosis of Nasopharyngeal Carcinoma. *Ann Surg Oncol* **17**, 1927-1936.

Xiong H, Zhang ZG, Tian XQ, Sun DF, Liang QC, Zhang YJ, Lu R, Chen YX & Fang JY (2008) Inhibition of JAK1, 2/STAT3 signaling induces apoptosis, cell cycle arrest, and reduces tumor cell invasion in colorectal cancer cells. *Neoplasia* **10**, 287-297.

Xu J, Menezes J, Prasad U & Ahmad A (1999) Elevated serum levels of transforming growth factor beta1 in Epstein-Barr virus-associated nasopharyngeal carcinoma patients. *Int J Cancer* **84**, 396-399.

Xu JB, Bao Y, Liu X, Liu Y, Huang S & Wang JC (2007) Defective expression of transforming growth factor beta type II receptor (TGFBR2) in the large cell variant of non-small cell lung carcinoma. *Lung Cancer* **58**, 36-43.

Yamada M, Tsuji N, Nakamura M, Moriai R, Kobayashi D, Yagihashi A & Watanabe N (2002) Down-regulation of TRF1, TRF2 and TIN2 genes is important to maintain telomeric DNA for gastric cancers. *Anticancer Res* **22**, 3303-3307.

Yamamoto H, Oue N, Sato A, Hasegawa Y, Yamamoto H, Matsubara A, Yasui W & Kikuchi A (2010) Wnt5a signaling is involved in the aggressiveness of prostate cancer and expression of metalloproteinase. *Oncogene* **29**, 2036-2046.

Yamato K, Koseki T, Ohguchi M, Kizaki M, Ikeda Y & Nishihara T (1997) Activin A induction of cell-cycle arrest involves modulation of cyclin D2 and p21CIP1/WAF1 in plasmacytic cells. *Mol Endocrinol* **11**, 1044-1052.

Yang H, Zhao R & Lee MH (2006) 14-3-3sigma, a p53 regulator, suppresses tumor growth of nasopharyngeal carcinoma. *Mol Cancer Ther* **5**, 253-260.

Yang J, Bielenberg DR, Rodig SJ, Doiron R, Clifton MC, Kung AL, Strong RK, Zurakowski D & Moses MA (2009) Lipocalin 2 promotes breast cancer progression. *Proc Natl Acad Sci U S A* **106**, 3913-3918.

Yardy GW, Bicknell DC, Wilding JL, Bartlett S, Liu Y, Winney B, Turner GD, Brewster SF & Bodmer WF (2009) Mutations in the AXIN1 gene in advanced prostate cancer. *Eur Urol* **56**, 486-494.

Yates JL, Warren N & Sugden B (1985) Stable replication of plasmids derived from Epstein-Barr virus in various mammalian cells. *Nature* **313**, 812-815.

Yau WL, Lung HL, Zabarovsky ER, Lerman MI, Sham JS, Chua DT, Tsao SW, Stanbridge EJ & Lung ML (2006) Functional studies of the chromosome 3p21.3 candidate tumor suppressor gene BLU/ZMYND10 in nasopharyngeal carcinoma. *Int J Cancer* **119**, 2821-2826.

Yauch RL, Gould SE, Scales SJ, Tang T, Tian H, Ahn CP, Marshall D, Fu L, Januario T, Kallop D, Nannini-Pepe M, Kotkow K, Marsters JC, Rubin LL & de

Sauvage FJ (2008) A paracrine requirement for hedgehog signalling in cancer. *Nature* **455**, 406-410.

Yi HM, Li H, Peng D, Zhang HJ, Wang L, Zhao M, Yao KT & Ren CP (2006) Genetic and epigenetic alterations of LTF at 3p21.3 in nasopharyngeal carcinoma. *Oncol Res* **16**, 261-272.

Yi M & Schnitzer JE (2009) Impaired tumor growth, metastasis, angiogenesis and wound healing in annexin A1-null mice. *Proc Natl Acad Sci U S A* **106**, 17886-17891.

Yip KW, Mocanu JD, Au PY, Sleep GT, Huang D, Busson P, Yeh WC, Gilbert R, O'Sullivan B, Gullane P, Bastianutto C & Liu FF (2005) Combination bcl-2 antisense and radiation therapy for nasopharyngeal cancer. *Clin Cancer Res* **11**, 8131-8144.

Yip WK, Abdullah MA, Yusoff SM & Seow HF (2009) Increase in tumour-infiltrating lymphocytes with regulatory T cell immunophenotypes and reduced zeta-chain expression in nasopharyngeal carcinoma patients. *Clin Exp Immunol* **155**, 412-422.

Yip YL & Tsao SW (2008) Regulation of p63 expression in primary and immortalized nasopharyngeal epithelial cells. *Int J Oncol* **33**, 713-724.

Yoo YA, Kang MH, Kim JS & Oh SC (2008) Sonic hedgehog signaling promotes motility and invasiveness of gastric cancer cells through TGF-beta-mediated activation of the ALK5-Smad 3 pathway. *Carcinogenesis* **29**, 480-490.

Yoo YD, Choi JY, Lee SJ, Kim JS, Min BR, Lee YI & Kang YK (1999) TGF-beta-induced cell-cycle arrest through the p21(WAF1/CIP1)-G1 cyclin/Cdks-p130 pathway in gastric-carcinoma cells. *Int J Cancer* **83**, 512-517.

Yoshizaki T, Endo K, Ren Q, Wakisaka N, Murono S, Kondo S, Sato H & Furukawa M (2007) Oncogenic role of Epstein-Barr virus-encoded small RNAs (EBERs) in nasopharyngeal carcinoma. *Auris Nasus Larynx* **34**, 73-78.

Young KA, Chen XS, Holers VM & Hannan JP (2007) Isolating the Epstein-Barr virus gp350/220 binding site on complement receptor type 2 (CR2/CD21). *J Biol Chem* **282**, 36614-36625.

Young LS, Lau R, Rowe M, Niedobitek G, Packham G, Shanahan F, Rowe DT, Greenspan D, Greenspan JS & Rickinson AB. (1991) Differentiation-associated expression of the Epstein-Barr virus BZLF1 transactivator protein in oral hairy leukoplakia. *J Virol* **65**, 2868-2874.

Young LS & Rickinson AB (2004) Epstein-Barr virus: 40 years on. *Nat Rev Cancer* **4**, 757-768.

Young LS, Yao QY, Rooney CM, Sculley TB, Moss DJ, Rupani H, Laux G, Bornkamm GW & Rickinson AB (1987) New type B isolates of Epstein-Barr virus from Burkitt's lymphoma and from normal individuals in endemic areas. *J Gen Virol* **68**, 2853-2862.

Yu MC, Ho JH, Lai SH & Henderson BE (1986) Cantonese-style salted fish as a cause of nasopharyngeal carcinoma: report of a case-control study in Hong Kong. *Cancer Res* **46**, 956-961.

Yu MC & Yuan JM (2002) Epidemiology of nasopharyngeal carcinoma. *Semin Cancer Biol* **12**, 421-429.

Yue J & Mulder KM (2001) Transforming growth factor-beta signal transduction in epithelial cells. *Pharmacol Ther* **91**, 1-34.

Zablow AI, Eanelli TR & Sanfilippo LJ (1992) Electron beam therapy for skin cancer of the head and neck. *Head Neck* **14**, 188-195.

Zavadil J & Bottinger EP (2005) TGF-beta and epithelial-to-mesenchymal transitions. *Oncogene* **24**, 5764-5774.

Zeng Z, Zhou Y, Zhang W, Li X, Xiong W, Liu H, Fan S, Qian J, Wang L, Li Z, Shen S & Li G (2006) Family-based association analysis validates chromosome 3p21 as a putative nasopharyngeal carcinoma susceptibility locus. *Genet Med* **8**, 156-160.

Zeng ZY, Zhou YH, Zhang WL, Xiong W, Fan SQ, Li XL, Luo XM, Wu MH, Yang YX, Huang C, Cao L, Tang K, Qian J, Shen SR & Li GY (2007) Gene expression profiling of nasopharyngeal carcinoma reveals the abnormally regulated Wnt signaling pathway. *Hum Pathol* **38**, 120-133.

Zhang F, Monkkonen M, Roth S & Laiho M (2002) TGF-beta induced G(1) cell cycle arrest requires the activity of the proteasome pathway. Transforming growth factor. *Exp Cell Res* **281**, 190-196.

Zhang W, Zeng Z, Zhou Y, Xiong W, Fan S, Xiao L, Huang D, Li Z, Li D, Wu M, Li X, Shen S, Wang R, Cao L, Tang K & Li G (2009) Identification of aberrant cell cycle regulation in Epstein-Barr virus-associated nasopharyngeal carcinoma by cDNA microarray and gene set enrichment analysis. *Acta Biochim Biophys Sin (Shanghai)* **41**, 414-428.

Zhao C, Chen A, Jamieson CH, Fereshteh M, Abrahamsson A, Blum J, Kwon HY, Kim J, Chute JP, Rizzieri D, Munchhof M, VanArsdale T, Beachy PA & Reya T (2009) Hedgehog signalling is essential for maintenance of cancer stem cells in myeloid leukaemia. *Nature* **458**, 776-779.

Zhao X, Li C, Paez JG, Chin K, Janne PA, Chen TH, Girard L, Minna J, Christiani D, Leo C, Gray JW, Sellers WR & Meyerson M (2004) An integrated view of copy number and allelic alterations in the cancer genome using single nucleotide polymorphism arrays. *Cancer Res* **64**, 3060-3071.

Zhao Y, El-Gabry M & Hei TK (2006) Loss of Betaig-h3 protein is frequent in primary lung carcinoma and related to tumorigenic phenotype in lung cancer cells. *Mol Carcinog* **45**, 84-92.

Zheng H, Li LL, Hu DS, Deng XY & Cao Y (2007) Role of Epstein-Barr virus encoded latent membrane protein 1 in the carcinogenesis of nasopharyngeal carcinoma. *Cell Mol Immunol* **4**, 185-196.

Zheng X, Yuan F, Hu L, Chen F, Klein G & Christensson B (1994) Effect of beta-lymphocyte- and NPC-derived EBV-LMP1 gene expression on in vitro growth and differentiation of human epithelial cells. *Int J Cancer* **57**, 747-753.

Zheng Z, Pan J, Chu B, Wong YC, Cheung AL & Tsao SW (1999) Downregulation and abnormal expression of E-cadherin and beta-catenin in nasopharyngeal carcinoma: close association with advanced disease stage and lymph node metastasis. *Hum Pathol* **30**, 458-466.

Zhou J, Ma J, Zhang BC, Li XL, Shen SR, Zhu SG, Xiong W, Liu HY, Huang H, Zhou M & Li GY (2004) BRD7, a novel bromodomain gene, inhibits G1-S progression by transcriptionally regulating some important molecules involved in ras/MEK/ERK and Rb/E2F pathways. *J Cell Physiol* **200**, 89-98.

Zhou L, Feng X, Shan W, Zhou W, Liu W, Wang L, Zhu B, Yi H, Yao K & Ren C (2007) Epigenetic and genetic alterations of the EDNRB gene in nasopharyngeal carcinoma. *Oncology* **72**, 357-363.

Zhou M, Liu H, Xu X, Zhou H, Li X, Peng C, Shen S, Xiong W, Ma J, Zeng Z, Fang S, Nie X, Yang Y, Zhou J, Xiang J, Cao L, Peng S, Li S & Li G (2006) Identification of nuclear localization signal that governs nuclear import of

BRD7 and its essential roles in inhibiting cell cycle progression. *J Cell Biochem* **98**, 920-930.

Zhou M, Xu XJ, Zhou HD, Liu HY, He JJ, Li XL, Peng C, Xiong W, Fan SQ, Lu JH, Ouyang J, Shen SR, Xiang B & Li GY (2006) BRD2 is one of BRD7-interacting proteins and its over-expression could initiate apoptosis. *Mol Cell Biochem* **292**, 205-212.

Zhou W, Feng X, Li H, Wang L, Zhu B, Liu W, Zhao M, Yao K & Ren C (2009) Inactivation of LARS2, located at the commonly deleted region 3p21.3, by both epigenetic and genetic mechanisms in nasopharyngeal carcinoma. *Acta Biochim Biophys Sin (Shanghai)* **41**, 54-62.

Zong YS, Zhang CQ, Zhang F, Ruan JB, Chen MY, Feng KT & Yu ZF (1993) Infiltrating lymphocytes and accessory cells in nasopharyngeal carcinoma. *Jpn J Cancer Res* **84**, 900-905.

zur Hausen H, Schulte-Holthausen H, Klein G, Henle W, Henle G, Clifford P & Santesson L (1970) EBV DNA in biopsies of Burkitt tumours and anaplastic carcinomas of the nasopharynx. *Nature* **228**, 1056-1058.